

**AN INVESTIGATION INTO SPINAL INJURY
FROM VEHICLE CRASHES
IN SAUDI ARABIA**

By

NAIF KHALAF AL-SHAMMARI

A thesis submitted to
The University of Birmingham
for the degree of
DOCTOR OF PHILOSOPHY

School of Engineering
The University of Birmingham
April 2011

UNIVERSITY OF
BIRMINGHAM

University of Birmingham Research Archive

e-theses repository

This unpublished thesis/dissertation is copyright of the author and/or third parties. The intellectual property rights of the author or third parties in respect of this work are as defined by The Copyright Designs and Patents Act 1988 or as modified by any successor legislation.

Any use made of information contained in this thesis/dissertation must be in accordance with that legislation and must be properly acknowledged. Further distribution or reproduction in any format is prohibited without the permission of the copyright holder.



**In the Name of Allah, the Most Gracious,
the Most Merciful**

Abstract

The primary purpose of this thesis is to present a comprehensive analysis of occupant kinematics and spinal injuries, during road traffic accidents in Saudi Arabia from the points of view of statistical analysis, modeling of occupant kinematics, and biomechanics.

An in-depth database containing information on 512 real world vehicle crashes was constructed. The study identifies the characteristics of the collisions and occupant spinal injuries in Saudi Arabia, and suggests measures to mitigate them.

A logistic model has been presented which can be used to provide information about the crashes and spinal injuries. The model may serve as an initial prediction to establish the risk of spinal injury sustained by occupants at road crash, and a paramedic's protocol, as part of the emergency response, could be revised according to the developed model.

State of the art techniques for accident reconstruction have been demonstrated as a tool to investigate the crashes, and the probable cause of crashes, and to make recommendations to prevent crashes and/or mitigate the severity of the accidents and resulting spinal injuries.

Computational simulations of crashes provide a tool for understanding the dynamics of crashes and injuries, and are being used worldwide to study dynamics of crashes and efficacy of safety devices. The work conducted here has demonstrated how crashes can be simulated to estimate the injury parameters, and the likelihood of injuries on various parts of the body.

While this study presents a detailed multi-dimensional study on road traffic crashes and spinal cord injuries therein, it remains a pilot study for Saudi Arabia. It demonstrates how this type of study can have far reaching consequences and the need to collect such data and carry out this kind of a study on a regular basis at the national level.

Acknowledgements

First and foremost all my thanks and praise is due to ALLAH (glorified be he) without whom this work would not have been undertaken, Second deep appreciation and thanks must go to my lead supervisor, *Prof. C.E. Neal-Sturgess*, for his continuous support, valuable suggestion, and endless encouragement. Without him, this work would not be have been possible to achieved, I shall always be grateful to him and his efforts, valuable assistance.

I have also been fortunate enough to be able to work closely, and secure advice and suggestions of my associate supervisor, *Dr. Ahamedali M. Hassan*. I would like to convey my special thanks and appreciation with gratitude for this invaluable suggestions, constructive comments, and timely guidance.

I'm also greatly indebted to my local supervisor, *Dr. Ali S. Al-Mejrad*, in King Saud University for his help and advisement during the last four years.

I would like to express my deep gratitude to *HRH Prince Fasial Bin Sultan Bin Abdulaziz Al-Saud*, Secretary General, Sultan Bin Abdulaziz Al-Saud Foundation, *HRH Mohammed Bin Naif Bin Abdulaziz Al-Saud*, Assistant Interior Minister for Security Affairs, *HH Prince, Dr. Turki Bin Saud Bin Mohammed Al-Saud*, Vice President for Research Institute, King Abdulaziz City for Science & Technology, for their support of my PhD.

My sincere appreciation goes to the multi-disciplinary team in GDT, SRCS, ADA, MPVI, NCCI, MoT and MoH for their invaluable contributions during my field work study.

Last, but not least, my deep thanks must go to my family for providing me with all the benefits of love, and patience. Thanks also go to all my friends for their encouragement.

I wish
To dedicate
This thesis
To my parents
And
To my daughter
Shaden

LIST OF PUBLICATIONS

- I. Al-Shammari, N. K.; Neal-Sturgess, C. E.; Hassan, A. M.; Al-Mejrad, A. S. (2008) *Modelling Human Body Movement in Road Accidents and Consequences for the Cervical Spine*, In the Proceedings of the Saudi International Innovation Conference (SIIC-2008), 93-97, University of Leeds, Leeds, UK, Jun 9-10 2008.
- II. Al-Shammari, N. K.; Neal-Sturgess, C. E.; Hassan, A. M.; Al-Mejrad, A. S. (2008) *Simulation of Spinal Injury in Camel–Vehicle Collision (CVC)*, In the Proceedings of the Saudi International Innovation Conference (SIIC-2008), 184, University of Leeds, Leeds, UK, Jun 9-10 2008.
- III. Hassan, A. M.; and Al-Shammari, N.K. (2009) *Investigation of Road Traffic Accident Disaster*, Internal Symposium on Disasters Management, Riyadh, KSA, Oct 3-6 2009.
- IV. Al-Shammari, N. K.; Bendak, S., Al-Gadhi, S. (2009) *In-Depth Analysis of Pedestrian Crashes in Riyadh*, J. Traffic Inj Prev, 10(6): 552-559, 20 November 2009.
- V. Al-Shammari, N. K.; Hassan, A. M.; Neal-Sturgess, C. E.; Al-Mejrad, A. S. (2010) *Mechanism of Spinal Injuries Sustained by Drivers of Passenger Cars during Collisions with Camels*, In the Proceedings of the 6th World Congress on Biomechanics 2010, pp. 49, Singapore, 1-6 August 2010.
- VI. Al-Shammari, N. K.; Hassan, A. M.; Neal-Sturgess, C. E.; Al-Mejrad, A. S. (2011) *Accident Reconstruction of Some Uncommon Spinal Injuries in Auto-Crashes in the Kingdom of Saudi Arabia*, Saudi Med J, 32(4): 2-3, March 2011.

CONTENTS OF THE THESIS

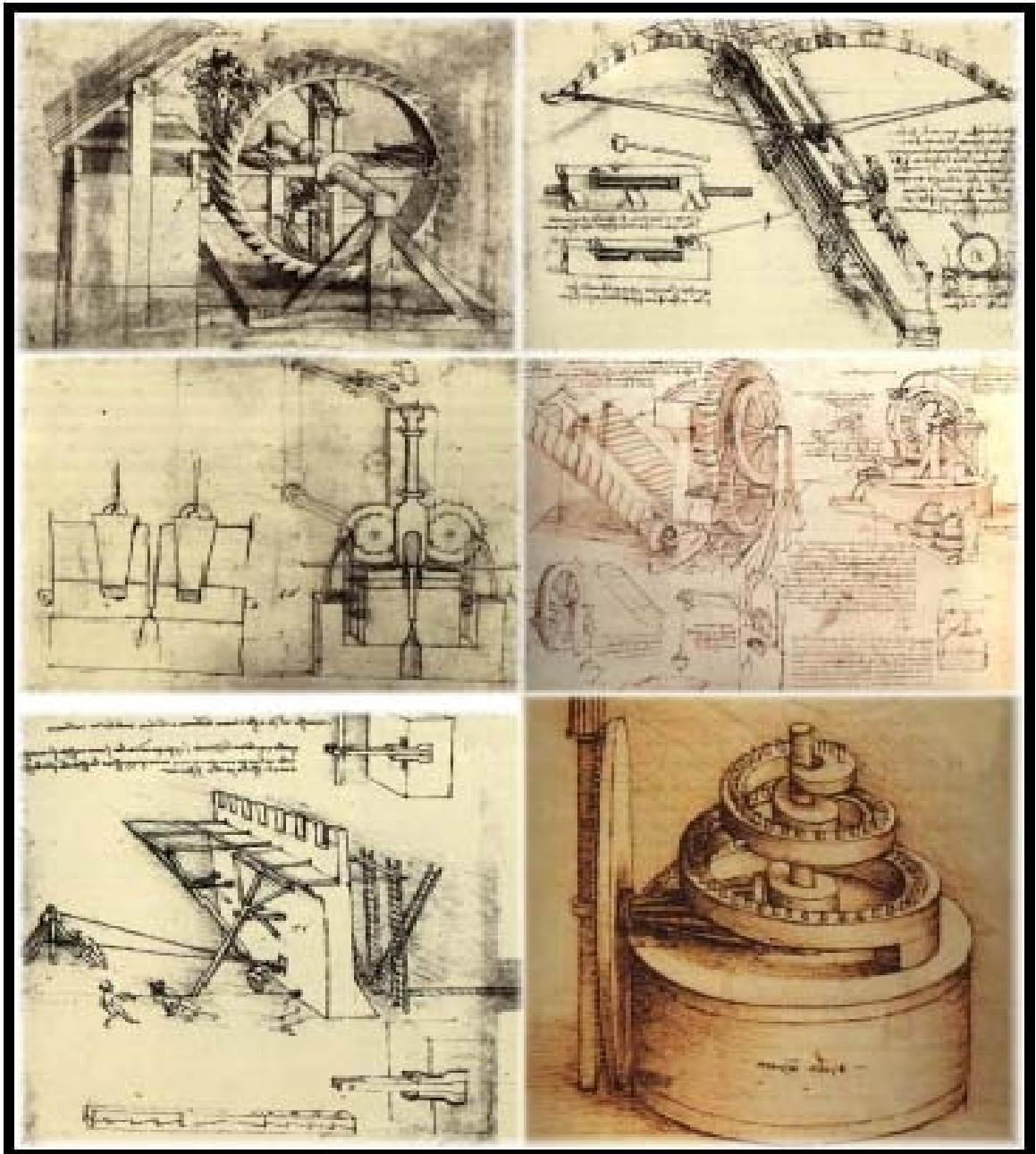
CHAPTER 1	INTRODUCTION	1
1.1	Statement of Research Problem	1
1.2	Research Purpose and Plan	3
1.3	Significance of the Study	5
CHAPTER 2	LITERATURE REVIEW ON-STATE-OF THE ART RESEARCH	6
2.1	Biomechanics of Spinal Injury	7
2.1.1	Anatomy of the Spine	7
2.1.2	Mechanisms of Spinal Injury	9
2.2	Neck Injury Crash-Test Criteria	11
2.2.1	Neck Injury Criterion (NIC)	11
2.2.2	Normalized Neck Injury Criterion (Nij)	12
2.2.3	Peak Virtual Power (PVP)	14
2.3	Field Studies Of Crash Factors Related To Spinal Injuries	16
2.4	Computational Models Of The Human Spine	17
2.4.1	Multi-Body Models (MBMs)	18
2.4.1.1	Cervical Spine Multibody Models	18
2.4.1.2	Lumbar Spine Multibody Models	21
2.4.2	Finite Element Models (FEMs)	24
2.4.2.1	FE Models of the Whole Human Spine	24
2.4.2.2	FE Models of the Cervical Spine	25
2.4.2.3	Whole Head and Neck Models	25
2.4.2.4	Thoracolumbar Spine Models	29
2.5	Conclusions	30
CHAPTER 3	ROAD TRAFFIC ACCIDENTS IN SAUDI ARABIA	32
3.1	Trends In Accidents, Injuries, And Deaths Of RTAs	33
3.2	Car Ownership And Vehicle Fleet	34
3.3	A Comparison Of RTA Rates	35
3.4	Characteristics Of Road Traffic Accidents	38
3.5	National Economic Loss Due To RTAs	40
3.6	Accident Forecasts And Safety Targets	42
3.7	Conclusions	44

CHAPTER 4	IN-DEPTH COLLISION CHARACTERISTICS OF SPINAL INJURIES	45
4.1	Methods and Materials	46
4.1.1	Purpose and Scope	46
4.1.2	Study Design	46
4.1.3	Case Selection Criteria	48
4.1.4	Study Location	48
4.1.5	Study Forms	49
4.1.6	Study Population	50
4.1.7	Definition of Variables	53
4.1.8	Statistical Analysis	54
4.2	Types of Spinal Injury	55
4.3	Types of Collision	56
4.4	Direction of Impact	58
4.5	Spinal Injury Causation	61
4.6	Deformation and Intrusion	63
4.7	Restraint Use And Spinal Injury	66
4.8	Ejection And Spinal Injury	68
4.9	Conclusions	73
CHAPTER 5	RISK OF SUSTAINING SPINAL INJURY FROM VEHICLE CRASHES IN SAUDI ARABIA	76
5.1	Methods and Materials	77
5.2	Development of the Logistic Model	80
5.3	Model Validation	84
5.4	Model Applications	86
5.5	Conclusions	92
CHAPTER 6	CONSEQUENCES OF SPINAL CORD INJURY (SCIs) IN SAUDI ARABIA	94
6.1	Materials And Methodology	95
6.1.1	Data Sources	95
6.1.2	Study Design	95
6.1.3	Poisson Regression Model of Spinal Cord Injury Trends	97
6.2	Overall Prevalence And Incidence	98
6.3	Etiology of SCIs	101
6.4	Pre-Hospital Care of SCI Casualties	102
6.5	Assessment Of Neurological Level Of SCI	103

6.6	Mechanisms Of SCI	104
6.7	Trends In Spinal Cord Injury In Saudi Arabia	105
6.8	Conclusions	107
CHAPTER 7	ACCIDENT RECONSTRUCTION OF SOME UNCOMMON SPINAL INJURIES IN AUTO-CRASHES IN SAUDI ARABIA	108
7.1	Methods And Materials	109
7.1.1	In-depth Investigation	111
7.1.2	Computer Simulation	111
7.2	CASE 1: Collision With A Pedestrian	112
7.2.1	Crash Reconstruction I	112
7.2.2	Mechanisms of Spinal Injury	114
7.3	CASE 2: Collision With A Fixed Object	116
7.3.1	Crash Reconstruction II	116
7.3.2	Mechanisms of Spinal Injury	118
7.4	CASE 3: Rollover Crash	120
7.4.1	Crash Reconstruction III	120
7.4.2	Mechanisms of Spinal Injury	122
7.5	CASE 4: Frontal Impact	124
7.5.1	Crash Reconstruction IV	124
7.5.2	Mechanisms of Spinal Injury	126
7.6	Conclusions	129
CHAPTER 8	MODELLING OF THE SPINE FOR DYNAMIC ANALYSIS DURING VEHICLE CRASHES	131
8.1	Methods And Materials	132
8.1.1	Modelling Process	133
8.1.2	Modelling Software	133
8.1.3	Basic Assumptions	135
8.1.4	Crash Data Collection	136
8.2	Simulation Of Spinal Injury In Frontal Impact	137
8.2.1	Model of the Deformable Front Barrier (DFB)	137
8.2.2	Model of the Car in the Sagittal Plane	138
8.2.3	Model of Driver in the Sagittal Plane	142
8.2.4	Frontal Impact Model Validation	153
8.3	Simulation Of Spinal Injury In Rear Impact	158
8.4	Simulation Of Spinal Injury In Side Impact	162
8.4.1	Model of Car in the Frontal Plane	163

8.4.2	Model of Moving Deformable Barrier (MDB)	165
8.4.3	Model of Driver in the Frontal Plane	167
8.4.4	Side Impact Model Validation	172
8.5	Simulation Of Spinal Injury In Rollover	175
8.5.1	Model of Dolly	178
8.5.2	Rollover Model Validation	179
8.6	Simulation Of Spinal Injury In Collision With Camels	184
8.6.1	The Anthropometry of the Dromedary Camel	185
8.6.2	Development of the Model of the Dromedary Camel	187
8.6.3	Camel Collision Model Validation	190
8.7	Development Of Spinal Injury Of Pedestrian	198
8.7.1	Model of Passenger Car in the Pedestrian Impact Simulation	199
8.7.2	Model of Pedestrian	200
8.7.3	Cadaver Tests	202
8.7.4	Pedestrian Model Validation	204
8.8	MAIS- ΔV Estimated Curves	210
8.9	Neck Injury Causation Analysis By PVP	217
8.10	Conclusions	231
CHAPTER 9	OVERALL CONCLUSIONS AND FUTURE WORK	233
9.1	Overall Conclusions	233
9.2	Future Work	237
BIBLIOGRAPHY		238
APPENDIX A	Fieldwork Of Real-World Accidents Study	254
APPENDIX B	Nationwide Survey of SCI	267
APPENDIX C	Clinical Symptoms Of Soft Tissue Neck Injury	275

Note: Computational Simulations Samples are included on the accompanying CD-ROM



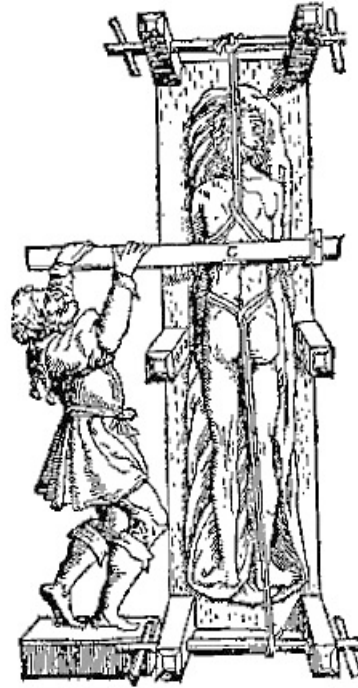
“Simplicity is the ultimate sophistication”

Leonardo da Vinci
(born 1452, died 1519)

HISTORICAL BACKGROUND

The clinical features of spinal cord injury were first described in great detail by Hippocrates in his insightful treatise *On The Articulations* believed to have been written around 400 BC*. In this work, Hippocrates Correctly described chronic paraplegia, mentions neurogenic bowel, neurogenic bladder and introduces the extension bench as a novel method for reducing spinal fractures (see figure).

In another work, Hippocrates also addressed the investigational merit of epidemiologic methodology when he stated “Whoever wishes to investigate medicine Properly should consider the greater particular nature of disease and what effects each produces, so he will not be in doubt as to treatment, or commit mistakes, as it likely to be the case provided one has not considered these matters”**. In this regard, Hippocrates has provided the philosophic substrate upon which the entire investigational component of the regional system of care for the spinal cord injured has been based.



* Adams F. The Genuine Works of Hippocrates I. William Wood and Company, NY, 1886; 156-183.

** Adams F. The Genuine Works of Hippocrates I. William Wood and Company, NY, 1886; 568-654.

List of Figures

Figure 1.1	Evolution in Road Casualties in UK and Saudi Arabia (1990-2010)	1
Figure 2.1	The human spinal column (adapted from Schmitt et al., 2004)	8
Figure 2.2	N_{ij} risk curves for neck injuries (adapted from Kleinberger et al., 1998)	13
Figure 2.3	Oblique and rear views of the MBM by Esat and Acar (2007)	22
Figure 3.1	Trends in injury and fatality rates of RTAs in Saudi Arabia (1970-2010)	33
Figure 3.2	The estimation and projection of CO in Saudi Arabia (1970-2025)	34
Figure 3.3	Comparison of fatalities per capita for the KSA and some countries	35
Figure 3.4	Fatalities per 10,000 vehicles for the KSA and some countries	36
Figure 3.5	Fatalities per billion vehicles kilometer for the KSA and other countries	36
Figure 3.6	Accident severity represented by odds ratio	37
Figure 3.7	Distribution of road accidents in Saudi Arabia by type of impact	38
Figure 3.8	Types of body injuries from road accidents in Saudi Arabia	39
Figure 3.9	Major causes of road accidents in Saudi Arabia	39
Figure 3.10	Place of death for victims from road accidents in Saudi Arabia	40
Figure 3.11	Distribution of costs for fatal and serious RTA in KSA (ADA, 2006)	41
Figure 3.12	Evolution in numbers of road fatalities, injury crashes and forecasts	43
Figure 4.1	Model design of the fieldwork study	47
Figure 4.2	Map of Riyadh showing the main districts and trauma centres	49
Figure 4.3	Classification of Collisions Severity in the Study	50
Figure 4.4	Tree classifications of collisions, vehicles, and injuries in the sample	52
Figure 4.5	Severity and type of spinal injury vs. type of collision	56
Figure 4.6	Site of spinal injury by PDoF for frontal impact	58
Figure 4.7	Site of spinal injury by PDoF for rear impact	59
Figure 4.8	Site of spinal injury by PDoF for side impact	59
Figure 4.9	Site of spinal injury by non-horizontal PDoF for rollover collisions	60
Figure 4.10	Sources of spinal injury types for occupants and pedestrians	62
Figure 4.11	Effect of maximum deformation on spinal injury in car collisions	63
Figure 4.12	Severity of spinal injury versus intrusion for car collisions	64
Figure 4.13	Distribution of occupant spinal injuries and intrusion for rollovers	65
Figure 4.14	Effect of belt wearing on outcome of spinal injury	66

Figure 4.15	Type of spinal injury versus restraint use	67
Figure 4.16	Effect of ejection on the fatality of spinal injuries in RTAs	69
Figure 4.17	Ejection risk by portal type	69
Figure 4.18	Impact classification for ejected occupants	70
Figure 4.19	Ejection type by belt use	71
Figure 4.20	Type of spinal injuries for ejected and non-ejected occupants	72
Figure 5.1	Schematic process of the spinal injury logistic modelling	77
Figure 5.2	Pearson residuals and high leverage plots for graphical assessment	84
Figure 5.3	ROC curve for various cut-off levels of ETS	85
Figure 5.4	Risk of spinal injury for occupants without seatbelt or airbag	86
Figure 5.5	Risk of spinal injury for occupants with airbag only	87
Figure 5.6	Risk of spinal injury for occupants with seatbelts and airbag	87
Figure 5.7	Probability of cervical spine injury at ETS test levels for safety legislations	88
Figure 5.8	Probability of thoracic spine injury at ETS test levels for safety legislations	89
Figure 5.9	Probability of lumbar spine injury at ETS test levels for safety legislations	89
Figure 5.10	Adjusted odds ratio of spinal injury by type of injury	90
Figure 5.11	Optimum ETS values for various crash modes by using ROC	91
Figure 6.1	Process chart of finding a verified study population	96
Figure 6.2	Prevalence of SCI per million per year by regions of Saudi Arabia	99
Figure 6.3	Incidence of SCI per million population by regions of Saudi Arabia	99
Figure 6.4	Global annual incidence of SCI per million population (Al-Shammari, 2008a)	100
Figure 6.5	Etiology of spinal cord injuries in Saudi Arabia	101
Figure 6.6	Evaluation of EMS service and the response time	102
Figure 6.7	Incidence of SCI by neurological level of injury at admission	103
Figure 6.8	Trend in cases, CR, ASR of SCI in Saudi Arabia during 2000-2010	106
Figure 7.1	Accident reconstruction process flowchart	110
Figure 7.2	Scene diagram and the contact locations of the pedestrian on the car	113
Figure 7.3	PC-Crash simulations for crash of pedestrian in Case 1	113
Figure 7.4	Radiographic images of spinal injuries for pedestrian in Case 1: <i>left</i> , axial CT scan shows Type II right occipital condyle fracture extending through skull base; <i>right</i> , plain radiograph of open-book pelvic fracture	114
Figure 7.5	Scene diagram and vehicle damage for Case 2	117
Figure 7.6	Snapshots from the PC-Crash simulations for Case 2	117

Figure 7.7	Radiographic images of spinal injuries for driver in Case 2: <i>left</i> , lateral radiograph of cervical spine showed Grade I Anterolisthesis of C6; <i>centred</i> , axial CT images revealed corticated cleft between bilateral C6 facets and spina bifida of C6; <i>right</i> , three-dimensional CT showed inferior facet fragments on side of the spondylolytic	118
Figure 7.8	Scene diagram and vehicle damage for Case 3	121
Figure 7.9	Snapshots from the PC-Crash simulations for Case 3	121
Figure 7.10	Radiographic images of spinal injuries for driver in Case 3: <i>left</i> , sagittal CT of T3 shows Anterolisthesis fracture (<i>black arrow</i>), disruption of ligament (<i>white arrow</i>); <i>right</i> , weighted MRI images of upper thoracic spine of T3 shows a compression of spinal cord with cord edema (<i>arrowheads</i>)	122
Figure 7.11	Scene diagram and vehicle damage for Case 4	125
Figure 7.12	Snapshots from the PC-crash simulation for Case 4	125
Figure 7.13	Radiographic images of spinal injuries for driver in Case 4	126
Figure 8.1	Simulation process of the whole model system	132
Figure 8.2	Window interface/tools menu of WM2D	135
Figure 8.3	Modelling setup of the frontal impact simulation	137
Figure 8.4	Modelling of the deformable front barrier	138
Figure 8.5	Geometry parameters of the Corolla car (Toyota, 2005)	139
Figure 8.6	Main components of the simulated Toyota car	140
Figure 8.7	Main components of the armchair in the model	141
Figure 8.8	Global and local coordinate systems for elements of models	142
Figure 8.9	Samples of the modelling of the spinal vertebra created by SolidWorks	143
Figure 8.10	Modelling of the head and the whole spine in the sagittal plane	144
Figure 8.11	Modelling of head and cervical spine in the sagittal plane	145
Figure 8.12	Modelling of the thoracic spine in the sagittal plane	145
Figure 8.13	Modelling of the lumbar spine and sacrum in the sagittal plane	145
Figure 8.14	Vertebral static compression strength (White and Panjabi, 1990)	150
Figure 8.15	The connections between the driver and car in the sagittal plane	152
Figure 8.16	Test setup of the NBDL volunteer experiments (Thunnissen et al., 1995), together with the model simulation setup. The four points seat belt (red color) means that driver is more rigidly fixed to the armchair than in typical car	154
Figure 8.17	NBDL experiments: Mean sled acceleration, T_1 acceleration, direction, and T_1 rotation angle in the plane of frontal impact (Thunnissen et al., 1995)	155
Figure 8.18	Kinematics of a 15g frontal simulation at successive times	156

Figure 8.19	Simulations of frontal impact compared to NBDL experiments at 15g	157
Figure 8.20	Initial configuration of rear impact model	158
Figure 8.21	Test setup of the rear sled experiments with model simulation setup	159
Figure 8.22	Simulations of human model for rear impact at successive times	160
Figure 8.23	Simulations of rear impact compared to the PMHS experiments at 12g	161
Figure 8.24	Simulation of side impact model	162
Figure 8.25	The test setup of IIHS (IIHS, 2005)	163
Figure 8.26	Model of a car with assumed masses in side impact	164
Figure 8.27	Slot joint and spring-damper elements between door and car body	164
Figure 8.28	IIHS test cart with deformable barrier element attached	165
Figure 8.29	Model of moving deformable barrier with assumed masses	166
Figure 8.30	IIHS deformable barrier element-version 4 (ESID, 1996)	166
Figure 8.31	Modelling of the head and the whole spine in the frontal plane	167
Figure 8.32	Modelling of head and cervical spine in the frontal plane	168
Figure 8.33	Modelling of the thoracic spine in the frontal plane	168
Figure 8.34	Modelling of the lumbar spine and sacrum in the frontal plane	169
Figure 8.35	Positioning of the driver inside the car in the frontal plane	171
Figure 8.36	The connections between the driver and car for side impact	171
Figure 8.37	Simulations of human model for side impact at successive times	172
Figure 8.38	Simulated response to 7g side impact for model and NBDL	173
Figure 8.39	Comparison of force application through door: (a) literature example (EEC, 2001; IIHS, 2005), (b) results of the model	174
Figure 8.40	The initial configuration for simulation of a rollover of a vehicle	175
Figure 8.41	The dolly test setup (Chou et al., 2005)	176
Figure 8.42	Car in rollover: geometry (Toyota), and model of car	177
Figure 8.43	Model of platform used in the dolly system	178
Figure 8.44	The vehicle kinematics during test of Viano and Parenteau, 2004 (upper) and simulation (lower) at successive times	180
Figure 8.45	Decelerations generated for the model and tests in SAE J2114	180
Figure 8.46	Roll angle of the SAE tests (Gopal et al., 2004) and model simulation	181
Figure 8.47	The vehicle CG height trajectory in the simulation	182
Figure 8.48	FMVSS 208 vehicle roll rate (deg/s) obtained from the laboratory tests (Parenteau et al., 2001) and the model simulations	182
Figure 8.49	FMVSS 208 driver head acceleration obtained from laboratory tests (Parenteau et al., 2001) and the model simulations	183
Figure 8.50	The typical characteristics of the camel's body (Al-Habardi, 2000)	186

Figure 8.51	Coordinates of the camel models for the sagittal plane	187
Figure 8.52	Coordinates of the camel models for the frontal plane	188
Figure 8.53	Model of camel collision in sagittal plane	189
Figure 8.54	Model of camel collision in frontal plane	189
Figure 8.55	A picture of the damaged vehicle (having CDC: 12FLEW1) showing the major contact points on the vehicle	192
Figure 8.56	Snapshots from the simulation of the Case I crash showing the contact of the camel with the vehicle	193
Figure 8.57	A picture of the damaged vehicle (having CDC: 12FLEW1) showing measurements: 1-position of first impact between the legs of animal and the vehicle, 2-second contact points due to sliding of the animal's legs over the bonnet of the vehicle, 3-third contact between the windscreen/roof and the back of the animal	196
Figure 8.58	Snapshots from the simulation of the Case II crash showing the contact of the camel with the vehicle	197
Figure 8.59	The initial configuration for the simulation of the pedestrian impact with a typical passenger car	198
Figure 8.60	Model of passenger car	199
Figure 8.61	New model of pedestrian	200
Figure 8.62	Model of limbs of pedestrian	201
Figure 8.63	Vehicle frontal geometry used cadaver tests (Ishikawa et al., 1993)	202
Figure 8.64	Sketches of pedestrian pre-impact positions (Ishikawa, 2000)	203
Figure 8.65	Pedestrian's kinematics at 40 km/h impact speed in the current 2D-Model and Linder's 3D-Model	205
Figure 8.66	Trajectories of head, pelvis, knee and foot in the experiments (Ishikawa et al., 1993) and model simulations	206
Figure 8.67	Comparison between the resultant head velocity relative to vehicle of the pedestrian in the experiments and computer simulations	207
Figure 8.68	Comparison between the resultant head acceleration of the pedestrian in the experiments and computer simulations	208
Figure 8.69	MAIS vs Delta-V for frontal impact, belted drivers, for spinal injures	210
Figure 8.70	MAIS vs Delta-V for rear impact, belted drivers, for spinal injures	210
Figure 8.71	MAIS vs Delta-V for side, belted drivers, for spinal injures	211
Figure 8.72	MAIS vs Delta-V for rollover, belted drivers, for spinal injures	211
Figure 8.73	MAIS vs Delta-V for camel impact, belted drivers, for spinal injures	212
Figure 8.74	MAIS vs impact speed for pedestrians, van cars, for spinal injures	212
Figure 8.75	MAIS vs Delta-V for frontal impact, unbelted drivers, for spinal injures	213

Figure 8.76	MAIS vs Delta-V for rear impact, unbelted drivers, for spinal injures	213
Figure 8.77	MAIS vs Delta-V for side impact, unbelted drivers, for spinal injures	214
Figure 8.78	MAIS vs Delta-V for rollover, unbelted drivers, for spinal injures	214
Figure 8.79	MAIS vs Delta-V for camel impact, unbelted drivers, for spinal injures	215
Figure 8.80	MAIS vs impact speed for pedestrians, passenger cars, for spinal injures	215
Figure 8.81	PVP for belted driver in frontal impacts	218
Figure 8.82	PVP for belted driver in rear impacts	219
Figure 8.83	PVP for belted driver in side impacts	220
Figure 8.84	PVP for belted driver in rollover collisions	221
Figure 8.85	PVP for belted driver in camel collisions	222
Figure 8.86	PVP for pedestrian impacts	223
Figure 8.87	Distribution vertebral injuries of crash data vs PVP from simulations for belted and unbelted drives at 80 km/h frontal impact	225
Figure 8.88	Distribution vertebral injuries in crash data vs PVP from simulations for belted and unbelted drives at 80 km/h rear impact	226
Figure 8.89	PVPn and MAIS based on the simulations	227
Figure 8.90	Graphical representation of N_{ij} for frontal and rear impacts	229
Figure 8.91	The Correlation between N_{ij} and PVPn for frontal and rear impacts	230

List of Tables

Table 2.1	Main functions of human spinal column	7
Table 2.2	A Revised classification of cervical spine injury	9
Table 2.3	AO fracture classification (adapted from Magerl et al., 1994)	10
Table 2.4	The force and moment intercept values used in N_{ij} (Lee et al., 2003)	13
Table 2.5	Comparison of model details for Merrill et al. (1984) and De Jager (1996)	19
Table 2.6	Overview of relevant neck multi body models	23
Table 2.7	Cervical spine FE model details as reported by various authors	26
Table 4.1	General statistics of the 552 casualties in the study	51
Table 4.2	Type of spinal injury by specific anatomic structure	55
Table 4.3	Incidence rates of spinal injury by crash type	57
Table 4.4	Injury contacts by type of collision for belted occupants	61
Table 4.5	Injury contacts by type of collision for non-belted occupants	61
Table 4.6	Incidence rates of spinal injury by restraint use	68
Table 5.1	Statistical methods used for the logistic regression model	79
Table 5.2	Hypothesis testing for proportions	80
Table 5.3	Estimated coefficients for the model variables after reduction	81
Table 5.4	The result of testing interactions	82
Table 5.5	Final model properties	83
Table 5.6	Goodness of fit statistics for the final model	83
Table 5.7	Comparison of observed and predicted outcomes	83
Table 6.1	Common mechanisms of spinal cord injury in Saudi Arabia	104
Table 6.2	Summary of Poisson model results	105
Table 7.1	Type of injuries sustained by pedestrian in Case 1	115
Table 7.2	Haddon' s matrix for pedestrian in Case 1	116
Table 7.3	Injuries of driver in Case 2	119
Table 7.4	Haddon' s matrix for Case 2	120
Table 7.5	Injuries of driver in Case 3	123
Table 7.6	Haddon' s matrix for Case 3	124
Table 7.7	Injuries of driver in Case 4	127
Table 7.8	Haddon' s matrix for Case 4	128
Table 8.1	Mechanical properties of the DFB (IIHS, 2008)	138
Table 8.2	Mechanical properties of vehicle components (Toyota, 2005)	140

Table 8.3	Mechanical properties of the armchair (Toyota, 2005)	141
Table 8.4	Moments of inertia, mass/dimensions of vertebrae (Al-Shammari et al., 2008b)	146
Table 8.5	Stiffness coefficients for the cervical spine (Yoganandan et al., 2000)	148
Table 8.6	Stiffness coefficients for the thoracic spine (White and Panjabi, 1990)	148
Table 8.7	Stiffness coefficients for the lumbar spine (Gardner-Morse and Stokes, 2004)	149
Table 8.8	Mechanical properties of driver body parts in the sagittal plane	151
Table 8.9	Stiffness and damping values for driver/car contact points	152
Table 8.10	Test conditions of the frontal and side NBDL experiments	155
Table 8.11	Test conditions for the rear end sled experiments	159
Table 8.12	Moments of inertia and mass of driver body parts in the frontal plane	170
Table 8.13	Test conditions of the side NBDL experiments	172
Table 8.14	Parameters of model's platform	179
Table 8.15	Ground properties	179
Table 8.16	Physical properties of a typical adult camel (Al-Habardi, 2000)	185
Table 8.17	Moments of inertia, and mass of parts of camel's body	188
Table 8.18	Brief description of Case I	191
Table 8.19	Injuries of the driver in Case I	191
Table 8.20	Brief description of injuries in Case II	194
Table 8.21	Injuries of the driver in Case II	195
Table 8.22	Moments of inertia and mass of main parts of the pedestrian body	201
Table 8.23	Delta-V measures for different impacts	217
Table 8.24	Statistical tests of PVP-Neck injury correlations (95% CL)	224
Table 8.25	Neck Injury Criteria results for frontal and rear impact simulation	228

Glossary of Terms

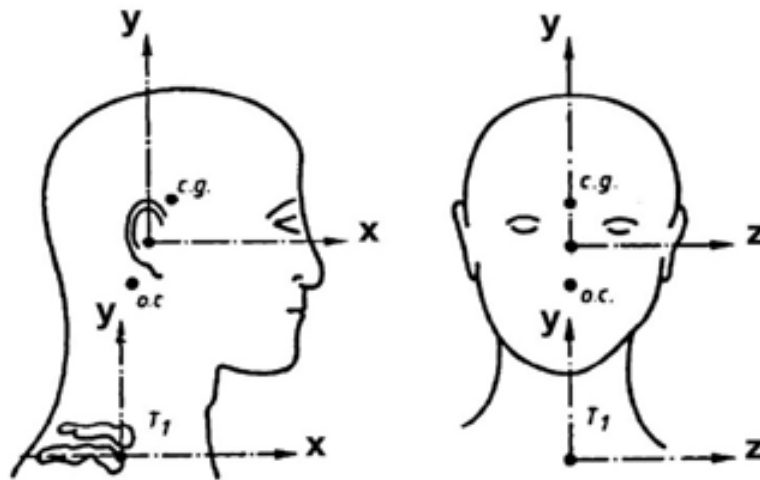
AAAM	Association for Advancement of Automotive Medicine
ADA	Arriyadh Development Authority
AIS	Abbreviated Injury Scale
AO	Classification of Thoracolumbar Fractures
ASIA	American Spinal Injury Association Scale
ATD	Anthropomorphic Test Device/Dummy
CCIS	Co-operative Crash Injury Study
CDC	Collision Deformation Classification
CDM	Continuum Damage Mechanics
CDSI	Central Department of Statistics and Information
CIREN	Crash Injury Research and Engineering Network
COC	Certificate of Confidentiality
CT	Computed Tomography
CVC	Camel Vehicle Collision
DFB	Deformable Front Barrier
ECMT	European Conference of Ministers of Transport
EEVC	European Enhanced Vehicle-Safety Committee
EMS	Emergency Medical Service
EMT	Emergency Medical Team
ESC	Electronic Stability Control
FE	Finite Element
FEM	Finite Element Model
FES	Functional Electrical Stimulation
FMVSS	Federal Motor Vehicle Safety Standards

GCS	Glasgow Coma Scale
GDP	Gross Domestic Product
GDT	General Directorate of Traffic
GIDAS	German In-Depth Accident Study
GNP	Gross National Product
H-III	Hybrid Three Anthropomorphic Test Dummy
ICD	International Classification of Diseases
IIHS	Insurance Institute for Highway Safety
IRD	Impact Reference Distance
IRTAD	International Road Traffic and Accident Database
KSA	Kingdom of Saudi Arabia
LTV	Light Truck and Van
MAIS	Maximum Abbreviated Injury Scale
MB	Multi-body
MBM	Multi Body Model
MDB	Moving Deformable Barrier
MoH	Ministry of Health
MoI	Ministry of Interior
MoT	Ministry of Transportation
MRI	Magnetic Response Imaging
MVPI	Motor Vehicle Periodic Inspection Programme
NASS	National Automotive Sampling System
NBDL	Naval Biodynamics Laboratory
NCAP	European New Car Assessment Programme
NFS	Not Further Specified
NHTSA	National Highway Traffic Safety Administration

PDoF	Principal Direction of Force
PGS	Pain Grief Suffering
PMHS	Post-Mortem Human Subject
PMP	Per Million Population
RTA	Road Traffic Accident
SAE	Society of Automotive Engineers
SCI	Spinal Cord Injury
SI	Spinal Injury
SRCS	Saudi Red Crescent Society
SUV	Sport Utility Vehicle
VRU	Vulnerable Road User
W.R.T	With Respect To
WHO	World Health Organization
WM	Working Model Software
WTP	Willingness to Pay
X-ray	Plain Film Radiography

NOMENCLATURE

Symbols



A	Resultant acceleration
AB	Airbag used
a_{rel}	Relative acceleration
ASR	Age-standardised incidence rate
b	Damping coefficient
CG	Centre of gravity
C_i	Cervical Vertebra ($i = 1 \dots 7$)
CO	Car ownership
CR	Crude incidence rate
Delta-V, ΔV	Change in velocity
d_i	The number of incidences for age group i
D_t	Number of incidences registered in year t
ETS	Equivalent Test Speed
F	Resultant force
F/P	Fatalities per 100,000 population

F/V	Fatalities per 10,000 vehicles
F/VK	Fatalities per one billion vehicle-kilometers traveled
F_Y	Axial force in y-direction
F_{YC}	Critical axial load of neck tension and compression
g	Acceleration due to gravity (9.81 m/s ²)
IMPDIR	Direction of impact
IV-NIC	Intervetebral Neck Injury Criterion
I_x	Mass moment of inertia about x-axis
I_y	Mass moment of inertia about y-axis
I_z	Mass moment of inertia about z-axis
k	Spring stiffness constant
ℓ	Length of the pig's cervical spine (0.2 m)
L_i	Lumbar Vertebra (i = 1 5)
LNL	Lower Neck Load Index
log_e	The natural logarithm to the base e
M	Bending moment
m	Mass
M_{OCZ}	Sagittal bending moment at the occipital condyle
M_{ZC}	Critical neck flexion moment at the occipital condyle
NA	Airbag not used
NB	Not Belted
NDC	Neck Displacement Criterion
NIC	Neck Injury Criteria
N_{ij}	Normalized Neck Injury Criterion
N_{km}	Neck Protection Criterion
N_t	The mid-year population in year t
P(MAIS ≥ 3)	Conditional probability of spinal injury
PI	Injury probability

PVP	Peak Virtual Power
PVPn	Peak virtual power for neck injury
q_i	The mid-year resident population for age group i
Q_i	Standard population in age group i
RESTUSE	Restraints System
r_i	Age-specific incidence rate for age group i
SB	Seat belted
SEV	Severity of spinal injury
S_i	Sacral Vertebra (i = 1 5)
SPINETYP	Type of spinal injury
S_t	Saturation level for car ownership
t	Time
T_i	Thoracic Vertebra ((i = 1 12)
V	Resultant linear velocity
V_{rel}	Relative horizontal velocity
X	X-axis
x_i	The proportion of class i of design variable
Y	Y-axis
Z	Z-axis
α	Incidence annual rate of change
B_i	Coefficients of the model parameters (i = 1 n)
θ	Angle of rotation
ω	Angular velocity

Statistics

AIC	Akaike's Information Criterion
ANOVA	One-way analysis of variance
AOR	Adjusted odds ratio
CI	Confidence interval at the 95% level
CL	Confidence level
D	Deviance test
<i>d.f</i>	Degree of freedom
e	The base of the natural logarithm (≈ 2.718)
G	Change in deviance
H_a	Alternative hypothesis test
HL	Hosmer–Lemeshow test
H₀	Null hypothesis test
LL	Lower limit of confidence
N	Total number of sample
n	Frequency number
OD	Odds ratio
P	Probability at 95% significance level
R, R²	Correlation coefficient of regression
R²_{CS}	Cox-Snell pseudo R-squared
R²_N	Nagelkerke pseudo R-squared
ROC	Receiver operator characteristic curve
Sen	Sensitivity
Spc	Specificity
U	Mann-Whitney test
UL	Upper limit of confidence
W	Wald statistic
σ, SE	Standard deviation
χ^2	Pearson chi-square test
Ψ	Relative risk
<i>g(x)</i>	The logistic function

Units

cm	Centimeter
deg	Degree
ft	Feet (1 m = 3.280840 ft)
Gb	Gigabyte (1 Gb = 10 ⁹ bytes)
h	Hour
Ibf	Pound force (1 N ≈ 0.224809 Ibf)
in	Inch (1 in = 2.54 cm)
k	Kilo
kg	Kilogram
km	Kilometer
m	Meter
M	Mega
min	Minute
mm	Millimeter
mph	Mile per hour (1 mph = 1.609344 km/h)
ms	Millisecond (1 ms = 10 ⁻³ s)
N	Newton
pa	Pascal
rad	Radian (1 rad = 57.2957 degrees)
s	Second

Superscript

<i>o</i>	<i>Degree</i>
"	Inch (1 in = 2.54 cm)
²	Square
³	Cubic

Subscript

g	Gravity
OC	Occipital condyle
t	Transitional
X	About x-axis
Y	About y-axis
Z	About z-axis
Φ	Rotational

CHAPTER 1

INTRODUCTION

1.1 STATEMENT OF RESEARCH PROBLEM

Road Traffic Accidents (RTAs) account for a large proportion of injuries and early deaths in the world. The road accident deaths are projected to increase from 1.3 million in 2004 to 2.4 million in 2030 (WHO, 2008). Today's, there are more than 3,000 die daily as a result of road crashes while 140,000 people are injured and about 15,000 are disabled for life.

Like other countries in the Middle East, RTAs are increasingly being recognized as a growing public health, social and economic problem in the Kingdom of Saudi Arabia (KSA).

Figure 1.1 shows that there has been an overall downward trend in road accident deaths in highly-motorised countries such as the UK during the late 1990s. In contrast, fatality rates of RTAs have risen steadily in Saudi Arabia (Hassan and Al-Shammari, 2009).

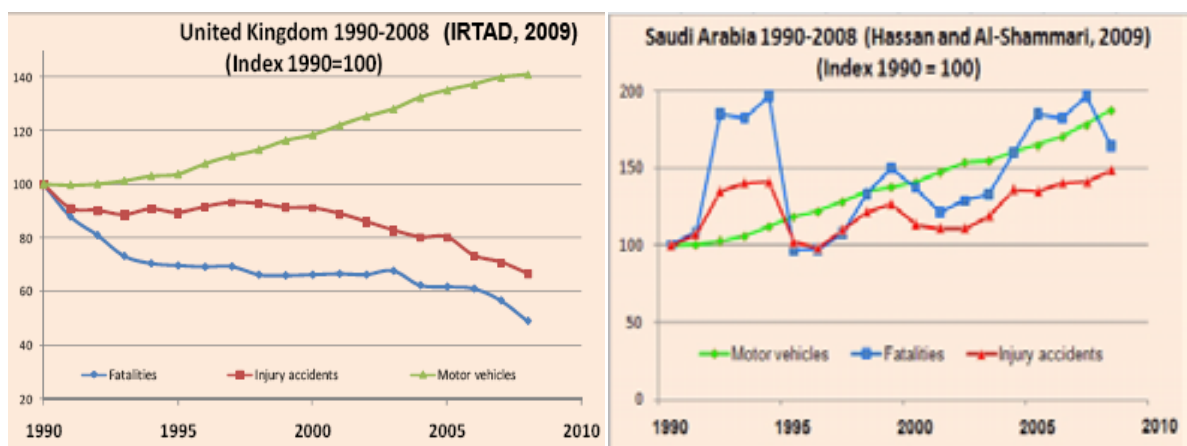


Figure 1.1: Evolution in road casualties in UK and Saudi Arabia (1990-2010)

This increase in vehicle crashes in Saudi Arabia may to some extent be attributed to increase in the number of cars per family, increase in the number of youths driving cars, and lack of respect of traffic regulations among young population (Bendak, 2005).

In Saudi Arabia, an estimated loss of between 2.2% and 4.7% of the **Gross National Product (GNP)** has been suggested by some researchers due to road accidents. Also, the cost of RTAs in the Kingdom is estimated to be 1.7 times greater than in the USA. It is thus a drain on the health as well as economic resources on an individual (Al-Ghamdi, 2003). In most developed countries, the problem of RTAs has attracted increasing research and safety interventions resulting in a reduction of the size of the problem in many of these countries.

Contrarily, although Saudi Arabia, have significantly higher rates of morbidity and mortality as well as traumatic **Spinal Cord Injuries (SCIs)** due to RTAs, no attempt has so far been made to study the gravity of the problem caused by spinal injuries either on a regional or at the national level (Nafal et al., 1996). An essential factor in the prevention, management and analysis of traffic accidents is understanding the demographic characteristics of the victims of such accidents. So far, the epidemiology of spinal injuries in Saudi Arabia has not been studied. Furthermore, there are no national crashes database and neuro-trauma centers serve as a database registry. This lack of data is an obstacle in analyzing such injuries and in developing measures that would mitigate those life threatening injuries.

This study, therefore, represents an attempt to fill some of the gaps in the information related to the principal characteristics of spinal injuries of vehicle crashes in the Kingdom. It aims to develop a methodology to collect data on RTAs, study their main causes, to study causes of SCIs in RTAs and to propose suitable engineering and management measures to minimize the existing consequences of spinal injuries in Saudi Arabia.

1.2 RESEARCH PURPOSE AND PLAN

The main purpose of this thesis is to understand the problem of spinal injuries from traffic accidents in Saudi Arabia and offer suggestions for its mitigation. The study involves collection data from real world traffic accidents in the Kingdom which could be analyzed and measures developed to mitigate these injuries, or even develop means of preventing such injuries. The methodology of this type of data collection is in accordance with standard international procedures and will be detailed in subsequent chapters. It is a study designed to improve the knowledge-base of the biomechanical characteristics of the most frequently injured spine regions during impacts. The study will also show how the severity of such injuries can be reduced. The crash characteristics which influence spinal injury severity will be explored in-depth so that biomechanical references of such injuries can be constructed.

In pursuit of main aim, a suite of four sub-studies will be conducted and the results summarised as in the following:

1. Study of RTAs: The primary purpose of this investigation is to gain insight into causes and factors which directly or indirectly lead to the occurrence of spinal injuries in Saudi Arabia and evaluating the management of road safety within the Saudi Arabia (**Chapter 3**). The data in this study were based on information obtained from insurance companies and governmental agencies.
2. Epidemiology of Spinal Injuries: The second objective of this research is an in-depth study of spinal injuries in vehicle crashes (**Chapter 4**). This analysis is aimed at identifying mechanisms of spinal injuries, various characteristics of occupants and type of collisions, and identifying which injury and body region requires further

research. A study based on data collected from real world crashes in Riyadh, Saudi Arabia during November 2004 to November 2008 is presented. The crash factors that might affect the severity of the spinal injury were identified using logistic modelling technique (**Chapter 5**). Finally, the consequences of spinal cord injuries and etiology of spinal casualties are also investigated in **Chapter 6**.

3. Reconstruction of Crashes: In order to understand the dynamics of a crash, crash reconstruction techniques are used worldwide. Reconstruction of a crash requires in depth data about the crash. Scientific reasoning then allows the dynamics to be reconstructed and correlated with the data to give an understanding of how the crash happened. Safety measures can then be designed accordingly. **Chapter 7** presents case studies done on a set of typical crashes in Saudi Arabia and demonstrates how this technology can be used in the context of crashes in the Kingdom.
4. Computer Simulations of crashes: In order to understand the behaviour of the human body during car crashes mathematical modelling, using the latest numerical methods has been done. For this purpose, six dynamic models were created in Working Model 2D to simulate spinal injuries of driver in situations similar to real world accidents from head-on, rear collisions, rollover and side impact car accidents, collision with camels, and pedestrian impacts. Results of numerical simulations allowed qualitative estimates of the most dangerous situations of spinal injuries during these types of accidents (**Chapter 8**).

1.3 SIGNIFICANCE OF THE STUDY

This study is original and makes an important contribution to knowledge, in that so far little is known about the causes of road accidents in Saudi Arabia. Information about causes of road accidents in the country is vital, as a basis for improving the traffic system and its safety.

The information provided by this study will, it is hoped, provide valuable insights into the nature of road safety problems in the Kingdom. In so doing, it will provide a basis on which planners and policy makers can consider the Kingdom's future needs as regards road engineering, driver education and so forth, and make the necessary provisions.

It is also necessary to carefully assess which appropriate interventions that can be implemented are most likely to be effective in improving recovery or survival among persons with life-threatening injuries occurred in vehicle crashes. These interventions could be in road design, vehicle design, infrastructure or even in trauma care systems. The epidemiological studies in this research will reveal attention areas like black spots, causes of accident, what time of the year and day and night, nature of injury, time lag between the accident and medical aid, to name a few. Availability of these figures will greatly help the health authorities to take necessary measures to reduce the incidence of accident by allocating fully equipped emergency mobile service to provide immediate and optimal care at the site, during mobilization and immediately after arrival care at the hospital. Reduction in injury is expected to reduce the disability and mortality to a great extent. The data obtained from this study will be of great value to establish guidelines for management of SCI casualties, training and formulating the recommendations for establishment of national neurotrauma centres, registry of SCI and to develop educational programs for enhancing public awareness about SCI.

CHAPTER 2

LITERATURE REVIEW ON-STATE-OF-THE-ART RESEARCH

There are few physical disabilities that are as complex and challenging as spinal injury. Vehicle crashes are considered to be the main cause of traumatic spinal injury. There has been considerable work done on understanding the behavior of the spine in impact conditions, understanding the mechanisms of spinal injury, and estimating its likelihood in different crash scenarios. This chapter gives a comprehensive survey of these aspects.

If the characteristics of the spinal injury in vehicle collisions are to be investigated, the biomechanical background of the spine must be represented in detail. **Section 2.1** describes the anatomy of the spine, and the common mechanisms of spinal injuries. The incidence, prevalence, and characteristics of spinal injury vary considerably from one country to another. Such variations are even found in many studies conducted in the same country. There was no available accurate information on SCI in Saudi Arabia. **Section 2.2** provides up to date literature review of studies on the crash factors related to spinal injuries.

Section 2.3 includes a review of the classifications of human spine models as well as a broad literature survey on numerous prominent models developed. The final classification approach used in this thesis serves for understanding the mainstream of spinal modelling and helps to demonstrate the rapid developments and improvements within each methodology.

2.1 BIOMECHANICS OF SPINAL INJURY

Spinal injuries can be categorized as a sprain, strain, disk disruption, vertebral fracture, or vertebral dislocation. Any one of the bony injuries may or may not involve the **Spinal Cord Injury (SCI)**. In order to understand the biomechanical aspects of spine trauma, it is essential to understand the basic anatomy, the mechanisms of injury, and the injury rank scales, as well as the crash tests and neck injury criteria. The detailed description of the anatomy and physiology can be found in the standard textbooks (e.g. Nahum, and Melvin, 2002)

2.1.1 Anatomy of the Spine

The spinal column is the principal load-bearing structure of the head and the torso. Despite its great strength and ability to serve a variety of purposes, it forms an intricately designed and delicate mechanical unit (Backaitis, 1995), see **Table 2.1**.

Table 2.1: Main functions of human spinal column

Function	Elements
Protection	<ul style="list-style-type: none">• Spinal Cord and Nerve Roots• Many internal organs
Bases for Attachment	<ul style="list-style-type: none">• Ligaments• Tendons• Muscles
Structural Support	<ul style="list-style-type: none">• Head, shoulders, chest• Connects upper and lower body• Balance and weight distribution
Flexibility and Mobility	<ul style="list-style-type: none">• Flexion (forward bending)• Extension (backward bending)• Side bending (left and right)• Rotation (left and right)• Combination of above

The spine is divided into *cervical*, *thoracic*, *lumbar*, and *sacral* regions. The spine is a complex structure with hard and soft tissue constituents. The bones of the spine, the *vertebrae*, are the hard elements of the structure. They also protect the vulnerable spinal cord and emanating nerves. The structure and function of the vertebrae vary somewhat along the length of the spine. The seven *cervical vertebrae* of the neck provide maximum flexibility and range of motion of head. As shown in **Figure 2.1**, these vertebrae are designated C1 through C7 in the cranial-to-caudal direction. The 12 *thoracic vertebrae* (T1 through T12) support the ribs and the organs that hang from them. In the thoracic region, the vertebral bodies are optimized for a combination of structural support and flexibility. The five *lumbar vertebrae* (L1 -L5) are subjected to the highest forces and moments of the spine (Schmitt et al., 2004). Consequently, they are largest and strongest of the vertebral bodies. These bones are optimized for structural support as opposed to flexibility. The *sacrum* attaches the spine (L5-S1) to the pelvis.

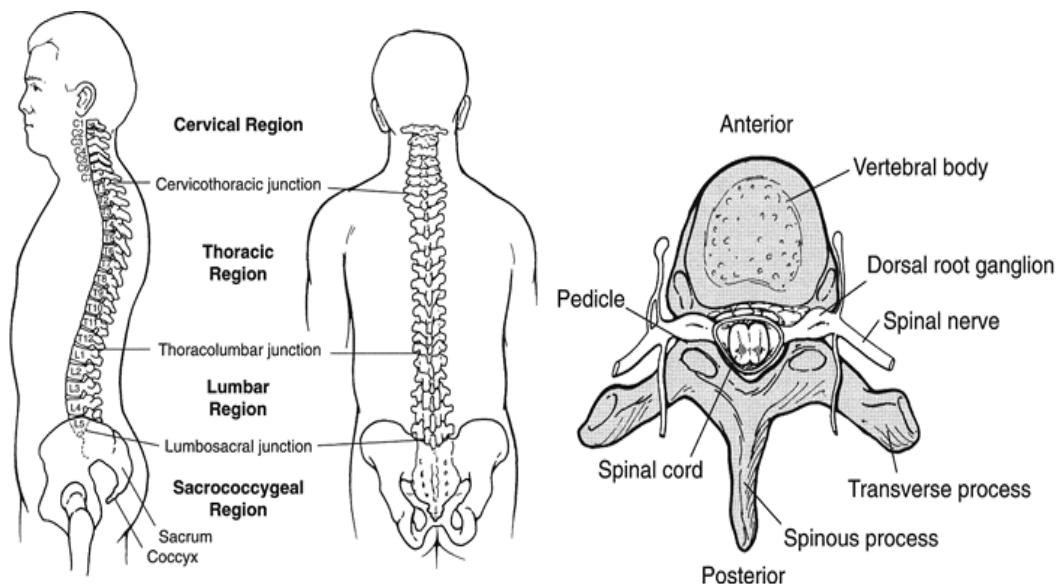


Figure 2.1: The human spinal column (adapted from Schmitt et al., 2004)

2.1.2 Mechanisms of Spinal Injury

While several classification systems for cervical spine injury co-exist, none of them has gained uniform acceptance among researchers or clinicians. **Table 2.2** results in a mapping of cervical injuries to classes (Myers and Winkelstein, 1995).

The thoracolumbar spinal injuries are usually specified by the **AO Classification** (Magerl et al., 1994), as provided in **Table 2.3**.

Table 2.2: A Revised classification of cervical spine injury

<i>Compression</i>	<i>Extension moment</i>
Jefferson fracture	Hangman's fracture
Multipart Atlas fracture	Anterior longitudinal ligamentous rupture
Multipart vertebral body Fracture	Disk rupture
<i>Compression flexion</i>	Horizontal fracture of vertebral body
Burst fracture	<i>Torsion</i>
Wedge compression fracture	Atlantoaxial rotary dislocation
<i>Compression extension</i>	Atlantoaxial uniside facet dislocation
Posterior element fractures	<i>Horizontal shear</i>
<i>Tension</i>	Transverse ligament rupture
Occipitoatlantal dislocation	<i>Multiple mechanisms</i>
<i>Tension extension</i>	Odontoid fracture
Hangman's fracture	Teardrop fracture
<i>Flexion moment</i>	Clay shoveler's fracture
Hyperflexion sprain	
Biside facet dislocation	
Uniside facet dislocation	

Table 2.3: AO fracture classification (adapted from Magerl et al., 1994)

Type A: vertebral body compression		Type B: anterior and posterior element injury with distraction		Type C: anterior and posterior element injury with rotation	
A1. A1.1 A1.2 A1.2.1 A1.2.2 A1.2.3	Impaction fractures Endplate impaction Wedge impaction fractures Superior wedge impaction Lateral wedge impaction fracture Inferior wedge impaction fracture	B1. B1.1 B1.1.1 B1.1.2 B1.1.3 B1.2 B1.2.1 B1.2.2 B1.2.3	Posterior disruption predominantly ligamentous (flexion-distraction injury) With transverse disruption of the disc Flexion-subluxation Anterior dislocation Flexion-subluxation / anterior dislocation with fracture of the articular processes. With Type A fracture of the vertebral body Flexion-subluxation +Type A fracture Anterior dislocation +Type A fracture Flexion- subluxation / anterior dislocation with fracture of the articular processes + Type A fracture	C1. C1.1 C1.2 C1.2.1 C1.2.2 C1.2.3 C1.2.4 C1.3 C1.3.1 C1.3.2 C1.3.3	Type A injuries with rotation (compression injuries with rotation) Rotational wedge fracture Rotational split fractures Rotational sagittal split fracture Rotational coronal split fracture Rotational pincer fracture Vertebral body separation Rotational burst fractures Incomplete rotational burst fractures Rotational burst-split fracture Complete rotational burst fracture
A2. A2.1 A2.2 A2.3	Split fractures Sagittal split fracture Coronal split fracture Pincer fracture	B2. B2.1 B2.2 B2.2.1 B2.2.2 B2.3 B2.3.1 B2.3.2	Posterior disruption predominantly osseous (flexion distraction injury) Transverse bicolomns fracture With transverse disruption of the disc Disruption through the pedicle and disc Disruption through the pars interarticularis and disc (flexion-spondylolysis) With Type A fracture of the vertebral body Fracture through the pedicle + Type A fracture Fracture through the pars interarticularis (flexion-spondylolysis) + Type A fracture	C2. C2.1 C2.1.1 C2.1.2 C2.1.3 C2.1.4 C2.1.5 C2.1.6 C2.1.7 C2.2 C2.2.1 C2.2.2 C2.2.3 C2.3 C2.3.1 C2.3.2 C2.3.3	Type B injuries with rotation B1 injuries with rotation (flexion distraction injuries with rotation) Rotational flexion subluxation Rotational flexion subluxation with unilateral articular process fracture Unilateral dislocation Rotational anterior dislocation without / with fracture of articular processes Rotational flexion subluxation without / with unilateral articular process + Type A fracture Unilateral dislocation + Type A fracture Rotational anterior dislocation without / with fracture of articular processes + Type A fracture B2 injuries with rotation (flexion distraction injuries with rotation) Rotational transverse bicolomn fracture Unilateral flexion spondylolysis with disruption of the disc Unilateral flexion spondylolysis + Type A fracture B3 injuries with rotation (hyperextension-shear injuries with rotation) Rotational hyperextension subluxation without / with fracture of posterior vertebral elements Unilateral hyperextension- spondylolysis Posterior dislocation with rotation
A3. A3.1 A3.1.1 A3.1.2 A3.1.3 A3.2 A3.2.1 A3.2.2 A3.2.3 A3.3 A3.3.1 A3.3.2 A.3.3.3	Burst fractures Incomplete burst fracture Superior incomplete burst fracture Lateral incomplete burst fracture Inferior incomplete burst fracture Burst split fracture Superior burst split fracture Lateral burst split fracture Inferior burst split fracture Complete burst fracture Pincer burst fracture Complete flexion burst fracture Complete axial burst fracture	B3. B3.1 B3.1.1 B3.1.2 B3.2 B3.3	Anterior disruption through the disc (hyperextension shear injury) Hyperextension subluxations Without injury of the posterior column With injury of the posterior column Hyperextension spondylosis Posterior dislocation	C3. C3.1 C3.2	Rotational-shear injuries Slice fracture Oblique fracture

2.2 NECK INJURY CRASH-TEST CRITERIA

With respect to neck injury, the Neck Injury Criteria (**NIC**) (Bostrom et al., 1996), N_{ij} (Klinch et al., 1996; Kleinberger et al., 1998), and N_{km} (Schmitt et al., 2001) are often used. Other proposed criteria are Intervetebraal Neck Injury Criterion (**IV-NIC**) (Panjabi et al., 1999), Neck Displacement Criterion (**NDC**) (Viano and Davidsson, 2001), Lower Neck Load Index (**LNL**) (Heitplatz et al., 2003), and Peak Virtual Power (**PVP**) (Sturgess, 2001).

A general limit of such injury criteria is the fact that they can be determined under controlled conditions, i.e. in experiments. Real world crashes cannot be assessed retrospectively through those criteria, because there is no possibility to measure the neck loads in the real world. With respect to soft tissue neck injuries, this poses a problem as those cases often result in legal procedures requiring an assessment by an expert witness to clarify the likeliness whether the injury claimed is causally linked to an accident. Therefore special schemes were developed to biomechanically assess this causality.

In this Section only **NIC**, N_{ij} and **PVP** are explained with respect to the main purposes of the present study. More details about other criteria can be found in the literature.

2.2.1 Neck Injury Criterion (**NIC**)

The Neck Injury Criterion (**NIC**) was developed by Bostrom et al. (1996). The definition of the **NIC** as a function of time was validated based on animal experiments. The **NIC** expression is given in Eq. (2.1) as

$$\text{NIC}(t) = a_{\text{rel}}(t) \times \ell + v_{\text{rel}}(t)^2 < 15 \text{ m}^2 / \text{s}^2 \quad (2.1)$$

Where NIC stands for Neck Injury Criterion, a_{rel} is the relative acceleration difference between C1-C7 in gs ($g = 9.81 \text{ m} / \text{s}^2$, ℓ is the length of the pig's cervical spine (0.2 m or 7.8 in) and v_{rel} is the relative horizontal velocity of neck C1-C7 in m/s in sled or car crash. The threshold value above which a significant risk of sustaining minor (AIS 1) neck injury is assumed to be inherent was set to be $15 \text{ m}^2 / \text{s}^2$ (Schmitt et. al. 2004).

2.2.2 Normalized Neck Injury Criterion (N_{ij})

Klinch et al. (1996) and Kleinberger et al. (1998) proposed this US-NHTSA criterion to assess neck injury. Recently, the N_{ij} criterion was included as part of FMVSS 208. The N_{ij} criterion developed implies a linear combination of the axial forces and the flexion/extension bending moment, both normalized by critical intercept values:

$$N_{ij} = \frac{F_Y}{F_{YC}} + \frac{M_{OCZ}}{M_{ZC}} \quad (2.2)$$

Where N_{ij} is the Normalized Neck Injury Criteria, F_Y and M_{OCZ} are the axial force and the sagittal bending moment at the occipital condyle, respectively. F_{YC} indicates the critical axial load values of neck tension and compression, and M_{ZC} indicates the critical values of neck flexion moment at the occipital condyle. The intercept values of M_{ZC} and F_{YC} in new FMVSS 208 are as shown in **Table 2.4**.

Table 2.4: The force and moment intercept values used in N_{ij} (Lee et al., 2003)

Dummy	M_{ZC} (Flexion/Extension)	F_{YC} (Compression/Tension)
	[Nm]	[N]
H-III 50%	310/ 135	6160/ 6806
H-III 5%	155/ 67	3880/ 4287
H-III 5%*	155/ 61	3880/ 3880
H-III 6 year	93/ 37	2800/ 2800
H-III 3 year	68/ 27	2120/ 2120

* Out of position

Currently there is very little correlation between neck injuries received by occupants in real accidents and this calculated injury criteria. The dummy neck loads (from the Hybrid III) obtained from New Car Assessment Program (NCAP) testing were compared with NASS accident, and data incidence of neck injury in the filed accident data. Kleinberger et al. (1998) proposed an AIS 5+ neck injury risk curves for human in frontal impacts, **Figure 2.2**.

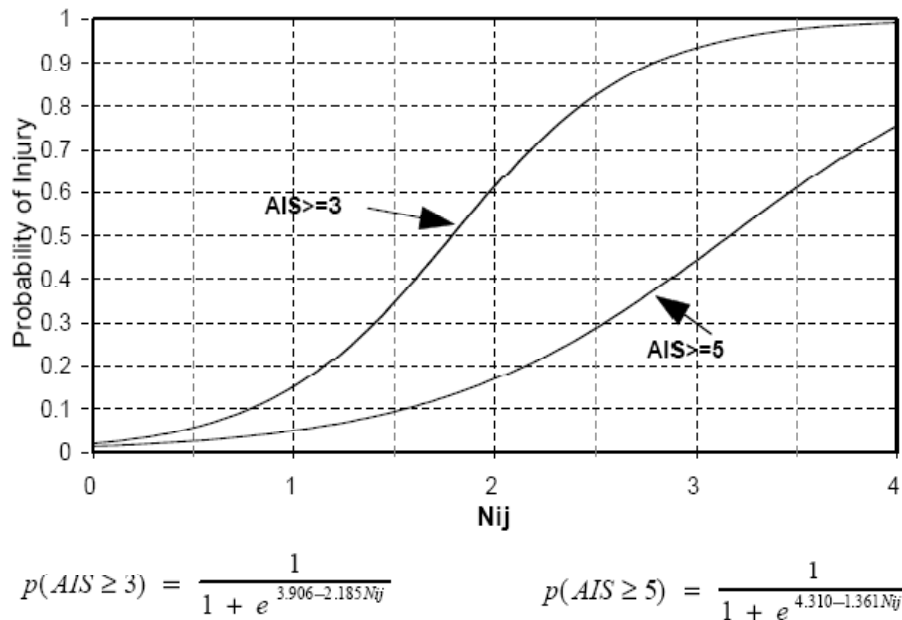


Figure 2.2: N_{ij} risk curves for neck injuries (adapted from Kleinberger et al., 1998)

2.2.3 Peak Virtual Power (PVP)

The concept of **Peak Virtual Power (PVP)** or the maximum rate of Entropy production was first introduced by Sturgess (2001) as a universal injury criterion in the following form:

$$PVP = \frac{\partial \hat{U}}{\partial t} = F \cdot \hat{V} = F \cdot V \quad (2.3)$$

Where $\frac{\partial \hat{U}}{\partial t}$ is the specific virtual power per unit mass, F is the force, and V is the impact velocity. For a particular impact, V is also the change in the velocity (ΔV).

In the research of Sturgess (2002a), it was assumed that injuries in Impact Trauma can be modeled as mechanical dissipative processes, and the formalism of **Continuum Damage Mechanics (CDM)** based on Irreversible Thermodynamics was applied to Impact Trauma. An objective, self-consistent injury criterion of “Peak Virtual Power” was derived.

In the research of Sturgess et al. (2001), it has shown that the PVP can model the severity of injury at the micro, and macro scales, and can model neck impact injuries as well, if not better than, NIC. Other scientifically valid injury criteria such as the “Viscous Criterion” (Viano and Lau, 1986), and “Margulies and Thibault” criterion (Margulies and Thibault, 1989) were also shown to be derivable from PVP, and taken as further confirmation of the concept of PVP as a universal injury criterion.

It was shown that PVP predicted the severity of injury, measured on AIS scale, in around 90% of cases for all types of injury to all body regions (brain, skull, thorax, spine, upper and lower extremities) for car occupants from Co-operative Crash Injury Study in the UK (CCIS – Phase 7) and NASS-CDC Databases. Values of the Correlation Coefficient (R^2) which are greater than 0.98 were routinely observed in that research (Sturgess, 2002a).

It was shown that in general the Lower Bound of severity of injury is proportional to ΔV^3 or (ETS^3) , for restrained vehicle occupants according to the form in Eq. (2.4):

$$\begin{aligned} \text{Severity of Injury} &\propto AIS \propto PI\% \propto PVP \\ &\propto aV_{max} \propto \hat{a} \propto a^2 \Delta t \propto V^3 \propto \Delta V^3 \text{ or } (ETS^3) \end{aligned} \quad (2.4)$$

For unrestrained occupants, the Upper Bound is proportional to ΔV^2 or (ETS^2) , Eq.(2.5):

$$AIS \propto PVP \propto aV_{max} \propto \hat{a} \propto a^2 \Delta t \propto V^2 \propto \Delta V^2 \text{ or } (ETS^2) \quad (2.5)$$

Where *AIS* is the **A**bbreviated **I**njury **S**cale, *a* is the acceleration, *ETS* is the **E**quivalent **T**est **S**peed and *PI%* is the probability of injury.

Sturgess et al. (2002b) have shown that the concept of Peak Virtual Power (PVP) as an injury criterion can predict injuries to pedestrians, and that the injury severity is proportional to V^2 , for slight injuries, and V^3 for serious and fatal injuries. Simulations using MADYMO for head and chest injuries showed that, to a first degree of approximation, the influence of vehicle contact stiffness on the acceleration of the body is approximately linear.

In a recent PhD work, Jiang and Sturgess (2008) developed a reconstruction simulation for head injury in rollover real world accidents. The MAIS results achieved from the “Master PVP Curve” indicates the head injury severity well which shows the PVP is a good indicator of head injury from both macro and micro viewpoints. It was concluded that PVP could be a suitable candidate for an objective universal injury criterion.

2.3 FIELD STUDIES OF CRASH FACTORS RELATED TO SPINAL INJURIES

There have been many studies on the biomechanics of spinal injury as a result of automobile crashes (White and Panjabi, 1990; Huelke et al., 1986; McElhaney and Myers, 1993; and others) and papers describing case studies of spinal injuries sustained in such crashes (Huelke et al., 1993; O'Connor, 2002; Thurman et al., 1995 and Hassan et al., 1997 and others). An earlier study of 30 RTA related SCI cases sought to identify various risk factors of collision type, driver impairment, restraint use, and road conditions, but reported only significant risks for unrestrained occupants (Cushman et al., 1991).

While there have been many studies on the biomechanics of spinal injury, to date, very few studies present the epidemiology of spinal injuries in detail. Hassan et al. (1996a) have studied 290 cases of spinal injury and presented their epidemiology. Yoganandan et al. (1989) have primarily looked at cervical injuries and studied the biomechanics of the injury. Variations due to age, gender and many other factors have not been covered.

Recently, Smith et al. (2005) have examined the effect of change in velocity (ΔV) and energy dissipation on impact, above and below the test levels for federal vehicle crash safety standards, on the incidence of spine fractures, spinal cord injury, spine fracture mortality and the associated injury patterns in frontal and lateral vehicle crashes.

Understanding the factors that contribute to spinal injuries is paramount in injury prevention. Thus, in spite of their importance and the very large burden they can cause to the society, spinal injuries and their relationship with RTAs has not been studied in detail.

In conclusion, unlike previous research there is a need to study all RTA-related risk factors with a relatively large sample of study subjects.

2.4 COMPUTATIONAL MODELS OF THE HUMAN SPINE

There are numerous human spine models in the literature that were developed and widely used by researchers who investigated the biomechanics of spinal injuries or provided an ergonomic environment for the human spine. Maquet (1992), reports that biomechanical modelling of the human spine and investigating the effects of spinal loadings dates back to the 17th century. If a computational model of the human spine is to be used for injury analysis the mechanical behavior of the spine and its components needs to be represented. A successful model must be able to reproduce the normal kinematics of the spine and predict its behavior when subjected to abnormal loads.

The human spine is categorized into four main areas, namely cervical (head-neck region), thorax, lumbar, sacral. Different computational models representing each of spinal regions are reported in literature. These computational human spine models are categorized into four groups according to the modelling technique used:

1. Multi-Body (MB)/ Discrete Parameter Models
2. Finite Element (FE) Models
3. Hybrid Multi-body/Finite Element Models

Continuum and two pivot models can only represent the spine in a simplified form whereas the multi body/discrete parameter models and finite element models can better represent the complex anatomical structure and mechanical behavior of the cervical spine. In the following sections, all of these groups are investigated, reflecting the developments in each category for each spinal region. First a brief overview of modelling software is presented followed by a review of multi-body and finite elements models.

2.4.1 Multi-Body Models (MBMs)

Multibody or discrete parameter models allow for a more detailed representation of the spine, in which rigid bodies with corresponding mass and inertial properties idealize the head and vertebrae. Mass-less spring and damper elements connected between adjacent rigid bodies represent the lumped characteristics of the intervertebral discs and surrounding soft tissues, such as ligaments, facet joints and sometimes muscles. Rigid bodies represent bony elements of the spine while connecting tissues are represented by connections of springs and dampers. Multi-body/discrete parameter models have the ability to simulate the global and local kinematics and kinetics of the human spine.

2.4.1.1 Cervical Spine Multibody Models



Williams and Belytschko (1983) developed a three-dimensional model of the head and neck. The vertebrae C1-C7 are modeled as rigid bodies interconnected by deformable elements representing the intervertebral disks, facet joints, ligaments and muscles. The model consisted of four different types of deformable elements:

1. Spring Elements; with stiffness along the axis joining the two elements they connect.
2. Beam Elements; with axial bending and torsional stiffness.
3. Muscle Elements; similar to spring elements but with the axial force being independent to the neck elongation to mimic the contraction of the muscle.
4. Pentahedral Facet Elements; special element developed to model the articular facet joint that has axial and shear stiffness.

Twenty-two muscle groups of the neck were included with the force from each muscle group being estimated from the product of its stress and cross-sectional area. The model was the first to include both passive and active properties of muscles.

Simulations for impact situations were performed with and without muscle activity to see the effects of the stretch-reflex response during impact. They showed that with frontal impact the compression, shear forces and bending moments in the disk were reduced with muscle activity but under side loading the stretch-reflex response increased compressive and shear force in the disk. This difference in response under side and frontal impact emphasizes the importance of modelling the head and neck in 3D for impact studies.

Table 2.5: Comparison of model details for Merrill et al. (1984) and De Jager (1996)

Parameters	Model Details	
Author	Merill, Goldsmith and Deng (1984)	De Jager (1996)
Software	Unknown	MADYMO
Head	Rigid	Rigid
Vertebrae	Rigid	Rigid
Occiput-Atlas-Axis	C1-C2 2D ball and socket joint	Hyper- ellipsoid frictionless contact
Discs	Lumped into intervertebral joint	Linear viscoelastic Kelvin elements
Ligaments	Lumped into intervertebral joint	Non-linear viscoelastic
Facet joints	Frictionless ball on plane	Hyper-ellipsoid frictionless contact
Muscles	7 passive linear elements	14 Hill type muscle elements
Validation	Volunteer and physical model tests	15g frontal, 7g side impacts (NBDL volunteer data)
Application	2D flexion whiplash, 3D side impact	Frontal and side impacts
Figure		

The two dimensional lumped parameter model developed by Reber and Goldsmith (1979) was extended to three dimensions by Merrill et al. (1984), shown in **Table 2.5**. The model was further improved by Deng and Goldsmith (1987). The resulting model consisted of head, neck and upper torso (C1 down to T2) with fifteen pairs of passive neck muscles. The mechanical behaviour of each individual spinal unit was lumped into a single intervertebral joint with a linear stiffness matrix characterising the segmental response.

Following the work of Deng and Goldsmith, de Jager (1996) implemented their model in the multibody software package Madymo developing a sophisticated model of the head and cervical spine. The new model consisted of head, neck (C1-C7) and the first thoracic vertebrae (T1). Summary and modelling comparison is listed in **Table 2.5**.

Recently van der Horst (1997, 2002) has made further improvements to the de Jager model by increasing the geometric detail of the vertebrae, updating the material properties of the soft tissues and modelling the neck muscles in greater detail. Apart from the material properties advancements, inclusion of contact between spinal processes was a new feature of the model. Ligaments in the model were represented by 2D non-linear viscoelastic spring-damper elements producing force in tension only. Sixteen cervical muscle groups sub-divided into 68 muscle elements were modeled with improved geometry and lines of action curving around the cervical vertebrae. The Hill type muscle model, as used by De Jager and available in the Madymo software was used to describe active and passive muscle behavior.

Winkelstein and Myers (2002) presented a study, which tries to quantify flexibility relationships for the cervical spine segments and investigate the nonlinear components of the flexibility matrix that forms the basis of multibody dynamics models.

Van Lopik and Acar (2002) developed and validated a 3D MBM of the human head and neck using the dynamic simulation package VisualNastran 4D. Van Lopik and Acar (2004) improved the previous model comprising 19 muscle groups of the head and neck. Muscle mechanics were governed by the external software Virtual Muscle 3.1.5 that runs within Matlab and Simulink providing both passive and active muscle behaviour. The effect of passive and fully active muscle behaviour has been investigated and validated against experimental data, yielding good agreement for both impact directions.

Van Lopik and Acar (2004) further validated the head-neck model by checking the accuracy of the individual components, motion segments and the model as a whole under different loading conditions. They claimed that the model had successfully reproduced the characteristic 'whiplash' motion and resulting head and vertebral rotations and displacements seen in the experimental results for rear impact accelerations. Model responses to 15g frontal impact and 7g side impact situations with 100% active musculature.

A head-neck computer model was built by Stemper et al. (2004) and comprehensively validated over a range of rear-impact velocities using experiments conducted by the same group of authors in the same laboratory. The validated model was used to investigate the effects of important kinematical factors in whiplash injury assessment.

2.4.1.2 Lumbar Spine Multibody Models

De Zee et al. (2003) developed a multi-body human spine model partially by using the AnyBody Modelling System, written in so-called AnyScript, which is a declarative, object-oriented language for development of multi-body dynamics models, and particularly for models of the musculoskeletal system. The model was incomplete in terms of including all

lumbar muscle groups and it was solely constructed around the lumbar region. Ishikawa. et al. (2005) developed a musculoskeletal multi-body spine model in order to perform Functional Electrical Stimulation (FES) effectively as well as to simulate spinal motion and analyse stress distribution within the vertebra. The muscles were joined to the skeletal model by using 3D analysis software Visual Nastran 4D. Intervertebral discs and ligaments were represented by spring-damper elements. Recently, Esat and Acar (2007) developed a novel MB model of the whole human spine to simulate a ligamentous cervical spine undergoing whiplash trauma. The MB model devoid of muscles was validated against test results, while most of the simulation results and model predictions showed good agreement with experiments, **Figure 2.3**.

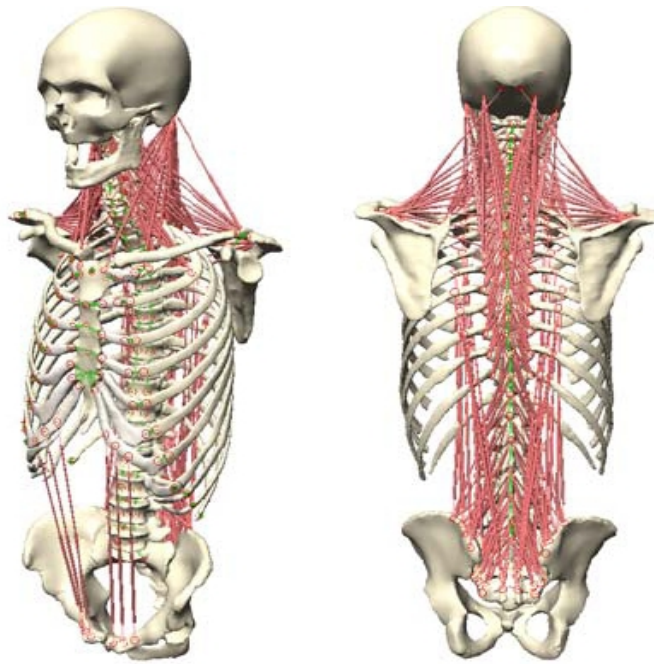

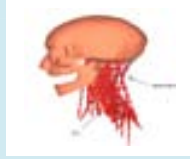




Figure 2.3: Oblique and rear views of the MBM by Esat and Acar (2007)

An overview of the most important neck multi-body models created using professional software is presented in **Table 2.6**.

Table 2.6: Overview of relevant neck multi body models

Reference	De Jager (1996)	Van der Marike (1997, 2002)	Esat and Acar (2007)	Stemper (2004)
Model	MB	MB	MB	MB
Code	MADYMO	MADYMO	MSC. Visual/Nastran 4D	MADYMO
Head	rigid	Rigid	rigid	rigid
Vertebrae	rigid	Rigid	rigid	rigid
Intervertebral joints	free	spring and damper	spring and damper	nonlinear elastic spring-damper
Discs	linear viscoelastic	3D nonlinear viscoelastic	linear viscoelastic	nonlinear viscoelastic
Ligaments	nonlinear viscoelastic	nonlinear viscoelastic	nonlinear viscoelastic	nonlinear viscoelastic
Facet joint contact	frictionless	frictionless and nonlinear elastic springs	frictionless	point restraint, nonlinear viscoelastic
Occiput-Atlas-Axis	frictionless	frictionless, force-displacement relation	-	-
Muscles	active and passive	active and passive, force generating Hill type	active and passive	active and passive, Hill type
Illustration				
Detail	13 pairs of muscles, 11 ligaments divides in many springs	9 rigid bodies, 16 types of muscle (total 68 elements) 15 ligaments divided in many springs	9 rigid bodies, 6 ligaments	16 types of muscle (136 Hill muscle elements)
Application	frontal and side acc.	frontal and side acc.	frontal and side acc.	rear impact
Validation	15g frontal, 7g side	15g frontal, 7g side	15g frontal, 7g side	1.3, 1.8, 2.6 m/s rear impact velocity

2.4.2 Finite Element Models (FEMs)

A finite element model is capable of simulating any type of geometry, material behavior, loading and boundary condition data. Bony geometry of the models varies widely between studies but the material properties are mostly based on the same literature sources.

2.4.2.1 FE Models of the Whole Human Spine

Dietrich et al. (1991) presented a finite element model of the complete human spine. A 20 noded element was used in for modelling to adopt different shapes and dimensions, and thus is suitable for modelling the complex shapes of the spinal system. The FEM model included rigid and deformable bodies as well as fluids. Muscle force was defined as a function of its elongation and stimulation by nerves. The resulting finite element model enabled static analysis of forces in the spinal system (muscles, vertebrae, ligaments, and joints) and pressure in nuclei pulposi and in the abdominal cavity and also investigation of the influence of the shape and dimensions of the spine as a whole.

Huang et al. (1994) developed an FEM of the human body to simulate the gross motion of cadavers in sled tests. To simplify the model and to reduce the computational time, the FE mesh of the whole human spine was relatively coarse. The model was used to predict the injury responses for the chest in side impact sled tests. Lee et al. (1995) generated a linear three dimensional finite element model in order to predict the vertebral displacements resulting from a postero-anterior force applied by a therapist. Consequently, intervertebral translations were predicted to be 1 mm or more at up to four intervertebral joints away from the point of load application. Lizee et al. (1998) constructed a relatively advanced FEM of the

human body, which was validated through various impactor and sled tests. The model included a limited number of 10,000 elements for the sake of simplicity. They have claimed to validate the results and showed the feasibility of a biofidelic FEM of the human body.

Jost and Nurick (2001) developed an FE human model for simulating damage during vehicle side impacts. The model predictions were claimed to show good agreement with the results of pendulum impactor tests.

2.4.2.2 FE Models of the Cervical Spine

Cervical spine FEMs vary according to the type of analysis to be carried out. FEMs types may include whole head and neck models, partial cervical spine models, a functional spine unit (two complete vertebra and a disc in between) models, disc segment (two vertebral bodies without processes and a disc in between) models or individual cervical vertebra/disc models. A number of FE studies have been reported in literature, for instance, Side, 1993; Dauvilliers et al., 1994; Yang et al., 1998; Cooper et al., 2001; and Jost and Nurick, 2001.

2.4.2.3 Whole Head and Neck Models

Whole head and neck FE models include the head on top of the cervical spine to obtain a better representation of the head-neck complex. Liu (1986) developed a finite element model of the head and the cervical spine. The 3D finite element model of a fluid filled skull had been used to simulate the spinal cord cavity. A summary of some of the significant cervical FE models is presented in **Table 2.7**. Most of these cervical spine models were used to study the mechanics of cervical injuries related to automobile crashes.

Table 2.7: Cervical spine FE model details as reported by various authors









Reference	Kleinberger (1993)	Dauvilliers (1994)	Camacho (1997)	Halidin (2000)
Model	FEM	FEM	FEM	FEM
Code	LS-DYNA	Radios	LS-DYNA	PAM-CRASH
Head	rigid	rigid	elastic	hyper viscoelastic
Vertebrae	rigid	rigid	rigid	linear elastic
Intervertebral Joints	-	free	-	-
Discs	linear elastic	linear elastic: 8 solid elements, 32 crossed spring-damper elements	lumped into intervertebral joint, nonlinear springs and linear dampers	linear elastic
Ligaments	linear elastic	linear viscoelastic, spring-damper elements	lumped into intervertebral joint	linear elastic
Facet joint contact	linear elastic	frictionless, contact between shell elements	lumped into intervertebral joint	sliding contact with friction
Occiput-Atlas-Axis	pivot joint for C0-C1 allowing flexion/extension only	C0-C1 flexion/extension only, C1-C2 AR only	lumped into intervertebral joint	sliding contact with friction
Muscles	absent	absent	nonlinear spring elements (passive)	absent
Illustration				
Detail		150 solids, 140 shells, 415 springs	639 rigid shells, 448 deformable shells, 25 springs, 108 springs	
Application	axial compression, frontal impact	frontal and side acc.	axial impact	analysis of roof design
Validation	8g frontal	15g frontal, 7g side	axial impact at 3.2 m/s	C4-C5 and C0-C3 segment loading, head and neck drop test

Table 2.7 - Continued

Reference	Yang (1998)	Nitsche (1996)	Hu (2008)	Zhang (2008)
Model	(FEM)	(FEM)	(FEM)	(FEM)
Code	PAM-CRASH	PAM-CRASH	LS-DYNA	ANSYS and LS-DYNA
Head	rigid or viscoelastic	no head modeled	isotropic linearelastic	4 noded shell, linear elastic, homogeneous
Vertebrae	elastic	elastic	isotropic linearelastic	8 node brick, linear elastic, homogeneous
Intervertebral Joints	free	free	disc with solid element	brick elemnt with low E (0.1 MPa)
Discs	viscoelastic	linear elastic	elastic-plastic and linear viscoelastic	8 node brick, linear elastic, homogeneous
Ligaments	nonlinear, tension only, membrane and bar elements	linear anisotropic	transversely isotropic, hyperelastic/elastic	nonlinear stress-strain curve
Facet joint contact	frictionless contact	frictionless contact	frictionless surface-to-surface	surface-to-surface sliding contact function
Occiput-Atlas-Axis	frictionless contact	no C0-C1 joint, C1-C2 frictionless facets	frictionless	-
Muscles	sixty tension only, spring elements (passive)	absent	active and passive Hill type	passive
Illustration				
Detail	7351 solids for head, 11498 solid for neck, 3071 membranes	1952 solids, 96 membranes	23 pairs of cervical spine, muscles (84 elemnts), total 32135 elements and 23933 nodes, 8 types of ligaments	total 27712 elements and 31749 nodes, 10 types of ligaments
Application	frontal and rear acc., axial impact	frontal and side acc., axial impact	rollover crashes	rear impact
Validation	8g rear acc., axial impact at 3.2 m/s	15g frontal, 7g side, axial compression	0°, ± 15° axial impact and rear end collision	3.5, 5, 6.5, 8g rear

3D finite element model reported by Side (1993) used the first thoracic and seven cervical vertebrae whose geometric properties were gathered from the physical models and published quantitative data. Although numerous assumptions and simplifications were employed in the model, Side reported that axial compression results showed good agreement with reported experimental data.

Dauvilliers et al. (1994) constructed a finite element model of the cervical spine based on cadaver X-rays. The vertebrae and head, modeled as rigid bodies, included only major geometrical features to achieve computational efficiency. While the modelling details are summarized in **Table 2.7**, the model elements material properties were calibrated to produce a response similar to that of NBDL volunteers for frontal and side impact. A reasonable response was achieved for frontal impact simulation but the vertical displacement of the head failed to meet the response corridors by a significant degree. The authors suggested this might be due to failing to prescribe the rotation of T1 during the loading phase. Satisfactory agreement was seen between the model response and the volunteer data for side impacts but acceleration spikes are present that greatly exceed the volunteer corridors; this is likely due to insufficient damping of the model's elements.

Camacho et al. (1997) developed a head neck model to study the dynamic response of the head and cervical spine to near-vertex head impact. Geometric characteristics were derived from 3D reconstructions of skull and vertebral CT scans from the Visible Human Data Set. It was shown that the computational spine model accurately portrayed the buckling behaviour of the spine with respect to resultant head and neck forces and resultant head accelerations. Camacho's model was extended by Van Ee et al. (2000) to include neck musculature and revised tensile properties of the intervertebral joints.

The new version of the model was validated against tensile loading tests on ligamentous cervical spine specimens. The results showed that the inclusion of muscular forces increased the tolerance of the cervical spine to tensile loading by a factor of 2.3.

Yang et al. (1998) developed a detailed FEM of the cervical spine from MRI scans of a 50th percentile male volunteer. The model was validated with reasonable success against the head and neck drop tests as well as cadaveric sled tests. Halidin et al. (2000) constructed a detailed finite element model of the head and neck in order to investigate the effect of axial impacts. A detailed FE model of the head was incorporated into the model to simulate load transfer accurately during near-vertex head impact simulation.

2.4.2.4 Thoracolumbar Spine Models

Shirazi-Adl and Pamianpour (1996) performed a nonlinear finite element study of the ligamentous thoracolumbar spine to investigate the stabilizing role of two plausible mechanisms of combined moments and pelvic rotation on the human spine in axial compression. Following this study, they developed a nonlinear finite element formulation Shirazi-Adl and Pamianpour (2000) of wrapping elements sliding over solid body edges in order to investigate the biomechanics of the human spine under a novel compression loading that follows the curvature of the spine. They concluded that the idealized wrapping loading stiffens the spine, allowing it to carry very large compression loads without hypermobility.

Zander et al. (2002) employed a 3D nonlinear finite element model of the lumbar spine with internal spinal fixators and bone grafts in order to study mechanical behavior after mono and bi-segmental fixation with and without stabilization of the bridged vertebra. They created a 3D consisting of about 8000 volume elements and has more than 30,000 degrees of freedom.

2.5 CONCLUSIONS

In this chapter, the anatomy of spine and mechanisms of spinal injuries have been studied. Also, the epidemiological studies on spinal injuries have been reviewed. Finally, the classification of the computational human spine models has been discussed. A number of conclusions are drawn as the following:

- 1- The human spine is a complex structure with the main function of providing the strength and support for the remainder of the human body.
- 2- The geometrical differences between vertebrae have been identified highlighting the importance of the cervical spine in the physiology and kinematics of the spine.
- 3- There was no agreement on the classification of mechanisms of cervical injuries. However, it was found that the best classification is based on upper and lower cervical spine classification. On the other hand, AO classification for the mechanisms of thoracolumbar injuries was preferred by most of authors.
- 4- There have been many studies on the biomechanics of spine and some studies on crash factors related to the spinal injuries. However, few studies have examined the risk of spinal injury from crash factors.
- 5- A comprehensive review of the various computational human spine models was presented. A relatively large number of computational models of the human have been developed over the last 30 years with each generation having greater anatomical detail as modelling techniques have improved and computers have advanced. However, no single model is suitable for all applications.

- 6- All models are limited by the available material properties, specifically for the soft tissues, intervertebral discs, and dynamic response of which is still largely uncharacterized, with most researchers choose linear properties based on quasi-static experimental data.
- 7- Multi body models offer a computational efficiency which is needed for simulations involving overall kinematics and longer time durations. Multi-body dynamics models have advantages such as less complexity, less demand on computational power, and relatively simpler validation requirements when compared to FE models. Due to the nature of multi-body models, it is not possible to conduct structural analysis directly in order to gain information on internal forces and deformations within the segments of the human spine.
- 8- FE modelling is very popular for being able to cover all types of analysis such as quasi-static and dynamic and also to provide detailed structural results such as stress and strain distributions. On the other hand, FE techniques may require high computational power, detailed and realistic description of material properties, and complex validation requirements depending on the nature of the problem.
- 9- A lot of work has been done to reconstruct crashes in many developed countries. However, no work has yet been done to reconstruct the kind of crashes that occur in the Kingdom of Saudi Arabia.
- 10- From the literature it is clear that both multi body and Finite Element simulations can be used to analyse crashes and understand the injury mechanism. However, SCIs are not very well understood and a lot needs to be done to understand their mechanisms as well as ways to mitigate them.

CHAPTER 3

ROAD TRAFFIC ACCIDENTS IN SAUDI ARABIA

The **K**ingdom of **S**audi **A**rabia or **KSA** (Arabic: المملكة العربية السعودية, Al-Mamlaka Al-'Arabiyya As-Su'ūdiyya) enjoys a long and rich history that traces its roots back to the earliest civilizations of the Arabian Peninsula (Menoret, 2005). KSA is located in Southwestern Asia. It is considered the largest country in the Middle East which occupies about fourth-fifths of the Arabian Peninsula with a total area of 2,250,000 square kilometers, which amounts to ten times the area of UK or slightly more than one fifth the size of the USA (MCI, 2008).

Although the Kingdom is categorized as a developing country, the discovery of oil around the middle of the last century has changed many aspects of life in KSA. This led to increase the problem of road accidents to an alarming level. This chapter provides an introduction about the size of RTAs and road safety management in Saudi Arabia.

There are several agencies linked to road traffic and road safety in KSA including the **G**eneral **D**irectorate of **T**raffic (**GDT**), **M**inistry of **T**ransportation (**MoT**), **M**inistry of **H**ealth (**MoH**), and **S**audi **R**ed **C**rescent (**SRCS**), in addition to other governmental organisations. GDT was established in 1960, under the **M**inistry of **I**nterior (**MoI**) to be held responsible for traffic regulations and surveillance, driver education, vehicle testing, and accident reporting (GTZ, 2005). The **M**otor **V**ehicle **P**eriodic **I**nspection programme (**MVPI**) has been in place since 1985. The introduction of compulsory third party insurance began in 2002. The seatbelt use was made compulsory for all drivers and front passengers in 2002.

3.1 TRENDS IN ACCIDENTS, INJURIES, AND DEATHS OF RTAs

The lifestyle of the people of Saudi Arabia has changed remarkably during the last 40 years following the boom in oil prices in 1974, 1980 and 1990/1991. Between 1970 and 2010, the Saudi population increased at an annual average growth rate of 3.91% (CDSI, 1970-2010). Likewise, the number of registered motor vehicles increased at an annual average growth rate of 12.14% (MoI, 1970-2010). The length of paved roads has increased from 8,500 to 57,645 km, a nearly six fold increase (MoT, 1970-2010). Rising numbers of RTAs and consequent increases in fatalities accompanied these changes.

It is estimated that more than one million (1,105,683) people have died or have been seriously injured in RTAs since 1970 (MoH, 1995-2010). The trend of road traffic accidents, injuries, and fatalities per vehicle declined, except during the period (1981-1990). Paradoxically, however, except for a short period (1970-1980), a steady increase in the risk of accident, injury and death per person accompanied were observed and presented in **Figure 3.1**.

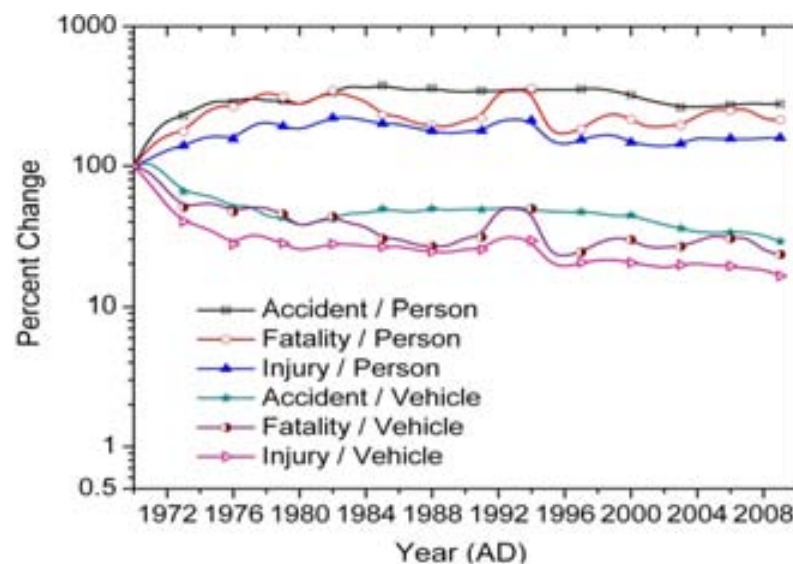


Figure 3.1: Trends in injury and fatality rates of RTAs in Saudi Arabia (1970-2010)

3.2 CAR OWNERSHIP AND VEHICLE FLEET

The forecasts of car ownership and use play a central role in the planning and decision making of numerous public agencies and private organisations. In this study, the logistic S-curve theory was employed to predict the car ownership in Saudi Arabia.

The Gompertz formula (Dargay et al., 1999) was found to fit the data (Eq. 3.1):

$$CO = S_t e^{(-a e^{(-b GDP)})} \quad 3.1$$

Where CO is the car ownership per capita, S_t is the saturation of cars ownership, GDP is the Gross Domestic Product (GDP), a and b are constants.

Figure 3.2 presents the model and the projected car ownership trends in Saudi Arabia for 2025. The GDP growth was assumed to be 3.7% based on the average growth rate between 1999 and 2004 (GTZ, 2005). According to the model forecasting, the CO will reach 396 Cars/Capita at the projection year 2025. However, the model forecasts are based on the continuous increase of GDP, which means they are not sensitive to an economic crisis.

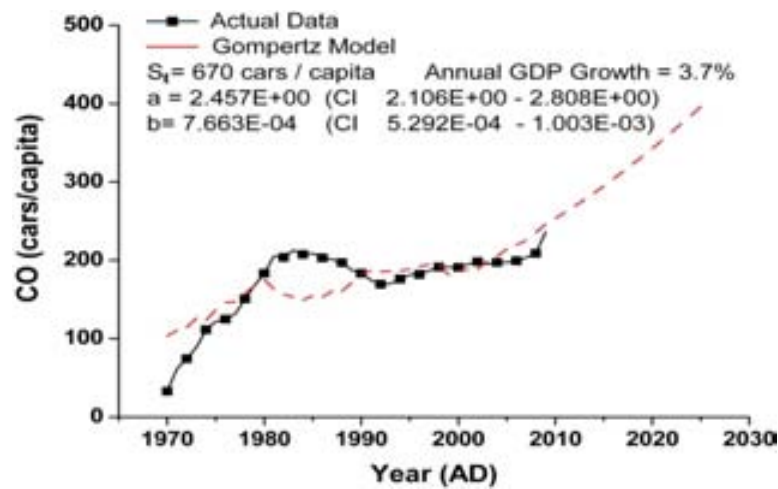


Figure 3.2: The estimation and projection of CO in Saudi Arabia (1970-2025)

3.3 A COMPARISON OF RTA RATES

There are some known measures or indicators can be used for accident comparisons when related to motorization rate. These Indicators are important tools not just for measuring the magnitude of a problem but also for setting targets and assessing performance. Two very common indicators are the: deaths per 100,000 population (F/P), and the number of deaths per 10,000 vehicles (F/V). Both of these indicators have limitations regarding their reliability and validity that place restrictions on how they can be used and interpreted (WHO, 2004). A better indicator of traffic safety risk is deaths per 1 billion vehicle-kilometers traveled (F/VK), but this also fails to allow for non-motorized travel. **Figures 3.3-3.5** shows these measures for some countries based on recent data obtained from IRF (2010), and author calculations.

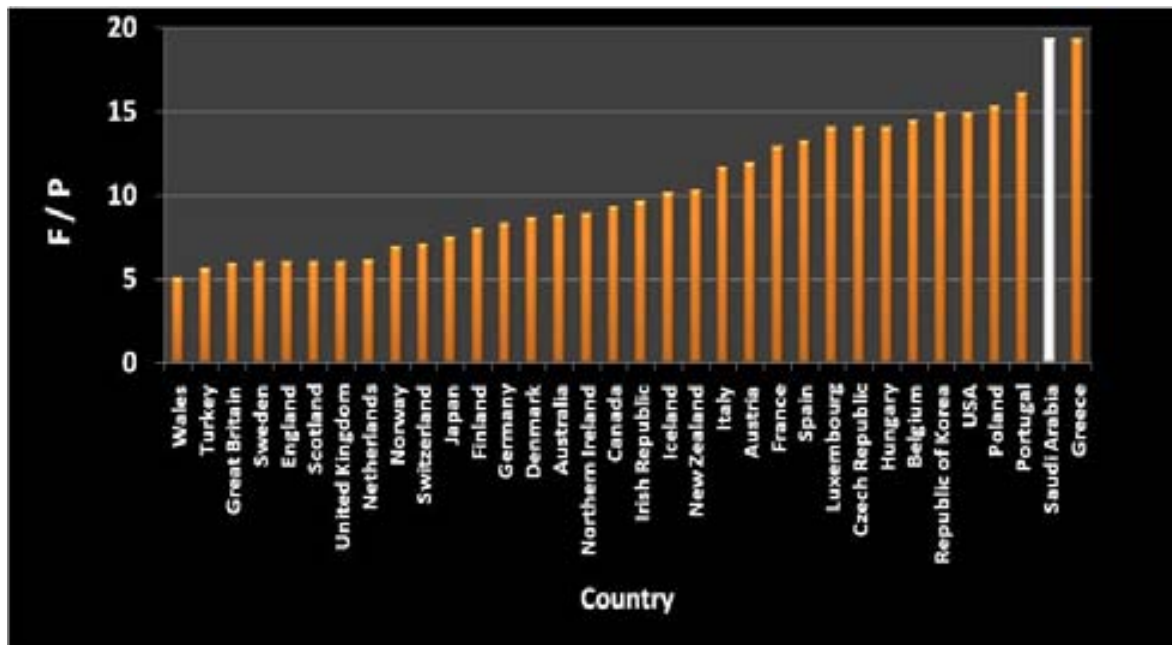


Figure 3.3: Comparison of fatalities per capita for the KSA and some countries

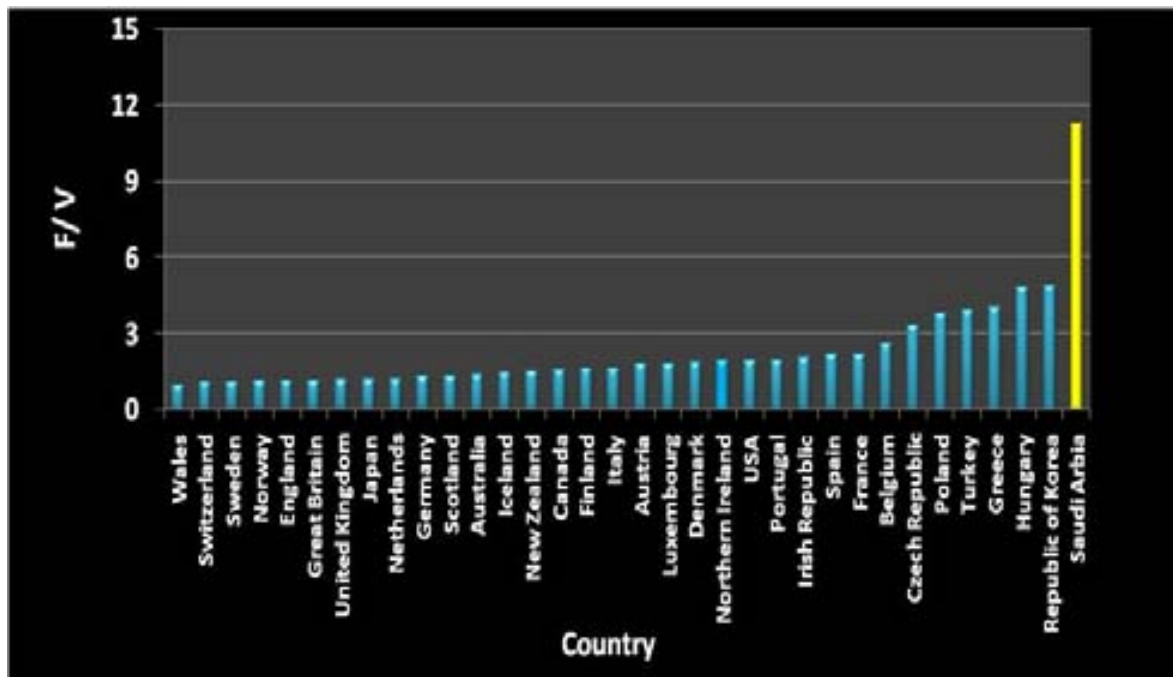


Figure 3.4: Fatalities per 10,000 vehicles for the KSA and some countries

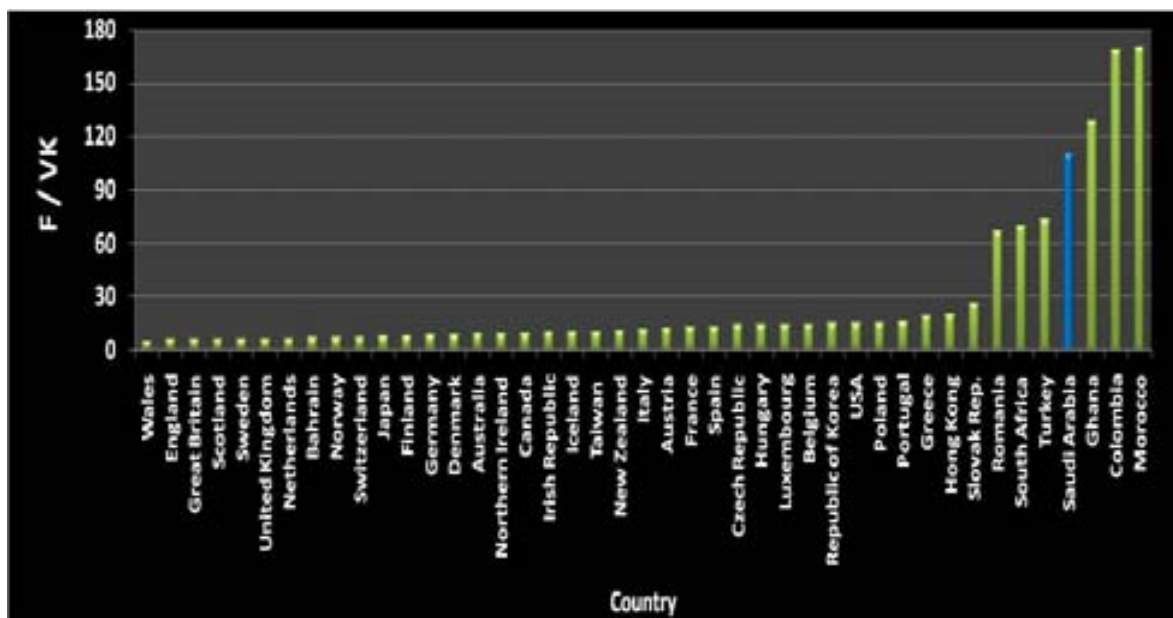


Figure 3.5: Fatalities per billion vehicles kilometer for the KSA and other countries

When the Saudi average mortality rate (19.25) from RTAs for the period 2000-2010 was compared with the equivalent rates in a number of developed countries, mortality rate (F/P) was at the upper-most limit being surpassed only by one country. The rank of Saudi's fatality rate based on its motorization level (F/V) was 11.23; three times higher than the average of that for other modern countries. Using the F/VK rate which is the best measure for making reliable comparison among nations, since it takes into consideration the total amount of travel, it appears that Saudi Arabia had by far the fourth highest rate in the scale. It can be easily noticed that, for example, the risk of F/VK in Saudi Arabia is 18 times that in UK.

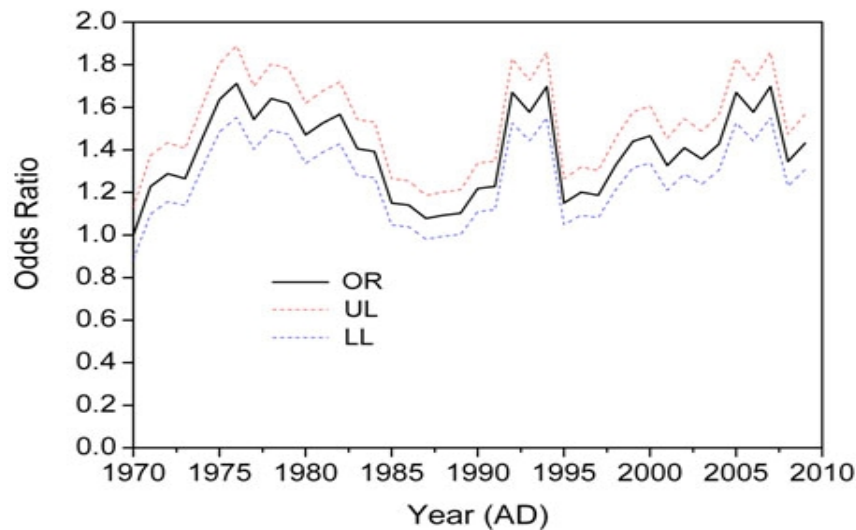


Figure 3.6: Accident severity represented by odds ratio

The level of accident severity in Saudi Arabia during the past decades was also assessed by using the concept of **Odds Ratio (OD)** as shown in **Figure 3.6**. The year of 1970 was taken as a reference. The trend of OD suggests that no improvement in this dimension seems to have taken place between these points of time, except a short period during 1985-1990.

3.4 CHARACTERISTICS OF ROAD TRAFFIC ACCIDENTS

In previous sections, high rates of road victims in Saudi Arabia were noticed. This section provides some insight into the main factors that might contribute to these accidents.

Figure 3.7 shows the percentage of road accidents according to type of impact. Among these accidents, the frontal (56%), and side impacts (27%) are the most frequent severe type of impact. Rollover crashes also occur less frequently than all other types of automotive crashes, however, they are far more likely to result in fatalities than non-rollover ones (10%).

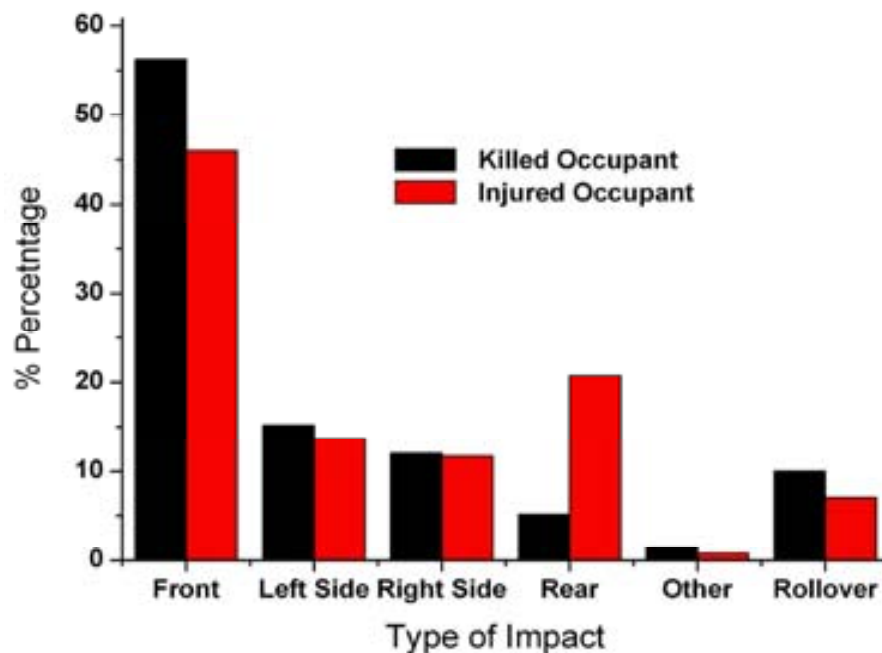


Figure 3.7: Distribution of road accidents in Saudi Arabia by type of impact

Figure 3.8 presents distribution of injuries by body regions for both killed and survivor occupants. The results show that the head (22%), thorax (19%) and spine (10%) are the parts of the human body most exposed to fatalities during different accidents.

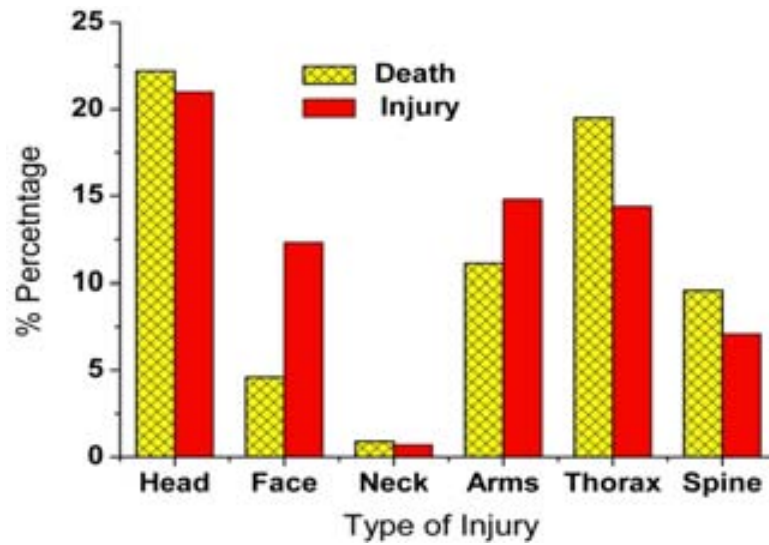


Figure 3.8: Types of body injuries from road accidents in Saudi Arabia

The distribution of accidents by cause is shown in **Figure 3.9**. Among other causes, careless driving (42%) was found to be the largest contributing factor for road accidents in Saudi Arabia, followed by sudden deviation (17%) and mechanical faults (15%).

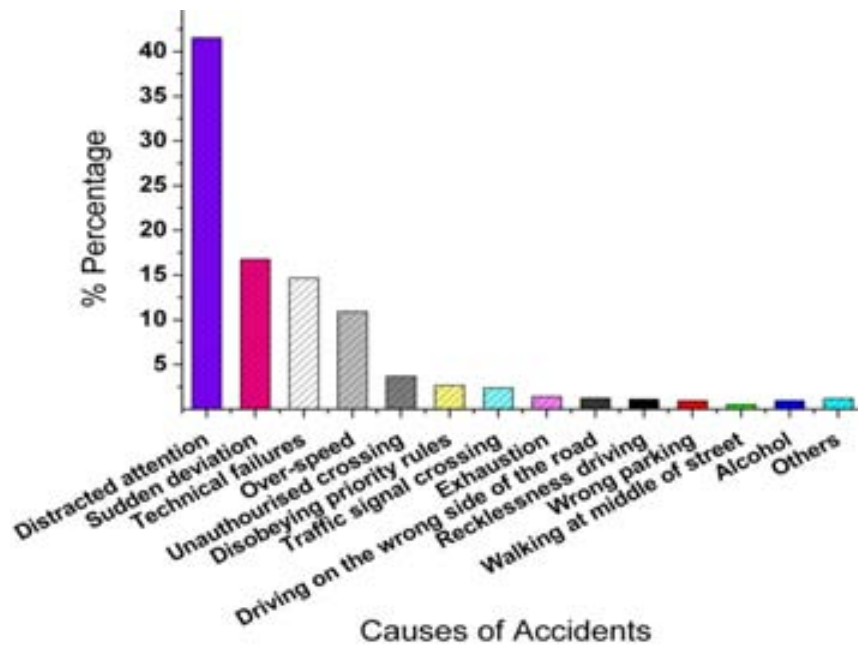


Figure 3.9: Major causes of road accidents in Saudi Arabia

Figure 3.10 shows the site of death identified for occupants. Most of the RTA victims were dead on scene/arrival in the hospital (63%). Only 12% died on the hospital wards proper.

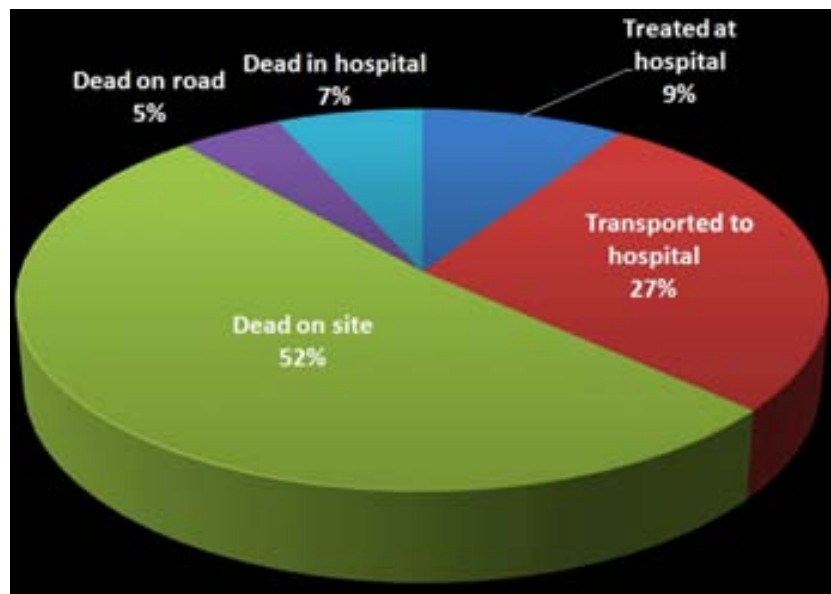


Figure 3.10: Place of death for victims from road accidents in Saudi Arabia

3.5 NATIONAL ECONOMIC LOSS DUE TO RTAs

In addition to fatalities, traffic accidents also cause disability and are a drain on the health resources as well as social and economic effects on an individual. Understanding the true cost of road traffic accidents will help decision makers to obtain a clear understanding of the vast economic sums that road traffic accidents cost the national and local economy. No accurate study has been conducted before on estimating costs of RTAs in Saudi Arabia.

Thus, the author has participated in a national study to investigate the economic costs of road traffic accidents in the Kingdom of Saudi Arabia in 2005 (ADA, 2006).

Costs have been calculated using only the resource costs, as assessed and calculated with amounts added for ‘Pain, Grief and Suffering’ (PGS) and then calculated with amounts added (as in the UK) for ‘Human’ costs assessed by the ‘Willingness to Pay’ (WTP) approach. **Figure 3.11** shows summary of resource costs for fatal and serious RTAs in Saudi Arabia.

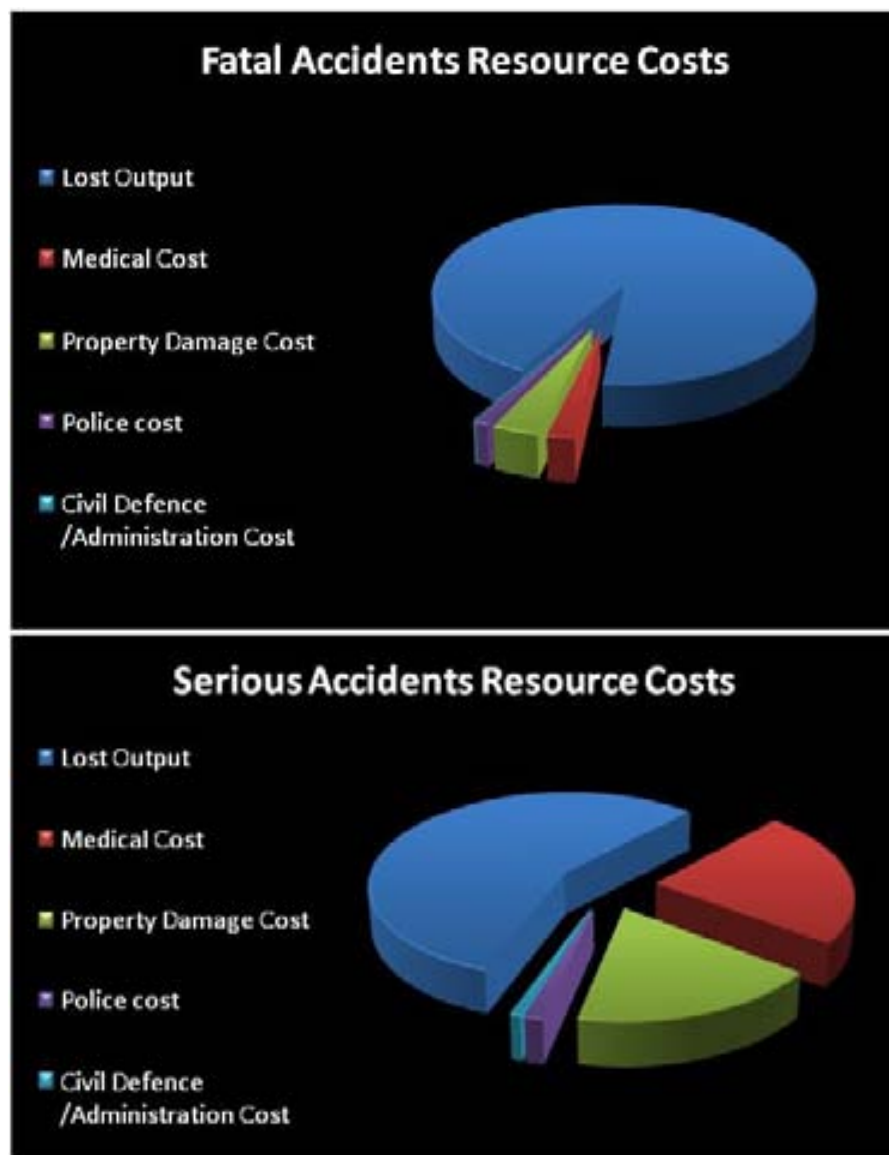


Figure 3.11: Distribution of costs for fatal and serious RTA in KSA (ADA, 2006)

Where an adjustment was made for the perceived under reporting of damage-only accidents for the Kingdom as whole, then the values increased to US\$ 2,551 million (Resource costs only), US\$ 3,522 million (including Pain Grief and Suffering), and US\$ 7,088 million with human costs included. Thus with this adjustment, the total costs including PGS values were increased in the Kingdom by about 12%. Finally, if the annual cost of road accidents in the Kingdom is a minimum of US\$ 3,148 million ($> 1\%$ of GNP) then detailed consideration should be given as to how much should be spent annually on road accident countermeasures.

3.6 ACCIDENT FORECASTS AND SAFETY TARGETS

A most effective management tool for road safety improvement has been proven to be the setting of overall casualty reduction targets. These may be set at a national or regional level but it is imperative that they are disaggregated to the local level. Setting such targets applicable, say to a local highway authority, has tended to focus those with safety responsibilities to begin to work very efficiently to achieve the set goals. It is, however, also important that such targets are achievable and their progress is monitored and charted.

The fatal road accident in Saudi Arabia is defined as death having occurred at the scene or within 24 hours of the accident. The European Conference of Ministers of Transport (ECMT) provides a standardized 30 days adjustment factor of 1.30 to make the statistical data comparable. If factored to the internationally accepted definition of road fatality, the total number of fatalities would be considerably higher. In fact studies have indicated that moving from a 24-hour to 30-day fatality definition would result in doubling of the numbers of accidents recorded as fatal (SIDA, 2002). This estimate of real number of fatalities using the 30-day definition for the past 30 years is shown in **Figure 3.12**.

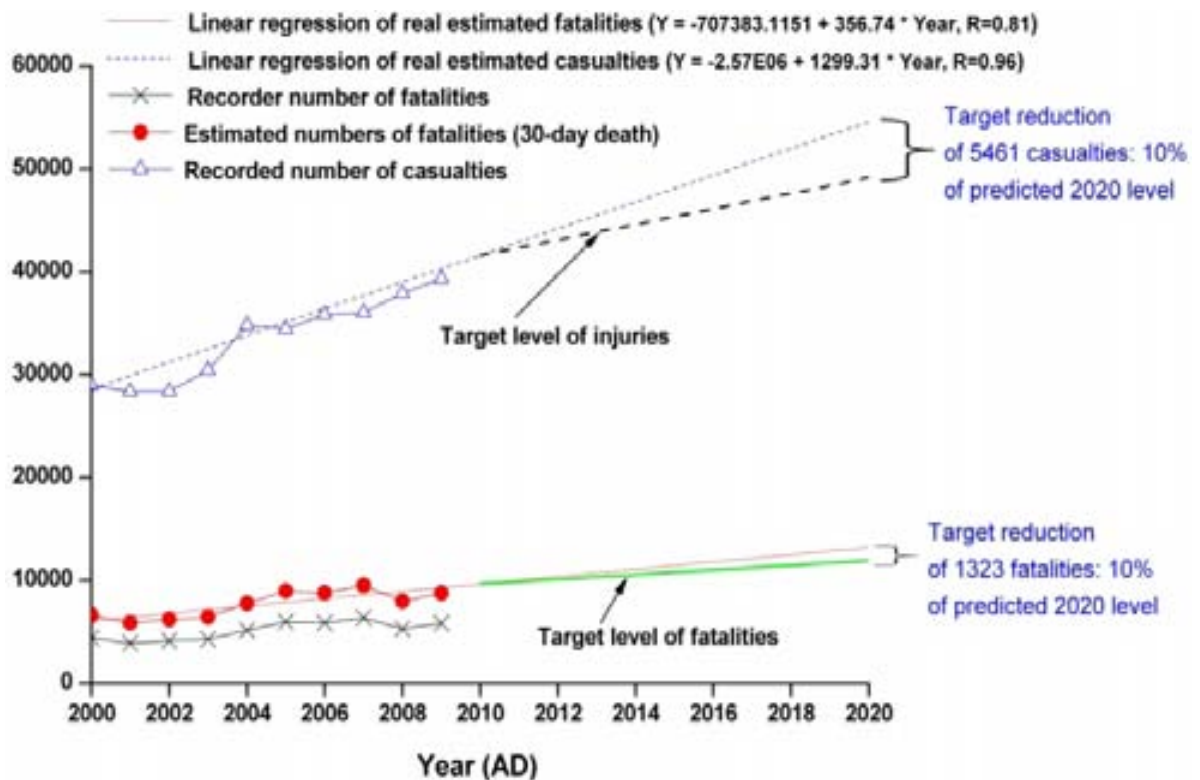


Figure 3.12: Evolution in numbers of road fatalities, injury crashes and forecasts

It is proposed that for the Kingdom a target reduction of 10% in the fatality and injury accident levels that have been forecast for the year 2010 should be set. To achieve 10% of the accidents, all the various sectors need to actively work together to save collectively about 1% each year. If the 10% target is ultimately achieved after 10 years, this would effectively be saving the Kingdom more than US\$ 823.47 million per year.

3.7 CONCLUSIONS

In this Chapter, a retrospective analysis was conducted, based on secondary data obtained from the Saudi official sources on RTAs, road injuries and deaths, on people of all ages in the thirteen regions of the Kingdom during the period 2000–2010 and, for international comparison, from IRF Statistics reports and the published literature. A number of key issues arise from this review are as follows:

- 1- The study has shown that despite the sharp increase in the registered vehicles in KSA, fatality rates (per vehicle) appear to have declined. However, these declines were accompanied by a persistent increase in the fatality rates per person.
- 2- The actual number of vehicles working on roads of Saudi Arabia was estimated to be 6 million cars by end of 2010, with an annual growth of car ownership of 2.8%.
- 3- Frontal (56%) and side impacts (27%) are the common types constituted RTAs.
- 4- The portion of spinal injury per human body including the neck was found to be 11% exceeding the international rates (3-6%) because of reckless and aggressive driving (52.45%) in this country. Hence, one person injured every two hours, and the injuries to every sixth person on the roads is due to spinal injury.
- 5- Most of victims (63%) died at spot before arrival to hospital. It is obvious that there is a lack of emergency services and shortage in the first aid coverage.
- 6- When the accident rates (F/P, F/V, and F/VK) were compared with some developed countries, the Saudi level far exceeded all other countries in the list.
- 7- The size of the problem of road crashes in Saudi Arabia and the size of the human and economic resources lost are therefore enormous. It is necessary to implement a national strategy to face this problem.

CHAPTER 4

IN-DEPTH COLLISION CHARACTERISTICS OF SPINAL INJURIES

Spinal Injuries (SIs) are a serious concern for all as they can have a very significant economic burden on the society. Their effects can be long lasting, and the cost of medical care as well as other indirect burden on the society can be large. A large number of this type of SIs is caused by RTAs. Safety technology is developed only with focused research on specific problem areas, which are identified on the basis of the epidemiology of the problem. It is therefore important to understand the epidemiology of SIs.

Even though spinal injuries are a major burden to the society, the epidemiology of SIs is not fully understood. In this work, an attempt has been made to study the epidemiology of SIs in Saudi Arabia. Saudi Arabia does not have a detailed crash database like those in developed countries (like the CIREN in USA, CCIS in UK, GIDAS in Germany, etc.).

This chapter describes a general methodology to develop an in-depth database which can then be interrogated to address the problem of spinal injuries related to vehicle crashes in Saudi Arabia and their characteristics.

4.1 METHODS AND MATERIALS

This section describes the methodology followed in this in-depth crash injury study. Data were collected for each individual vehicle, occupant and injury sampled. It is intended that this section should also describe the general method of data collection that was used for sub-studies in this thesis since these studies use data from the same sources and therefore the method of data collection was identical in each case. Subsequent chapters describe the methodology that was unique only to the particular sub-study in question.

4.1.1 Purpose and Scope

The reported incidence of SCIs in Saudi Arabia is high at 63 per million per year which exceeded all reported values worldwide (AboAbat, 1999). At the time of writing this thesis, a detailed real world accidents database does not exist in Saudi Arabia. Therefore, this study involves collection of data from real world traffic accidents in Saudi Arabia.

4.1.2 Study Design

A Prospective Study was used to obtain detailed collision characteristics of spinal injuries in Saudi Arabia. The author was involved in the project design, planning and implementation phases of the survey and in developing the official letters and forms. The required data was provided by collaborators which included the police, fire departments, emergency medical services, and trauma centres based in the city of Riyadh (**Figure 4.1**). This method was considered to be the most efficient approach to collect accurate and timely data on the mechanisms of spinal injury resulting from vehicle crashes.

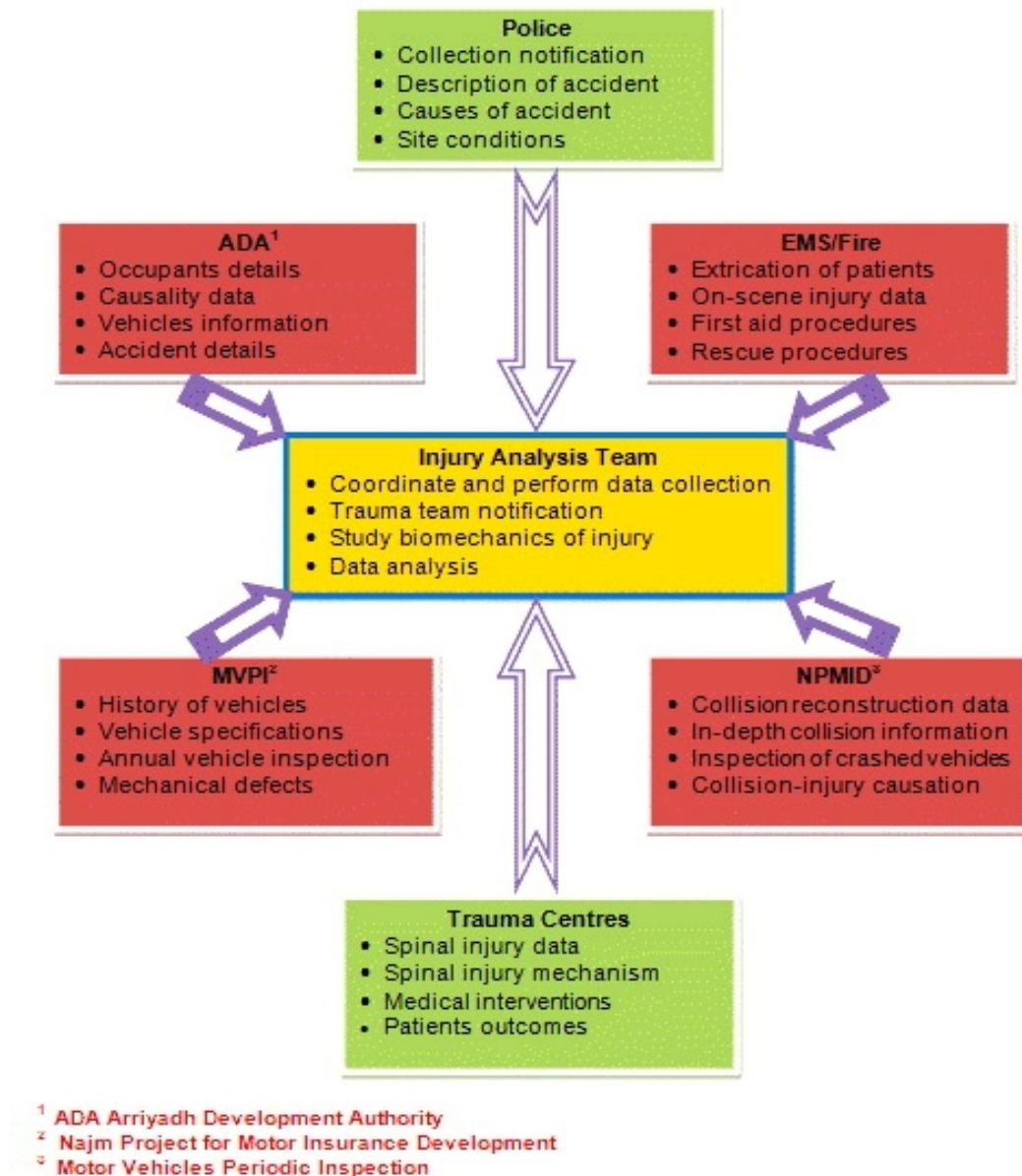


Figure 4.1: Model design of the fieldwork study

The method of data collection was largely in accordance with the international standards of the National Accident Sampling System (NASS, 2005), and general practice of the Co-operative Crash Injury Study (CCIS). A comprehensive overview of the CCIS methodology can be found in Mackay et al (1985) and Mackay and Hassan (2000).

4.1.3 Case Selection Criteria

The study population was restricted to occupants or pedestrians who were involved in a vehicle crash and sustained a spinal injury of $\text{MAIS} \geq 2$. Passenger cars, pickup trucks, mini vans or Sport Utility Vehicles (SUVs) involved in car collisions, fixed objects, camel, and pedestrian or rollover crashes were selected for inclusion in this study. The vehicle was inspected at the scene of the accident, at the garage or at the police compound within few days of the crash. Only persons who were hospitalized or who died were included, and persons with lesions due to degenerative disc disease were excluded.

4.1.4 Study Location

The city of Riyadh (plural of *rawdha*, oasis) was founded on the ruins of several communities around 1740. Although it was chosen as the capital of the second Saudi state in 1824, it came to prominence only after its independent governor, *Abdulaziz Al-Saud*, began a campaign to consolidate modern Saudi Arabia in 1902. The speed and scale of Riyadh's transformation since, particularly during the 1970s, has had few parallels. From a walled city of less than 1 square kilometer in 1920, it has grown into a sprawling modern capital of 1,782 square kilometers. Its population has increased from an estimated 14,000 in 1902, to 666,480 in 1974, to an estimated 6.7 million by 2010. Indeed about 30% of RTAs casualties and 25% of the country's fatalities happen within the city limits. Every year around 23% of SRCS emergencies in the kingdom are attended in Riyadh. In addition, one fifth of the national spinal injuries are treated in the seven trauma centers in Riyadh (SRCS, 1970-2010). Therefore, it was believed that the spinal casualties of Riyadh are indicative sample for the urban population of spinal injuries related to vehicle crashes in Saudi Arabia (**Figure 4.2**).

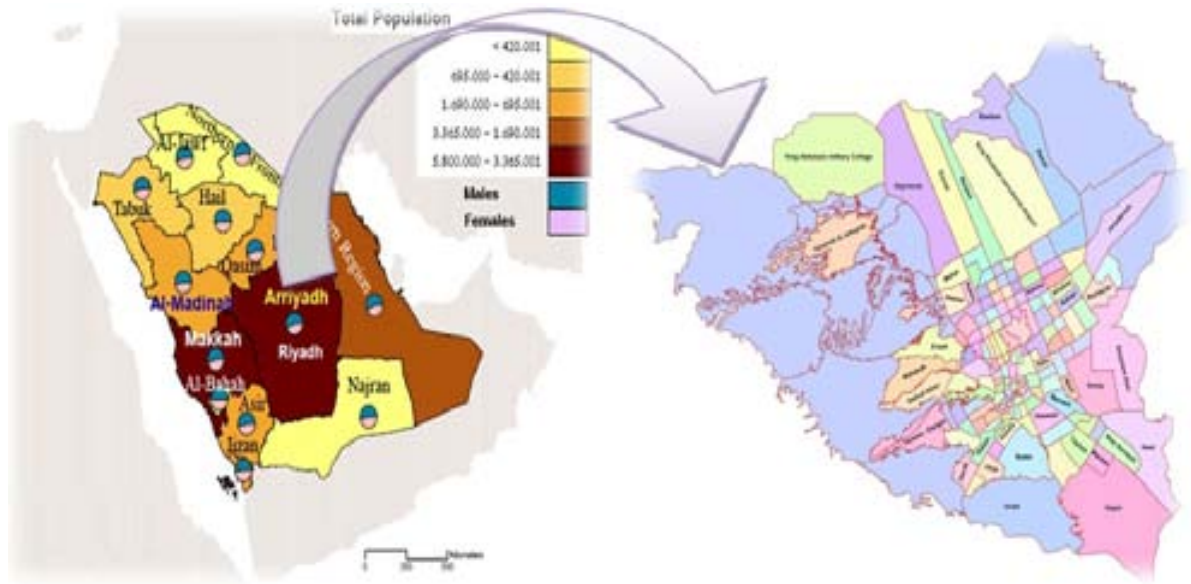


Figure 4.2: Map of Riyadh showing the main districts and trauma centres

4.1.5 Study Forms

A standard porforma including around 500 pieces of information was designed especially for the data collection. There were five levels of datasets including: (1) accident information; (2) vehicle's exterior characteristics; (3) vehicle's interior; (4) casualty details; and (5) Injury details. This study was approved by the Institutional Review Boards of **Ministry of Interior (MOI)**, **Ministry of Health (MOH)**, **Ministry of Transportation (MOT)**, **Saudi Red Crescent Society (SRCS)**, and **Arriyadh Development Authority (ADA)**. The data sources used in this study utilized under a **Certificate of Confidentiality (COC)** authorized by each hospital under a specific law passed by MOH. Copies of the data forms and COCs are included in the **Appendix A.1**. The standard investigation forms in English and Arabic Languages can be found in **Appendixes A.2** and **A.3**.

4.1.6 Study Population

The final data bank of 512 car collisions acquired over a four year period (2004-2008) forms the basis on which the main analysis of this thesis was performed. In these collisions, there were 1211 casualties who received between them 1843 spinal injuries and other serious injuries ($\text{MAIS} \geq 2$). In all, information on 778 spinal injuries sustained by 552 casualties in 512 vehicle crashes met the selection criteria for this study.

Of the 552 casualties, 296 (54%) were involved in serious crashes, while 256 (46%) were involved in fatal crashes. Figures produced by the police classification during the same accidents time showed that the actual severity distribution was 45% fatal, 49% serious, and 6% slight respectively as shown in **Figure 4.3**. It can be seen therefore that the data collected in this study is significantly biased towards the more serious end of the severity ($P < 0.001$).

This would suggest that official statistics do not accurately reflect the true size of the problem because they are restricted to those who die at the scene and do not take into account those who die during treatment (Al-Ghamdi, 1998).

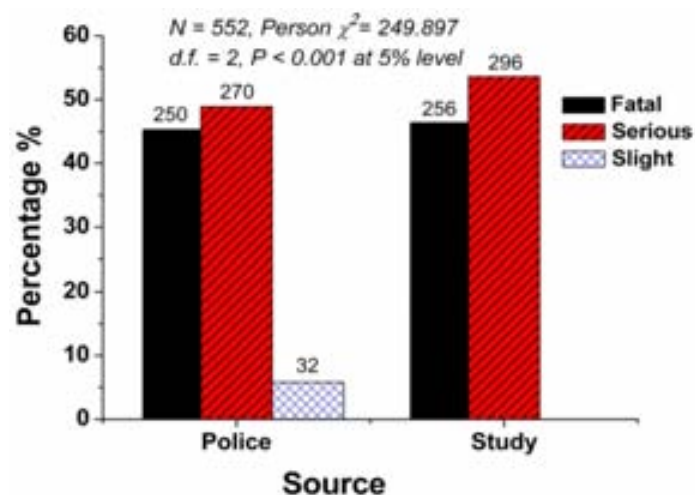


Figure 4.3: Classification of collisions severity in the study

Table 4.1: General statistics of the 552 casualties in the study

Characteristic	Spinal Injury	95% CI
Type of Collision	2.45 (0.94); 2; 1-5 ^a	2.37-2.53
1- Car	323 (58.5) ^b	0.55-0.61
2- Fixed object	83 (15)	0.13-0.18
3- Pedestrian	82 (14.9)	0.12-0.17
4- Rollover	47 (8.5)	0.06-0.10
5- Camel collision	17 (3.1)	0.02-0.04
Impact Type	1.57 (0.94); 1; 1-4	1.50-1.65
1- Frontal	363 (65.8)	0.62-0.69
2- Side	105 (19)	0.16-0.22
3- Rear end	37 (6.7)	0.05-0.08
4- Rollover	47 (8.5)	0.07-0.10
ETS (km/h)	45.10 (26.98); 39.2; 5.28-186.23	42.33-47.87
Vehicle body type	1.11 (0.31); 1; 1-2	1.08-1.13
1- Passenger car	490 (88.8)	0.87-0.91
2- SUV, Truck, Van	62 (11.2)	0.09-0.13
Vehicle curb weight (kg)	1112 (244.5); 1070; 668-2850	1091.5-1132.4
1- Small ($\leq 1,089$)	303 (54.9)	0.51-0.58
2- Mid-size (1,090 - 1,587)	226 (40.9)	0.37-0.44
3- Large ($\geq 1,588$)	23 (4.2)	0.03-0.06
Classification of casualty	1.14 (0.35); 1; 1-2	1.11-1.17
1- Car occupant	470 (85.1)	0.83-0.88
2- Pedestrian	82 (14.9))	0.12-0.17
Age (years)	2.08 (0.35); 2; 1-3	2.05-2.11
1- Child (≤ 12)	15 (2.7)	0.02-0.04
2- Adult (13-59)	478 (86.6)	0.84-0.89
3- Senior (≥ 60)	59 (10.7)	0.09-0.13
Gender	1.23 (0.42); 1; 1-2	1.19-1.26
1- Male	423 (76.6)	0.74-0.80
2- Female	129 (23.4)	0.20-0.26
Seating position	1.55 (0.76); 1; 1-3	1.50-1.61
1- Driver	422 (60.89)	0.57-0.64
2- Front occupant	156 (22.51)	0.19-0.25
3- Rear occupant	115 (16.59)	0.13-0.19
Restraint used	209 (44.46)	0.40-0.47
Ejection	63 (11.4)	0.09-0.14
Overall mortality	217 (39.3)	0.36-0.43
Type of spinal injury (MAIS ≥ 2)	1.86 (2); 0.90; 1-4	1.79-1.92
1- Cervical	292 (52.90)	0.49-0.56
2- Thoracic	161 (29.17)	0.26-0.32
3- Lumbar	122 (22.10)	0.19-0.25
4- Sacral	29 (5.25)	0.04-0.07

^a Values are mean (σ); median; range

^b Values are n (%)

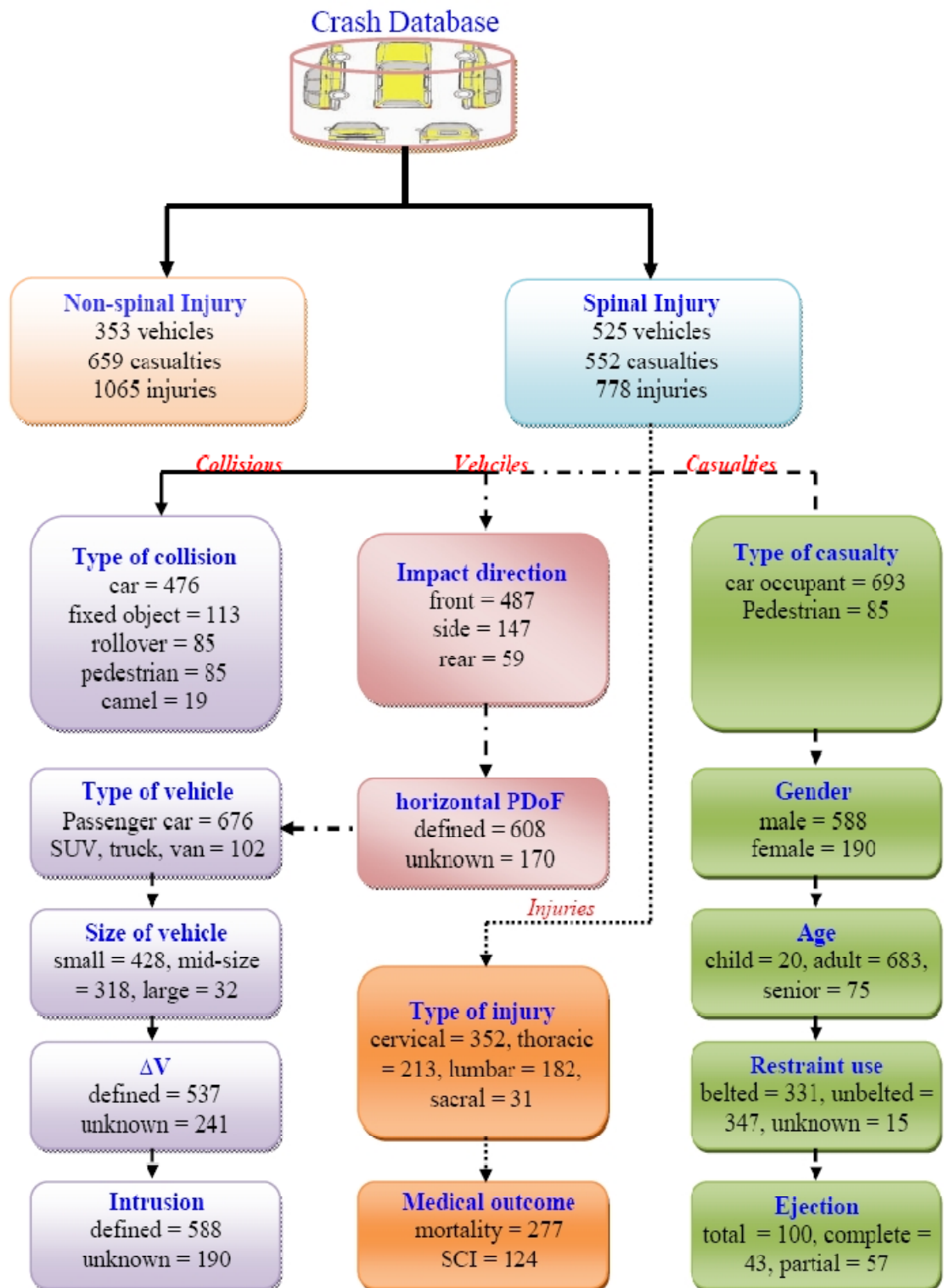


Figure 4.4: Tree classifications of collisions, vehicles, and injuries in the sample

4.1.7 Definition of Variables

Table 4.1 and **Figure 4.4** show collision, vehicle, and injury characteristics for the sample. The frequencies of the variables were sufficiently large to perform confidence-interval analyses. A collision was defined as a road vehicle crash in which the first harmful event is a collision of a road vehicle with another road vehicle, other property or pedestrians (ANSI, 1996). For the purposes of this study, collisions were categorised according to the type of object struck: *Car*; *Fixed object*; *Pedestrian*; *Rollover*; and *Animal collisions*.

All vehicles sampled in this study were inspected and photographed extensively both internally and externally. The data collected on the vehicle exterior including information on car components such as doors, door latches, pillars, vehicle glazing, bonnet hinges and latches and certain contents of the engine bay.

The data collected on the interior of the vehicle included information on seats and seat performance, steering wheel and steering column, measurement of any intrusion into the passenger survival cell, information on seat belt usage and identification of specific and exact occupant contacts within the vehicle. Sometimes, points of contacts of the occupant's body can be determined from skin smudges, skin and hair transfers, facial cosmetic smears, dents or deformities and blood stains on the interior of the vehicle.

Where possible, the damage profile of the vehicle was measured so that severity indicators known as collision Delta-V (ΔV) and/or Equivalent Test Speed (ETS) could be attained (Gabler et al., 2003). The rollover speed and impact speed of pedestrian were reconstructed based on the physical evidence present at the scene. For pedestrian crashes, the procedure developed by NASS (1996) was followed. These parameters were computed by using PC-CRASH ver 7 (DSD, 2006) and AiDamage ver 3 packages (Aits, 2003).

The impact direction was classified as front (PDoF = 1, 11, and 12), side (PDoF = 2, 3, 4, 8, 9 and 10), and rear (PDoF = 5, 6, and 7). This method used the **P**roduct **D**irection of **F**orce of the impact (**PDoF**) and the standardised **C**ollision **D**eformation **C**lassification (**CDC**) code as recommended by 'SAE Practice J224b' (SAE, 1984).

Vehicle body types were classified into 2 categories: passenger and **LTV** (**L**ight **T**ruck, and **V**an), and **SUV** (**S**port **U**tility **V**ehicle). Vehicles were also classified according to curb weight (i.e. small, $\leq 1,089$ kg; mid-size, $1,090 - 1,587$ kg; or large, $\geq 1,588$ kg).

Information including age, gender, restraint use, and seating position was obtained for each attended casualty. Occupants' use of airbags and seatbelts was primarily determined through crash scene vehicle inspection, police and interviews.

Details of the injuries were obtained from medical and emergency department records. Injury severity was classified according to the AIS, 2005 Rev (AAAM, 2005). The highest AIS or Maximum AIS value (MAIS) was used to represent the overall severity of injury sustained by a casualty. The level of spinal injury examined was confined to cervical, thoracic, and lumbar spinal regions regardless of neurologic injury (WHO, 2007).

4.1.8 Statistical Analysis

The data used for statistical analysis were entered into a computer generated relational database and the statistical analysis using one-way analysis of variance (ANOVA) and χ^2 test where applicable was performed. Mann-Whitney U and Median tests were used for comparisons of means. The rejection for the null hypothesis was set at probability levels of $\leq 5\%$. Data were analysed by using SPSS Package version 17 (Norusis, 2010). It should be noted that the statistical parameters are shown on each figure.

4.2 TYPES OF SPINAL INJURY

There were 552 casualties who suffered an injury ($\text{MAIS} \geq 2$). Of the 778 AIS 2+ spinal injuries the majority was of vertebral fractures (75%), following by 124 cord injuries (16%). Of these 47 SCIs were associated with fracture, 13 with dislocation, 54 with fracture and dislocation, and 10 without fracture or dislocation. Vertebral subluxation is not prevalent, which occurred even less frequently than spinal cord injuries. There appear to be some differences in the type of injuries suffered by spinal region (*Person* $\chi^2 = 81.83$, *d.f.* = 12, $P < 0.001$ at 5% level). Injuries to the cervical are both cordal and vertebral.

The cervical cord injuries (86%) mainly involve fractures and dislocation and injuries to the cervical vertebrae and to a lesser extent dislocation. Around one quarter (24%) of the injuries to the cervical spine involved an insult to the cord. In contrast, injuries to the thoracic, lumbar, and sacral spines were fractures without associated cord damage (77%, 96%, and 90% respectively). The types of injuries to the spine are shown in **Table 4.2**.

Table 4.2: Type of spinal injury by specific anatomic structure

Specific Anatomic Structure	Cervical	Thoracic	Lumbar	Sacral
Vertebral fracture without cord injury[†]	213 (61%)	163 (77%)	174 (95.60%)	28 (90%)
Cord injury	86 (24%)	32 (15%)	3 (1.65%)	3 (10%)
Vertebral subluxation without fracture or cord injury	26 (7%)	7 (3%)	1 (0.54%)	0
Disk injury	11 (3%)	9 (4%)	3 (1.67%)	0
Nerve root injury	16 (5%)	2 (1%)	1 (0.54%)	0
Total	352 (100%)	213 (100%)	182 (100%)	31 (100%)

[†] Values are N (%)

4.3 TYPES OF COLLISION

This section describes the effect of car collision type on the level and severity of spinal injury. Injuries in frontal, rear, side and rollover impacts are being presented along with those in pedestrian impacts and in impacts with camels.

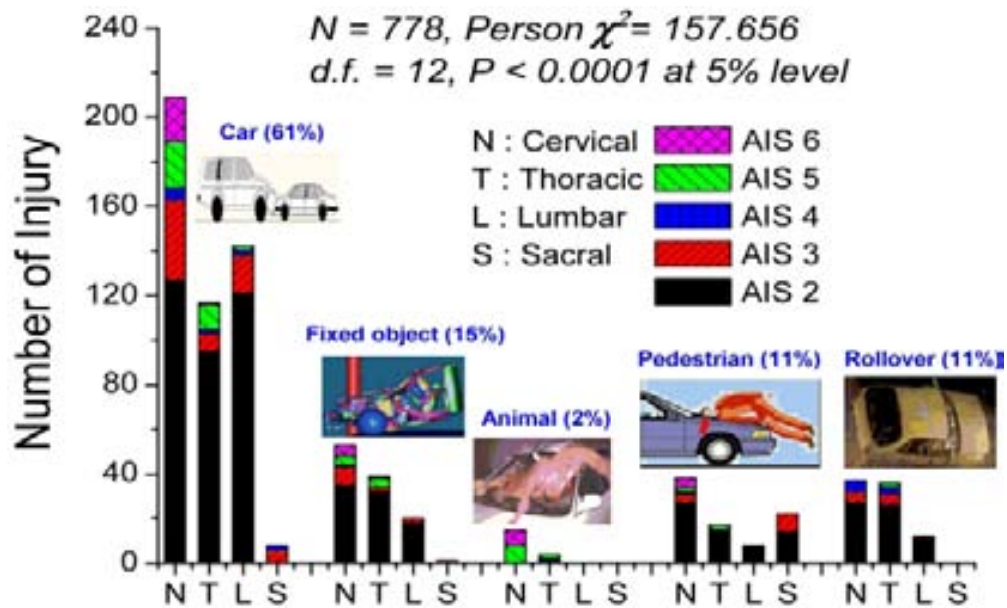


Figure 4.5: Severity and type of spinal injury vs. type of collision

Figure 4.5 shows the severity of spinal injuries for various collisions. Out of 778 cases 61% of the injuries are caused by crashes with cars. Of these, the cervical vertebrae are injured the most (44%). Fractures of thoracic vertebrae were reported in 117 (25%) cases. The lumbar spinal injuries were reported in 142 cases which are mostly AIS 2 (85%). Few cases of serious injuries (12%) and only 2 cases of critical injuries (AIS 5) were reported. Very few cases (mostly AIS 3) were reported for sacral vertebral injuries.

Impacts with fixed objects on the road accounted 15% of the spinal injuries in this study. Most of these injuries found in cervical region (47%), followed by thoracic injuries (35%).

In spite that only less (2%) of the collisions in this study were classified as an impact with camels, but all the cases resulted either in critical injury (AIS 5) or in fatal injury (AIS 6).

The pedestrian impacts considered 11% of the injuries. Most of these injuries were AIS 2 and occurred in cervical spine (45%) followed by sacral segments (26%).

Rollover collisions were responsible for 11% injuries. Out of these, 37 (44%) cases (including 25 AIS 2 injuries, and the remaining AIS 3 and 4) were reported on cervical vertebra injuries. Thoracic vertebrae (42%) also had a similar pattern of injury. 10 cases (all AIS 2) of lumbar injuries were observed. No injuries were reported in sacral vertebrae.

From **Table 4.3**, it can be observed out of 512 crash cases considered 294 cases (58%) are impact with another car. Followed by 82 cases (16%) of pedestrian impact and 79 cases (15%) of fixed object impact. 61% of the spinal injuries are caused by car crashes. It can be observed that in all the cases car crashes are the most frequent. The highest injury rate was observed in rollovers followed by car collisions, and fixed object collisions.

Table 4.3: Incidence rates of spinal injury by crash type

Collision Type	Crashes		Casualties				Spinal Injuries		
			Fatal		Serious				
	N	%	N	%	N	%	N	%	Injury/Casualty
Car Occupants									
Car	294	57.42	129	59.45	194	57.91	476	61.18	1.47
Fixed object	79	15.43	38	17.51	45	13.43	113	14.52	1.36
Rollover	43	8.4	7	3.23	40	11.94	85	10.93	1.81
Animal	14	2.73	3	1.38	14	4.18	19	2.44	1.12
Road Users									
Pedestrian	82	16.02	40	18.43	42	1.54	85	10.93	1.04
Total	512	100	217	100	335	100	778	100	1.41

4.4 DIRECTION OF IMPACT

In addition to the type of collision, the **Principal Direction of Force (PDoF)** plays an important role in the mechanism and location of the spinal injury. The effect of PDoF on the severity of spinal injuries are shown in **Figures 4.6-4.9** for frontal, rear, side impacts in horizontal plane, and rollovers in non-horizontal plane.

Figure 4.6 compares the severity of spinal injury with the horizontal PDoF for frontal impact. Out of 330 cases, 48% and 16 % cases are of MAIS 2 and $\text{MAIS} \geq 3$ respectively. In all, 64% of the injuries are when the PDoF is 12 o'clock, and 25% at 30 degrees.

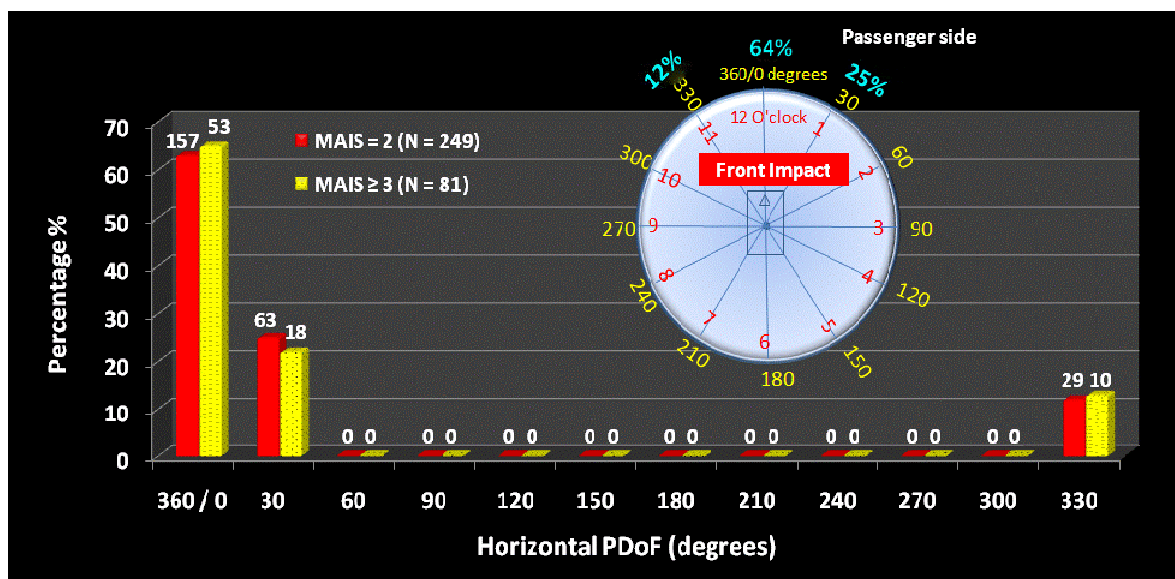


Figure 4.6: Site of spinal injury by PDoF for frontal impact

Figure 4.7 compares the severity of injury in spinal column with the horizontal Principle Direction of Force (PDoF) for rear impact. Out of 54 cases in the study, 35% sustained $\text{MAIS} = 2$ injury at 6 o'clock and another 24% sustained $\text{MAIS} \geq 3$.

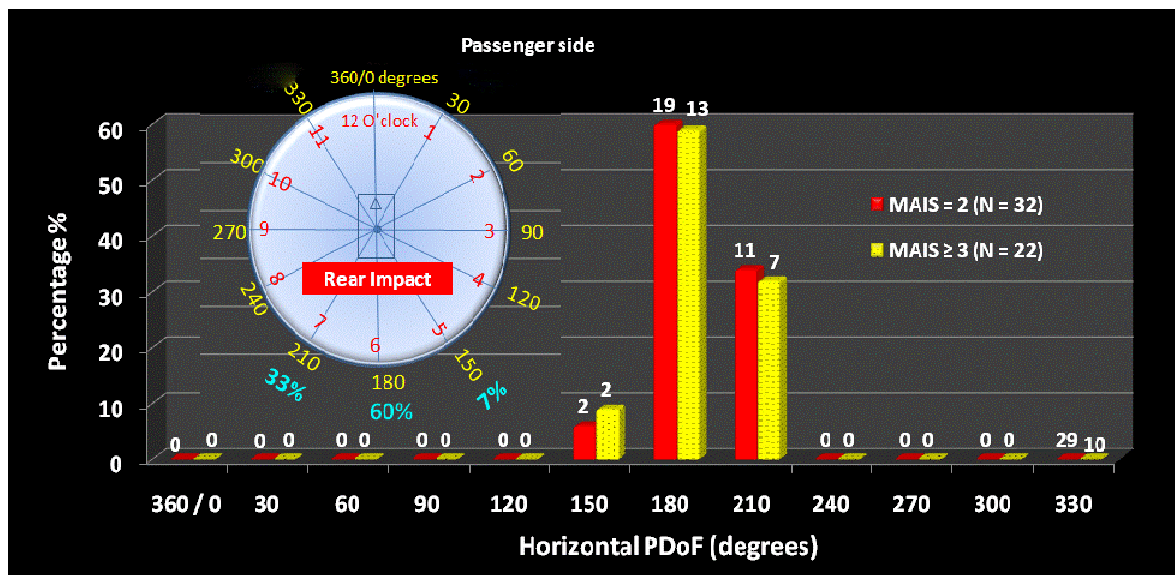


Figure 4.7: Site of spinal injury by PDoF for rear impact

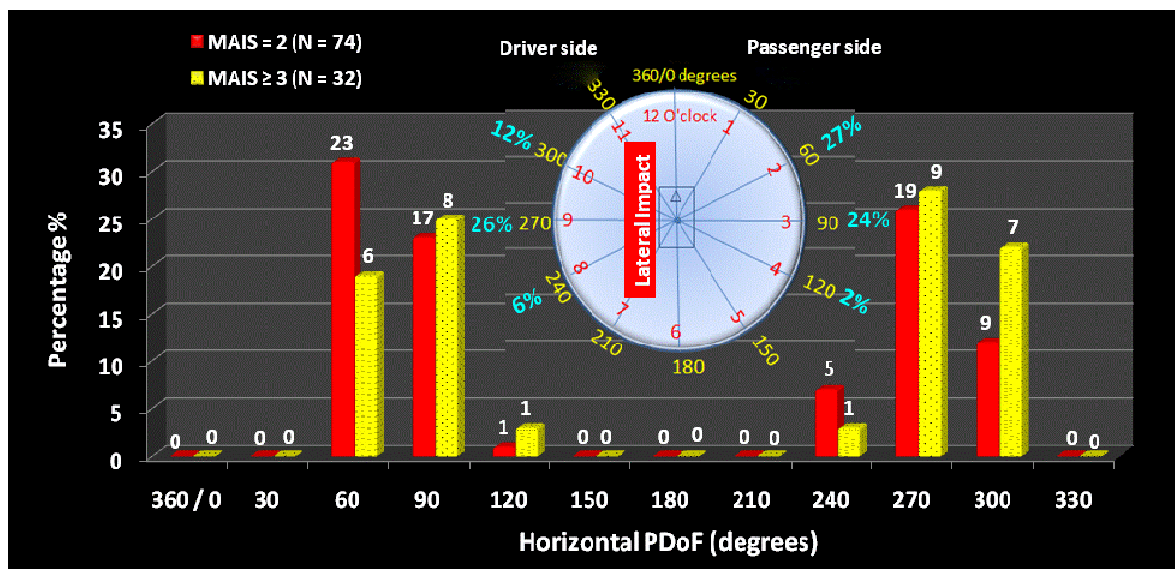


Figure 4.8: Site of spinal injury by PDoF for side impact

Figure 4.8 compares the severity of injury in spinal column with the horizontal PDOF for side impact. It can be observed that the maximum casualties are in the 3 o'clock and 9 o'clock orientations. At 9 o'clock direction of impact, which happens to be on the driver side, 18% cases of MAIS = 2 injury and 9% cases of MAIS \geq 3 injury are observed. At 3 o'clock direction of impact 16% cases of MAIS = 2 injury and 8% cases of MAIS \geq 3 injury are observed. 10 o'clock direction of impact resulted in 7% of MAIS \geq 3 injuries and 2 o'clock direction of impact induced 6% of MAIS \geq 3 injuries.

Figure 4.9 presents the severity of injury in spinal column with the non-horizontal PDoF for rollover. It can be seen that during the rollovers, most of the severe spinal injuries (MAIS \geq 3) occur in rollover when the vehicle tips over to its 1-3 o'clock positions.

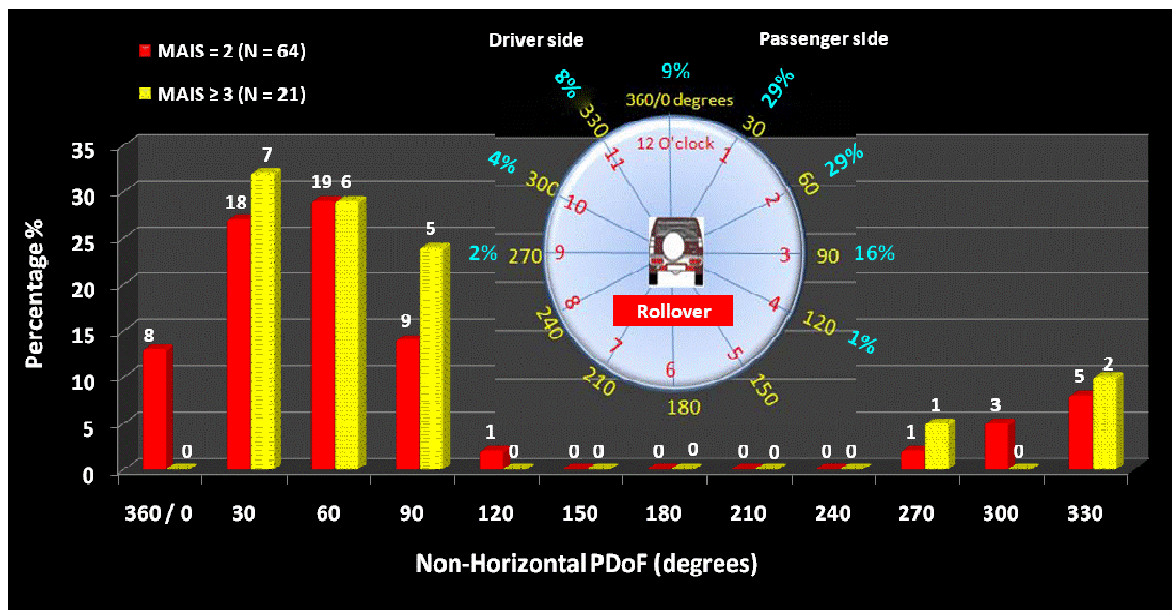


Figure 4.9: Site of spinal injury by non-horizontal PDoF for rollover collisions

4.5 SPINAL INJURY CAUSATION

This section describes the contacts of spinal injury for different types of collision.

Tables 4.4 and 4.5 indicate injury contacts for belted and unbelted occupants respectively.

Table 4.4: Injury contacts by type of collision for belted occupants

Injury Source	Rollover		Vehicle		Fixed object		Camel		Total	
	N	%	N	%	N	%	N	%	N	%
Vehicle glazing	2	6	27	13	5	9	0	0	34	11
Steering wheel / facia	3	9	18	8	10	18	1	11	32	10
Stiff forward structures	2	6	7	3	7	13	0	0	16	5
Seat	1	3	14	6	2	4	0	0	17	5
Restraint components	4	13	20	10	3	5	0	0	27	9
Stiff side structures	4	13	12	5	6	11	1	11	23	7
Other side structures	2	6	13	6	3	5	0	0	18	6
Roof	7	23	9	4	0	0	4	44	20	6
Occupant / luggage	2	6	5	2	0	0	0	0	7	2
Intruding object	2	6	18	9	9	16	0	0	29	10
Non-contact	3	9	72	34	12	22	0	0	87	28
Camel's body	0	0	0	0	0	0	3	33	3	1
Total	32	100	215	100	57	100	9	100	313	100

Table 4.5: Injury contacts by type of collision for non-belted occupants

Injury Source	Rollover		Vehicle		Fixed object		Camel		Total	
	N	%	N	%	N	%	N	%	N	%
Vehicle glazing	20	39	40	18	3	6	0	0	63	19
Steering wheel / facia	0	0	16	7	5	9	0	0	21	6
Stiff forward structures	0	0	9	4	6	9	0	0	15	4
Seat	0	0	22	10	15	28	0	0	37	11
Restraint components	0	0	2	1	0	0	0	0	2	1
Stiff side structures	5	9	13	6	2	4	0	0	20	6
Other side structures	1	2	29	13	3	6	0	0	33	10
Roof	13	25	11	5	0	0	4	33	28	8
Occupant / luggage	4	7	7	3	1	2	0	0	12	3
Intruding object	9	18	27	12	13	23	0	0	49	14
Non-contact	0	0	47	21	7	13	0	0	54	16
Camel's body	0	0	0	0	0	0	7	67	7	2
Total	52	100	223	100	55	100	11	100	341	100

The influence of injury mechanism on spinal injuries for both occupant and pedestrian was also investigated and shown in **Figure 4.10**. For occupants, it can be noticed that interior sources and non-contact are the main causes for cervical injuries. Injuries to thoracic spine were mainly due contact with stiff side structures. Also, the seat, luggage, and other side structures predominated in the cause of lumbar spine. For pedestrians, the probable causes for cervical injuries are the bonnet surface and windshield glazing. Bonnet edge/trim and ground are the frequent causes for sacral injuries (Al-Shammari et al., 2010b).

4.6 DEFORMATION AND INTRUSION

In this section the effect of deformation and intrusion on spinal injury outcome was evaluated. Injuries were categorized according to AIS, separately for car collisions and rollovers. They were then plotted against the maximum intrusion and depth of deformation.

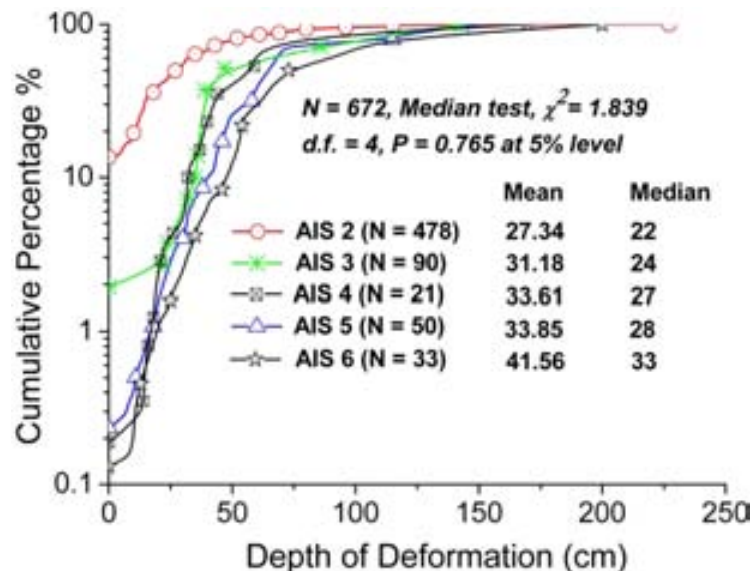


Figure 4.11: Effect of maximum deformation on spinal injury in car collisions

Figure 4.11 plots the severity of spinal injuries as a function of vehicle deformations. It is observed that probability of an $\text{AIS} \geq 4$ injury is significantly less in low deformation crashes. This supports the hypothesis that low deformations often cause low injuries.

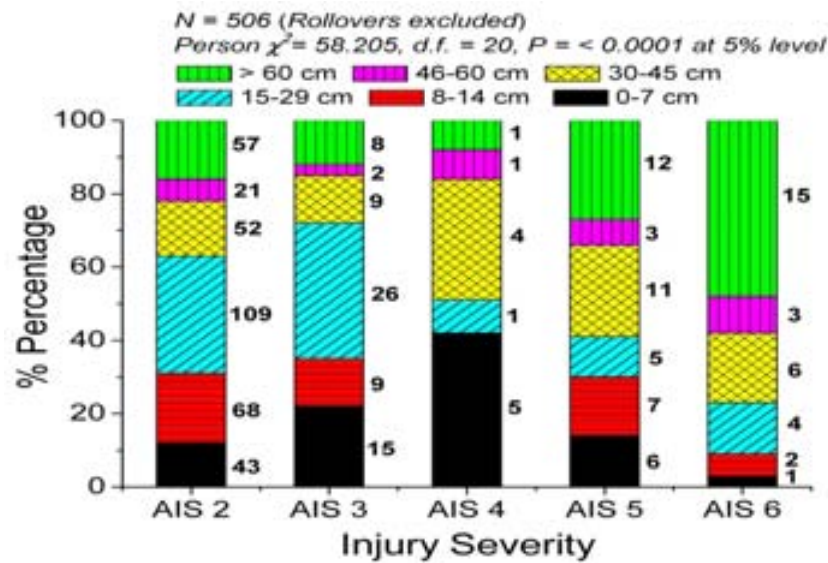


Figure 4.12: Severity of spinal injury versus intrusion for car collisions

Severity of spinal injury versus intrusion is summarized in **Figure 4.12**. It can be observed that spinal injuries of AIS 2 and 3 levels can occur even at lower levels of intrusion distances (< 30 cm). On the other hand higher levels of spine injury severity ($\text{AIS} \geq 4$) are observed at higher intrusion levels. It can be concluded that extent of intrusion has a significant influence on the likelihood of spinal injury.

The distribution of occupant spinal injuries in intrusion for rollover type collisions were also identified in this study and are shown in **Figure 4.13**. It is observed that 11% of all injuries occurred at roof deformation more than 15 cm which exceeded the requirement of the FMVSS 216 standard (NHTSA, 2005).

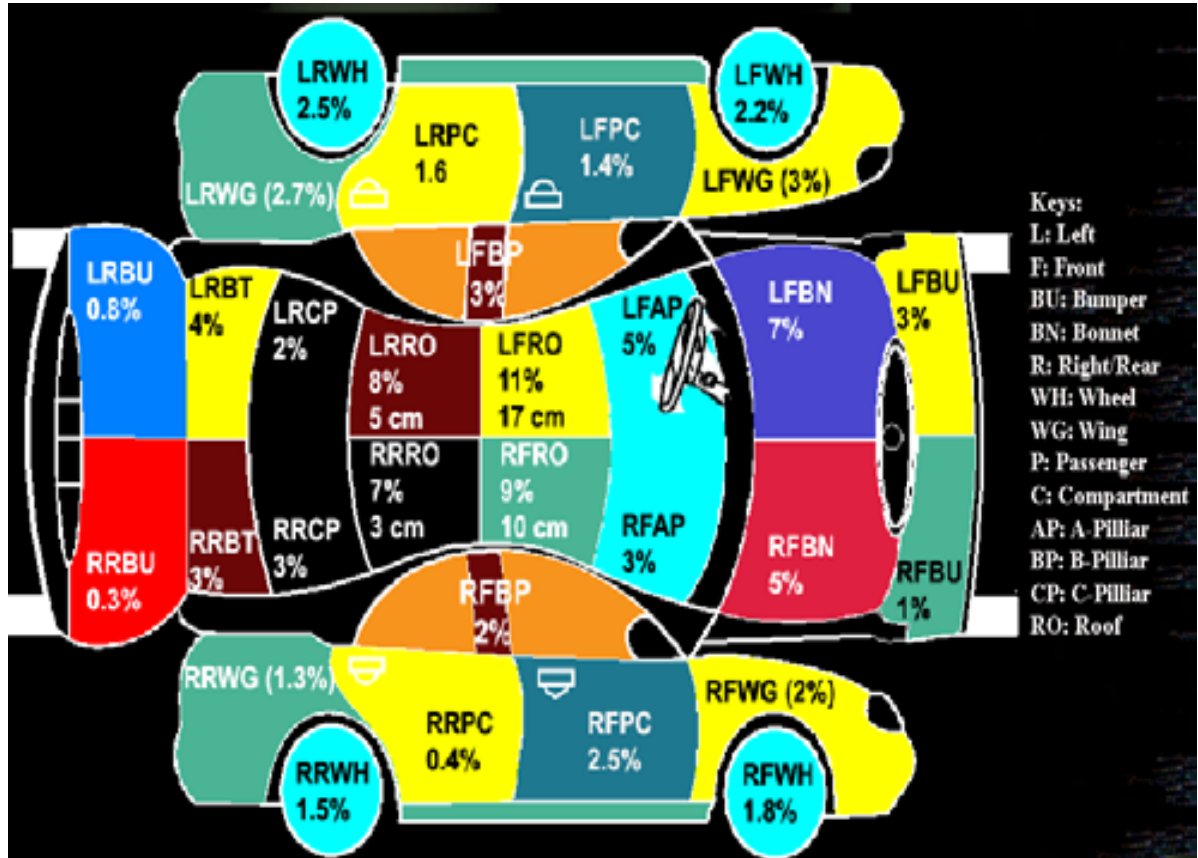


Figure 4.13: Distribution of occupant spinal injuries and intrusion for rollovers

In case of rollovers spinal injuries due to roof intrusion are the most frequent (Conroy et al., 2006). In this study, 11% injuries are observed when there is a driver roof intrusion followed by the co-driver side roof intrusion. Injuries due to roof intrusions are followed by A-pillar intrusion and roof intrusion at rear passenger side roof. In around 5-7% cases of spinal injury bonnet intrusion was observed. In general it is observed that the maximum intrusion was measured at the area adjacent to the struck-side occupant.

4.7 RESTRAINT USE AND SPINAL INJURY

The relationship between belt use and spinal injury outcome was examined in all cases where the belt use conditions could be verified. 209 (44%) occupants had used a restraint as opposed to 261 (56%) who had not. An association was found, so that unrestrained occupants are more likely to sustain spinal injury as shown in **Figure 4.14**. This is as expected, as there are several mitigating circumstances (Rivara et al., 2000).

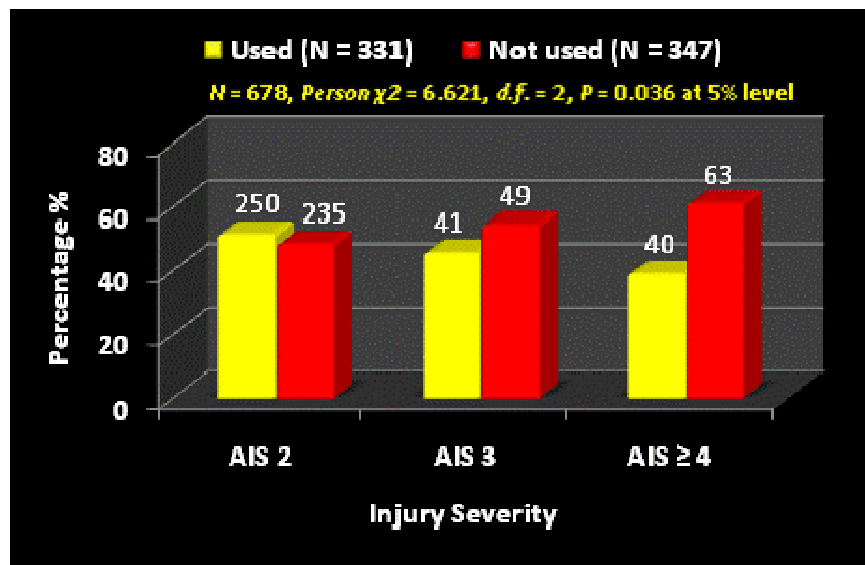


Figure 4.14: Effect of belt wearing on outcome of spinal injury

In addition, **Figure 4.14** gives the impression of a slight trend towards more severe injury if the belt was not used. In contrast, there was a reduction in severity of spinal injuries when the seat belt was used. Although only 44% of occupants were used their seatbelt in this study, this result indicates that a high proportion of spinal injuries in Saudi Arabia can be prevented if the usage of seat belts increases (Bendak, 2005).

Further analysis conducted to test the relationship between the belt use and type of spinal injury as illustrated in **Figure 4.15**. Restraint use was found to significantly influence the type of spinal injury sustained in vehicle crashes. It can be seen that the neck and thoracic injuries are less for belted occupants. However, more lumbar injuries are more common for belted occupants. This result is expected because chance injuries are mostly associated with seatbelt use as shown in **Section 7.4.2**. Seatbelt use is shown to reduce the incidence of sacral injuries, since these type of injuries are mainly caused by ejection.

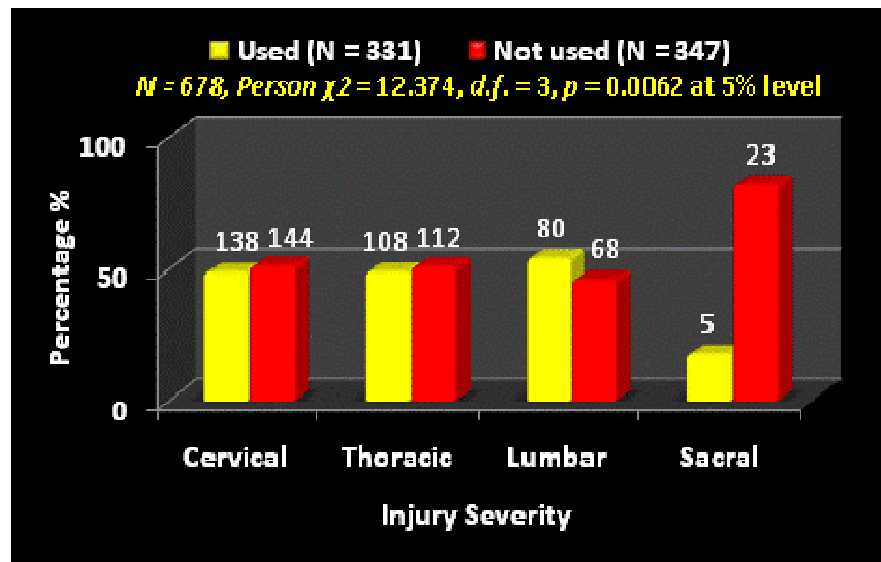


Figure 4.15: Type of spinal injury versus restraint use

It is clear that seat belt use significantly alters the dynamics of the head-neck complex as drivers in frontal impacts often suffer a head strike on the steering wheel when the seat belt is not used. Similarly, when the seat belt is not used a high proportion of the thoracic and lumbar spine injuries are due to contact with side structures, and loads transmitted through the seat from occupants or luggage.

Table 4.6 shows the injury rate by seatbelt use. For belted occupants, 12% experienced AIS ≥ 4 injuries at an incidence rate of 0.71; while for the unbelted occupants, the rate was 1.70 which was more than twice that for the belted occupants.

Table 4.6: Incidence rates of spinal injury by restraint use

Restraint Use	Severity of Spinal Injury (AIS)					
	Unrestrained			Restrained		
	AIS 2	AIS 3	AIS ≥ 4	AIS 2	AIS 3	AIS ≥ 4
Spinal Injury	235	49	63	250	41	40
Occupants	210	38	37	174	39	56
Incidence Rate	1.12	1.28	1.70	1.43	1.05	0.71

4.8 EJECTION AND SPINAL INJURY

Occupant ejection from motor vehicles has long been considered to be a contributor to death and serious injury in RTAs (Campbell, 1966). The following analysis related to occupants who were ejected to assess the risk of fatality in both the ejected and the non-ejected occupants. Occupant ejection was deemed to have occurred after careful study of the data obtained from vehicle examination, injury details and their causes. A total of 100 injuries of 63 occupants were identified as being ejected indicating an ejection incidence of 13%, and 1.58 injury rate per occupant. Incidence of ejection was identified to be high in Saudi Arabia, suggesting that further investigation of these parameters is needed.

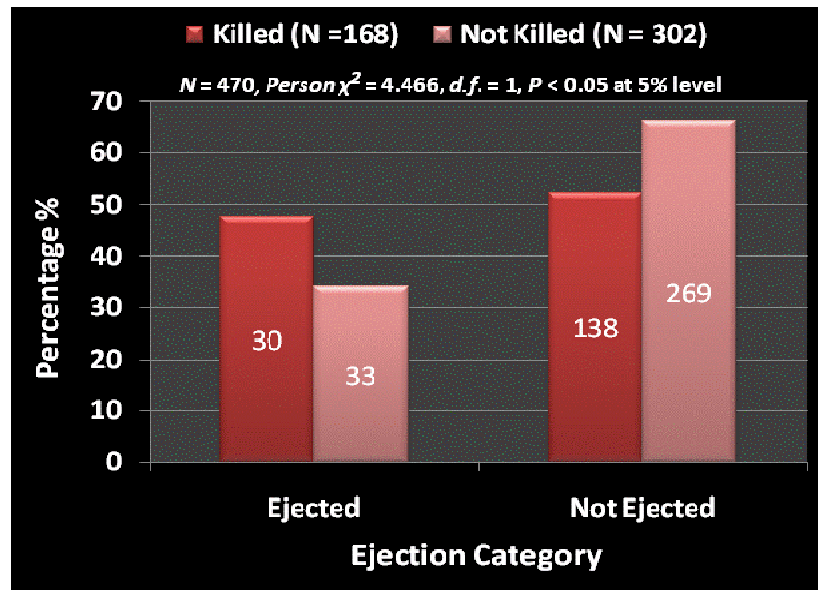


Figure 4.16: Effect of ejection on the fatality of spinal injuries in RTAs

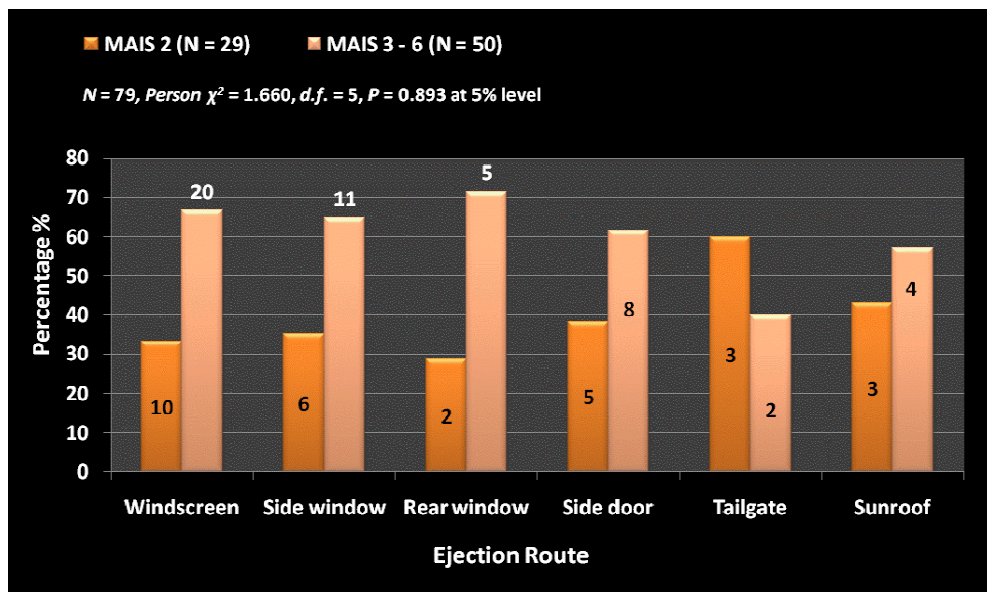


Figure 4.17: Ejection risk by portal type

Ejection tends to result in more severe spinal injuries to the occupants in vehicle crashes. **Figure 4.16** shows the relationship between numbers of occupants killed and not killed against the number of occupants ejected and not ejected. It can be seen that the risk of fatal injuries is significantly higher among ejected occupants.

In this analysis, the actual egress routes were identified for 52 occupants as shown in **Figure 4.17**. The major ejection portal was the windscreen (38% or 30/79) which would normally be as a result of a frontal impact. Side windows followed by side doors accounted for 22% and 17% of ejection routes respectively. Occupants ejected via these routes will almost certainly have exited during side impact and rollover accidents since occupant motion during these two types of collision would normally be towards these apertures.

There is no statistical relationship between ejection portal and MAIS. Therefore, an occupant is ejected through, for example a side window, is as likely to sustain non-to-moderate MAIS injury as a serious-to-maximum AIS spinal injury.

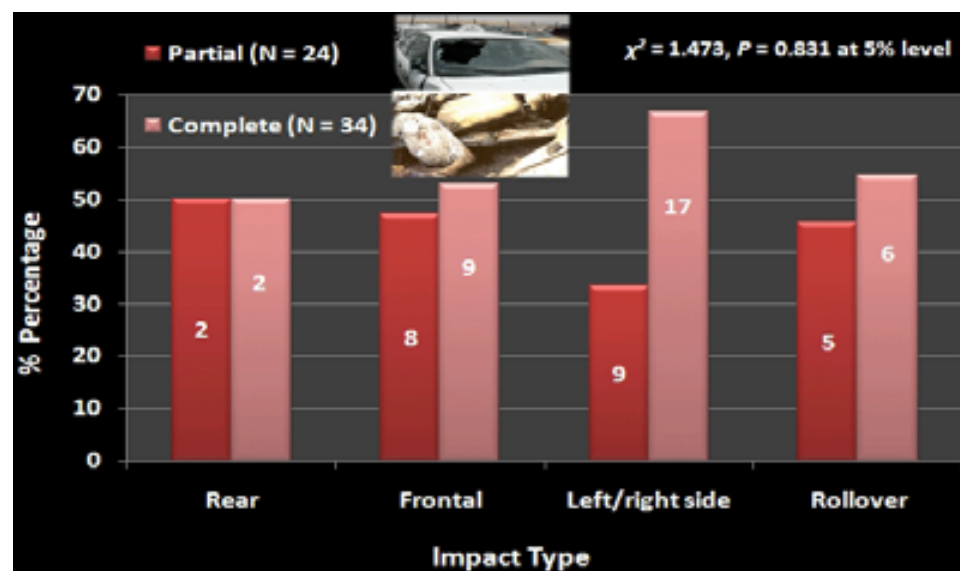


Figure 4.18: Impact classification for ejected occupants

The influence of impact direction on the ejection type was also investigated and presented in **Figure 4.18**. Side impacts account for 45% of all ejections, while frontal impacts account for only 29%. Rollover crashes account for 17% of ejections and rear impacts 7%.

The effectiveness of seat belts in preventing ejection was also analysed. The results are shown in **Figure 4.19**. The analysis shows quite clearly that there is a significantly greater risk of partial ejection if the seat belt is worn and also a significantly greater risk of total ejection if the seat belt is not worn. 86% of ejected occupants who had worn the belt were partially ejected and only 14% were completely ejected. Of occupants not using seat belts, 37% were partially ejected while 63% were completely ejected. The evidence presented overwhelmingly supports the notion that total ejections are a rarity among restrained occupants and are far likely for unrestrained occupants.

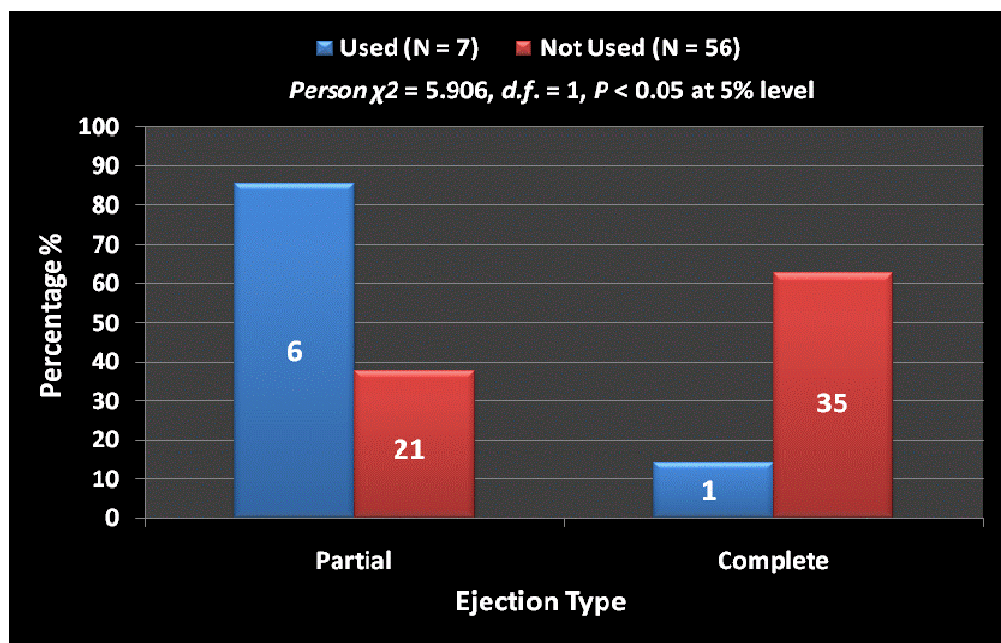


Figure 4.19: Ejection type by belt use

The distribution of spinal injuries for both ejected and non-ejected occupants were also identified as shown in **Figure 4.20**. Ejected occupants are more likely to sustain cervical (55%), and sacral (8%) injuries than the non-ejected occupants. This high rate of incidence is expected since the cervical region is most likely to strike the glazing (and ejection portal) during the ejection sequence (Parenteau et al., 2001).

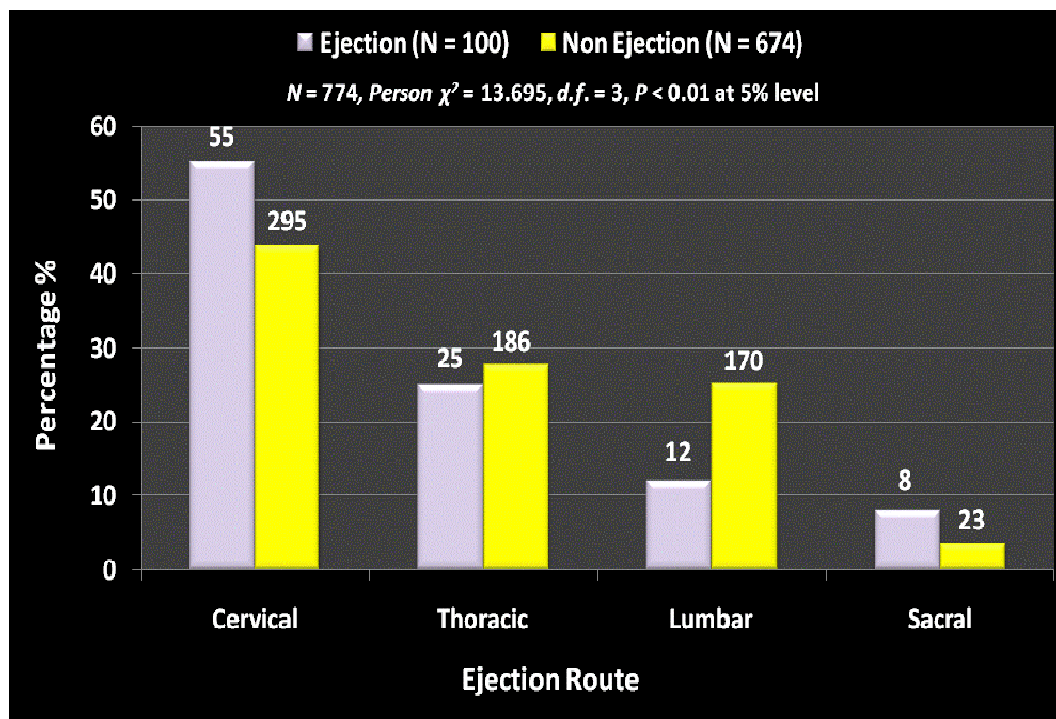


Figure 4.20: Type of spinal injuries for ejected and non-ejected occupants

4.9 CONCLUSIONS

In this study, the epidemiology of spinal injuries due to RTAs has been studied on the basis of data collected through from the city of Riyadh, Saudi Arabia. This is the first attempt to collect crash data and study spinal injury in the Saudi Arabia, where until the time of writing this thesis, no in-depth crash database was available. This study has been successful in developing a sufficiently in-depth database which can then be interrogated to address the problem of spinal injuries in Saudi Arabia. A number of conclusions are drawn as follows:

- 1- Over half of the spinal injuries sustained are cervical, and a significant number of those involve cord damage. Thoracic and lumbar spinal injury is predominately fracture, without associated cord damage.
- 2- While at all levels of injury severity, car to car impacts accounted for about 61% of the injuries in the study. It was interesting to note that 34% of injuries were generated in collisions with vehicles other than cars. This suggests that these injuries may not be adequately addressed by the European or US test standards and tests since the mass and the height of the test barrier in either test cannot compare to the mass and height of a standard European/US heavy goods vehicle.
- 3- Correlation between the spinal region injured and the direction of impact was studied. While cervical, thoracic and lumbar spine injuries were associated with frontal impacts followed by side impacts, sacral injuries were more sustained in side crashes which might be associated with ejection.
- 4- Most of the spinal injuries associated with rollover accidents were mainly found to be in the cervical region with a high severity.

- 5- The study has identified the sources of contact in spinal injuries. The cervical spine is particularly prone to deceleration injury. The thoracic spine is particularly prone to injury from impacts to the side of the occupant. Lumbar injury occurs frequently when the seat is loaded by occupants or luggage.
- 6- The common source of contact for AIS 2 spinal injuries was found to be the vehicle interiors, such as front stiff components, while about a quarter are non-contact type injuries. Only 25% of the AIS 3 and 27% of the AIS ≥ 4 spinal injuries occurred through contact with exterior objects. It can be concluded that the detailed distribution of the source of injury gives an insight into which parts of the vehicle cause injury to the different parts of the spine.
- 7- The high incidence of injury to all areas of the spine from the roof illustrates the vulnerability of the spine to compressive loads transmitted via a head contact. However, the complex dynamics of vehicles in rollovers involves a number of different timings of occupant motion in the vehicle during roof crush events.
- 8- Spinal injury severity is seen to correlate with the extent of intrusion. AIS ≥ 4 injuries were more common in cases of intrusion above 30 cm.
- 9- The current frontal barrier, and side impact test requirements do not take into account differences in the mechanism of the spinal injury. Furthermore, they do not address the issue of spine contacts on exterior objects. Thus, further refinement of the Neck Injury Criteria is required to ensure a more comprehensive injury coverage.
- 10- The dynamic biofidelity of the **Anthropomorphic Test Device (ATD) Neck** (accuracy of load transmission to the neck via head/face contact) is required for credible injury assessment using ATD neck force and moment measurements.

- 11- Restraint use was found to reduce the ejection, and affect the severity and the level of spinal injury sustained in cervical, thoracic or lumbar regions. This is expected as in an impact the seatbelt reduces head velocity at time of vehicle contact. This indicates that a large number of spinal injuries in Saudi Arabia can be saved.
- 12- Even though a distinction could not be made based on the type (full / partial) of ejection and the ejection portal, this study has shown that almost half of ejected occupants (48%) were killed compared to 34% of the non-ejected occupants.
- 13- It is also important to note that the most common routes for partial and full ejections are the windscreen (38%), followed by side windows (22%) and the side doors (17%) respectively. Ejections are found to be most frequent in side impact followed by frontal impact and then rollover collisions. It is also observed that the cervical and thoracic are the most likely spinal areas to be injured in ejection accidents (83%).
- 14- It was found that a significant number of the cervical injuries were life threatening, whereas almost all the thoracic and lumbar injuries were not.
- 15- Moderate to fatal spinal injury rarely occurs in isolation. The head and face is very often fatally injured as well, as is the chest. The location of other moderate to fatally injured body regions are generally close to the spinal injury site.
- 16- In addition to the spinal injuries in this study (AIS 2+), there were less catastrophic spine injuries, such as fractures, whiplash injuries (AIS 1), and degenerative conditions that are produced by motor vehicle crashes in Saudi Arabia. While less severe, these also create significant rates of disability and costs in health care system.

CHAPTER 5

RISK OF SUSTAINING SPINAL INJURY FROM VEHICLE CRASHES IN SAUDI ARABIA

Accident severity is of special concern in traffic safety. The present research is aimed not only at prevention of spinal injury but also at reduction of its severity. One of the steps in accomplishing the latter is to identify the most probable factors that affect crash severity. In recent years, crashes related to spinal injuries have been of interest because their influence on the casualties' social and financial environment is significant. There have been numerous studies on the biomechanics of spine, and spinal injuries as found in literature. However, few studies have defined the risk of spinal injury and no studies have examined the risk factors and patterns of severe spinal injuries in vehicle crashes.

The concept of risk can be interpreted according to its scientific context. In traffic safety, it is common to define the risk of spinal injury as the probability of serious injury using the Maximum Abbreviated Injury Scale (MAIS), given that the occupant was injured during a vehicle crash. This study aims to derive improved logistic regression models which relate occupant, vehicle and impact characteristics to the probability of spinal injury based on real-world accidental data. The resulting risk curves should offer assistance and guidance for future occupant safety strategies. In particular, they would be useful for quantifying benefit and effectiveness of proposed safety measures.

5.1 METHODS AND MATERIALS

The purpose of this study is to examine the contribution of crash variables to the risk of spinal injury. Collision data were derived from the multi-centred study which was described in **Chapter 4**. The conceptual model for this study is shown in **Figure 5.1**.

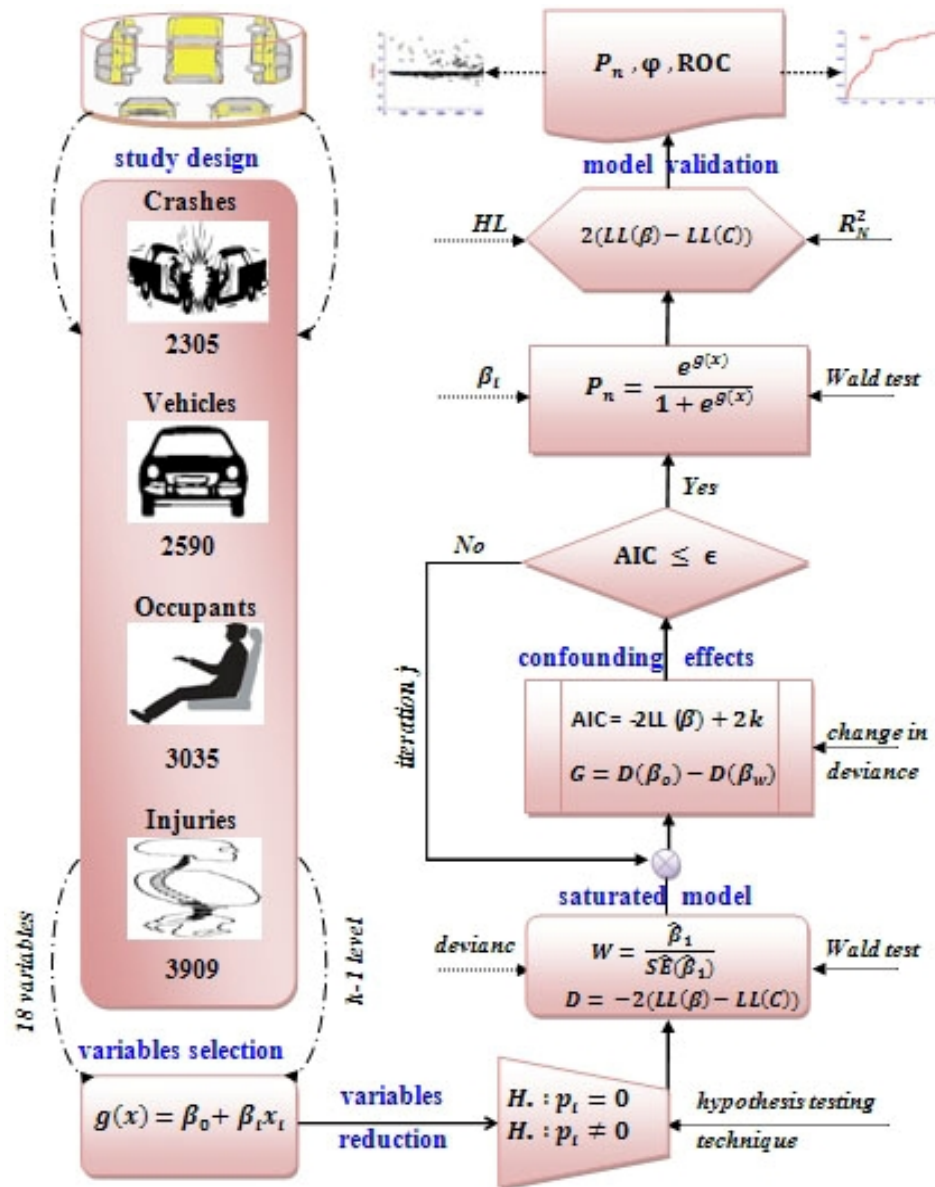


Figure 5.1: Schematic process of the spinal injury logistic modelling

Equivalent Test Speed (ETS) has traditionally been used as a measure of crash severity and predictor for occupant injury for vehicular crashes. All vehicle crashes where ETS or any other crash data was missing were excluded from the study. Due to the differences in the spine anatomy between children and adults, children were deleted from the sample. As a result, 906 occupants were excluded from the sample. Hence, the final sample consisted of 3,035 occupants who sustained 3,909 MAIS ≥ 1 spinal injuries.

In this study, the hypothesis that a crash event will result in a serious to fatal spinal injury based on input crash variables was tested. The response variable, severity of spinal injury (MAIS ≥ 3 or MAIS 1-2), is a binary or dichotomous variable. Therefore, logistic regression statistical modelling is a suitable technique as it predicts the likelihood of a binary dependent variable as a function of predictor variables (Hooper et al., 2006; Asbridge et al., 2005). The probability of serious spinal injury can be given by

$$P(MAIS \geq 3) = \frac{e^{g(x)}}{1 + e^{g(x)}} \quad (5.1)$$

Where $g(x)$ is a function of the independent variables.

$$g(x) = \beta_0 + \beta_1 x_1 + \beta_2 x_2 + \dots + \beta_n x_n \quad (5.2)$$

The model was constructed by an iterative maximum likelihood procedure by using multi-dimensional logistic regression in SPSS 17 (Norusis, 2010). The various statistical parameters and a brief description of the statistical test used for the analysis are summarised in **Table 5.1**. The variable definitions were explained in details in **Chapter 4**. More details of the technique can be found in literature (Cramer, 2003; Feinberg, 1980; Agresti, 2002; Hooper et al., 2006; Asbridge et al., 2005 and others).

Table 5.1: Statistical methods used for the logistic regression model

Task	Method	Comments
Study design	Variables, from occupant, vehicle, and crash characteristics, that significantly influence spinal injuries, were designed based on past studies, current knowledge and expert judgment.	<ul style="list-style-type: none"> The final sample included 3,035 occupants and 3,909 MAIS ≥ 3 spinal injuries
Variables selection	Dummy variables were selected using the generalized linear method to have $k-1$ design variables for the k levels of the nominal scale of that variable.	<ul style="list-style-type: none"> 18 variables including 56 levels were selected for analysis of this study
Variables reduction	The hypothesis testing technique for proportions was used to decide whether the number of levels for a design variable could be reduced.	<ul style="list-style-type: none"> $H_0: p_i = 0, H_a: p_i \neq 0$ where p_i is the proportion of class i (level i) within the design variable. 16 levels were reduced
Saturated model	All variables with no interactions (saturated model) were tested on the basis of the deviance (D) and the Wald (W) statistic. The goal was to eliminate in the beginning, those variables that were not significant.	<ul style="list-style-type: none"> $W = \frac{\hat{\beta}_1}{SE(\hat{\beta}_1)}$ $D = -2(LL(\beta) - LL(C))$ 5 variables found to be significant by W and D tests
Interaction effects	The confounding effect was tested using the change in deviance (G). Final variables were selected at a minimum value of Akaike's (AIC).	<ul style="list-style-type: none"> $G = D(\beta_o) - D(\beta_w)$ $AIC = -2LL(\beta) + 2k$ Cofounding was presented in two variables
Final logit model	The coefficients of the final model, their confidence intervals, and the p -values were determined.	<ul style="list-style-type: none"> $g(x) = \beta_0 + \beta_i x_i$ 4 variables were retained
	95% Wald CI for $\exp(\hat{\beta}_j)$	<ul style="list-style-type: none"> $\exp(\hat{\beta}_j \pm z_{1-\frac{\alpha}{2}} SE_{\hat{\beta}_j})$
Validation of the model	The overall goodness-of-fit was tested by using Pearson χ^2 , D , W , and the Hosmer–Lemeshow (HL) tests.	<ul style="list-style-type: none"> $\chi^2_{HL} = \sum_{k=1}^g \frac{(O_{1k} - E_{1k})^2}{E_{1k}(1 - \xi_K)}$
	The Cox-Snell R^2 and Nagelkerke R^2 were attempted to provide a logistic analogy to R^2 in ordinary linear regression.	<ul style="list-style-type: none"> $R_N^2 = \frac{R_{CS}^2}{1 - L(B^{(0)})^{2/n}}$
Model interpretation	The interpretation involved three measures: probability(P), Odds Ratio (ϕ), and Receiver Operator characteristic Curve (ROC)	<ul style="list-style-type: none"> $P(MAIS \geq 3) = \frac{e^{g(x)}}{1 + e^{g(x)}}$ $\phi = e^{\beta_a - \beta_b}$ ROC

5.2 DEVELOPMENT OF THE LOGISTIC MODEL

To achieve the goal of this study, 18 crash variables were selected for this purpose.

Table 5.2 summarizes the hypothesis testing for all categorical variables in the study.

Table 5.2: Hypothesis testing for proportions

Variable Description (<i>ABBREVIATION</i>)		x_i	<i>P</i> -value	95% CI		Comments
				Lower	Upper	
Severity <i>SEV</i>	1= MAIS \geq 3	365	0.120	0.097	0.147	The dependent (response) variable
	2= MAIS<3	2670	0.880	0.856	0.902	
Seat type <i>SEATTYP</i>	1=Single seat	2910	0.959	0.944	0.972	Categories 2-3 were combined as a new category
	2=Full width hinged	106	0.035	0.019	0.043	
	3=50/50 split	19	0.006	0.001	0.011	
Occupant seating position <i>POS</i>	1=Driver	1814	0.598	0.556	0.639	Categories 3-5 were combined as a new category
	2=Front seat passenger	690	0.227	0.192	0.263	
	3=Rear seat – centre	90	0.03	0.015	0.044	
	4=Rear seat – nearside	175	0.058	0.038	0.077	
	5=Rear seat – offside	266	0.088	0.054	0.12	
Type of spinal injury <i>SPINETYP</i>	1=Cervical	1306	0.43	0.388	0.472	Categories 3-4 were combined
	2=Thoracic	808	0.266	0.229	0.304	
	3=Lumbar	870	0.287	0.249	0.325	
	4=Sacral	51	0.017	0.006	0.028	
Vehicle type <i>VEHTYP</i>	1=Automobile	2769	0.912	0.889	0.936	Categories 2-4 were combined as a new category (Non-Automobile)
	2=Sport utility vehicle	158	0.052	0.033	0.071	
	3=Van/minivan	17	0.006	-0.001	0.012	
	4=Pickup truck	90	0.03	0.015	0.044	
Seat belt use <i>RESTUSE</i>	1=Neither belted nor airbag	1731	0.570	0.536	0.605	
	2=Aigbag only	132	0.043	0.029	0.057	
	3=Both belted and airbag	1172	0.386	0.352	0.420	
Type of belt <i>BELTTYP</i>	1=Lap and diagonal belt	2956	0.974	0.936	1.1012	Categories 2-3 were combined as Other
	2=Lap belt	62	0.02	0.009	0.032	
	3=Full harness	17	0.006	-0.001	0.012	
Occupant age (years) <i>AGE</i>	1=Adult	2768	0.912	0.892	0.931	
	2=Senior	267	0.088	0.068	0.107	
Impact direction <i>IMPDIR</i>	1=Frontal	2040	0.672	0.633	0.712	
	2=Side	706	0.233	0.197	0.269	
	3=Rear end	288	0.095	0.07	0.12	
Occupant height <i>HEIGHT</i>	1=Lower quartile	927	0.305	0.266	0.344	
	2=Medium	1424	0.469	0.427	0.511	
	3=Upper quartile	684	0.225	0.19	0.261	
Size of vehicle <i>VEHSIZE</i>	1=Small	1729	0.57	0.528	0.612	The category large and mid-size were merged
	2=Midsize	1187	0.391	0.35	0.432	
	3=Large	119	0.039	0.023	0.056	
Occupant weight <i>WEIGHT</i>	1=Light	842	0.277	0.24	0.315	
	2=Well-nourished	1498	0.493	0.451	0.536	
	3=Obese	695	0.229	0.194	0.265	
Ejection status <i>EJEC</i>	1=Ejected	418	0.138	0.109	0.167	
	2=Non Ejected	2617	0.862	0.833	0.891	
Gender of occupant <i>GEND</i>	1=Male	2312	0.762	0.726	0.798	
	2=Female	723	0.238	0.202	0.274	

* The levels indicated in bold are insignificant.

Table 5.3 shows the number of design variables after reduction. For the explanatory variables, ETS is the only continuous variable; the others are categorical.

Table 5.3: Estimated coefficients for the model variables after reduction

Variable	Before Reduction		After Reduction		B_i	SE	$W\text{-test}$	$P\text{-value}$
	Levels	Design Variables	Levels	Design Variables				
COLLTYP (1)	2	1	2	1	-0.005	0.433	0.000	0.991
IMPDIR	3	2	3	2			8.857	0.012
IMPDIR (1)					-1.112	0.496	5.035	0.025
IMPDIR (2)					-0.158	0.538	0.086	0.769
INTR (1)	2	1	2	1	-0.226	0.499	0.206	0.650
EJEC (1)	2	1	2	1	0.262	0.421	0.387	0.534
VEHTYP (1)	4	3	2	1	0.248	0.581	0.182	0.670
VEHSIZE (1)	3	2	2	1	-0.129	0.345	0.139	0.709
RESTUSE	4	3	3	2			7.379	0.025
RESTUSE (1)					-0.776	0.537	2.087	0.149
RESTUSE (2)					0.261	0.488	0.286	0.593
BELTYP (1)	4	3	2	1	0.918	0.664	1.914	0.167
SEATTYP (1)	6	5	2	1	0.084	0.644	0.017	0.896
SEATORT	4	3	4	3			3.722	0.293
SEATORT (1)					0.544	0.587	0.861	0.354
SEATORT (2)					0.077	0.410	0.035	0.852
SEATORT (3)					-0.807	0.626	1.663	0.197
POS (1)	6	5	2	1	-0.687	0.488	1.980	0.159
AGE (1)	3	2	2	1	-0.72	0.619	1.352	0.245
GEND(1)	2	1	2	1	1.271	0.745	2.905	0.088
HEIGHT	3	2	3	2			1.657	0.437
HEIGHT (1)	3	2	3	2	0.260	0.608	0.183	0.669
HEIGHT (2)					-0.295	0.465	0.403	0.526
WEIGHT	3	2	3	2			3.243	0.198
WEIGHT (1)					-0.734	0.942	0.608	0.435
WEIGHT (2)					0.353	0.487	0.526	0.468
BMI (1)	2	1	2	1	-0.002	0.575	0.000	0.997
SPINETYP	4	3	3	2			33.149	0.000
SPINETYP (1)					4.174	0.755	30.54	0.000
SPINETYP (2)					3.19	0.782	16.635	0.000
ETS					0.053	0.008	48.582	0.000
CONSTANT					-9.145	1.664	30.192	0.000

The backward selection process of logistic regression was followed. First, all the variables with no interactions (referred to here as the saturated model) were tested on the basis of the deviance and the Wald (W) statistic. **Table 5.3** presents the results from fitting all the explanatory variables simultaneously. From the W -statistic it appeared that the variables *IMPDIR*, *RESTUSE*, *GEND*, *SPINETYP* and *ETS* showed some significant effect.

Each of these five variables was then removed from the saturated model, one at a time and the change in the value of $-2\log\text{-likelihood}$ was noted. From **Table 5.4**, it can be interpreted that the change on removing the variable *GEND* of the occupant from the model is non-significant ($P = 0.084$). The other four variables were found to be significant.

The four variables found to be statistically significant in the current study were investigated further with the possible terms of interaction by adding each interaction term to the full model. The interaction was found to be statistically significant for the variables *ETS* and *SPINETYP* and hence confounding is seen to be present. According to the previous analysis, the logit model with significant variables was obtained.

Table 5.4: The result of testing interactions

Variable dropped from the saturated model	Change in deviance	$d.f$ (associated with change in deviance)	P -value
IMPDIR*SPINETYP	*	*	*
IMPDIR*ETS	5.064	2	0.0795
SPINETYP*ETS	17.395	2	< 0.001
IMPDIR*RESTUSE	*	*	*
SPINETYP*RESTUSE	*	*	*
ETS*RESTUSE	0.572	2	0.751263

* The cases where model does not converge are not included in the model

Table 5.5 gives the parameter estimates, their confidence intervals, standard error and the P -values for the logistic regression model predicting the spinal injury ($\text{MAIS} \geq 3$).

Table 5.5: Final model properties

Crash Variable	B_i	SE	$W\text{-test}$	$d.f$	$P\text{-value}$	$Exp(B_i)$	95% CI for $Exp(B_i)$	
							Lower	Upper
<i>IMPDIR</i>			14.818	2	0.001			
IMPDIR (1)	1.109	0.469	10.384	1	0.001	3.031	1.209	7.601
IMPDIR (2)	0.368	0.505	0.718	1	0.397	1.445	0.537	3.888
<i>SPINTYPE</i>			3.054	2	0.217			
SPINTYPE (1)	0.2888	1.141	0.012	1	0.912	1.335	0.143	12.493
SPINTYPE (2)	0.768	1.179	1.350	1	0.245	2.155	0.214	21.733
<i>ETS</i>	0.028	0.015	1.919	1	0.166	1.028	0.999	1.059
ETS \times SPINETYP			15.222	2	< 0.001			
ETS \times SPINETYP (1)	0.055	0.018	9.958	1	0.002	1.057	1.020	1.094
ETS \times SPINETYP (2)	0.019	0.018	0.359	1	0.549	1.019	0.984	1.056
<i>RESTUSE</i>			7.018	2	0.03			
RESTUSE (1)	0.126	0.457	2.690	1	0.101	1.134	0.463	2.778
RESTUSE (2)	-0.668	0.427	0.155	1	0.694	0.513	0.222	1.184
CONSTANT	-5.618	1.260	16.95	1	< 0.001	0.004		

Table 5.6: Goodness of fit statistics for the final model

Model Summary			Hosmer and Lemeshow Test		
-2 Log likelihood	Cox & Snell R Square	Nagelkerke R Square	χ^2	$d.f$	$P\text{-value}$
295.021	0.228	0.412	7.366	8	0.498

Table 5.7: Comparison of observed and predicted outcomes

Observed		Predicted		
		Severity of Spinal Injury (<i>SEV</i>)		Percentage Correct
		MAIS 1-2	MAIS ≥ 3	
Severity of Spinal Injury (<i>SEV</i>)	MAIS 1-2	2543	68	97.39
	MAIS ≥ 3	283	141	33.25
Overall Percentage				88.44

5.3 MODEL VALIDATION

The next step is to validate the model. The goodness of fit statistics for the final model is shown in **Table 5.6**. If the final model is used for predicting severity of spinal injury, the observed and predicted outcomes are as shown in **Table 5.7**. It can be interpreted that the model can predict the outcome quite well in the cases when the injury is MAIS 1-2 and predicts poorly in the cases when the spinal injury is $\text{MAIS} \geq 3$. The goodness of fit statistics also indicates that there is scope for model improvement. This can be done either by considering more data points or including more variables in the data set.

Once the model has been fitted, several tests including *Pearson chi square* and *deviance*, the *Wald statistic*, and the *Hosmer–Lemeshow* tests, can be used to determine how effective the model is in describing the response variable, or its goodness of fit (Hosmer and Lemeshow, 1989). These tests resulted in a χ^2 criterion to make the decision on the model fit. The validity of the model was first checked by examining the statistical level of significance using deviance and the Wald statistic, as discussed earlier.

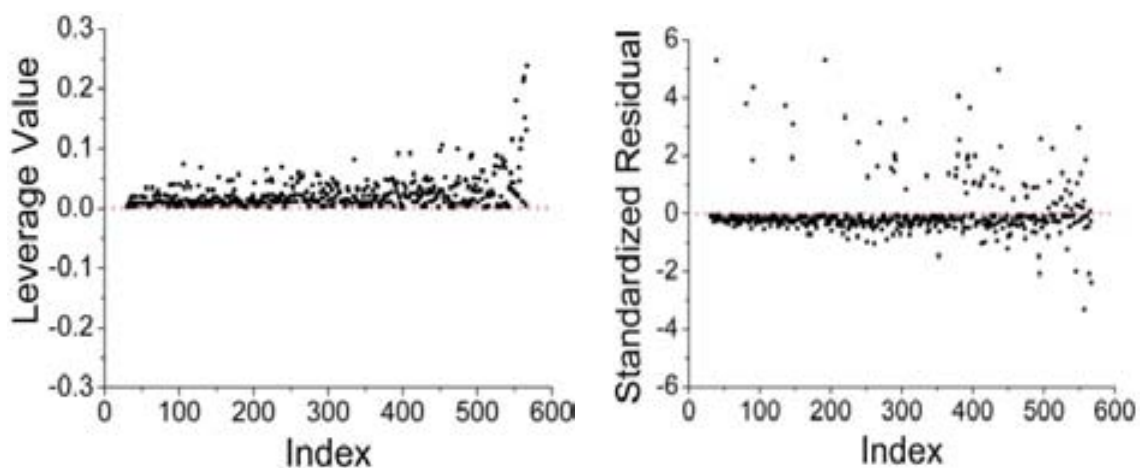


Figure 5.2: Pearson residuals and high leverage plots for graphical assessment

Figure 5.2 shows the plot of Pearson residuals, in which no trend can be detected. Also it shows Hi-Leverage points in which very few points appear to be outliers. The leverage for almost all the cases is very small due to very large number of cases and small number of independents in the model. It is important to note here that influential cases may nonetheless have small leverage values when predicted probabilities < 0.1 or > 0.9 .

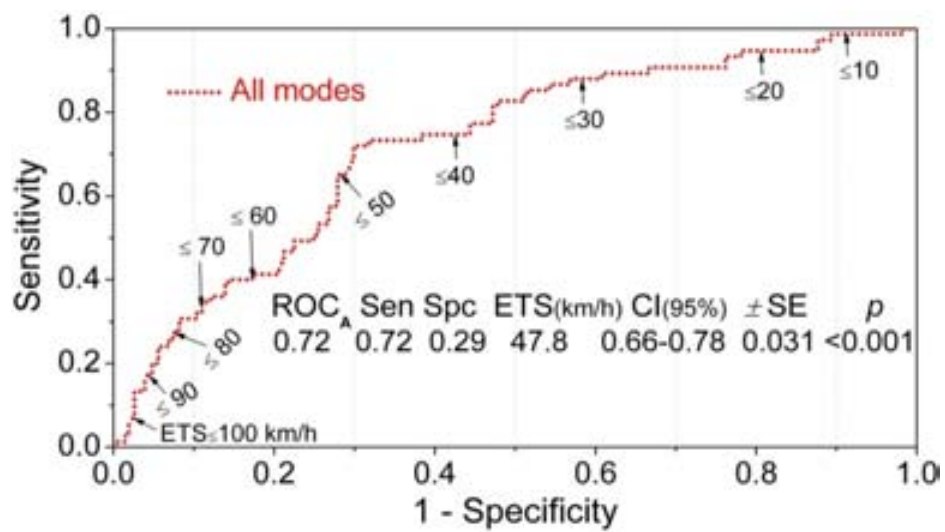


Figure 5.3: ROC curve for various cut-off levels of ETS

Figure 5.3 provides an evaluation for the model accuracy using the **Receiver Operator characteristic Curve (ROC)** at various cut-off ETS-levels. Sensitivity is a numerical measure of how well the model can predict serious injury when serious injury is observed while specificity is a measure of how well the model can avoid predicting injury when no injury is present. The previous graphical assessment provides that while the logistic model fits the data reasonably, there is also a scope to improve it further either by considering more data points or including variables in the data set. However, while this model can be strengthened; the logistic model is fairly robust at this point and can be used for further interpretation.

5.4 MODEL APPLICATIONS

Interpretation of any fitted model requires the ability to draw practical inferences from the estimated coefficients. The relationship between the logistic regression coefficient and the odds ratio provides the foundation for interpretation of all logistic regression results as explained in this section (McCullagh and Nelder, 1989).

Figures 5.4-5.6 show the probability of spinal injury for frontal, side and rear impact for all regions of the spine and equivalent testing speed (ETS). Graphs are plotted for three cases, viz, when the occupant neither belted nor airbag (NB+NA), when only airbag is used (AB) and when both seat belt and airbag are used (SB+AB).

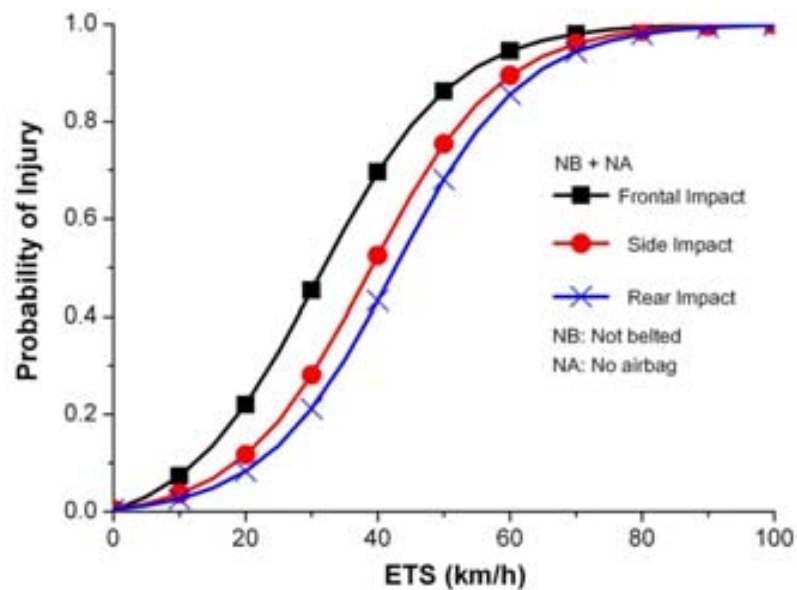


Figure 5.4: Risk of spinal injury for occupants without seatbelt or airbag

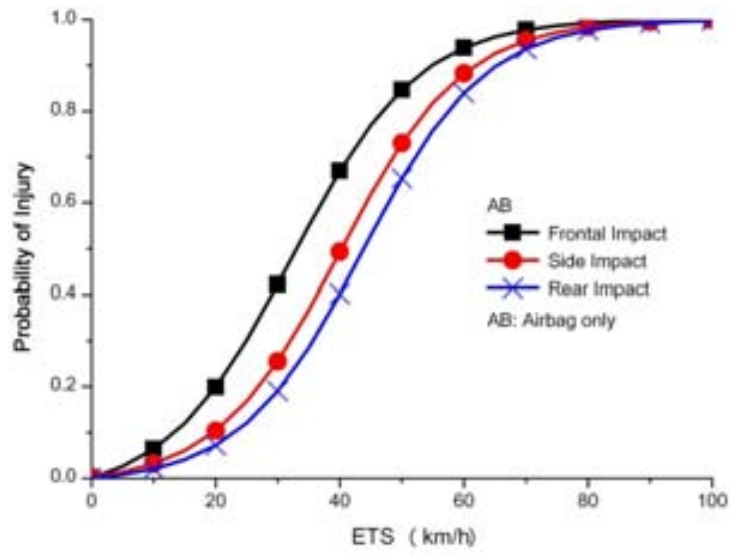


Figure 5.5: Risk of spinal injury for occupants with airbag only

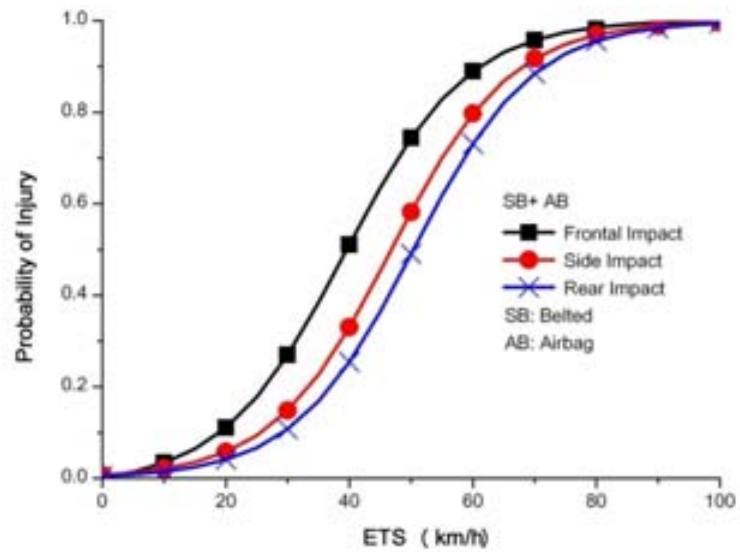


Figure 5.6: Risk of spinal injury for occupants with seatbelts and airbag

The probability of $\text{MAIS} \geq 3$ injuries is the highest in the NB+NA case as compared to the AB case, and are all the lowest in the SB+AB case. In these three cases the graphs tend to shift towards the left (as more restraints are used, that is, from NB+NA to AB to SB+AB).

At low speeds (10-20 km/h), the NB+NA case shows 0.4 to 2 more probability of MAIS ≥ 3 injury in the three directions of impact when compared with the AB case.

The probabilities of MAIS ≥ 3 injuries in frontal impact at 20 km/h are 22%, 19.9% and 11.07% respectively. However at 50 km/h the probability of MAIS ≥ 3 injury in the NB+NA case is 2%, 2% and 3% more than the AB case for front, side and rear impact respectively.

When comparing NB+NA case with the SB+AB case, the probability of MAIS ≥ 3 injuries is 12%, 7% and 19% more when no restraints are used for front, side and rear impact respectively. Additionally, a common observation is that MAIS ≥ 3 spinal injuries are more likely in frontal impacts, then in side impacts and then in rear impacts.

Figures 5.7-5.9 show a comparison of probability of MAIS ≥ 3 in terms of different restraint systems and impact directions for cervical, thoracic and lumbar injuries. Standard ETS test levels (FMVSS 208, 214, and IIHS) of 64, 50 and 32 km/h for front, side and rear impacts respectively are considered (Oagana, 2010).

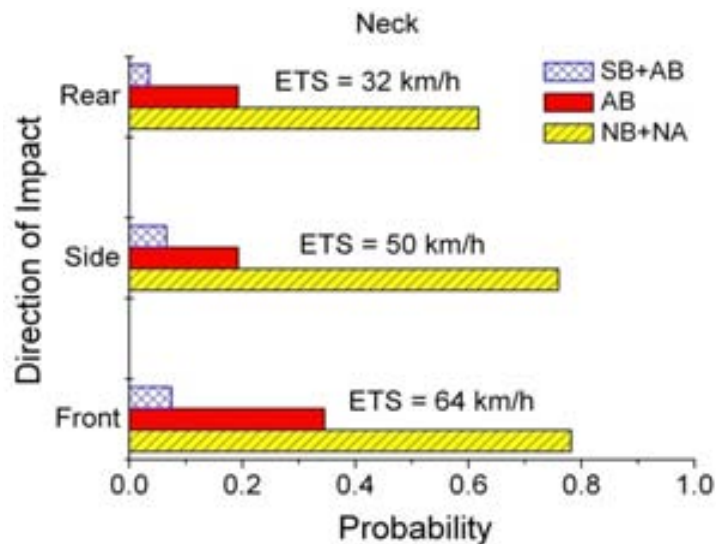


Figure 5.7: Probability of cervical spine injury at ETS test levels for safety legislations

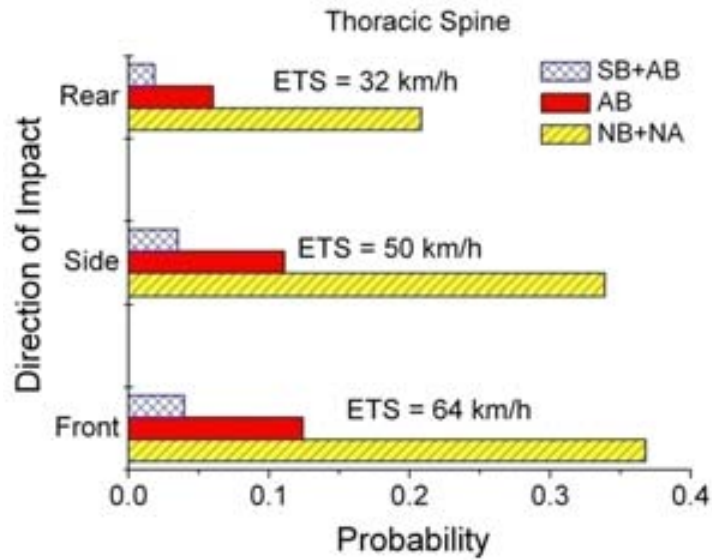


Figure 5.8: Probability of thoracic spine injury at ETS test levels for safety legislations

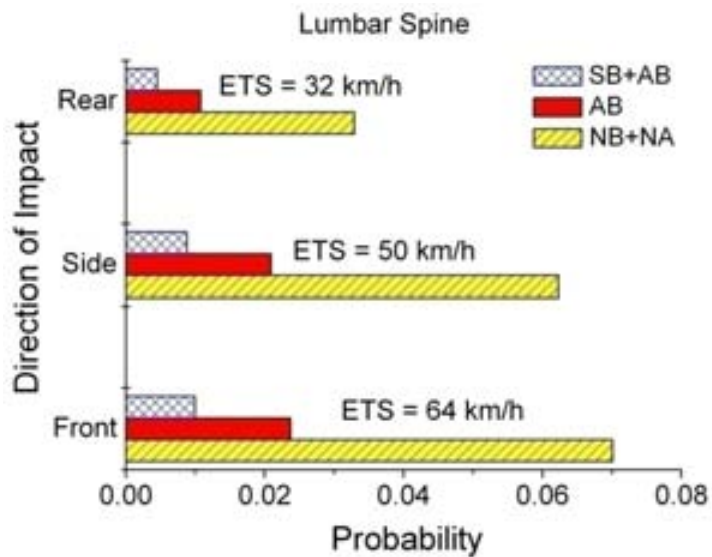


Figure 5.9: Probability of lumbar spine injury at ETS test levels for safety legislations

The pattern of variation is very similar in all the three cases. Occupants without seat belts and without airbags are more prone to injuries. Airbags reduce the probability of moderate to fatal cervical injury (MAIS ≥ 3) by 44% (front impact), 57% (side impact) and 43% (rear impact) (see **Figure 5.7**). Thoracic injuries are reduced by 25% (front impact), 23% (side impact) and 15% (rear impact) (see **Figure 5.8**) and lumbar injuries are reduced by 5% (front impact), 4% (side impact) and 2% (rear impact) (see **Figure 5.9**).

It can also be observed that when both seat belt and airbag are used, the chances of cervical injury are significantly reduced. Cervical injuries are reduced by 71% (front impact), 70% (side impact) and 58% (rear impact) (see **Figure 5.7**). Thoracic injuries are reduced by 33% (front impact), 30% (side impact) and 19% (rear impact) (see **Figure 5.8**) and lumbar injuries are reduced by 6% (front impact), 5% (side impact) and 3% (rear impact), as shown in **Figure 5.9**. It can be concluded that both seat belts and air bags contribute significantly towards reducing the probability of serious spinal injuries in vehicle crashes.

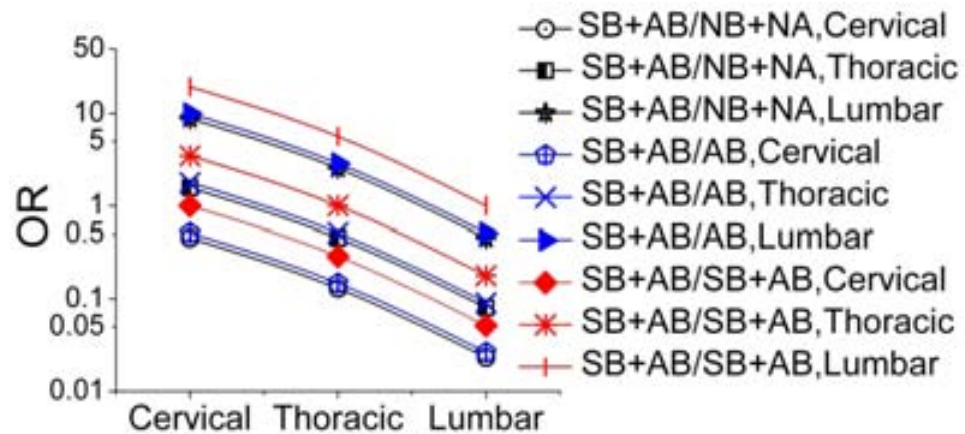


Figure 5.10: Adjusted odds ratio of spinal injury by type of injury

Figure 5.10 assesses the **Adjusted Odds Ratio (AOR)** for some crash parameters with relative to (/) other factors. It is classified into three groups by type of spinal injury, type of impact, and type of restrained used. For instance, the curve titled “*SB+AB/AB, Cervical*” shows that occupants using an airbag alone were 1.96 times (OR=0.51) more likely to suffer a cervical spine fracture than occupants restrained with an airbag and a seatbelt.

Also, occupants without any protective device “*SB+AB/NB+NA, Cervical*” were 2.23 times (OR=0.45) more likely to suffer a cervical spine fracture than those protected with an airbag and a seatbelt. Presentation of odds in a matrix format, as described in this study, provides a simple method for interpretation.

The model can thus be used to estimate the odds ratio in order to assess the odds of an occupant being injured in a crash by a serious spinal injury as compared to his chance of getting a serious spinal injury in other crash scenarios. This method can help in determining the most likely risk-factors in spinal injury-related crashes.

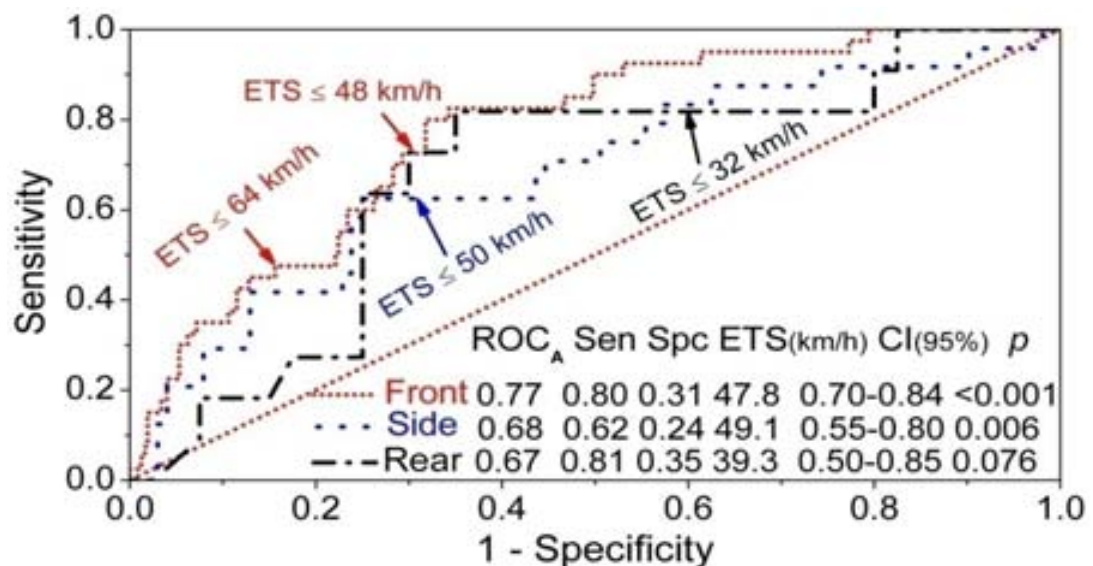


Figure 5.11: Optimum ETS values for various crash modes by using ROC

ROC graph curves as generated by SPSS are shown for three of impact directions in **Figure 5.11**. Optimum sensitivity and specificity values, as well as the ETS thresholds returned, are shown for each factor. The analysis indicates that the current criterion may exclude a substantial body of severe neck injuries involved in different modes of impacts. This would suggest that higher or lower thresholds may be adapted.

5.5 CONCLUSIONS

This study was conducted at deriving an improved logistic regression models which relate occupant, vehicle and impact characteristics to the probability of spinal injury based on real-world accidental data. A total of 3,035 occupants involved in serious traffic accidents and sustained spinal injuries were sampled. The main conclusions are:

- 1- Since the response variable is of a binary nature (i.e. has two categories - serious or non-serious), the logistic regression technique was used to develop the model in this study. The intent was to provide a demonstration of a model that can be used to assess the most important factors contributing to the severity of spinal injury in Riyadh, Saudi Arabia. On the basis of the real-world accidental data, 18 explanatory factors were used in the model development process.
- 2- Using the concept of deviance together with the Wald statistic, the study variables were subjected to statistical testing. The significant factors that contribute to the severity of spinal injury were found to be the type of spinal injury, restraint system, impact direction, and ETS. The observed level of significance for regression coefficients for the two variables was less than 5%, suggesting that these 5 variables

were indeed good explanatory variables. The results presented in this study show that the model provided a reasonable statistical fit.

- 3- It is clear that the final parameters will contribute to the severity of spinal (*SEV*) injury from a biomechanical view point. The crash mode (*IMPTYP*) and impact speed (*ETS*) pre-determine the kinematics of vehicles which cause injury to the occupant. In relation to the anatomical sections of spine (*SPINETYP*), cervical and thoracic regions are more prone to certain fracture mechanisms. Also, the occupant restraint system (*RESTUSE*) was reported to have a major effect on the incidence of spinal injury.
- 4- Presentation of odds in a matrix format, as described in this study, provides a simple method for interpretation. The columns and rows of the matrix correlate the factors in the logistic model, and each cell shows the impact of a certain factor on the odds with respect to another factor (a corresponding factor).
- 5- This model may be served as an initial prediction to establish the severity of spinal injury sustained by occupants at road crash. Thus a paramedic protocol as part of emergency response may be revised according to the developed model.

CHAPTER 6

CONSEQUENCES OF SPINAL CORD INJURY (SCIs) IN SAUDI ARABIA

Spinal Cord Injury (SCI) is often lethal, and usually imposes permanent physical damage to the victim leaving them as paraplegics or tetraplegics. RTAs are considered the leading cause of lifelong disability and mortality for young Saudi adults. The high prevalence of neurotrauma not only affects the disabled individual but also exerts tremendous socio-economic burden on the family as well as the nation as a whole.

As the incidence of spinal cord injury is highest among people 18 to 24 years of age, increased survival rates will be accompanied by increased demands on the social and medical systems. Consequently, reducing the incidence of spinal cord injury will not only prevent social and family disruption but will substantially reduce direct health care costs and the social costs from lost productivity. Knowledge gained from surveillance may lead to the development of intervention strategies capable of preventing injuries leading permanent disabilities, such as SCIs. Even though studies on SCIs have been reported from Saudi Arabia, the reports are few and limited to data from single hospitals.

Thus, this national study was conducted to evaluate the spinal trauma in the Saudi Arabia with a broader and comprehensive perspective. This chapter provides an overall analysis of the incidence, prevalence, risk factors, and socio-economic consequences of the SCI individuals, with special emphasis on factors associated with RTAs.

6.1 MATERIALS AND METHODOLOGY

6.1.1 Data Sources

In this study, persons who sustained SCI in the major cities of Saudi Arabia were identified through population-based registers, local registers and informal sources. Records of all casualties admitted with a SCI from January 2000 to December 2010 were reviewed. Cases were selected through seven steps as illustrated in **Figure 6.1**, comprising: (1) Definition of selection criteria, (2) The combined use of several data sources and (3) The use of various methods for verification. Cases with incomplete information were excluded.

6.1.2 Study Design

Spinal Cord Injury (SCI) has been defined *as an acute, traumatic lesion of the spinal cord, including trauma to the nerve resulting in varying degrees of motor and/or sensory deficit or paralysis* (Kaplan, 1995). A request for data was made including all **ICD-10** codes (International Classification of Diseases) that conceivably might represent cases comprising the target population (WHO, 2007). Severity of injury was defined by complete or incomplete lesion, as specified by ICD coding. Mechanism of injury was determined based on radiograph review, clinical information, and other available data from the medical records. Fracture type in the cervical region was classified according to Myers and Winkelstien (1995), and the thoracolumbar fracture was classified according to the AO classification (Magerl et al., 1994).

The neurological deficits were classified according to the American Spinal Injury Association (ASIA) scale (ASIA, 2002). Outcome was defined by the state of the casualty on discharge, which can be ASIA A-E or death. Structured, closed question data sheets were used for data collection (see **Appendixes B.1 and B.2**).

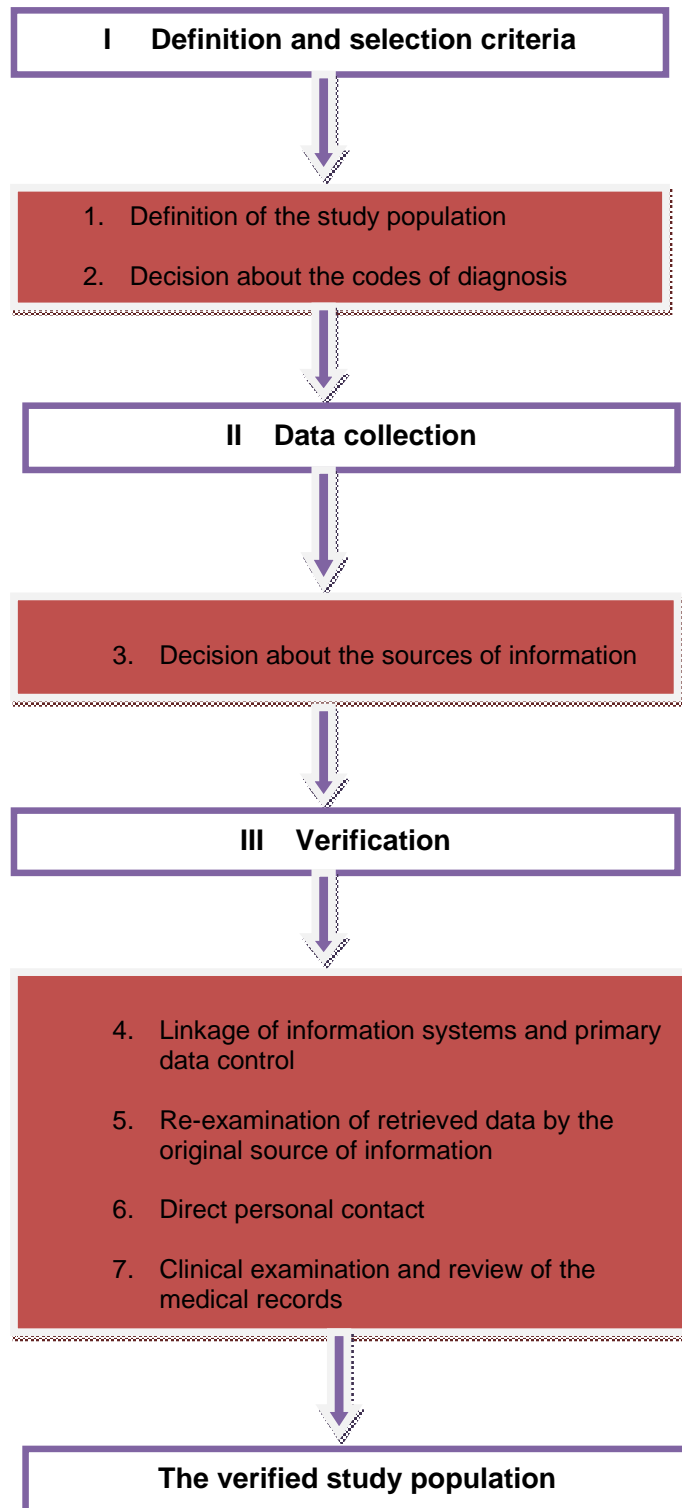


Figure 6.1: Process chart of finding a verified study population

6.1.3 Poisson Regression Model of Spinal Cord Injury Trends

Four types of incidence measures were considered: case numbers, age and sex specific incidence rates, crude incidence rates and age-standardised incidence rates:

The incidence rates measures were calculated according to the following formulae:

$$r_i = \frac{d_i}{q_i} \quad CR = \frac{\sum d_i}{\sum q_i} \quad ASR = \frac{\sum r_i Q_i}{\sum Q_i}$$

Where r_i is the age-specific incidence rate for age group i , CR is the crude incidence rate, ASR is the age-standardised incidence rate, d_i , the number of incidences for age group i , q_i is the mid-year estimated resident population for age group i , and Q_i is the standard population in age group i . An appropriate model for this type of data was the Poisson regression model, with a Poisson error distribution. A log link function and the natural log of population treated as an 'offset' (McCullagh and Nelder, 1989; Valkonen, 1989). For a particular incidence measure, the model may be expressed in Eq. (6.1):

$$\log_e(D_t) = \log_e(N_t) + \text{constant} + \alpha t \quad (6.1)$$

Where t is the year of registration of incidence, D_t the expected number of incidences registered in year t (dependant variable), N_t , the mid-year population in year t (offset), and α is the estimated annual rate of increase or decrease in incidence. Based on α , an average annual rate of change has been derived as follows:

$$\text{Percentage change} = [e^\alpha - 1] \times 100 \quad (6.2)$$

The 95 % confidence interval is obtained for α and the model constant. The decision to accept or reject the null hypothesis was based on an alpha level of 0.05.

6.2 OVERALL PREVALENCE AND INCIDENCE

Traumatic spinal injury accounted for 93% of all spinal injury recorded in Saudi Arabia. A total of 35,977 casualties with SCIs were admitted to the main hospitals in Saudi Arabia during the period from 2000 to 2010. The proportion of spinal casualties has increased by 6 times during the past decade at 22% average annual growth.

AIS level 3 vertebral fractured occurred at the rate of 23.65 per 100,000, and admissions for less severe spinal injuries occurred at the rate of 47.22 per 100,000. As a result, vertebral and spinal cord injuries accounted for 8.43% of hospital admissions for trauma centres during this period. The cervical spine injuries were the most common spine injuries accounting for 39.73% with an incidence rate of 9.20 per 10⁵, followed by lumbar (32.38%), thoracic (22.69%), and sacral (5.20%) injuries.

There were 8,129 new incident cases of SCI during 2000-2010. Based on the Saudi census population statistics (CDSI, 1970-2010), an average incidence rate of 37.92 cases per million per year for the residents of Saudi Arabia was estimated for this period of time. In 2010, the Saudi population was estimated at 25,634,675 and the prevalence of spinal cord injury in Saudi Arabia was 960 casualties per million that year. As a result, the total number of SCI in Saudi Arabia was estimated at 24,609 casualties.

Figures 6.2-6.3 show the prevalence and incidence of spinal cord injuries over the 13 provinces of Saudi Arabia. The low prevalence was found in Najran (11). It is surprising to discover that Makkah has the highest prevalence in the Kingdom (254). Millions of people come every year during Hajj and Ramadan seasons to visit the holy places in this city. Residents of the Northern Frontier, and Al-Madinah had a ten-year annual average incidence rate persisting SCI that was significantly higher than the national incidence rate.



Figure 6.2: Prevalence of SCI per million per year by regions of Saudi Arabia

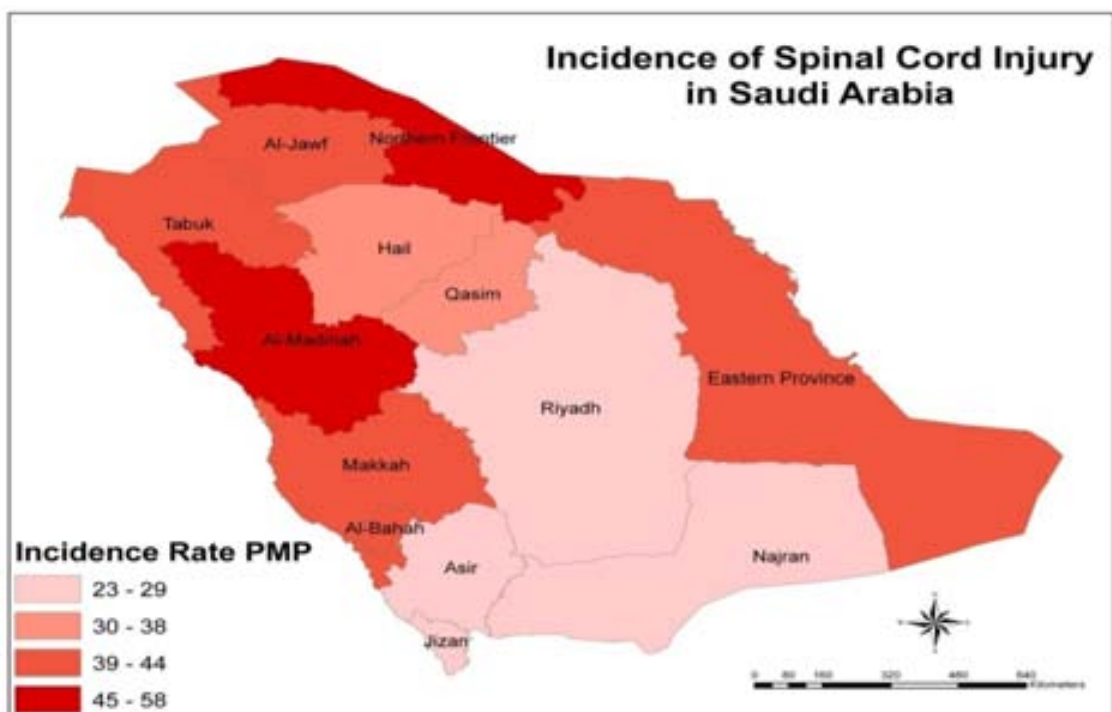


Figure 6.3: Incidence of SCI per million population by regions of Saudi Arabia

Of the 28 studies found on prevalence and the incidence of SCI in this research, the present incidence of SCI in Saudi Arabia is the highest rate ever reported in 85% of developed and developing countries in literature as shown in **Figure 6.4**.

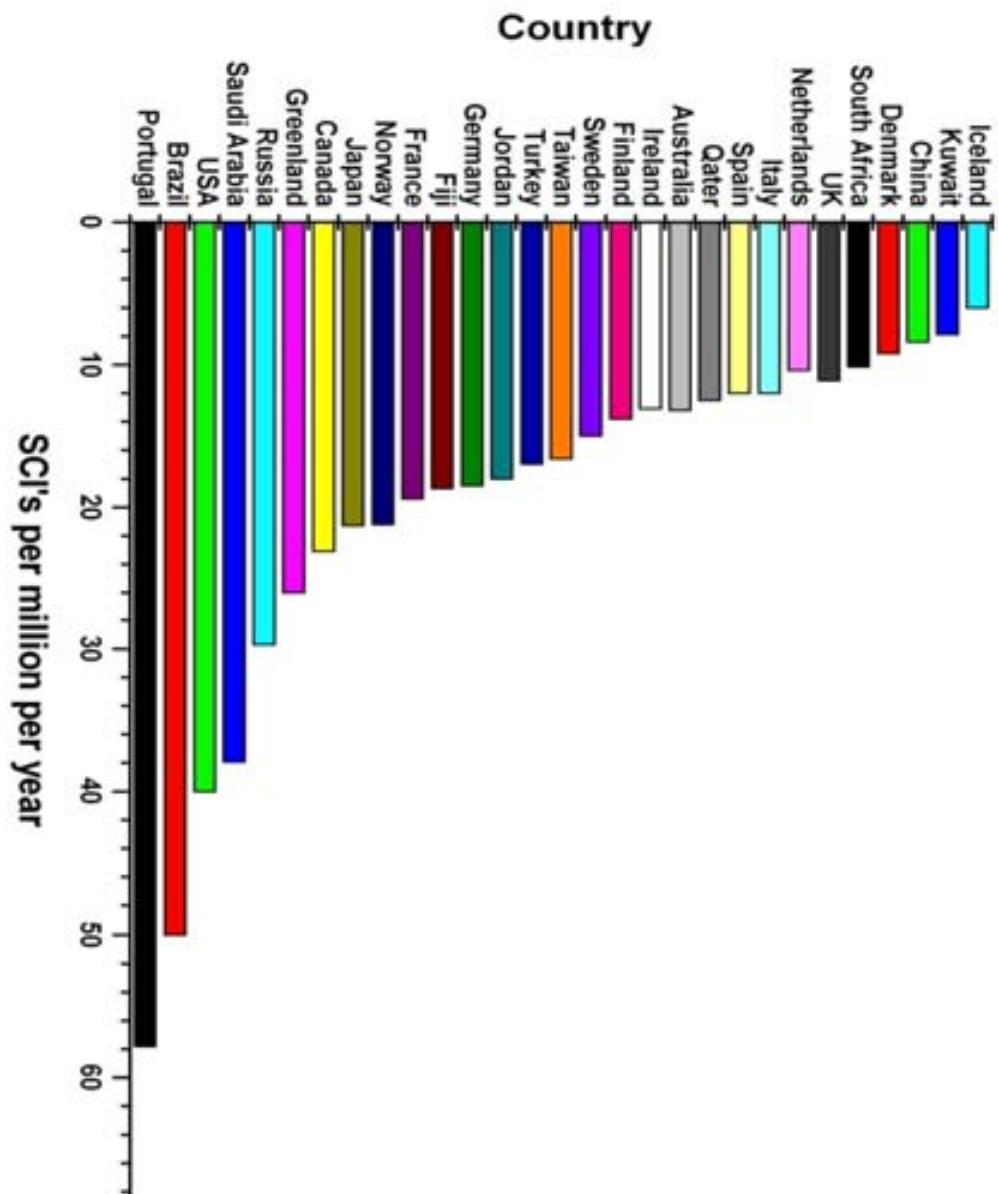


Figure 6.4: Global annual incidence of SCI per million population (Al-Shammari, 2008a)

6.3 ETIOLOGY OF SCIs

Figure 6.5 shows the external causes of SCI casualties in Saudi Arabia.

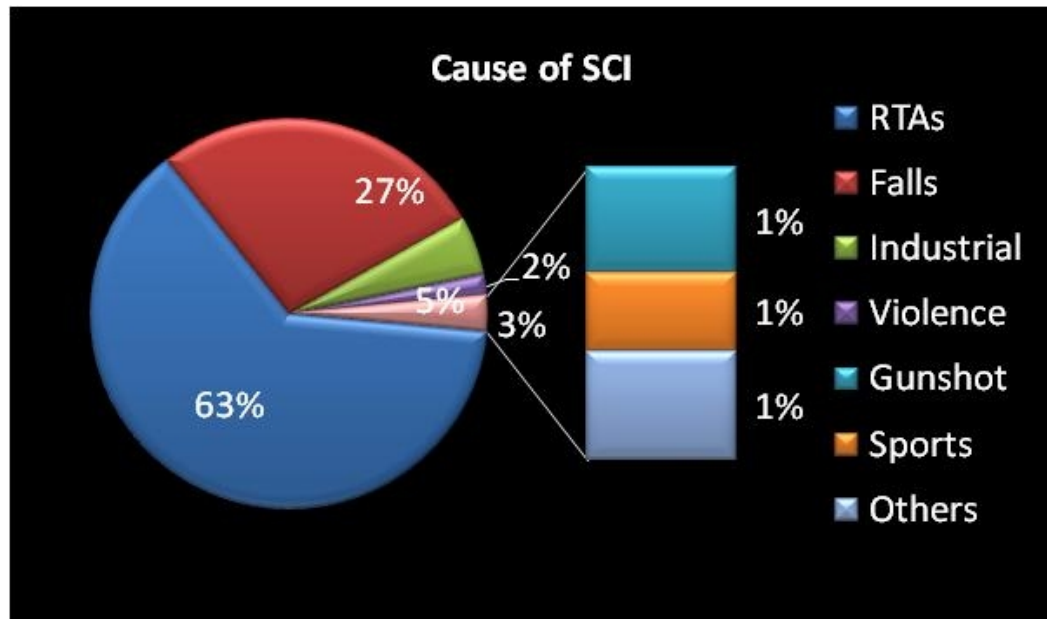


Figure 6.5: Etiology of spinal cord injuries in Saudi Arabia

Motor vehicle occupants accounted for 63% of the cases of SCI ($n=5119$). Seventy-one percent were motor vehicle occupants ($n=3648$) and 23% were Vulnerable Road Users (VRUs) i.e. pedestrians, and motor cycle riders ($n=1177$). Three quarters ($n=3824$) of these cases were in the age group 25–44 years. Most of the motor vehicle accidents occurred during leisure activities ($n=2457$, 48%) or travelling to or from work, or from other work related activities ($n=1382$, 27%). Further assessment of the crash types of motor vehicle occupants ($n=3646$) using structured injury narrative, revealed that 58% were due to vehicle rollover, 23% were due to collision with another vehicle or roadside hazard (i.e. tree, pole or other fixed object) and 7% were due to collision with a camel.

6.4 PRE-HOSPITAL CARE OF SCI CASUALTIES

Pre-hospital management seeks primarily to protect the casualty from further injury and to provide early resuscitation and transport to an appropriate acute care facility. In this study, two of the factors which may affect the function of spine during accident, viz, the first aid provider and the response time in care being made available were considered (**Figure 6.6**).

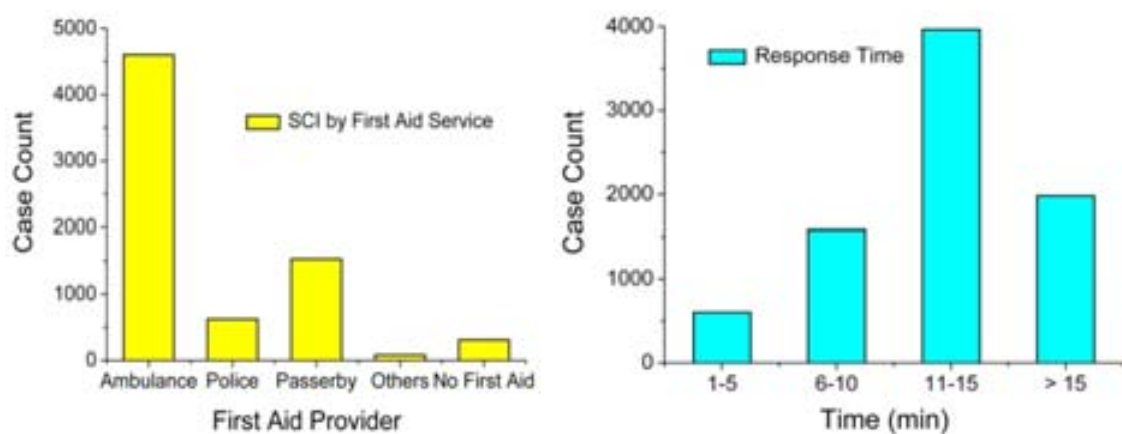


Figure 6.6: Evaluation of EMS service and the response time

Out of all SCI casualties, 7153 (88%) were provided first aid at site of accident, out of which 4603 (57%) received first aid by the **E**mergency **M**edical **T**eam (**EMT**) of SRCS, 1531 (19%) by passerby, 625 (8%) by police and 82 by relatives and friends. Surprisingly, 311 (4%) casualties did not receive first aid at site. There were 5283 (65%) casualties transported to the hospital by an ambulance, 2032 (25%) by normal transport, and 650 (8%) were airlifted. Only 2183 (27%) of the SCI casualties received first aid within the first ten minutes, while 3965 (49%) received first aid within 11-20 minutes, and 1981 (24%) received first aid after 15 minutes. 2845 (35%), and 3577 (44%) of casualties reached hospital within 15-30 minutes, and 31-45 minutes respectively, while, 488 (6%) reached hospital after 1 hr.

6.5 ASSESSMENT OF NEUROLOGICAL LEVEL OF SCI

The neurological level of SCI at admission is presented in **Figure 6.7**.

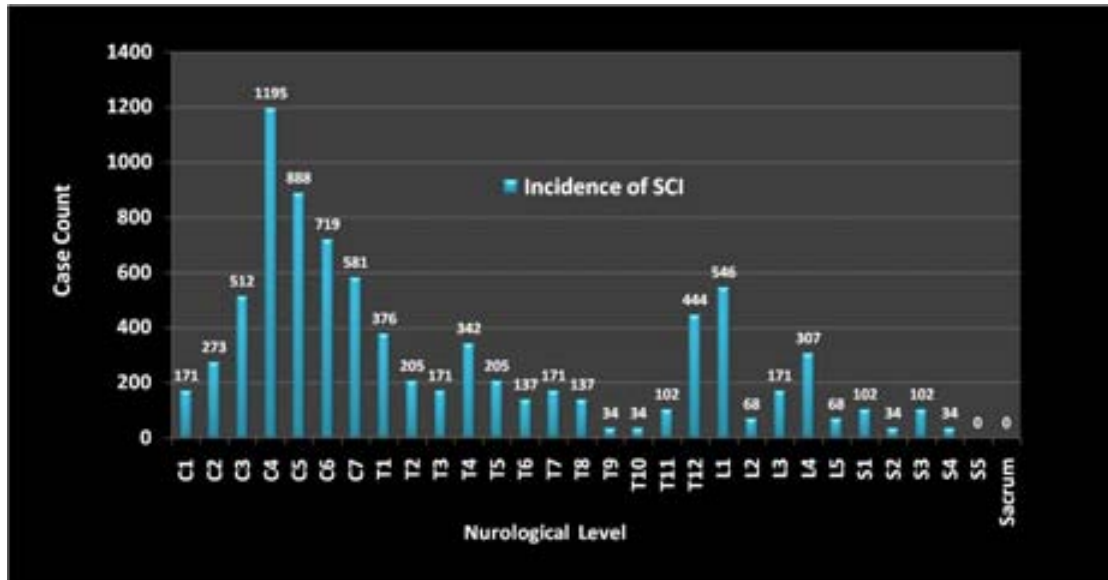


Figure 6.7: Incidence of SCI by neurological level of injury at admission

The most commonly injured spinal cord segments were: the cervical segments, particularly C4 (15%, $n=1195$), C5 (11%, $n=888$), and C6 (9%, $n=719$); the lumbar segment L1 (7%, $n=546$); and the lower thoracic segment T12 (5%, $n=444$).

A Frankel grade of 'A' (major impairment to normal motor ability function) was the most frequent grade observed ($n=5527$, 68%), followed by Grade B in 1219 (15%). The most common neurologic category was incomplete tetraplegia (42% of total, $n=3414$), followed by incomplete paraplegia (22% of total, $n=1788$), complete paraplegia (17% of total, $n=1382$), and complete tetraplegia (19% of total, $n=1545$). Motor vehicle occupants most often suffered from injury to the cervical segments of the spine, resulting in tetraplegia, with incomplete damage to the cord being most common at this level (67%, $n=3430$).

6.6 MECHANISMS OF SCI

Table 6.1 summarises the different types of SCIs in the study and the mechanisms hypothesized to have caused the injury, progressing from cranial to the caudal of the spine.

Table 6.1: Common mechanisms of spinal cord injury in Saudi Arabia

Injury Description	Frequency	Hypothesized Mechanism
Upper Cervical (Occiput-C2) <i>n</i> = 444		
Basilar skull fracture	28	Tension-extension
Occipitoatlantal dislocation	45	Hyperextension
Atlantoaxial dislocation	87	Extension-shear, Flexion-shear
Jefferson fracture	62	Vertical compression
Other Atlas fractures	24	Compression-extension
Odontoid fracture	133	Hyperflexion, Hyperextension
Axis fracture	3	Extension
Hangman's fracture (Spondylolysis)	62	Tension-extension
Lower Cervical Region (C3-C7) <i>n</i> = 3895		
Burst fracture/Compression fractures	659	Vertical compression
Transverse process	263	Lateral bending
Hyperextension dislocation	94	Hyperextension
Unilateral comminuted facet fracture	151	Extension-rotation
Wedge fracture	207	Compression-flexion
Teardrop fracture	1242	Compression-flexion
Spinous process	696	Compression-extension
Bilateral facet dislocation	169	Tension-flexion
Unilateral facet dislocation	414	Flexion-rotation
Thoracolumbar (T1-L5) <i>n</i> = 3518		
Wedge fracture	1033	Compression-flexion
Teardrop fracture	347	Hyperextension
Chance fracture	18	Tension-flexion
Transverse process	667	Flexion-rotation
Spinous process	37	Hyper-extension
Burst fracture/Compression fractures	1005	Vertical compression
Fracture/dislocations	292	Flexion-rotation, hyperflexion
Disruption of intervertebral disk	119	Tension-extension
Sacral (S1-Coccyx) <i>n</i> = 272		
Zone (I, II, III)	228	Hyperflexion, Hyperextension
Longitudinal and Central fractures	44	Tension-flexion
Total	8129	

6.7 TRENDS IN SPINAL CORD INJURY IN SAUDI ARABIA

Table 6.2 shows a summary of results using the Poisson model along with the 95% confidence interval, the *P*-value and the percentage change (see **Appendix B.3**).

Table 6.2: Summary of Poisson model results

Descriptive Statistics			α			P-value	Annual % Change
			Value	95% CI			
Trend Parameter	Mean	σ			Lower		
Cases	812.9	88.319	0.033	0.026	0.041	0	3.387
ASR	3594.5	167.096	-0.008	-0.011	-0.004	0	-0.752
CR	3523.6	171.381	-0.016	-0.019	-0.012	0	-1.541
Age/sex group							
Male 0-14 yrs.	1213.8	204.915	0.018	0.012	0.024	0	1.788
Male 15-24 yrs.	3700.7	300.485	-0.036	-0.04	-0.033	0	-3.559
Male 25-34 yrs.	9996.3	1038.73	0.001	-0.001	0.003	0.325	0.109
Male 35-44 yrs.	5725.6	949.507	-0.071	-0.074	-0.068	0	-6.869
Male 45-54 yrs.	7611.4	1927.819	-0.105	-0.107	-0.102	0	-9.966
Male 55-64 yrs.	9341.2	2765.399	-0.001	-0.003	0.001	0.463	-0.084
Male 65+ yrs.	8928	4228.514	-0.011	-0.014	-0.009	0	-1.14
Female 0-14 yrs.	471.6	116.583	-0.073	-0.083	-0.063	0	-7.051
Female 15-24 yrs.	979.8	272.028	0.05	0.043	0.057	0	5.168
Female 25-34 yrs.	2762.7	424.225	-0.061	-0.066	-0.057	0	-5.954
Female 35-44 yrs.	2963.4	423.86	-0.057	-0.061	-0.053	0	-5.508
Female 45-54 yrs.	2450.6	662.553	-0.074	-0.078	-0.07	0	-7.133
Female 55-64 yrs.	3443.1	349.814	-0.025	-0.029	-0.021	0	-2.476
Female 65+ yrs.	3036.2	642.034	-0.019	-0.023	-0.015	0	-1.877
Cause							
Transport	2221.8	95.638	-0.022	-0.027	-0.018	0	-2.187
Fall	969.3	112.366	-0.018	-0.025	-0.011	0	-1.763
Other cause	332.7	63.607	0.035	0.023	0.047	0	3.589
Neurological group							
Complete tetraplegia	284.8	37.944	-0.046	-0.059	-0.033	0	-4.511
Incomplete tetraplegia	589.5	186.2	-0.101	-0.111	-0.092	0	-9.65
Complete paraplegia	601.8	68.847	-0.047	-0.056	-0.039	0	-4.63
Incomplete paraplegia	1303.6	314.868	0.044	0.038	0.05	0	4.501

The analysis revealed that the changes in the overall case numbers (2000-2010) were fairly high, while the changes for the CR and ASR were very small as shown in **Figure 6.8**.

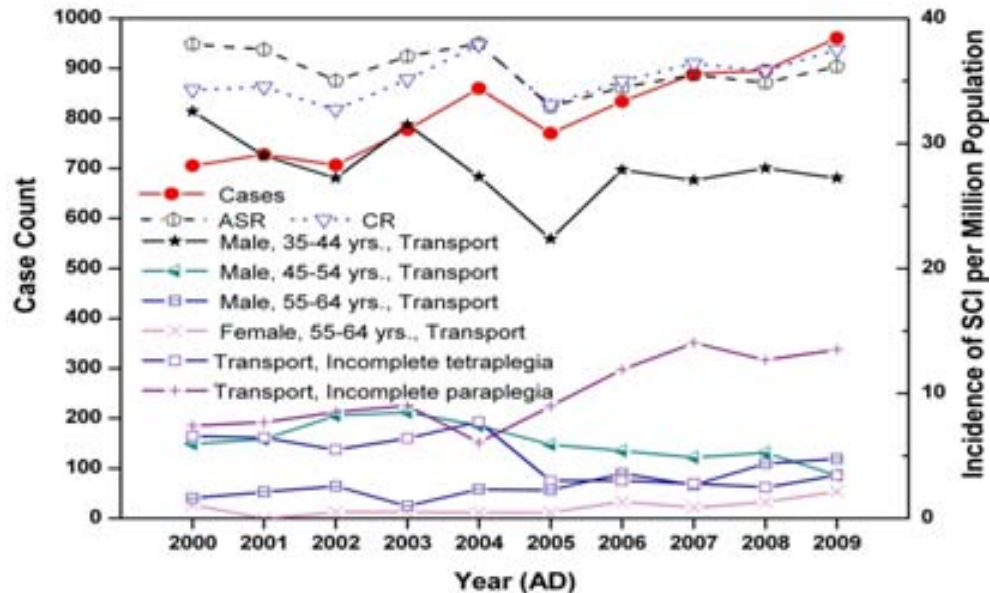


Figure 6.8: Trend in cases, CR, ASR of SCI in Saudi Arabia during 2000-2010

There was a significant increase of 3% annually in the total number of SCI cases. But when we look at the age standardized rate there is a decrease of -0.75%, this indicates that for different age groups the trend is different, the net result being a masking of the actual trends.

A significant (10%) increase in number of injuries for males (55-64 yrs) was observed when the SCIs were caused due to transport. On the other hand males in the age group 35-44 and 45-54 have shown a decrease of 4% and 8% respectively when the SCIs were caused due to transport. An alarming increase of 15% has been observed in the SCI incidences for females in the age group 55-64 when the SCIs were caused due to transport. In the neurological group of incomplete tetraplegia, transport related incidents have shown a decrease of 13%, while an increase of 6% has been observed for the group of incomplete paraplegia.

6.8 CONCLUSIONS

The aim of this chapter was to present an overview of epidemiological characteristics of Spinal Cord Injury (SCI) in Saudi Arabia. In this study, a retrospective and descriptive survey of 8,129 casualties managed for SCI in Saudi Arabia over the period from December 2000 to January 2010 was carried out. The main conclusions are as follows:

- 1- The estimated overall average incidence of SCI was 35 per million, with a prevalence of 812 new cases every year.
- 2- The leading cause of SCI was road traffic accident, accounting for 63% of all causes; accidental falls injuries 27% and others 10%.
- 3- The male/female ratio of SCIs was 6.40:1 which is higher than in other studies.
- 4- The highest age-specific rate occurred in the age group 15–24 years. Male rates of persisting SCI from traumatic causes were higher than female rates at all ages.
- 5- Seventy-one (71%) of the transport related cases were vehicle occupants and 23% were unprotected road users, predominately pedestrians (96%).
- 6- Only 57% of all SCI casualties were received first aid at site by EMT, and the majority of casualties (49%) were reached by EMT within 11-20 minutes.
- 7- Of these with a neurological deficit, 68% in this study were ASIA “A”. A large number of occupants (67%) sustained a cervical injury resulting in a tetraplegia.
- 8- Compression-flexion (31%) and vertical compression (21%) were the most common mechanisms associated with spinal cord injuries in this study.
- 9- There was a significant increase in the SCIs related to the RTAs cause for males aged 55-64 years, while there was a sharp increase for females aged 55-64 years.

CHAPTER 7

ACCIDENT RECONSTRUCTION OF SOME UNCOMMON SPINAL INJURIES IN AUTO-CRASHES IN SAUDI ARABIA

Accident reconstruction is an important tool to investigate crashes, to determine their probable cause, and to make recommendations to prevent them and/or mitigate the severity of the accidents and resulting injuries. Advances in safety systems have had a profound effect in reducing injury in motor vehicle accidents. Despite improvements in protection, crashes involving late model vehicles may still result in injury to the spine.

Blunt spinal injuries occur frequently as a result of trauma, and their diagnosis, pathomorphological pattern have been extensively reported in the medical literature. However, in some cases uncommon mechanisms of spinal fractures can be observed. It is unclear whether these fractures are rare or under-diagnosed.

This Chapter conducts in-depth investigations, and accident reconstructions for four occupants who sustained unique conditions of spinal injuries due to vehicle crashes in Saudi Arabia. The knowledge from the injury reconstruction can be used to better understand the injury mechanics behind spinal injuries, and to develop measures to aid in the identification of safety issues such as roadway design, human factors, vehicle design and crashworthiness related to occupant protection from spinal injuries.

7.1 METHODS AND MATERIALS

Motor vehicle crash prevention requires a multi-disciplinary approach and encompasses multiple factors. Understanding the many intersecting concepts can be challenging. In 1968 William Haddon (Haddon, 1968), a pioneer of motor vehicle safety, proposed that to better understand the factors associated with motor vehicle crash safety it should be conceptualized in three phases: pre-crash, crash, and post-crash. Although there are many prevention strategies, the methods used in this study will be considering the ten counter measures later proposed by Haddon (1999). These 10 counter measures are as follows:

1. Prevent the creation of the hazard (e.g., stop selling cars to teenagers).
2. Reduce amount of the hazard (e.g., reduce speed limits).
3. Prevent inappropriate release of the hazard (e.g., lower vehicle power).
4. Modify rate or spatial distribution (e.g., hydraulic bumpers on vehicles).
5. Separate release of the hazard in time or space (e.g., install pedestrian sidewalks).
6. Put a barrier between the hazard and people at risk (e.g., install guard rails between busy roads and sidewalks).
7. Change basic nature of the hazard (e.g., alternative active and passive safety systems).
8. Increase resistance of people to the hazard (e.g., prevent fractures due to weak bones and osteoporosis by regular exercise or estrogen intake).
9. Begin to counter damage already done (e.g., rapid rescue of trauma victims).
10. Stabilization, definitive care, and rehabilitation (e.g., rapid availability of trauma care systems, and provide best practice standards of emergency).

Figure 7.1 shows the conceptual framework of accident reconstruction process.

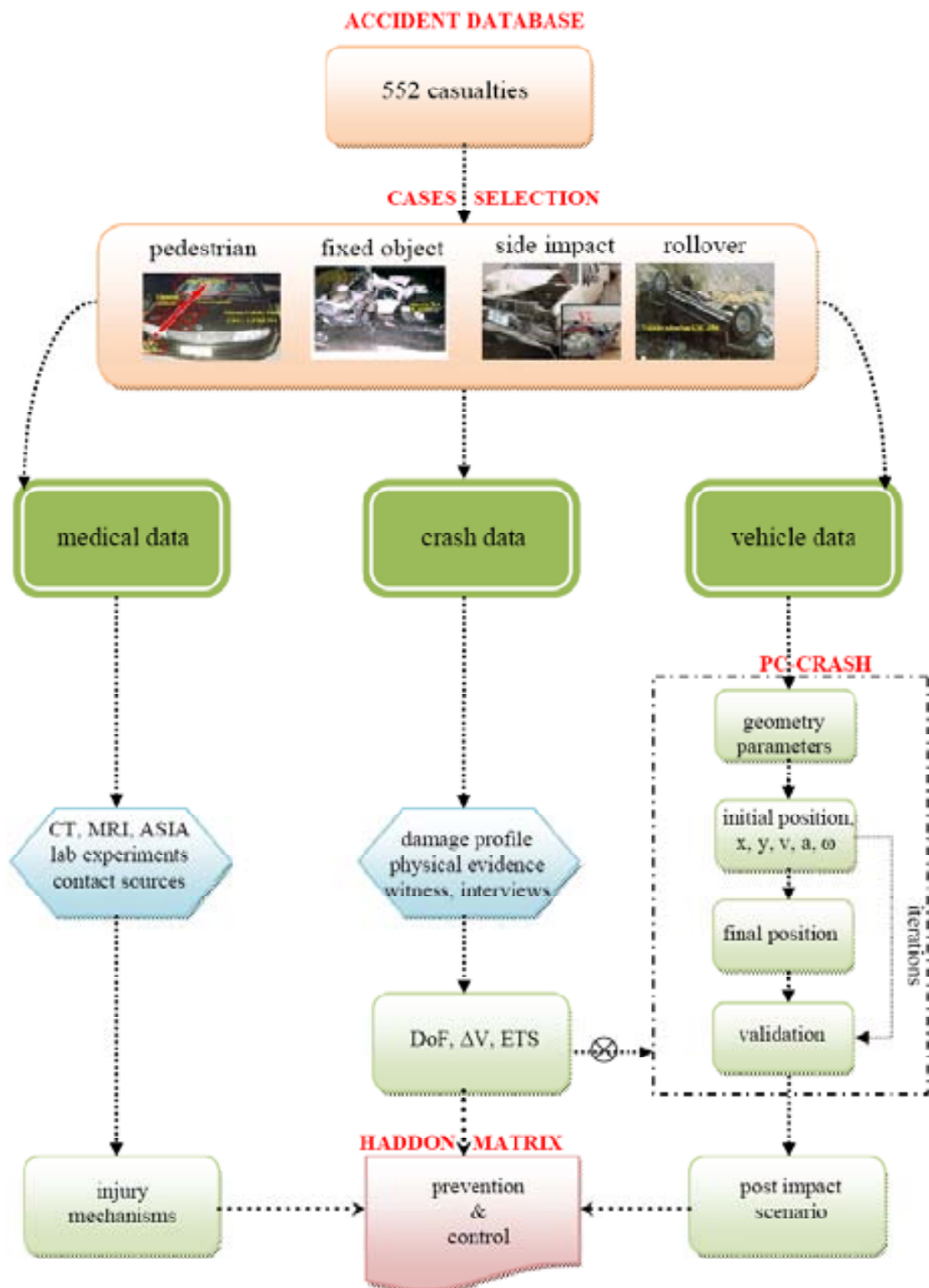


Figure 7.1: Accident reconstruction process flowchart

7.1.1 In-depth Investigation

To assess the details of specific crash scenarios resulting in spinal injury, four cases were selected from the 552 casualties considered in this study. Detailed descriptions of the general methods involved in data collection and analysis have been previously explained in **Section 4.1**. Crashes qualifying for inclusion in the study were those that involved 1995 or newer model vehicles, and those involving at least one adult occupant or pedestrian > 15 years of age. Qualifying crashes were limited to those that occurred in Riyadh region.

7.1.2 Computer Simulation

These cases were reconstructed and simulated using PC-CRASHTM ver 7 (DSD, 2006). Reconstruction by PC-CRASH gives the benefit that a scale diagram of the main screen, tables, and diagrams defining the vehicle motion can be viewed and animations of the simulation, from a fixed or moving camera position, can be rendered. This helps understand how the crash occurred and safety measures can then be planned accordingly.

If the vehicle model was not available, an apriori custom model was made. Scene information was then input, by loading or creating a 2D or 3D drawing in a DXF format. The vehicles were then positioned at the start points by entering the X and Y coordinates. The initial velocities including directions were also input. Sequences that control the wheel braking, steering and acceleration forces, and other functions that affect vehicle motion were then applied to each vehicle as per available initial estimates. An impact analysis was then performed along with a post-impact trajectory analysis. The estimated parameters were then iterated and the above steps were repeated until the comparisons are valid. After the impact scenario and post-impact motion were solved for, the pre-impact motion was examined.

7.2 CASE 1: COLLISION WITH A PEDESTRIAN

7.2.1 Crash Reconstruction I

On a clear evening in November, 2005, a young male driver of a 2000 Nissan Cedric (1604 kg) was attempting to make a left (southbound) turn at an intersection un- controlled by a traffic signal light in Riyadh. As the driver was completing the left turn and crossing the intersection, a pedestrian (38 years-male, 168 cm, 88 kg) emerged quickly from behind a small building on the right side of the passenger car and proceeded to cross the road at a non pedestrian sidewalk. The driver was unable to avoid the pedestrian due to the shadow cast by the building, and struck the pedestrian at an estimated speed of 34 km/h.

The car's bumper struck the man's left leg projection him up onto the bonnet, his head striking the windshield. He then rolled onto the bonnet and was thrown away for 5 m onto the ground. Damage to the vehicle included a dent on the grill and a large dent on the bonnet (0.54 m from front right corner of bonnet and 0.45 m back from the front of the bonnet). Evidence of pedestrian contacts on the car is shown in **Figure 7.2**.

The pedestrian was transported by EMS to King Fahad Hospital trauma center with a **Glasgow Coma Scale (GCS)** of 9. He was placed in a cervical collar and on a backboard at the scene. He reportedly lost consciousness, but was alert and oriented on arrival at EMS and remained so throughout transportation. The paramedics noted severe left shoulder pain.

During reconstruction using PC-Crash based simulations, a number of scenarios were simulated. One scenario that appeared likely was when the car had an initial speed of 30 km/h, and the pedestrian had an initial speed of 7 km/h based on a reasonable walking speed (Ishaque and Noland, 2006) and the car orientation during impact being -10^0 with the lane and pedestrian orientation was 110^0 with the same lane.

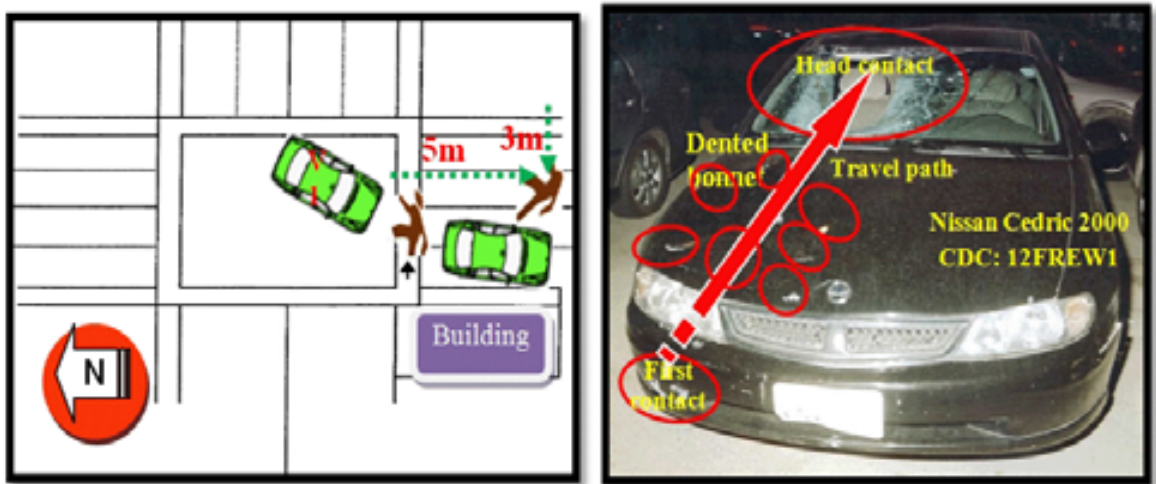


Figure 7.2: Scene diagram and the contact locations of the pedestrian on the car

Figure 7.3 shows the sequential events of PC-Crash simulation in this case. This reconstructed case was validated by impact positions (the car's bumper struck the man's left leg and the car's windshield struck the man's head) and final positions (the man rolled onto the bonnet and was then thrown away for 5 m on the ground).

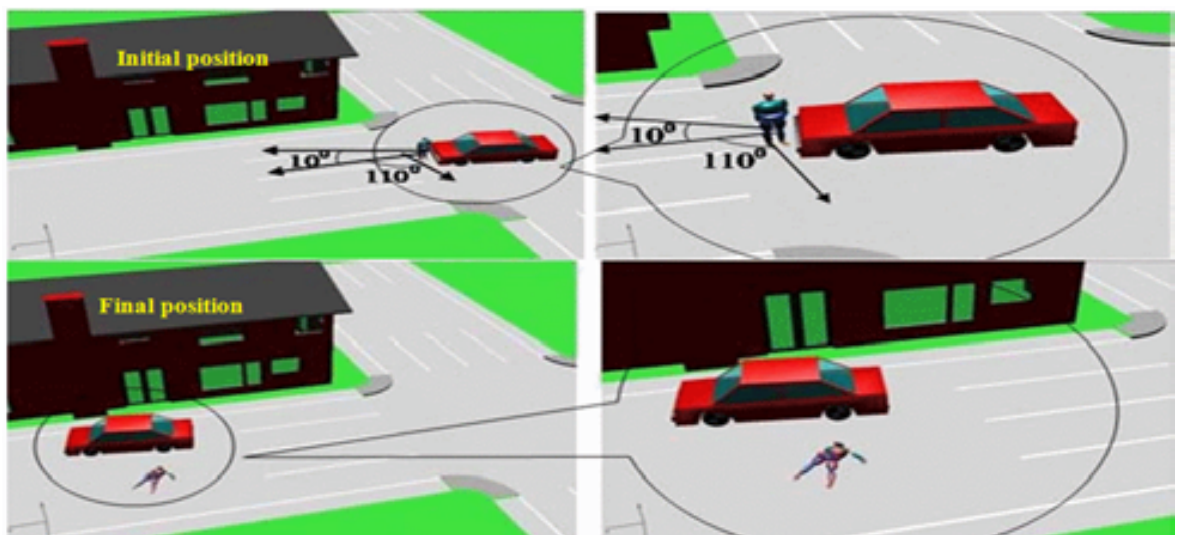


Figure 7.3: PC-Crash simulations for crash of pedestrian in Case 1

7.2.2 Mechanisms of Spinal Injury

The pedestrian subsequently underwent a head, cervical spine and abdominal-pelvic Computed Tomography (CT) scan. The laboratory studies demonstrated a skull base fracture that extends through the occipital condyle (Type II) and pelvic fracture at the sacroiliac complex as shown in **Figure 7.4**. In addition, there were multiple other injuries including head, facial, multiple thorax, abdomen, and extremities injuries (see **Table 7.1**).

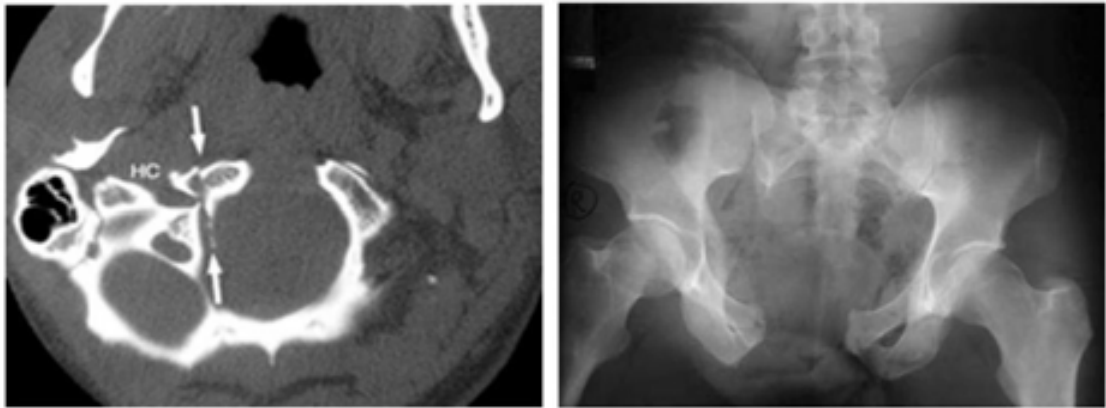


Figure 7.4: Radiographic images of spinal injuries for pedestrian in Case 1: *left*, axial CT scan shows Type II right occipital condyle fracture extending through skull base; *right*, plain radiograph of open-book pelvic fracture

The hypothesised mechanism of injury to the occipito-atlantal joint, dictated by the pedestrian kinematics, involves hyperextension of the cervical spine. It is believed that when the legs of the pedestrian impacted on the bumper corner, a rapid rotational acceleration was applied to the long axis of the body during the scooping-up- motion. The strike by the head and face body regions with the windscreen produced a transitional force causing extension at the occipital with concomitant sheering. This series of events resulted in complete disruption of the occipito-atlantal ligament complex and C0/C1 dislocation.

Table 7.1: Type of injuries sustained by pedestrian in Case 1

Injury	ISS Body Region	AIS	Source of Injury
Subarachnoid hemorrhage of cerebellum	Head	140466.3	Ground
Dislocation fracture of atlanto-occipital joint	Cervical spine	650228.3	Ground
Laceration, left temple to the upper scalp	Head	110602.1	Windshield
Bruising is present behind the left ear	Head	110402.1	Windshield
Multiple fractures of the zygomatic bones	Face	251800.2	Ground
Nose fracture	Face	251000.1	Ground
Upper lobe of the left lung is traumatised	Thorax	441499.3	bonnet edge
The liver shows some bruising	Abdomen	541810.2	Bonnet edge
The spleen shows multiple lacerations	Abdomen	544220.2	Bonnet edge
The left kidney is contused	Abdomen	541610.2	Bonnet edge
Disruption of sacroiliac joint	Sacral	852604.3	Ground
Mid-shaft fracture of right femur	Extremities	851814.3	Bonnet edge
Right tibia multiple compound fractures	Extremities	853404.2	Bonnet edge
Tibia contusion	Extremities	853402.1	Front grill
Shallow Lac's on the left shoulder 11 × 5 cm	Extremities	710602.1	Front grill
Fractured left hip, NFS	Extremities	852600.2	Bumper
ISS			27

Occipital condyle fractures seem to be rare. These injuries are typically indicative of high-velocity blunt force trauma (Anderson and Montesano, 1988). The most frequently encountered occipital condyle fractures are Type I, Type II, and Type III (Bell, 1817). Blunt force trauma secondary to a motor vehicle collision has been reported as the most common cause of occipital condyle fractures (Momjian, 2003).

Casualties with occipital condyle fractures resulting from motor vehicle collisions have been diagnosed with other blunt trauma and torsion injuries such as atlanto-axial dislocation, duodenal hematoma, and lumbar vertebra fractures and etc (Kaushik et al., 2002).

Table 7.2 shows the Haddon's matrix preventive measures for Case 1.

Table 7.2: Haddon' s matrix for pedestrian in Case 1

Phase	Factor		
	Host	Vehicle	Environment
Pre-event	<ul style="list-style-type: none">• Driver inattention• Pedestrian awareness• Pedestrian not wearing a reflective clothes	<ul style="list-style-type: none">• Brakes in proper working order• No anti lock brakes	<ul style="list-style-type: none">• No crosswalk
Event	<ul style="list-style-type: none">• Middle aged pedestrian• Strong bone strengths	<ul style="list-style-type: none">• Low bumper• High speed• Driver not wearing safety belt	<ul style="list-style-type: none">• Road surface
Post-Event	<ul style="list-style-type: none">• Middle aged pedestrian in good physical condition	<ul style="list-style-type: none">• Proper tire tread for stopping	<ul style="list-style-type: none">• Lack of EMS

7.3 CASE 2: COLLISION WITH A FIXED OBJECT

7.3.1 Crash Reconstruction II

This incident took place in July 2006 in the evening, in Al-Kharj province, South of Riyadh. A 44 year old male driver was driving a 4-door 1995 BMW-730i se (1878 kg) westbound at a high speed (≈ 155 km/h) in the first lane of a divided two-way road. The road was unlit. The driver appeared to lose control and hit the right shoulder of the road, somersaulted and did a 180 degree turn in the air. The vehicle then struck a light pole with a Principal Direction of Force (PDOF) of 110 degrees. The driver's side of the car struck the pole with a CDC estimated to be 10LPAN4. The total ΔV of the impact was estimated to be 125 km/h. The pole was damaged and sheared at its mounting and fell on to the car.

The damage to the vehicle consisted of a broken windshield, separation of the door skin, a buckled A-pillar, intrusion of the driver side door, and the right side of the roof over the driver was depressed into the occupant compartment as shown in **Figure 7.5**.

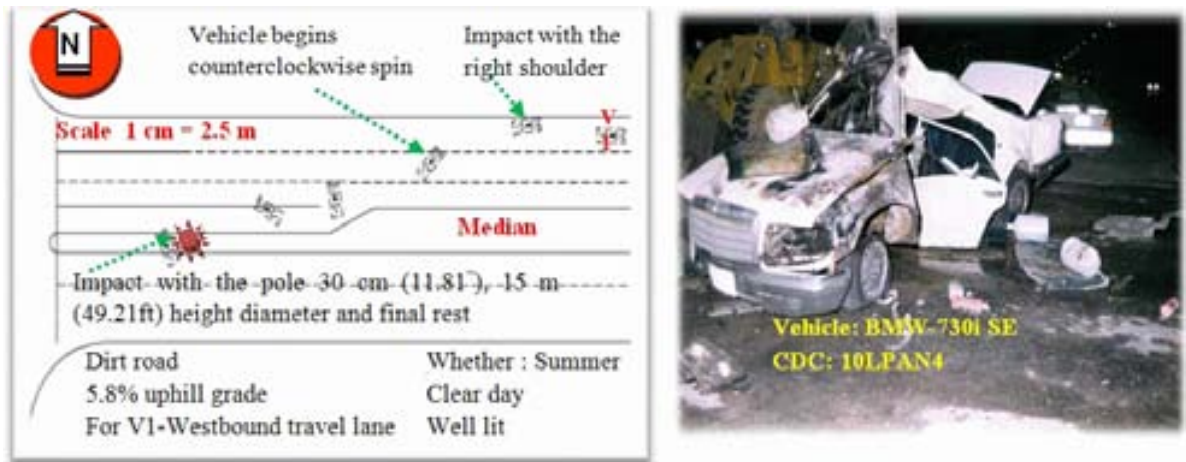


Figure 7.5: Scene diagram and vehicle damage for Case 2

In this particular crash one car and fixed objects were involved. A number of variations in the scenario were simulated. One of the scenarios that matched the result reasonably well was when the car orientation just before impact was 9° with the right shoulder. Finally the car struck a light pole (which was on the divider) with a Principal Direction of Force (PDOF) of 110° . This reconstructed simulation matches well with the known impact positions and kinematics. **Figure 7.6** shows the sequential events of PC-Crash simulation for Case 2.

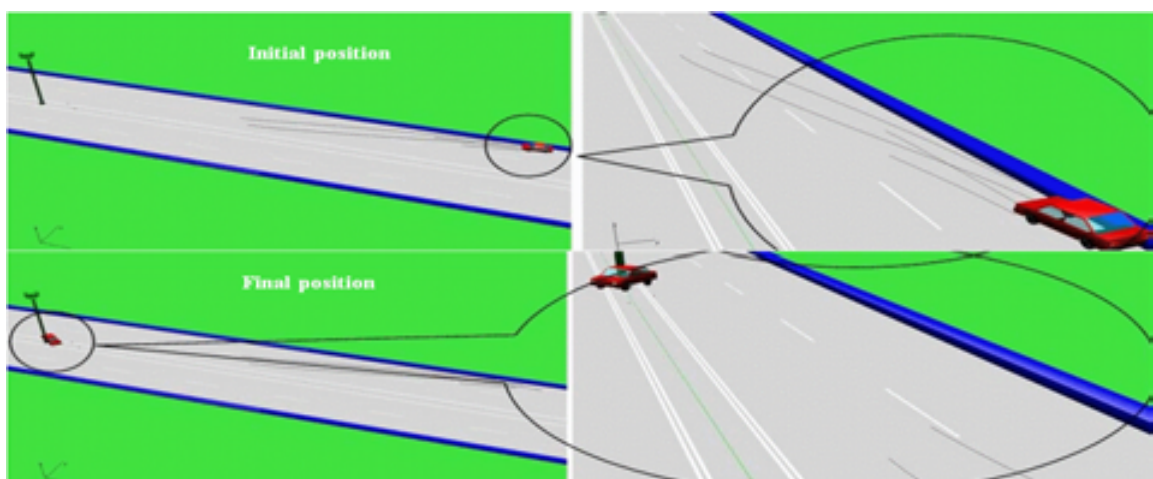


Figure 7.6: Snapshots from the PC-Crash simulations for Case 2

7.3.2 Mechanisms of Spinal Injury

A physical examination revealed mild tenderness over the driver's forehead and the left side of his neck. Nonetheless, a side radiography and multi-detector CT scan of the cervical spine showed a cleft between the superior and inferior facets of the articular pillar of C6 and grade I spondylolisthesis at C6 anteriorly with respect to C7 as shown in **Figure 7.7**.



Figure 7.7: Radiographic images of spinal injuries for driver in Case 2: *left*, lateral radiograph of cervical spine showed Grade I Anterolisthesis of C6; *centred*, axial CT images revealed corticated cleft between bilateral C6 facets and spina bifida of C6; *right*, three-dimensional CT showed inferior facet fragments on side of the spondylolytic

The associated injuries by the driver and the probable sources of these injuries are shown in **Table 7.3**. A physical examination revealed mild tenderness over the left side of his neck. The diagnosis of spinal injury was confirmed to be a biside cervical spondylolysis at C6 anteriorly with respect to C7. Examination of the vehicle interior showed that there was evidence of occupant contact on the left side sun visor. The likely occupant kinematics in this collision would suggest that the head of the driver has contacted the A pillar which would be the cause of the head injury. This may have been further confounded by contact with the pole.

Table 7.3: Injuries of driver in Case 2

Injury	ISS Body Region	AIS	Source of Injury
Brain mild contusion	Head	150202.3	A pillar
Biside C6 cervical spondylolysis	Cervical spine	650222.3	A pillar
Three linear abrasions on left cheek	Face	210202.1	A pillar
Laceration of forehead	Face	210600.1	Windshield
Multiple abrasions over right side chest	Thorax	410202.1	Side door
Multiple ribs fractures posteriorly	Thorax	450264.4	Side door
Transverse fracture through sternum	Thorax	450804.2	Side door
Extensive lacerations of parietal pleura	Thorax	441802.3	Side door
Biside lung contusions	Thorax	441410.4	Side door
Multiple abrasions over right flank	Abdomen	510202.1	Side door
Multiple fractures of pelvis	Extremities	852608.4	Steering wheel
Displaced fracture of right femur	Extremities	851815.3	Steering wheel
Multiple abrasions right upper thigh	Extremities	810202.1	Steering wheel
ISS			41

The fracture injury to the cervical vertebra is likely to have occurred as a result of either forced extension or flexion of the cervical spine due to head contact with the A pillar. Such type of loading can occur with an impact to the top of the head and the force being directed along the neck. The head contact with the A pillar suggests that the occupant has been ejected from the seat during which the upper thigh would have contacted the steering wheel and dash board. This would then be the likely source of injury for the pelvis and the upper thigh. The rarity of this condition means the natural course of cervical spondylolysis has not been well described. The common mechanisms of this type of spinal injury were described by many authors such as Yochum et al., 1995; and Mofidi et al., 2007. The severity of injury can be ameliorated or the accidents even eliminated by introducing highway safety measures (Hassan and Mackay, 1996b). **Table 7.4** shows the Haddon's matrix preventive measures for Case 2.

Table 7.4: Haddon's matrix for Case 2

Phase	Factor		
	Host	Vehicle	Environment
Pre-event	<ul style="list-style-type: none">• Fatigue• Driver education on effects of speed• Behavior modification	<ul style="list-style-type: none">• Brakes in working order	<ul style="list-style-type: none">• Poor lighting
Event	<ul style="list-style-type: none">• Middle age driver• Reduction time• No seatbelt use	<ul style="list-style-type: none">• High speed• No airbags	<ul style="list-style-type: none">• No guard rails
Post-Event	<ul style="list-style-type: none">• Middle age driver• Average physical condition	<ul style="list-style-type: none">• No engine cutoff	<ul style="list-style-type: none">• 911 Emergency number• EMS• Trauma care• Rehabilitation systems

7.4 CASE 3: ROLLOVER CRASH

7.4.1 Crash Reconstruction III

On a clear and sunny day, a 19 year old male (184 cm, 68 kg) driver of a 2003 suburban GMC (Chevrolet, 2085 kg) was negotiating a right-hand curve at an estimated speed of 160 km/h. According to the police report, the driver was trying to avoid hitting an object in front of him. The vehicle rolled over, swerving to the left side of the road and rolling to the left 6 quarter turns for a total of 40 m, and came to rest on its roof in a steep valley. The rollover resulted in moderate roof crush. The automobile sustained severe intrusion on the driver's side. The driver was found with his legs protruding through the driver's side window and, was lying supine on the seat unconscious. He was wearing the seatbelt. The air bag was not deployed, and the steering wheel was deformed. Crash scene is shown in **Figure 7.8**.

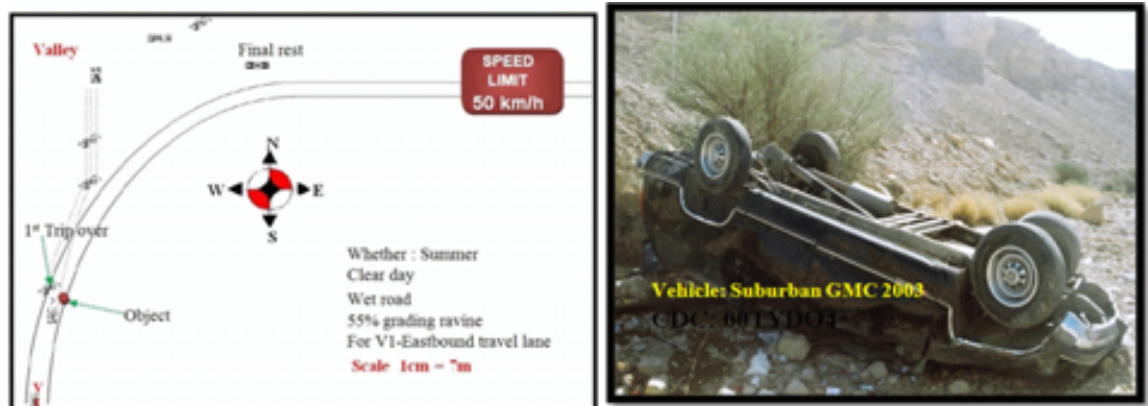


Figure 7.8: Scene diagram and vehicle damage for Case 3

The crash site and the vehicle have been modeled in PC-Crash. In this particular crash one car and a number of fixed objects were involved. A number of variations in the rolling scenario were simulated. One of the scenarios that matched the result reasonably well was considered for further discussion. The reconstruction result was compared with the accident scenario. The vehicle tripping over and swerving to the left side of the road rolling left 6 quarter turns and its final position (vehicle came to rest on its roof in a steep valley) matched well. **Figure 7.9** shows the simulation outputs at different events during series of crash.

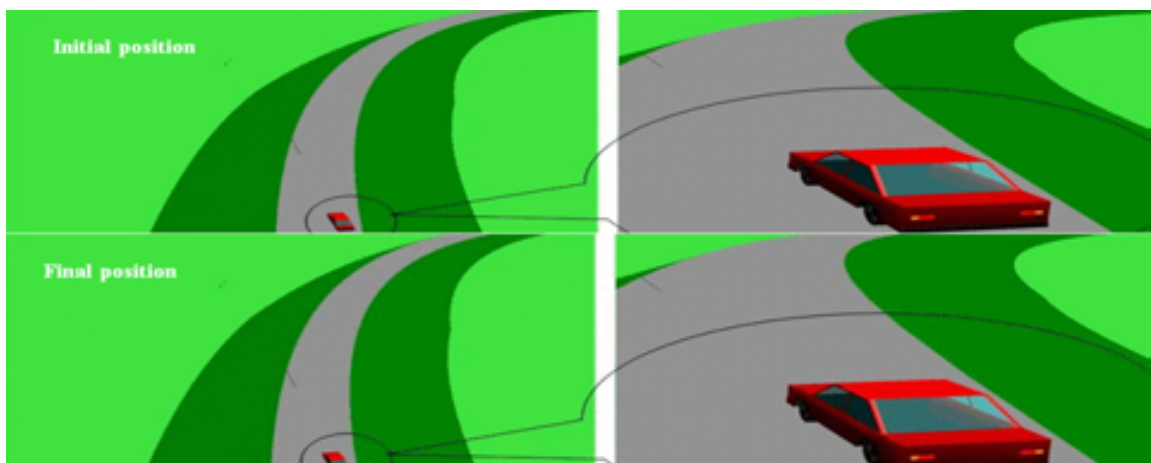


Figure 7.9: Snapshots from the PC-Crash simulations for Case 3

7.4.2 Mechanisms of Spinal Injury

The driver was seen initially at an external facility, with a reported GCS score of 3 and no visual, verbal, or motor responses. He presented with a transverse abdominal ecchymosis (seatbelt sign) but was not injured intraabdominally. In addition, he presented bruising on his upper chest, particularly around the shoulders.

On arrival at the hospital, he underwent CT and MRI of the cervical and thoracic spine that showed bilateral pulmonary contusions; a paraspinal hematoma; right first and second rib fractures; and complex fractures of the upper thoracic spine, specifically fractures through the transverse processes of T1, T2, T4, and T5 on the left as well as bilateral transverse process fractures of T3 (Chance), fractures of the pedicle and fractures of the T4 and T5 vertebral bodies lamina and posterior facets of T3, and compression (**Figure 7.10**). In addition, he sustained associated injuries as presented in **Table 7.5**.

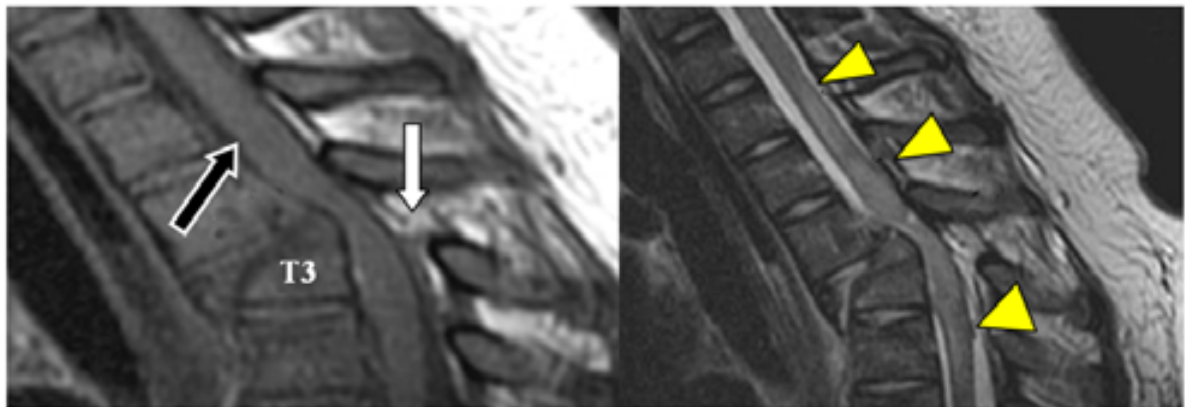


Figure 7.10: Radiographic images of spinal injuries for driver in Case 3: left, sagittal CT of T3 shows Anterolisthesis fracture (*black arrow*), disruption of ligament (*white arrow*); right, weighted MRI images of upper thoracic spine of T3 shows a compression of spinal cord with cord edema (*arrowheads*)

Table 7.5: Injuries of driver in Case 3

Injury	ISS Body Region	AIS	Source of Injury
Comminuted fracture of parietal bone	Head	150404.3	Roof/ A pillar
Contusion of the right temporal lobe	Head	140606.3	Roof/ A pillar
Acute traumatic subarachnoid haemorrhage	Head	140684.3	Roof/ A pillar
Multiple bruising left cheek and chin	Face	210202.1	Windshield
Facial contusions right side & bridge of nose	Face	210402.1	Windshield
Couple of small right pulmonary contusions	Thorax	441406.3	Side door
Cord contusion extending from C7 to T4	Thorax	640404.3	Seatbelt
Ligamentary chance fracture of T3	Thoracic spine	650622.3	Seatbelt
Multiple rib fractures NFS	Thorax	450220.2	Steering wheel
Deep lacerations in the lobes of the liver	Abdomen	541820.2	seatbelt
Bruising to abdomen (iliac spines)	Abdomen	510202.1	Seatbelt
Compound fractures of the leg & foot	Extremities	851823.3	Steering column
Fracture right scapula of the upper arms	Extremities	753000.2	Steering wheel
Bruising dorsum of the right and left hands	Extremities	710402.1	Steering wheel
ISS			27

Although Seatbelt fracture known as Chance fractures are relatively common injury in the lumbar spine (Chance, 1948; Nicoll, 1949), few cases of Chance fractures in the upper thoracic spine have been reported (Anderson et al., 1991).

The mechanism of action for the present case has been thoroughly described as a flexion distraction around a fulcrum, most commonly the seatbelt. The point of motion in the body impacting against this fulcrum is normally the spine itself. In the Chance fracture mechanism, the fulcrum (lap belt) is anterior to the spine and high-energy motion results in tension failure of the spine. Because the tensile strength of ligaments is greater than that of bone, the bone elements fail before the ligaments (Howland et al., 1965).

Table 7.6 shows the Haddon's matrix preventive measures for Case 3.

Table 7.6: Haddon's matrix for Case 3

Phase	Factor		
	Host	Vehicle	Environment
Pre-event	<ul style="list-style-type: none">• Driver inattention• Driver inexperience on road	<ul style="list-style-type: none">• Brakes in poor conditions• Install ESC	<ul style="list-style-type: none">• Road curvature• Sun in direction of driver• No warning signs
Event	<ul style="list-style-type: none">• Wearing seatbelt properly• Sit further back from steering wheel	<ul style="list-style-type: none">• Excessive speed before curve• Side airbags present• Roof deformation	<ul style="list-style-type: none">• Asphalt• Dirt on road• Defective road surface• No side fencing
Post-Event	<ul style="list-style-type: none">• Young age• Good physical condition	<ul style="list-style-type: none">• Tires traction in non-proper conditions for stopping	<ul style="list-style-type: none">• 911 Emergency number• EMS• Trauma care• Rehabilitation systems

7.5 CASE 4: FRONTAL IMPACT

7.5.1 Crash Reconstruction IV

In March, 2007, at approximately 10:40 AM on a spring weekend, a 1998 model year Nissan Datsun was proceeding on a wet, 2% uphill grade, two-way road approaching an uncontrolled intersection intending to continue straight on. A 1989 model Chevrolet Caprice (mass of 1926 kg) was travelling eastbound on this same roadway, with a 2% downhill grade, approaching the same intersection intending to turn left. The front of the Datsun collided with the front of the Caprice on the westbound way. The police estimated a speed of 125 km/h, and a force coming from “12 o’clock” with 75% right front to right overlap. The Datsun sustained severe frontal crash to the engine bay. The airbags failed during the crash. The driver of the Caprice was transported to hospital due to severe injuries where he died at the trauma centre. The driver of the Datsun was transported to hospital as he had sustained spinal injury and other moderate injuries. The crash overview of this case is shown in **Figure 7.11**.



Figure 7.11: Scene diagram and vehicle damage for Case 4

A reconstruction was developed for the crash using the software PC-Crash. A number of initial conditions were tried. The conditions that best matched the crash data included a vehicle1 speed of 120 km/h and orientation of 0° with the lane and vehicle-2 speed of 60 km/h and an orientation of -154° with the same lane. This reconstructed case was compared with the available data. The impact positions and damage of vehicle compared well (**Figure 7.12**).

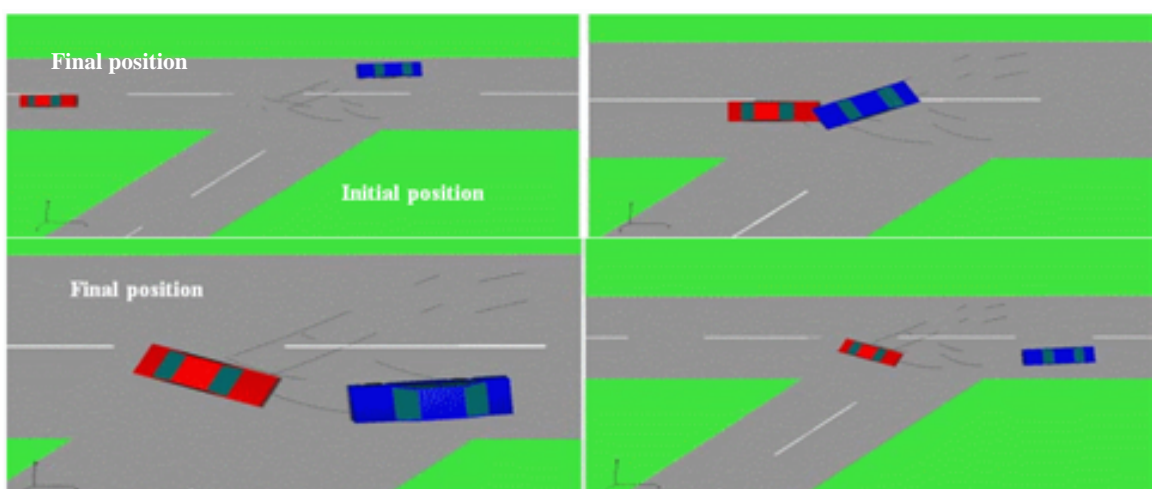


Figure 7.12: Snapshots from the PC-crash simulation for Case 4

7.5.2 Mechanisms of Spinal Injury

The anteroposterior radiograph and computed tomography (CT) examinations of the lumbar spine revealed a biside locked facet dislocation at L4-5 as well as fractures of the right transverse processes of L4 and L5 as can be seen in **Figure 7.13**.

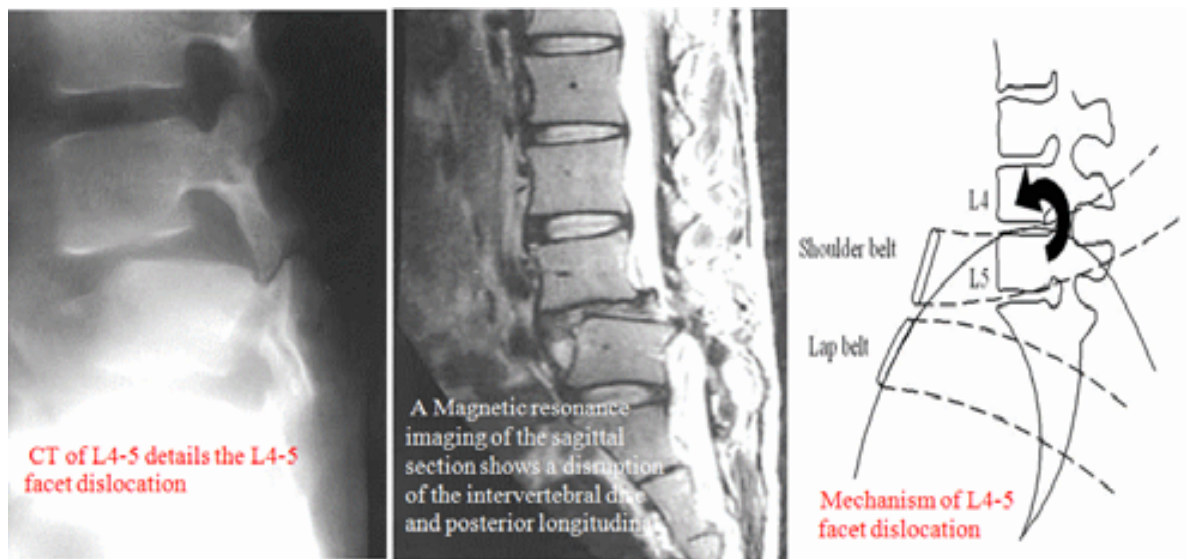


Figure 7.13: Radiographic images of spinal injuries for driver in Case 4

The driver was transferred to the unit for surgical treatment. He had no motor deficit or sensory disturbance in the lower limbs, and his bladder functions were normal. MRI revealed a severe constriction of the dural tube near the posterior-upper edge of the L5 vertebral body, and a sagittal view of the L4-5 level showed a disruption of the posterior longitudinal ligament. During surgery, It was found that the articular capsules of the zygapophyseal joints and the supra- and interspinous ligaments were completely torn, the ligamentum flavum was partially ruptured, and the bilateral L4-5 facets were locked bilaterally.

A posterior interbody fusion with cages, reinforced by a bilateral posterior rod and pedicle screw fixation was also performed. One year and 6 months later, he reported no lowback pain and had no neurological deficit. Radiographs showed no breakage of the implants, and satisfactory alignment. The mechanism of this spinal injury was identified to be identical to Magerl's Type B1.1.2 associated with seatbelt injury (Magerl et al., 1994). This type of injury also corresponds to Denis' Type C fracture dislocation injury (Denis, 1983). Therefore, it is speculated here upon the mechanism of this unusual condition.

The crash reconstruction was conducted to establish causation between the resulted injuries and the probable sources as indicated in **Table 7.7**. The driver was wearing a three-point lap/shoulder, and after inspection was found to have fitted his seatbelt in an improper manner, positioning the shoulder harness under his armpit.

Table 7.7: Injuries of driver in Case 4

Injury	ISS Body Region	AIS	Source of Injury
1 cm laceration on right posterior scalp	Head	110602.1	A pillar
3 cm laceration above left eye	Face	210602.1	A pillar
Fracture to nose with 2.5 cm laceration	Face	251004.2	A pillar
Focal ruptures of large bowel	Abdomen	540826.4	Seatbelt assembly
Torn mesentary	Abdomen	542024.3	Seatbelt assembly
Haemorrhagic across abdominal wall	Abdomen	510402.1	Seatbelt assembly
Right transverse process fracture at L4-L5	Lumbar spine	650620.3	Seatbelt assembly
Lacerations to left hand	Extremities	710602.1	Instrument panel
Lacerations to right hand	Extremities	710602.1	Instrument panel
Lacerations to left leg and foot	Extremities	810602.1	Toe pan
ISS			21

Examination of the vehicle interior showed that there was evidence of occupant contact on the A-pillar. Therefore, it is most likely that deceleration of the driver's body, such as in frontal vehicle collisions forced his head to travel toward the left A-pillar roof-rail region which would be the cause of the head and face injuries. On impact, as the upper body of driver was moving forward, the lap belt portion restrained his body at the waist and abdomen. This suggests that the driver sustained a dislocation of L4-5 facet joints due to a flexion moment of the trunk around the pelvis, immobilized by a lap seatbelt. This is supported by the evidence that the seatbelt webbing was stretched and frayed at the buckle point. Additionally, he had several intra-abdominal injuries. Together, all these injuries are consistent with loading to the abdomen and lumbar spine from the lap belt. The stretching and frying of the seatbelt at the latch plate provided certain evidence for this mechanism.

Table 7.8 shows the Haddon's matrix preventive measures for case 4.

Table 7.8: Haddon' s matrix for Case 4

Phase	Factor		
	Host	Vehicle	Environment
Pre-event	<ul style="list-style-type: none"> • Using hand mobile • Driver inexperience 	<ul style="list-style-type: none"> • No anti lock brakes • Windshield needs cleaning • No daytime running lights 	<ul style="list-style-type: none"> • Road design • Poor signage
Event	<ul style="list-style-type: none"> • In proper seatbelt fastening 	<ul style="list-style-type: none"> • High speed • No airbags 	<ul style="list-style-type: none"> • Asphalt • Road is wet • No side fencing
Post-Event	<ul style="list-style-type: none"> • Physically fit 	<ul style="list-style-type: none"> • Proper tire tread depth for stopping 	<ul style="list-style-type: none"> • 911 Emergency number • EMS • Trauma care

7.6 CONCLUSIONS

In this work four typical crashes with uncommon spinal injuries were reconstructed and the kinematics was correlated with injury information to develop confidence on the analysis of the mechanisms of injuries in these crashes. Haddon's matrix was used to present intervention measures for different stages of each impact. Since these crashes are typical crashes in Saudi Arabia, they demonstrate the ability of the methodology to give suggestions of these injuries can be prevented in future. The main conclusions are summarised as the following:

- 1- Case 1 represents a typical pedestrian collision occurred at an intersection in Riyadh. The pedestrian sustained a dislocation fracture of atlanto-occipital joint (AIS 3). In conclusion, occipital condyle fractures seem to be rare. In order to prevent such pedestrian crash, a dedicated signal and crosswalk should be installed which would prevent vehicles and pedestrians entering the intersection at the same time.
- 2- Case 2 was a side impact struck with a light pole. The spinal injury of the driver was identified as a bilateral cervical spondylolysis. Recognition of the anomaly and differentiating it from acute cervical fracture or dislocation is important in casualties with recent neck injuries. This injury could have been prevented or greatly reduced had the driver been wearing a seatbelt and had the vehicle design included side airbags.
- 3- Case 3 demonstrated a rollover in a suburban environment. The driver sustained an uncommon Chance fracture in the thoracic spine at T3. Since this crash could not be prevented, possible means of reducing the impact energy could have been applied. The presence of the roof-mounted side impact airbag will possibly prevent the driver from sustaining serious spinal injuries.

- 4- The crash in Case 4 is a frontal offset impact between two vehicles. The laboratory examination for the driver confirmed he has sustained a bilateral locked facet at L4-5. It is concluded that this rarely encountered condition of the unusual L4-5 level facet interlocking was attributed to misuse of the automobile shoulder harness. Since the crash could not be avoided in the pre-crash stage, applying some safety means such as road rumble strips could have reduced or eliminated the serious injuries. Use of safety restraint systems and availability of side airbags in the car seat and door would have mitigated the severity of these injuries.
- 5- Insufficient training of the EMS in better management of road design are among the factors believed to be impediments in spinal injury reduction in the Saudi society.
- 6- This work has demonstrated a methodology how crashes can be analysed, the cause of neck injuries understood and counter measures designed.
- 7- This kind of scientific analysis is essential to reduce the number of road traffic accidents and injuries. The current study has demonstrated how it can be done, but there is a long way to go in order to get the full benefits of such a study.
- 8- The study has demonstrated the need to do such an analysis for crashes in Saudi Arabia. It is now important to follow this up and start crash analysis and reconstruction on a regular basis. The benefits to the society will be immense.

CHAPTER 8

MODELLING OF THE SPINE FOR DYNAMIC ANALYSIS DURING VEHICLE CRASHES

In order to understand the behaviour of the human body and the neck injury mechanism during car crashes, mathematical modelling, using numerical methods has been done. For this purpose, six dynamic models were created in Working Model 2D to simulate spinal injuries of driver in frontal collisions, rear collisions, rollover crashes, side impact car crashes, crashes with pedestrians and crashes with camels. Results of these numerical simulations allowed qualitative estimates of the most dangerous situations of spinal injuries during these types of accidents. While most of the earlier neck injury criterion (like NIC, and N_{ij}) are force or acceleration based, it is postulated that Peak Virtual Power (PVP) gives better estimates of neck injury at each inter-vertebral level. These injury indices have then been compared with injury data from hospitals to study their correlations. It is observed that PVP correlates well with the injury data on spinal injuries.

This chapter describes the models developed, their validations, and the kinematics obtained in the different simulations. The MAIS of neck injuries has been correlated with ΔV from the accident data available. The PVP at each inter-vertebral level has been obtained and compared with the injury likelihood data obtained from real world crashes.

8.1 METHODS AND MATERIALS

The aim of this chapter is to analyse six types of vehicle crashes in the context of neck injuries similar to the situations in real world accidents. The models created are: front, rear, side impact, rollover, car to pedestrian collisions, and car to camel collisions in the vertical two-dimensional plane. Methodologies for modelling of the motion of the human spine vary dramatically in complexity. While providing detailed 3D modelling of the human spine can be computationally expensive. Alternatively, 2D nonlinear multibody dynamics representations are often used because of their simplicity. These formulations employ rigid models of vertebrae interconnected via conventional mechanical joints. However, it is well documented that inter-vertebral motion can depart significantly from conventional mechanical joint constraints. **Figure 8.1** gives the process of models in this study.

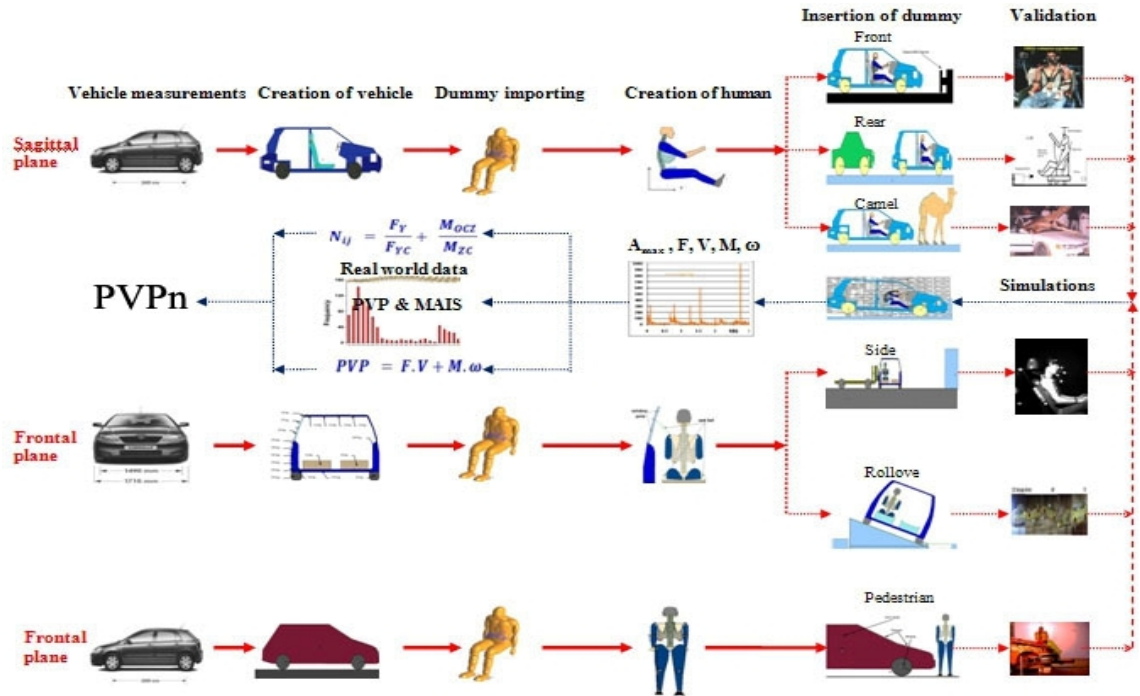


Figure 8.1: Simulation process of the whole model system

8.1.1 Modelling Process

In order to conduct the study, six dynamic 2-Dimensional models for a 50%ile male were created using the Working Model Software ver. 7.0 (MSC, 2004) as the following:

- I. Driver for frontal impact analysis.
- II. Driver for rear impact analysis.
- III. Driver for camel collision analysis.
- IV. Driver for side impact analysis.
- V. Driver for rollover analysis.
- VI. Pedestrian for car-pedestrian collision analysis.

Simplified models were formulated including the main car body parts with the appropriate size, mass, centre of gravity and stiffness. The modelling processes in this study have been performed on the basis of the principles of multibody dynamics (MBD), where rigid bodies are connected by articulated joints and spring-damper elements.

8.1.2 Modelling Software

Working Model (WM) is a powerful engineering analysis and motion simulation software on PC. Working Model was first released in 1993 by MSC Software Corporation for the engineering community. It was created by adding engineering functionality to **Interactive Physics (IP)** and importing DXF drawings from CAD packages such as AutoCAD. Working Model was renamed Working Model 2D in 1996. The latest version of WM2D is R5, released in 1999. Working Model 3D was first introduced in 1996. When MSC acquired Knowledge Revolution in 1999, dynamic FEA capability was added and Working Model 4D was born.

A user can sketch a problem using a variety of simple geometric primitives. Then sketch additional constraints (joints, springs, and dampers) and actuators (cylinders and motors). WM applies Newton's law along with physical constraints and external forces to calculate the internal forces and acceleration of each rigid body. Using numerical integration, the velocity and position of each body can be calculated (Wang, 2001).

Since no closed form formula is used in WM for the animation, users can use WM to verify answers obtained from using loop closure equations. For a complex control problem, WM can establish real-time links with Excel, MATLAB, or other programs that support Windows DDE to carry out calculations. WM can import drawings with AutoCAD DXF format. AutoMotion can also create and attach WM constraints to AutoCAD geometry. Once a mechanism is constructed and run in WM, a user can play "what if" scenarios by using the Smart Editor to manipulate objects on screen and change the property and appearance of each body. This flexibility gives an active learner a virtual prototyping tool.

WM2D can analyze a mechanical system by measuring the forces and motions of any part in the system. The measured data can be shown in graphs, digital displays, and bar charts, and can be customized with the versatile WM2D formula language. With its user-friendly interface, WM2D is a conceptual design tool as shown in **Figure 8.2**. A design can be optimized with the fast build-run-analyze-refine cycle before a physical prototype is built.

Theoretical background information on multibody dynamics are provided, among others, by Roberson and Schwertassek (1988) and Norton (1992).

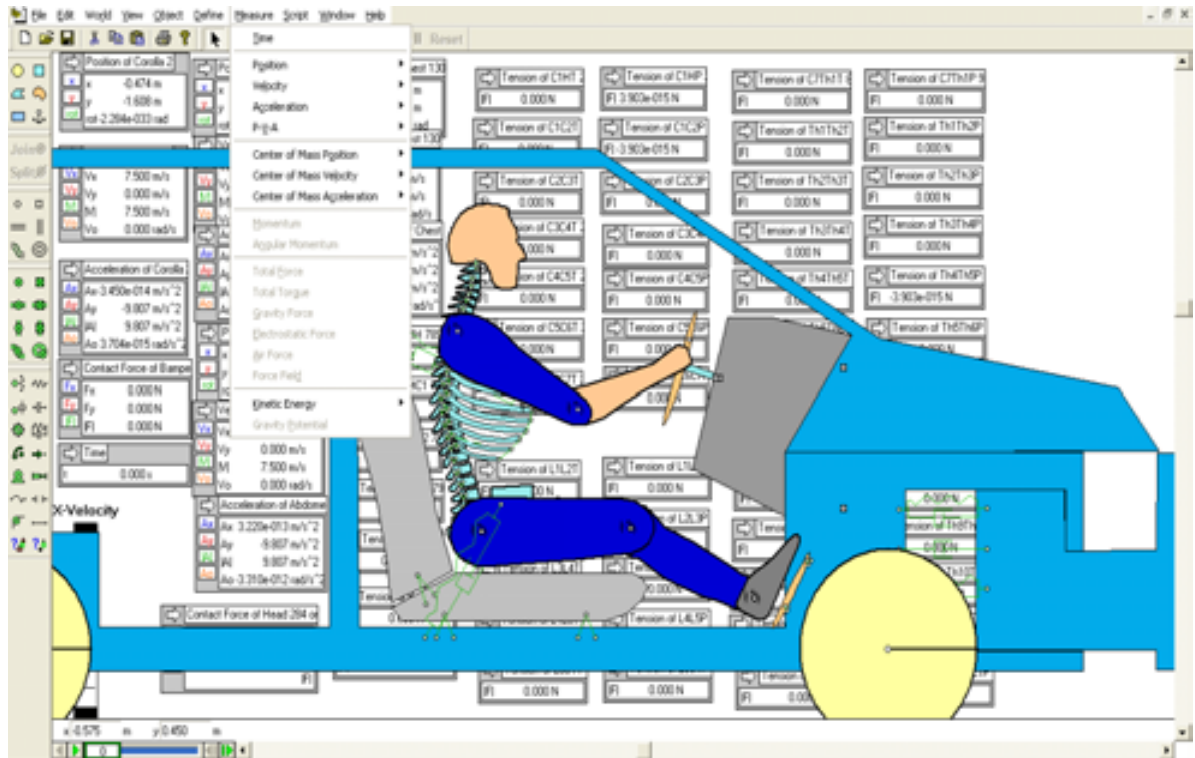


Figure 8.2: Window interface/tools menu of WM2D

8.1.3 Basic Assumptions

The models were created on the basis of the following general assumptions:

- the driver model corresponded to the parameters of a 50th percentile male of 1.74 m standing height and 75.7 kg weight (Schneider et al., 1983),
- the main parts involved in the modelling process are: the head, cervical, thoracic and lumbar spine, rib cage and the upper and lower limbs including 24 vertebrae, main muscles, ligaments, intervertebral joints and discs,
- the elements of the structures were treated as rigid bodies, connected with steering wheel, armchair and pedals by linear spring-damper elements,

- the head, vertebrae and trunk are joined by articulated joint and linear spring- damper elements representing natural connections,
- the interaction of soft tissues are represented by non-linear spring-damper elements,
- the armchair is divided into an immovable seat, movable head-rest and backrest, and are assumed to be rigid bodies,
- the excitations were assumed to be kinematical excitation adequate to respect the conditions during real car accidents, and
- the vehicle was modelled according to the geometrical parameters of the Toyota Corolla model (2002), 1200 Kg (Toyota, 2005).

The basic details of the model parts and material properties are given in the subsequent sections. Materials properties were assumed on the basis experiments and literature data.

8.1.4 Crash Data Collection

The collisions and injury data were compiled from on-site collected data and hospital records based on the general methodology used in **Chapter 4**. In particular, whiplash details were obtained from medical notes and interviews with the occupants. A follow-up of possible medical symptoms was carried out at least six months after the collision.

The questionnaire of symptoms and injury severity were structured in co-operation with a medical doctor. The symptoms noted were those associated with pain, stiffness and musculoskeletal signs, and with neurological symptoms, such as numbness. The duration of symptoms was defined as follows: no injury, symptoms less than one month, symptoms between one and six months, and symptoms for more than six months (see **Appendix C**).

8.2 SIMULATION OF SPINAL INJURY IN FRONTAL IMPACT

Frontal impact simulations have been developed to study the neck injury likelihood for the driver in frontal impacts. The model for frontal impact has been developed according to the Insurance Institute for Highway Safety (IIHS) frontal offset crash Test (IIHS, 2008).

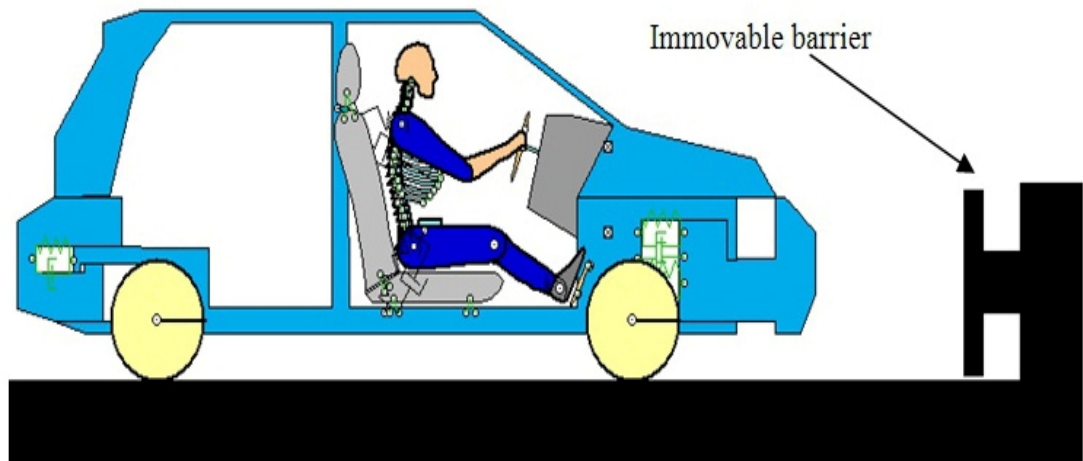


Figure 8.3: Modelling setup of the frontal impact simulation

The initial configuration of the model is shown in **Figure 8.3**. The modelling of frontal impact consisted of three systems combined in one MBD model: the car; the front barrier; and the driver dummy in the sagittal plane. These systems are described in the following sections.

8.2.1 Model of the Deformable Front Barrier (DFB)

The front barrier is composed of three elements: base unit, extension, and deformable face (IIHS, 2008) as shown in **Figure 8.4**. The base unit is 184 cm high, 366 cm wide and 542 cm deep. The extension is 91 cm high, 183 cm wide and 125 cm deep. The modelling of the front barrier has been simulated by a combination of rigid parts, connected through a set of springs and dampers. The mechanical coefficients are given in **Table 8.1**.

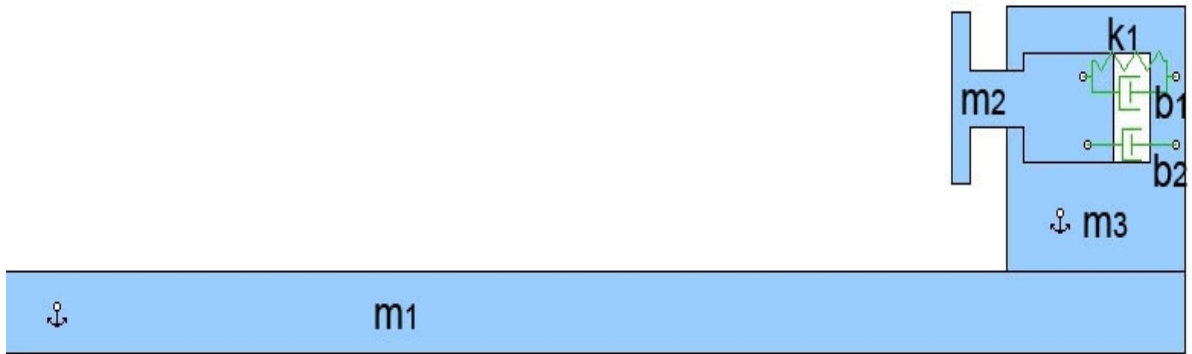


Figure 8.4: Modelling of the deformable front barrier

Table 8.1: Mechanical properties of the DFB (IIHS, 2008)

Mechanical Parameter	Unit	Value
Base mass (m_1)	kg	5×10^5
Deformable face mass (m_2)	kg	100
Extension mass (m_3)	kg	100
Spring stiffness, k_1	N/m	1508.50
Damping coefficient, b_1	N.s/m	1000
Damping coefficient, b_2	N.s/m	8.5×10^5

8.2.2 Model of the Car in the Sagittal Plane

The car model for frontal impact was initially developed using the data for a typical passenger car. In this case a 2002 Toyota, Corolla model is selected for the simulation. The technical specifications were obtained from the manufacturer (Toyota, 2005). The original dimensions of the simulated car are presented in **Figure 8.5**.

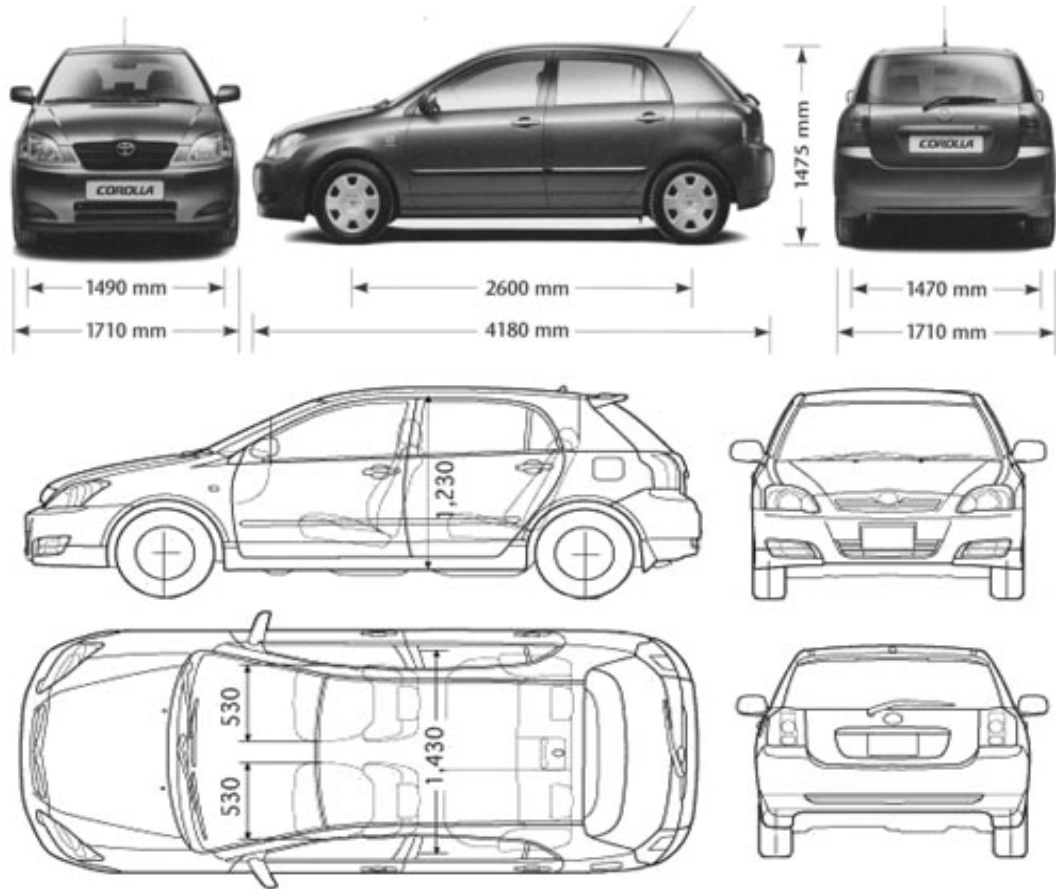


Figure 8.5: Geometry parameters of the Corolla car (Toyota, 2005)

The vehicle has been modeled from regular geometrical shapes representing rigid bodies which are joined in an appropriate way to consider the effect of the energy dissipation at the moment of collision as well as characteristics of body deformation. The rigid bodies are part of a model in the software WorkingModel™ and capture impact through force deflection characteristics in a multi-body modelling paradigm. The vehicle has moreover taken into account car equipment having the major influence on the driver's body behaviour during the crashes, i.e. accelerator/brake pedals and steering wheel. The pedals and the wheel were modeled as rigid elements jointed to the body through bracket joints. The details of the main car parts used in the simulations are provided in **Figure 8.6** and **Table 8.2**.

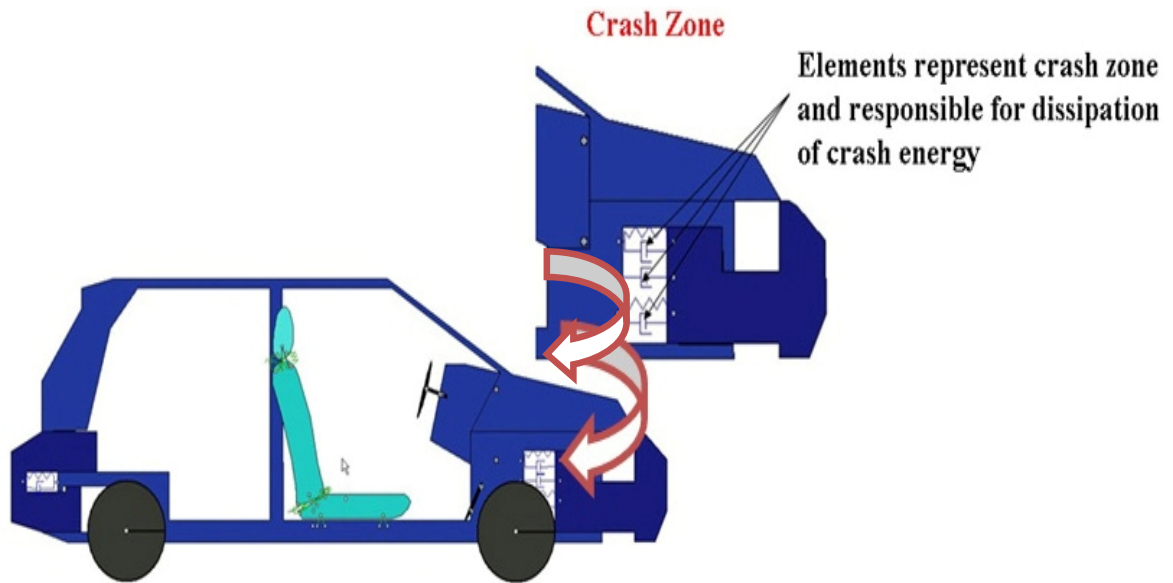


Figure 8.6: Main components of the simulated Toyota car

Table 8.2: Mechanical properties of vehicle components (Toyota, 2005)

Mechanical Element	Parameter (Unit)	Value
Body of vehicle including main parts	Mass (kg)	800
Front bumper	Mass (kg)	150
Rear bumper	Mass (kg)	150
Armchair assembly	Mass (kg)	22
Steering wheel, pedals, and dashboard	Mass (kg)	28
Wheels	Mass (kg)	50
Crash zone	Stiffness, k_t (N/m)	1500
	Coefficient of damper, b_t (N.s/m)	7×10^5

The initial seating and the head restraint positions are among those factors that might influence the risk of neck injury. In this model, the driver's armchair was divided into seat, backrest and movable headrest joined by articulated joints as well as spring-damper elements representing the characteristics of joints in real driver's armchair (**Figure 8.7** and **Table 8.3**).

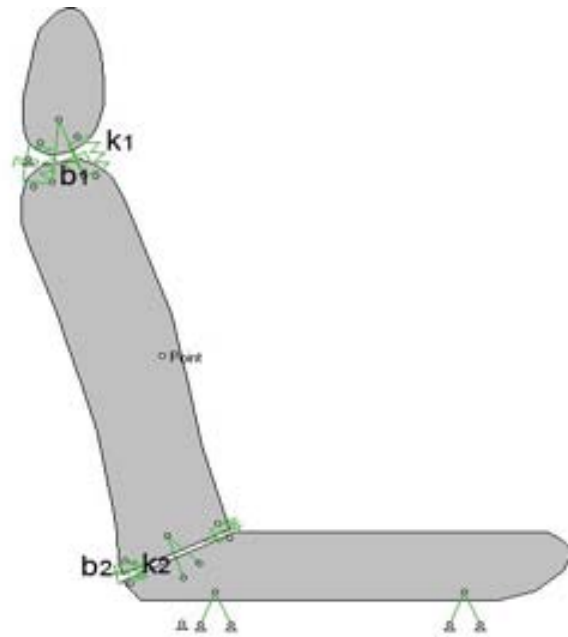


Figure 8.7: Main components of the armchair in the model

Table 8.3: Mechanical properties of the armchair (Toyota, 2005)

Mechanical Parameter	Unit	Value
Seat mass	kg	10
Backrest mass	kg	10
Movable headrest mass	kg	2
Spring stiffness, k_{t1}	N/m	8×10^4
Damping coefficient, b_{t1}	N.s/m	5000
Spring stiffness, k_{t2}	N/m	1×10^6
Damping coefficient, b_{t2}	N.s/m	5000

8.2.3 Model of Driver in the Sagittal Plane

The kinematics of each rigid body element is described after fixing the origin of the local coordinate system at the centre of mass of the body from which the displacement, velocity and acceleration are defined in accordance the global coordinate system (**Figure 8.8**). The movement of the human body in the front and rear impacts and camel collision has been analysed in the sagittal plane (XY) of the coordinate system. The motion of the human body in the side, rollover, and pedestrian models were analysed in the frontal (YZ) plane.

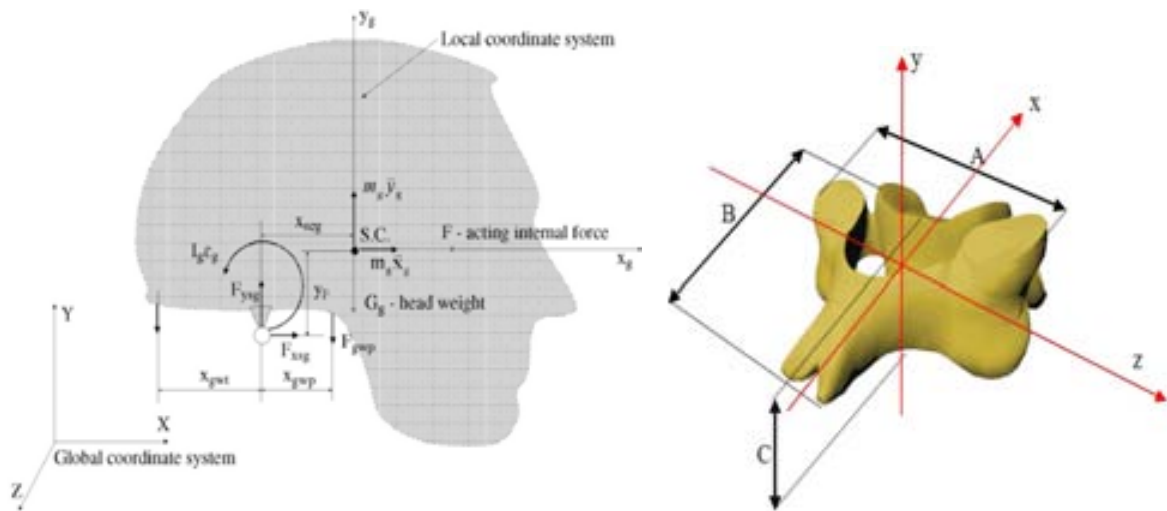


Figure 8.8: Global and local coordinate systems for elements of models

The human anatomical data needed to define the geometry and inertial properties of the rigid bodies in the model are scarce. The geometry of the whole spine for a 75 kg male was preliminary downloaded from an internet resource (www.3dcafe.com). The model of the human spine was then rescaled by using Rhinoceros Nurbs Modelling v3.0 SR5 according to the dimensions of a real adult male spinal column (Campbell-Kyureghyan et al., 2005).

The inertial parameters of each spinal vertebra were calculated separately about the X, Y, and Z axes by using SolidWorks Office Pro 2007 (**Figure 8.9**). Material properties were assumed to be homogenous bone structure with a density of $1.5 \text{ (g/cm}^3\text{)}$ which is the median value for cortical and trabecular tissues of vertebra bone (Jorgensen, 2005; Panjabi, 1998). The stiffness values used are quoted later.

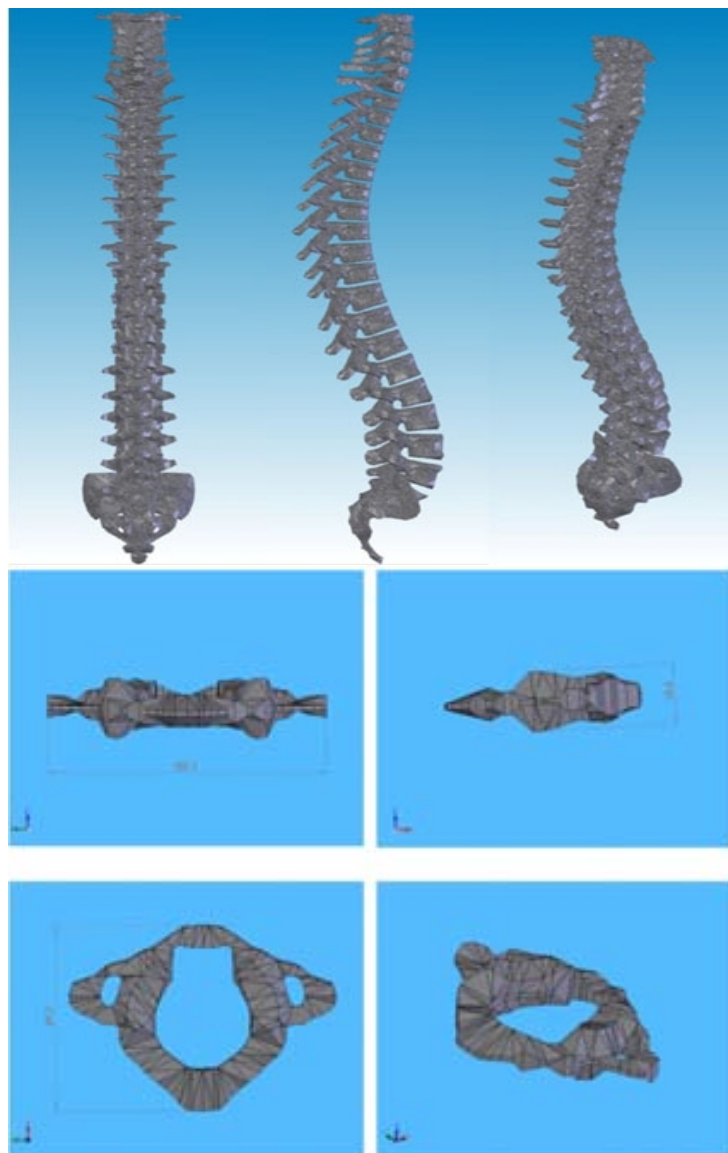


Figure 8.9: Samples of the modelling of the spinal vertebra created by SolidWorks

The main parts involved in the modelling process are: the head, spine, rib cage and the upper and lower limbs. The elements of the model were joined by articulated joints as open kinematic chains and additionally joined with spring-damper elements. Each of the muscles and ligaments have been modeled using appropriate spring and damper elements. The vertebral spine model includes 24 solid vertebrae, muscles, ligaments, inter-vertebral joints and discs as shown in **Figures 8.10-13**. The mass and moment of inertias of the vertebral spine in the sagittal plane (I_z) are presented in **Table 8.4**.

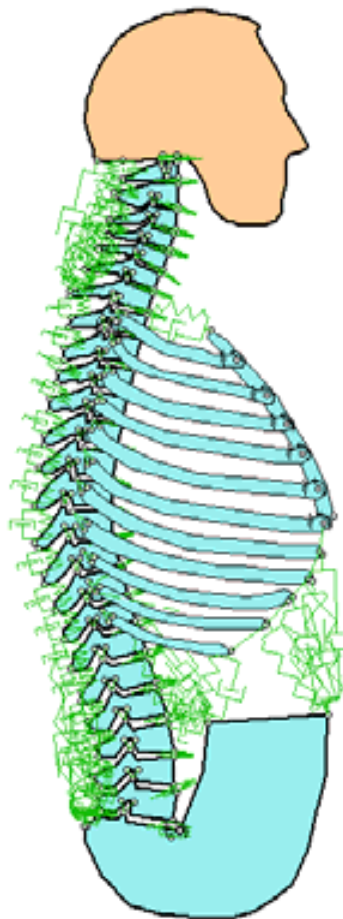


Figure 8.10: Modelling of the head and the whole spine in the sagittal plane

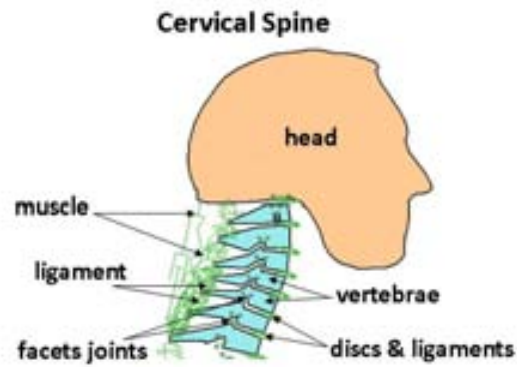


Figure 8.11: Modelling of head and cervical spine in the sagittal plane

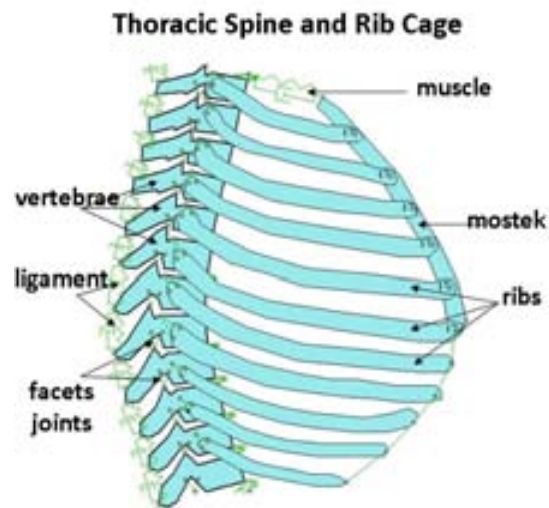


Figure 8.12: Modelling of the thoracic spine in the sagittal plane



Figure 8.13: Modelling of the lumbar spine and sacrum in the sagittal plane

Table 8.4: Moments of inertia, mass/dimensions of vertebrae (Al-Shammari et al., 2008b)

Vertebrae	Mass [g]	Mass Moments of Inertia			Dimensions		
		I_x [g.mm ²]	I_y [g.mm ²]	I_z [g.mm ²]	A [mm]	B [mm]	C [mm]
C1	21.1	8093.4	4248.45	11924.4	85.1	59.7	18.6
C2	23.5	3436.8	4901.4	7257	57.8	60.3	29.7
C3	22.6	3222.45	4871.85	7067.55	56.2	61.2	14.6
C4	24.3	3990	5199.45	8079.9	58.3	61.2	14.6
C5	28.7	4940.25	8316.75	12170.1	63.3	68.9	14.6
C6	29.4	5626.95	8392.65	12822.15	71.1	68.9	14.4
C7	40.4	8143.8	9644.1	14731.2	73.6	72	19.4
T1	40.3	9093.9	9937.95	14545.2	94.9	70.1	19.3
T2	40.0	7128.15	9721.95	12623.55	73.2	72.6	20
T3	48.5	9570.75	13664.55	17698.5	77.8	78	21.2
T4	55.9	11912.25	17352	22233	76.4	82.9	22.3
T5	56.3	11804.1	17302.5	22215	76.4	82.3	22.3
T6	60.8	12942	22192.5	27441	76.4	87.1	22.4
T7	62.4	13263.6	22480.5	27634.5	79.9	79.7	23.4
T8	68.4	15633	22884	29808	79.9	74.7	23.4
T9	73.3	16186.5	24618	31246.5	66.8	76.8	23.1
T10	88.0	20677.5	32013	37747.5	56.3	79	27.5
T11	89.3	20241	34623	40461	56.3	82.3	28
T12	89.3	20220	34683	40542	56.3	82.4	28
L1	89.7	21642	33895.5	40257	75.1	77.4	29.4
L2	86.4	20587.5	33579	39921	75.1	77.3	33.1
L3	95.9	24291	38938.5	46333.5	77.4	79.4	34.2
L4	96.8	24697.5	39570	46929	77.5	80.7	34
L5	84.7	21019.5	28614	37368	77.5	77.9	32.8
Sacrum	250.1	299895	170580	207240	113.9	80.7	121.9

Material properties of the intervertebral discs are required for all directions of loading as flexion, extension, tension, compression, anterior and posterior shear, lateral shear, axial rotation and lateral bending. Due to the mid-sagittal symmetry of the cervical spine, the disc response are assumed to be the same for left and right lateral bending, lateral shear and axial rotation. Vertebral disc responses are obtained by subjecting a motion segment (vertebra-disc-vertebra) or a disc segment (body-disc-body) to external loading. Disc stiffnesses reported by Moroney et al. (1988) and Yoganandan et al. (2000) were used for the cervical spine.

As no other data on cervical disc stiffnesses can be found Moroney's values have been used for axial rotation, lateral bending and all shear stiffness coefficients. Camacho et al. (1997) presented non-linear load-displacement curves at various levels.

The translational damping coefficients of the discs are set to 1000 kg/s and rotational coefficients to 1.5 Nm/s as based on those used by de Jager as no actual disc damping coefficients have been reported in the literature. These damping coefficients were shown not to account for the dynamic stiffening of the disc but instead were employed to attenuate vibration accelerations of the head (de Jager, 1996).

In the model, the dynamic stiffness of the disc is assumed to be twice the static stiffness to approximately allow for strain-rate effects. Material properties for cervical spine discs are tabulated in **Table 8.5**. For thoracic spine, the stiffness values in **Table 8.6** were employed in the modelling. For lumbar spine, the motion segment stiffness matrix results of the study of Gardner-Morse and Stokes (2004) was utilized in the modelling as shown in **Table 8.7**.

Table 8.5: Stiffness coefficients for the cervical spine (Yoganandan et al., 2000)

Loading Direction	Stiffness k [N/mm]						Damping b
	C2-C3	C3-C4	C4-C5	C5-C6	C6-C7	C7-T1	C2-T1 [N.s/m]
Anterior Shear	62	62	62	62	62	62	1000
Posterior Shear	50	50	50	50	50	50	1000
Lateral Shear	73	73	73	73	73	73	1000
Tension	63.5	69.8	66.8	68	69	82.2	1000
Compression	637.5	765.3	784.6	800.2	829.7	973.6	1000
	[Nm/rad]						[Nms/rad]
Flexion		Load Curve from Camacho et al., (1997) /2					1.5
Extension		Load Curve from Camacho et al., (1997)/2					1.5
Lateral Bending	0.33	0.33	1.5	0.33	0.33	0.33	1.5
Axial Rotation	0.42	0.42	0.42	0.42	0.42	0.42	1.5

Table 8.6: Stiffness coefficients for the thoracic spine (White and Panjabi, 1990)

Authors	Stiffness Coefficients	Maximum Load	Spine Region
Compression(-F_y)			
Virgin, 1951	2.5 MN/m	4500 N	Lumbar
Hirech & Nachemson, 1954	0.7 MN/m	1000 N	Lumbar
Brown et al., 1957	2.3 MN/m	5300 N	Lumbar
Markolf, 1970	1.8 MN/m	1800 N	Thoracic & Lumbar
Moroney et al., 1988	0.5 MN/m	74 N	Cervical
Tension(+F_y)			
Markolf, 1970	1.0 MN/m	1800 N	Thoracic & Lumbar
Shear (F_x, F_z)			
Markolf, 1970	0.26 MN/m	150 N	Thoracic & Lumbar
Moroney et al., 1988	0.06 MN/m	20 N	Cervical
Axial Rotation(M_y)			
Fairfan et al., 1970	2.0 Nm/deg	31 Nm	Lumbar
Moroney et al., 1988	0.42 Nm/deg	1.8 Nm	Cervical

Table 8.7: Stiffness coefficients for the lumbar spine (Gardner-Morse and Stokes, 2004)*

Level	Δ_1	Δ_2	Δ_3	Δ_4	Δ_5	Δ_6
Axial compression preload at 0 N (mean of L2-L3 and L4-L5)						
F ₁	438±92					-1370±519
F ₂		251±42				6510±969
F ₃			332±64	11000±2000	-696±1100	
F ₄				564000±89000	-235000±38200	
F ₅	(symmetric)				174000±20500	
F ₆						
Axial compressive preload at 250N						
F ₁ L2-L3	1700±67					-4280±1130
L4-L5						
F ₂ L2-L3		346±63				
L4-L5		389±76				
F ₃ L2-L3			447±68	12100±1740	-9360±971	
L4-L5						
F ₄ L2-L3				668000±1444000	-25000±34200	
L4-L5				744000±137000		
F ₅ L2-L3					211000±17900	
L4-L5					301000±29900	
F ₆ L2-L3						266000±33000
L4-L5						467000±80500
Axial compressive prelaod at 500 N						
F ₁ L2-L3	2420±158					-4280±1130
L4-L5						
F ₂ L2-L3		3676±68				
L4-L5		473±78				
F ₃ L2-L3			523±73	13400±1890	-10400±1760	
L4-L5					-11600±1250	
F ₄ L2-L3				734000±170000	-272000±33500	
L4-L5				832000±129000		
F ₅ L2-L3					236000±12900	
L4-L5					377000±44800	
F ₆ L2-L3						287000±27000
L4-L5						575000±137000

* Units are N, mm and rad. Δ_1 through Δ_3 are translations and Δ_4 through Δ_6 are rotations. Similarly, F₁ through F₃ are the three forces and F₄ through F₆ are the three torques. Stiffness values are tabulated in the format of the stiffness matrix for the upper vertebra center relative to the fixed lower vertebra.

The determination of the compression strength of the human vertebrae has been the subject of research from the early days of biomechanics. One of motivations behind the research was the problem of pilot ejection. Basically, it involves ejecting the pilot from a high-speed aircraft with the help of a rocket attached to the seat. To minimize the injury to the spine at the time of ejection, it is necessary to use a safe ejection acceleration. This requires a knowledge of the strength thresholds of the vertebrae. The results of some studies, in the form of strength vs. vertebral level, are summarized in **Figure 8.14**.

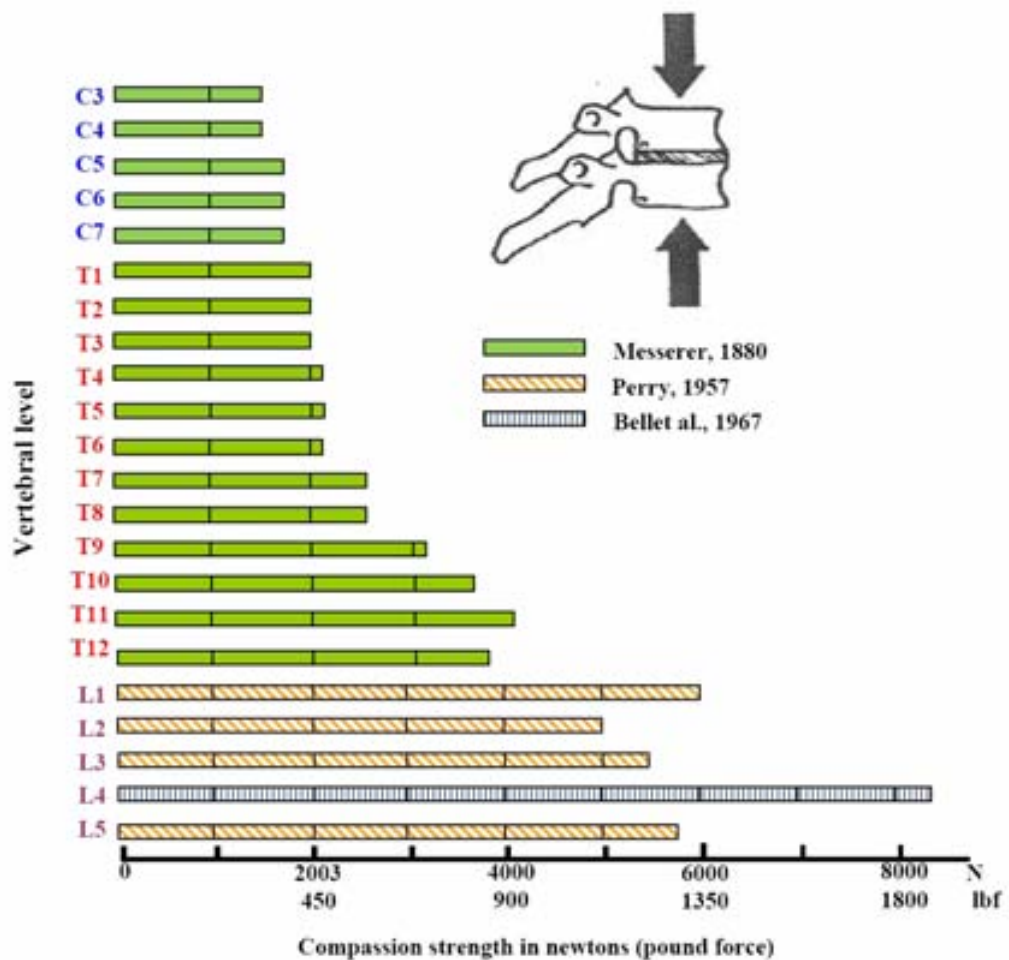


Figure 8.14: Vertebral static compression strength (White and Panjabi, 1990)

The mass and moment of inertias of the different parts of the body used in the modelling of driver in the sagittal plane are provided in **Table 8.8**. The upper and lower limbs were connected by a pivot with a rotational spring-damper systems (Silva and Ambrosio, 2004).

Table 8.8: Mechanical properties of driver body parts in the sagittal plane

Parts of Driver Body	Mass [kg]	I_z [kg.m ²]	k_ϕ [Nm/rad]	b_ϕ [Nms/rad]
Head	4.2	0.021		
Upper thorax	14	0.1		
Lower thorax	10	0.081		
Abdomen	8	0.05		
Upper arm	4	0.013	100	0
Lower arm	3.8	0.053	1000	0
Upper leg	20	0.515	1000	100
Lower leg	8	0.157	1000	100
Foot	2	0.009		

The driver has been then inserted in the vehicle and joined by spring-damper elements representing the flexible connections between the human body with armchair, pedals, seat belts and steering wheel as can be seen in **Figure 8.15**. The stiffness and damping coefficients of these elements are given in **Table 8.9** (Wismans et al., 1994).

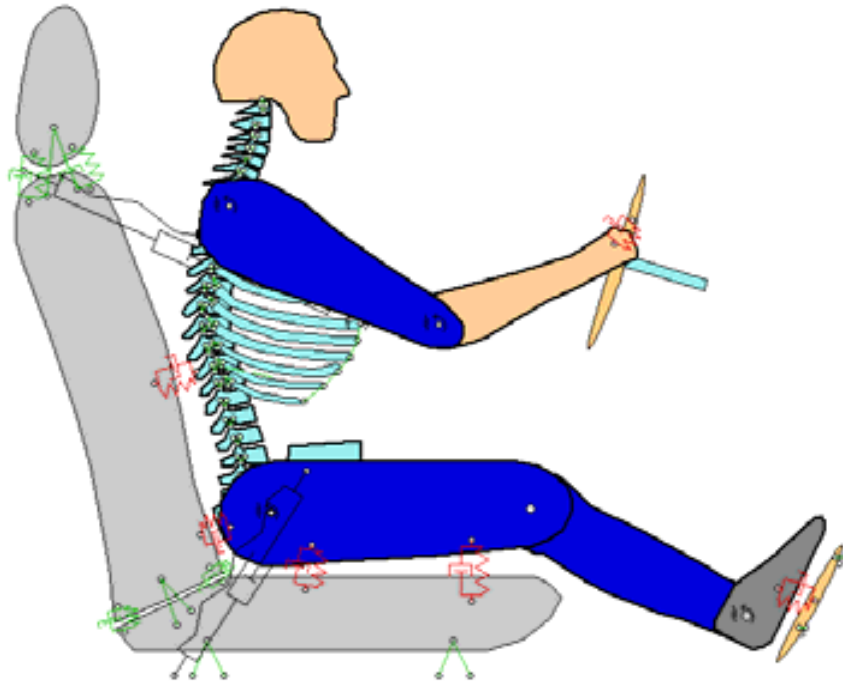


Figure 8.15: The connections between the driver and car in the sagittal plane

Table 8.9: Stiffness and damping values for driver/car contact points

Contact Point	Stiffness [N/m]	Damping [N.s/m]
Hand-Steering wheel	5000	50
Foot-Pedal	500	50
Leg-Seat	5000	1000
Sacrum-Seat	3000	1000
Sacrum-Backrest	8000	1000
Thorax-Backrest	1500	1000
Lower seatbelt	3×10^5	5000
Upper seatbelt	1×10^5	500

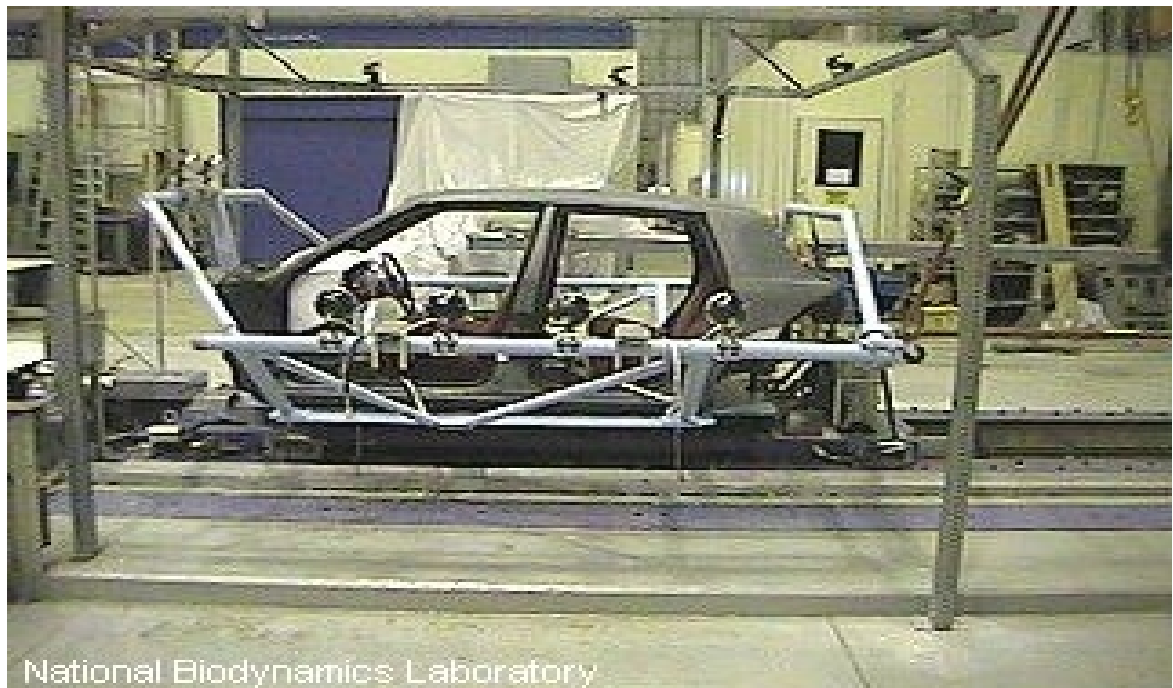
8.2.4 Frontal Impact Model Validation

Data for the validation of the neck model for frontal impact are taken from studies on human volunteers subjected to sled tests accelerations ranging from 3-15 g ($1g = 9.81 \text{ m/s}^2$), respectively, performed at the **Naval Biodynamics Laboratory (NBDL)** as in Ewing et al. (1977). Accelerations were recorded using a head bracket and a lower neck bracket which was strapped to the back at the T1 level. These tests were analyzed by Wismans et al. (1987) and by Thunnissen et al. (1995) resulting in response corridors. These corridors were used for validation of the whole human body model. A detailed description of the instrumentation and test methods is provided in Ewing and Thomas (1972).

Figure 8.16 shows the test experiments used for validation of front model. The subjects are restrained by shoulder straps, a lap belt and an inverted V-pelvic strap tied to the lap belt. Upper arm and wrist restraints are used to prevent flailing (Ewing and Thomas, 1972). In addition a lightly padded wooden board is placed against the right shoulder of the subject to limit the upper torso motion.

The volunteers were asked to take a normal automotive posture. The initial head angle was 0 degrees, where the head angle was defined as the angle between the Frankfort plane and the horizontal plane. The Frankfort plane is defined as the imaginary plane passing through the external ear canals and across the top of the lower bone of the eye sockets.

The test conditions are summarized in **Table 8.10**. Mean values of the sled acceleration-time histories for frontal are shown in **Figure 8.17**.



National Biodynamics Laboratory

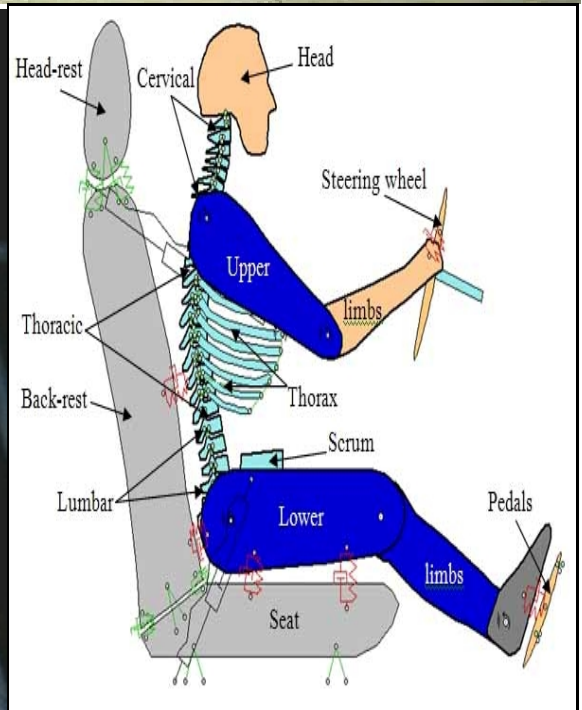
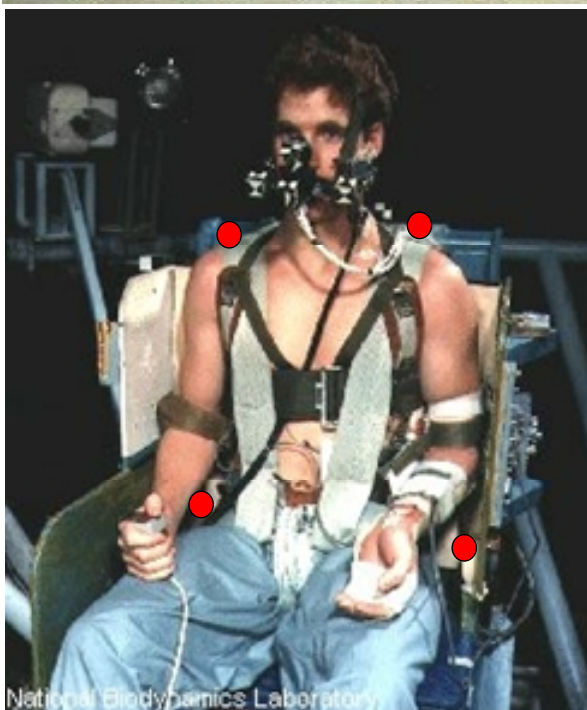


Figure 8.16: Test setup of the NBDL volunteer experiments (Thunnissen et al., 1995), together with the model simulation setup. The four points seat belt (red color) means that driver is more rigidly fixed to the armchair than in typical car

Table 8.10: Test conditions of the frontal and side NBDL experiments

Parameter	Unit	Frontal
Reference		Thunnissen et al., 1995
Subject		Volunteer
Total number of subjects		5
Total number of tests		9
Average mass	kg	68.6
Average height	m	1.69
Seat type		Rigid
Max sled pulse	g	15

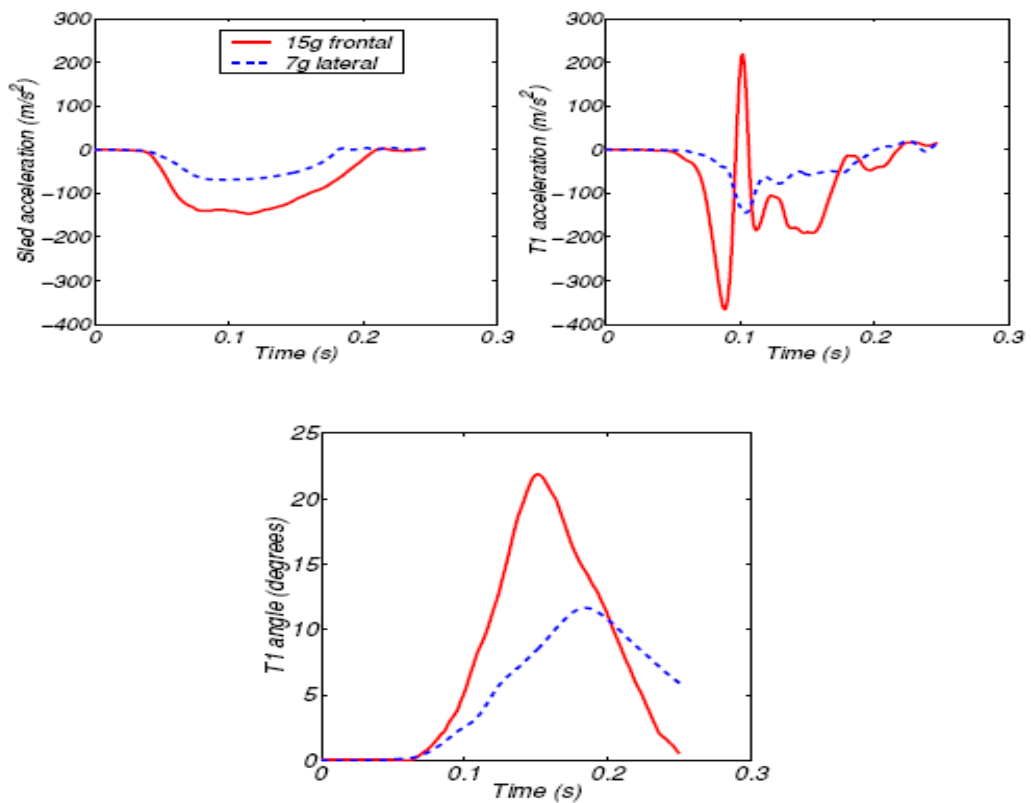


Figure 8.17: NBDL experiments: Mean sled acceleration, T_1 acceleration, direction, and T_1 rotation angle in the plane of frontal impact (Thunnissen et al., 1995)

For this study, the validations were considered to be *good* if the response was within the corridor of the experimental data, it was considered to be *reasonable* if the response was within a 25% deviation, while it was considered to be *poor* if the deviation was more than 25%. The simulation of a frontal impact of 300 ms required 12150 CPU-seconds using Working Model 2004-SPI version 7.0.0.0 with variable time step ($\geq 10^{-6}$ s) on a Pentium Core II Duo based workstation with 4Gb RAM.

The overall response of the model for frontal impact is shown in **Figure 8.18**. During the first 20 ms the head translates without any rotation with respect to inertial space (this is called head lag, Wismans, 1987). After this the head starts to rotate forward, resulting in the maximum head flexion at about 80 ms.

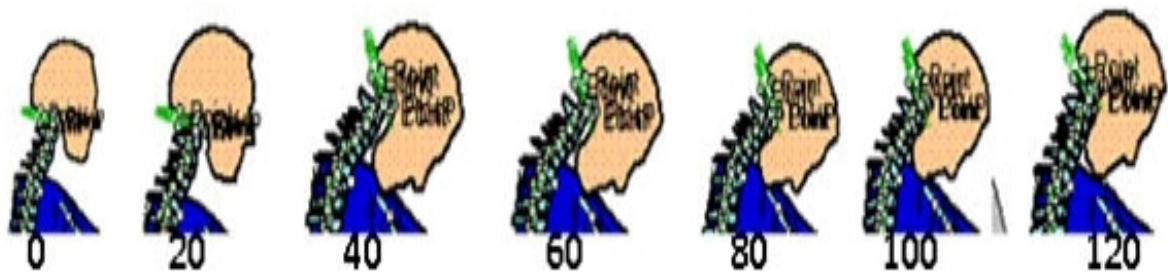


Figure 8.18: Kinematics of a 15g frontal simulation at successive times

Figure 8.19a shows that the head CG resultant acceleration follows the same double peak trend as that observed in the experiment. The peak head acceleration is slightly higher than 300 m/s^2 and the second peak is about 275 m/s^2 . Also, the head forward rotation (**Figure 8.19b**) in the simulations is very similar to that in the experimental data. The overall correlation was within 25% deviation of the corridor, and the correlation was therefore considered reasonable according to the criteria defined above.

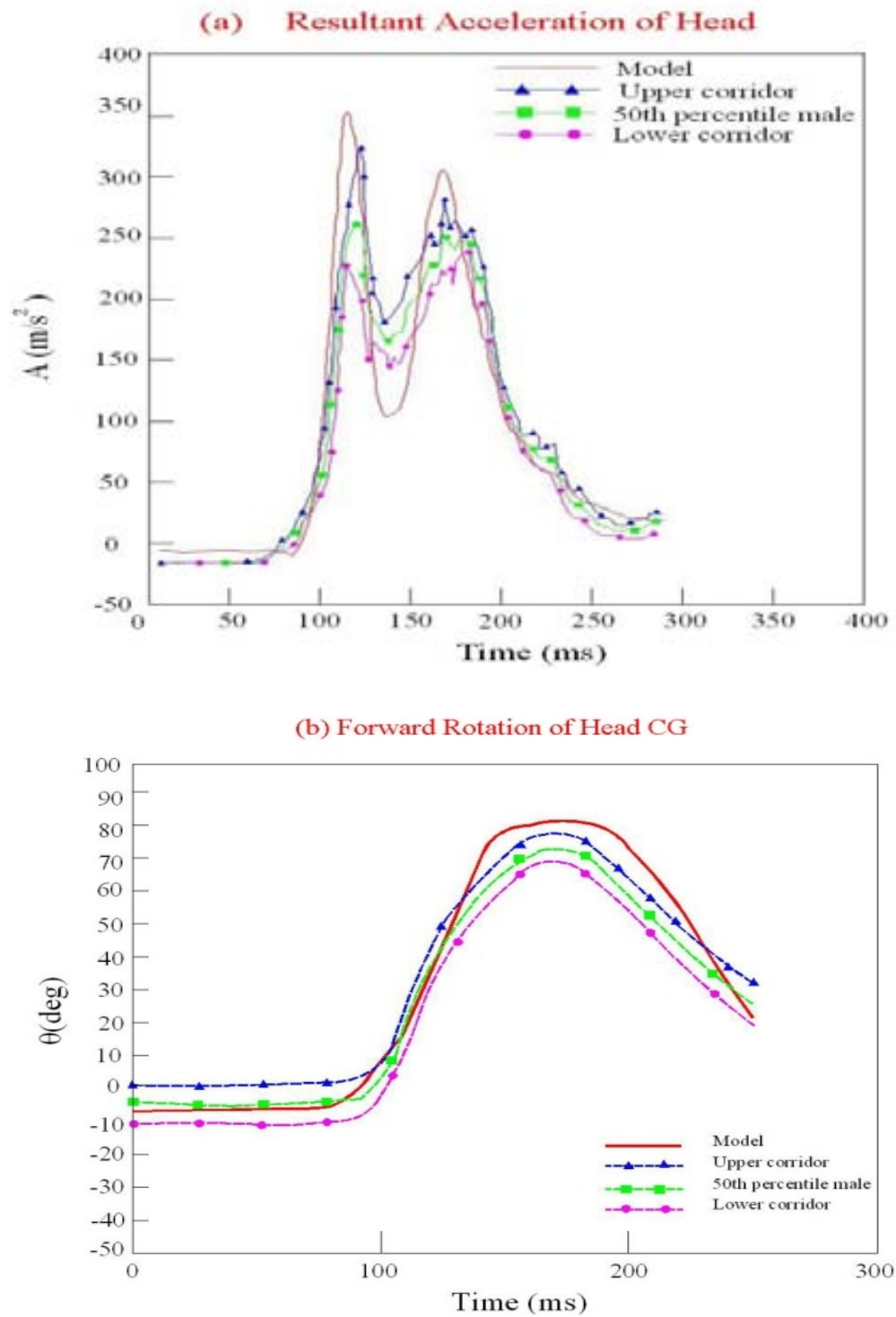


Figure 8.19: Simulations of frontal impact compared to NBDL experiments at 15g

8.3 SIMULATION OF SPINAL INJURY IN REAR IMPACT

Rear impact simulations have been developed to study the neck injury likelihood for the driver when a typical passenger car is impacted by another vehicle from behind (1100 kg).

Figure 8.20 shows the initial configuration in the rear impact simulations. The car and the driver models specifications are as described before in **Section 8.2**.

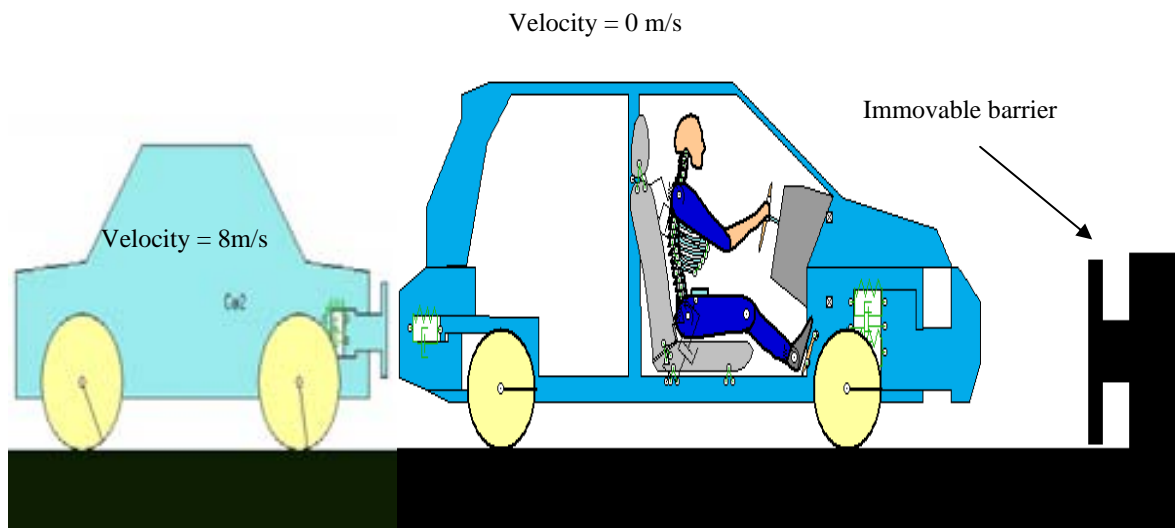


Figure 8.20: Initial configuration of rear impact model

The human body model of rear impact was validated with **Post-Mortem Human Surrogates (PMHS)** experiments performed at $\Delta V=10$ km/h by the Laboratory of Accidentology Biomechanics (Bertholon et al., 2000).

Figure 8.21 shows the setup of experiments used for the validation of rear impact model. The test conditions are summarized in **Table 8.11**.

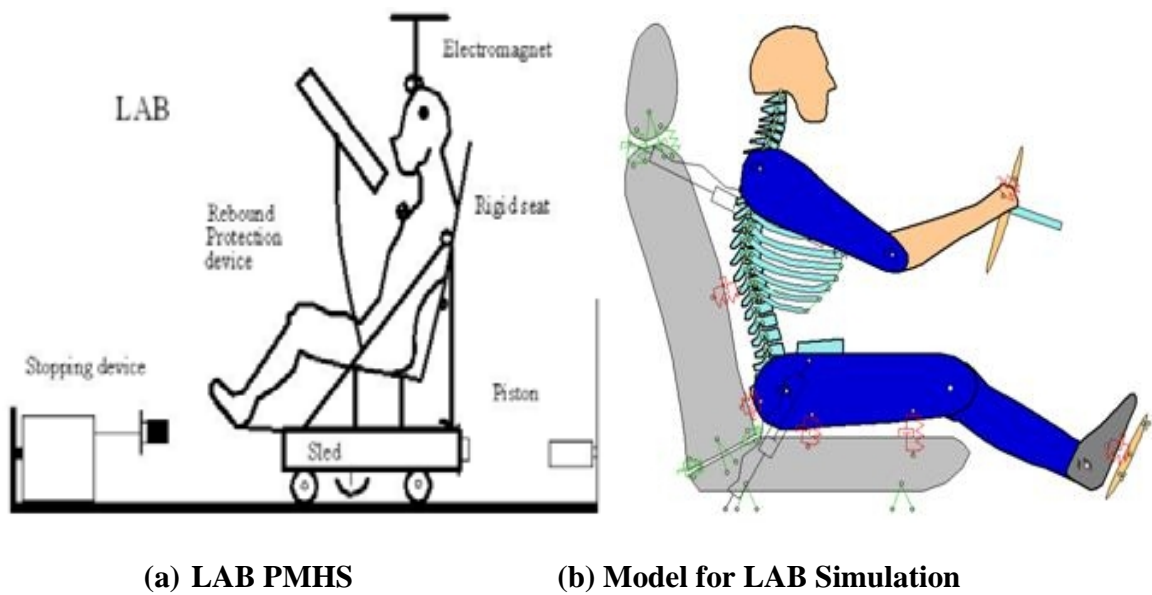


Figure 8.21: Test setup of the rear sled experiments with model simulation setup

Table 8.11: Test conditions for the rear end sled experiments

Parameter	Unit	Rear
Reference		Bertholon al., 2000
Subject		PMHS
Total number of subjects		3
Total number of tests		6
Average mass	kg	50
Average height	m	1.64
Seat type		Rigid
Head restraint		No
Belt system		Single belts over limbs, pelvis and thorax
ΔV	km/h	10
Max sled pulse	g	12

The overall response is shown in **Figure 8.22**, whereas the head kinematics versus time of the model behaviour and LAB PMHS response are presented in **Figure 8.23**.

In the first 40 ms of the response, the head continues to translate forward as the restraints have not slowed it down by then. The model response shows similar head-neck response until about 150 ms. The rebound of the model starts at 200 ms after the beginning of the input pulse. This is also observed in the PMHS experiments on films.

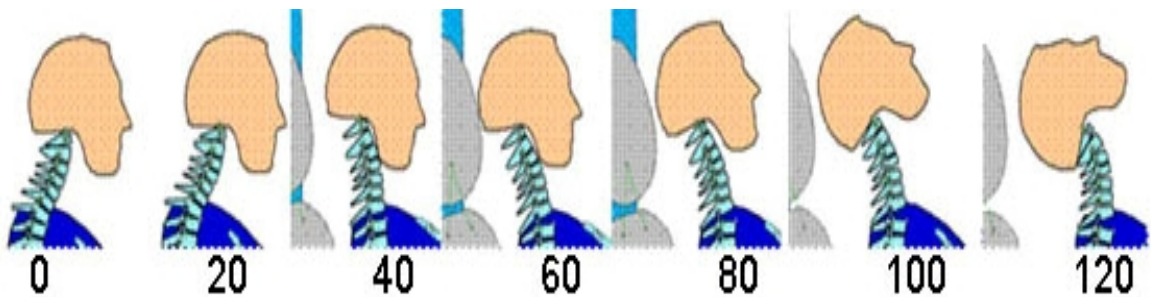


Figure 8.22: Simulations of human model for rear impact at successive times

The head rotation with respect to the sled is shown in **Figure 8.23**. The agreement of the model and test responses of each subject is clearly visible. Comparison with the model shows that the timing of the head rotation of model is good, and the maximum head rotation is within the response envelope (**Figure 8.23a**). The CG X-displacement with respect to T1 was also consistent for all the PMHS results (**Figure 8.23b**). The model falls within the envelope during the first 160 ms, but finally shows a smaller CG X-displacement. It is concluded that the correlation between the simulation model and tests predicts the head and neck response are good, and suitable for use in further rear impact simulations.

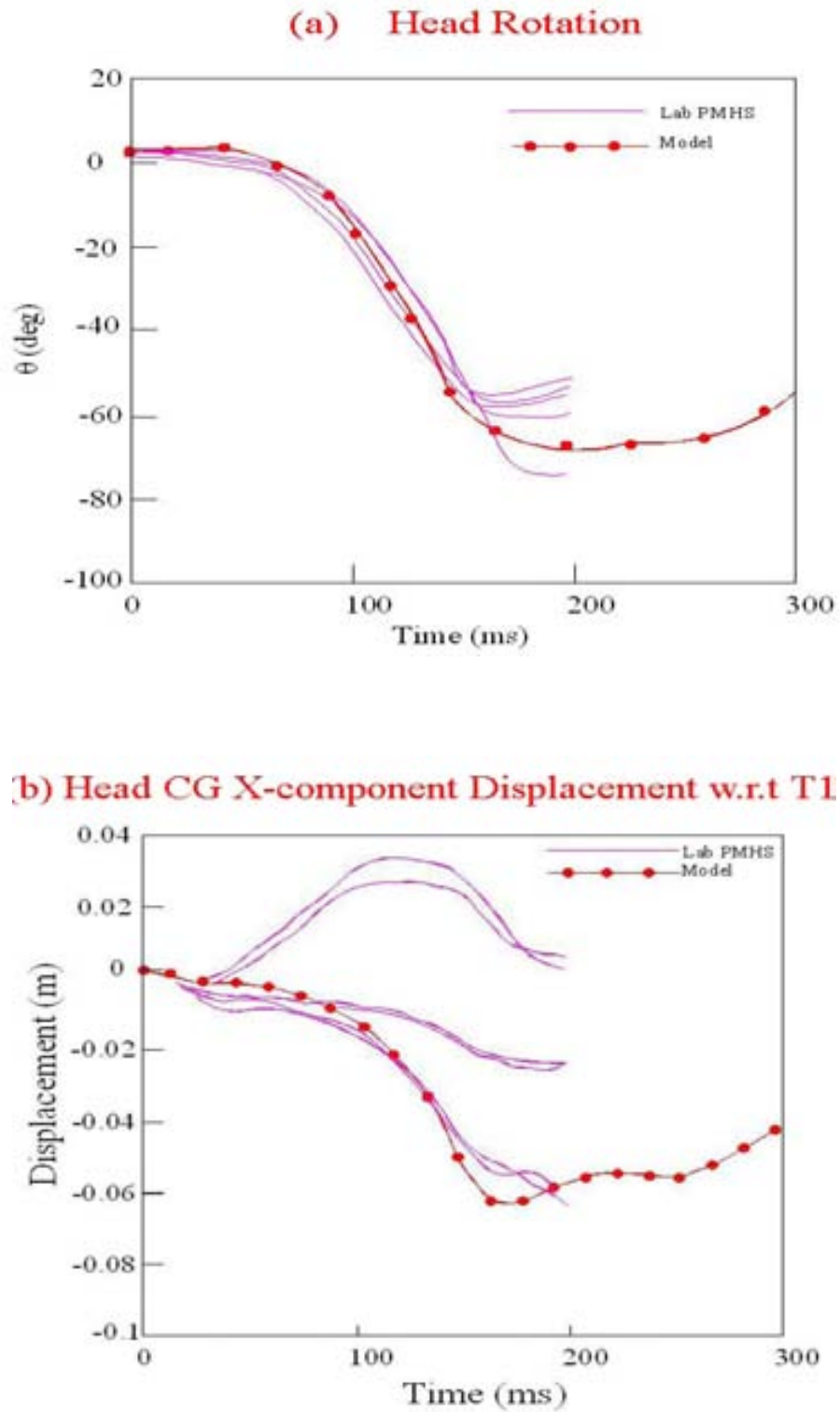


Figure 8.23: Simulations of rear impact compared to the PMHS experiments at 12g

8.4 SIMULATION OF SPINAL INJURY IN SIDE IMPACT

Side impact simulations have been developed to study the neck injury likelihood for the occupant (the driver) when the vehicle is impacted by another vehicle from the side. The initial configuration of side impact simulations is shown in **Figure 8.24**.

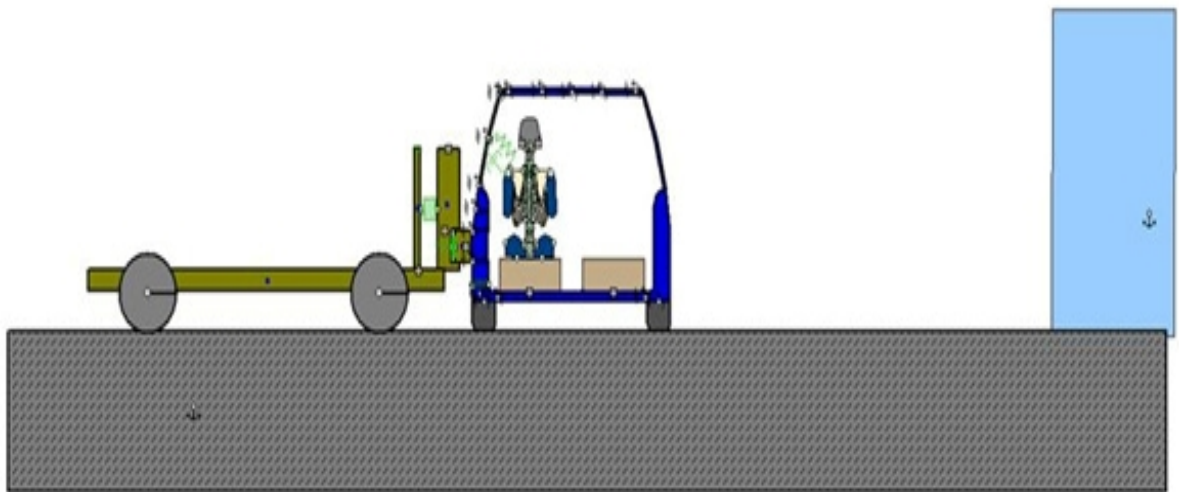


Figure 8.24: Simulation of side impact model

The simulation of side impact was performed according to the IIHS Lateral Impact Test specifications (IIHS, 2005). Side impact crash tests consist of a stationary test vehicle struck on the driver's side by a crash cart fitted with an Insurance Institute for Highway Safety (IIHS) deformable barrier element (version 4). The 1,500 kg Moving Deformable Barrier (MDB) has an impact velocity of 50 km/h (31.1 mph) and strikes the vehicle on the driver's side at a 90-degree angle. The longitudinal impact point of the barrier on the side of the test vehicle is dependent on the vehicle's wheelbase. The Impact Reference Distance (IRD) is defined as the distance rearward from the test vehicle's front axle to the closest edge of the deformable barrier when it first contacts the vehicle as shown in **Figure 8.25**.

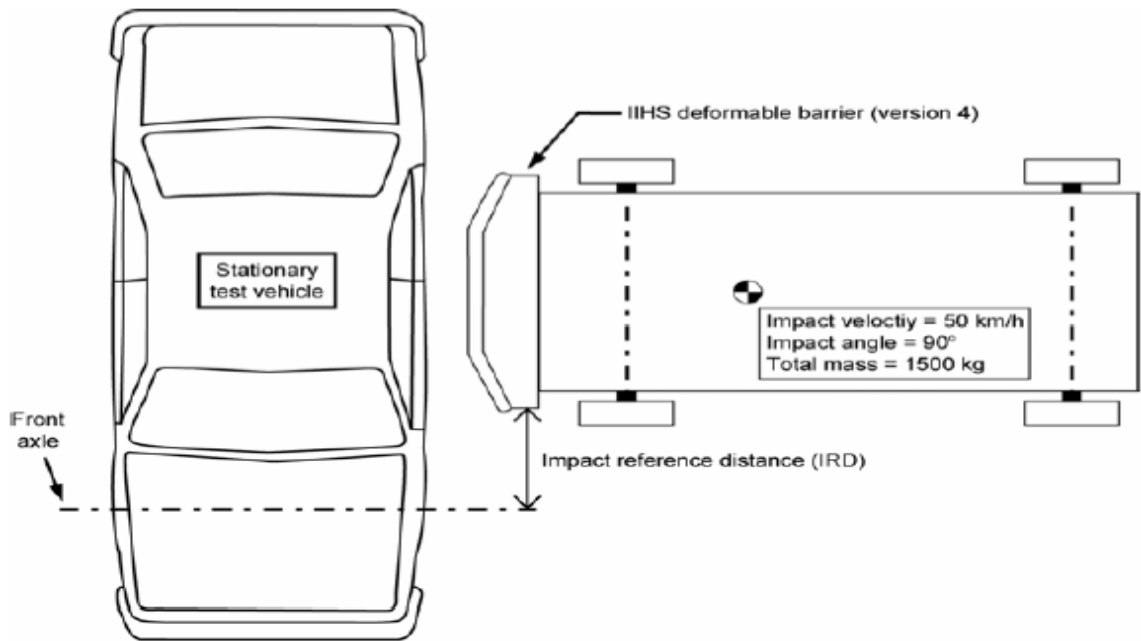


Figure 8.25: The test setup of IIHS (IIHS, 2005)

The model of side impact process consisted of three parts: (a) the side-impact vehicle model; (b) the MDB; and (c) the side impact dummy model.

8.4.1 Model of Car in the Frontal Plane

For side impact, the same typical car described in **Section 8.2.2** is also used here. In addition to the car seat the role of the steering wheel and the dashboard are not relevant. These have therefore not been modeled. The car body has been modeled in parts so as to get the appropriate stiffness of the side and the roof. The car consists of three elements body; the main body of the vehicle (1130 kg), seats (20 kg) and wheels (50 kg). The vehicle body is divided into several parts joined by rotational joints as well as spring-damper elements ($k_{\phi} = 100 \text{ Nm/rad}$, $b_{\phi} = 200 \text{ Nms/rad}$). **Figure 8.26** shows the main components of car.

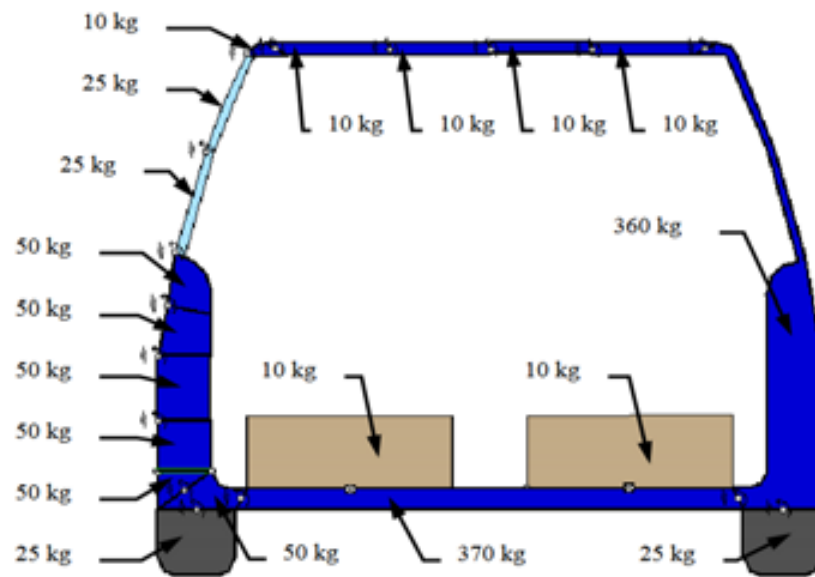


Figure 8.26: Model of a car with assumed masses in side impact

The possibility of the door thrusting into the vehicle interior is provided by an additional slot joint and nonlinear spring-damper elements ($k_t = 7 \times 10^5$ N/m, $b_t = 4000$ N.s/m) connecting the two body elements as provided in **Figure 8.27**.

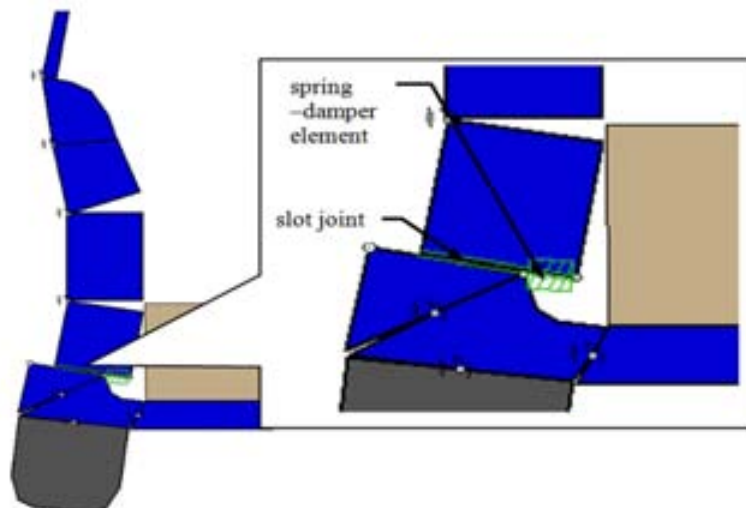


Figure 8.27: Slot joint and spring-damper elements between door and car body

8.4.2 Model of Moving Deformable Barrier (MDB)

The moving deformable barrier consists of an impactor and a trolley. The material of the impactor is usually aluminium honeycomb forming several independent joined parts. The MDB is modeled appropriately as per the Insurance Institute for Highway Safety (IIHS) recommendations (IIHS, 2005). The setup of IIHS is shown in **Figure 8.28**.

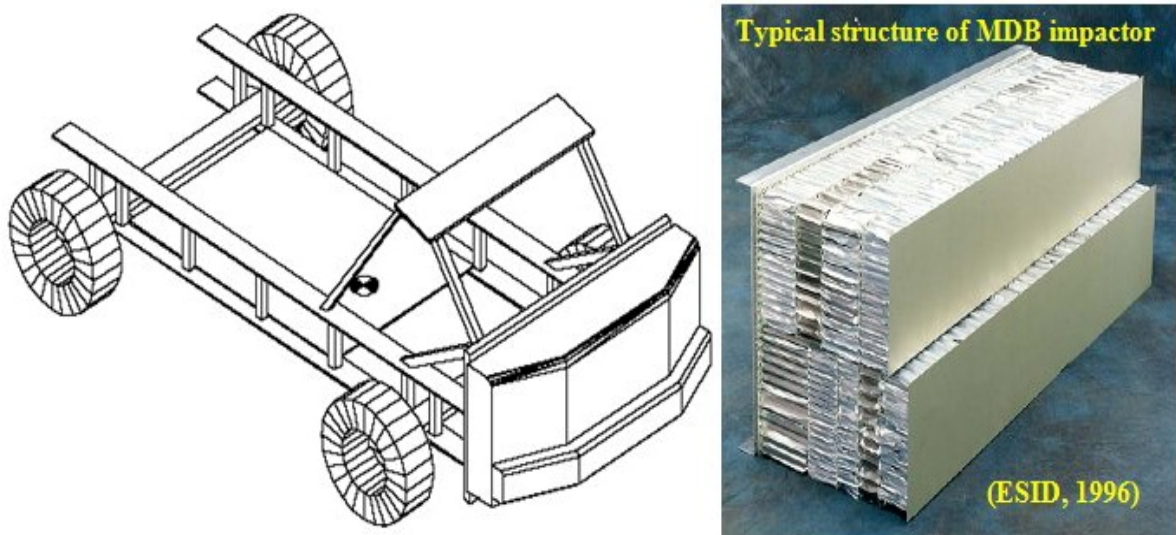


Figure 8.28: IIHS test cart with deformable barrier element attached

The MDB consists of the frame (950 kg), deformable element divided into three parts (400 kg) and wheels (25 kg each). The total MDB weight is 1500 kg and corresponds to the real cart mass. The deformable element is 1676 mm wide, has a height of 759 mm and a ground clearance of 379 mm when mounted on the test cart. The deformation of the MDB front part was captured by dividing deformable elements into parts connected with slot joints and dampers. The properties of MDB are shown in **Figures 8.29** and **8.30** (ESID, 1996).

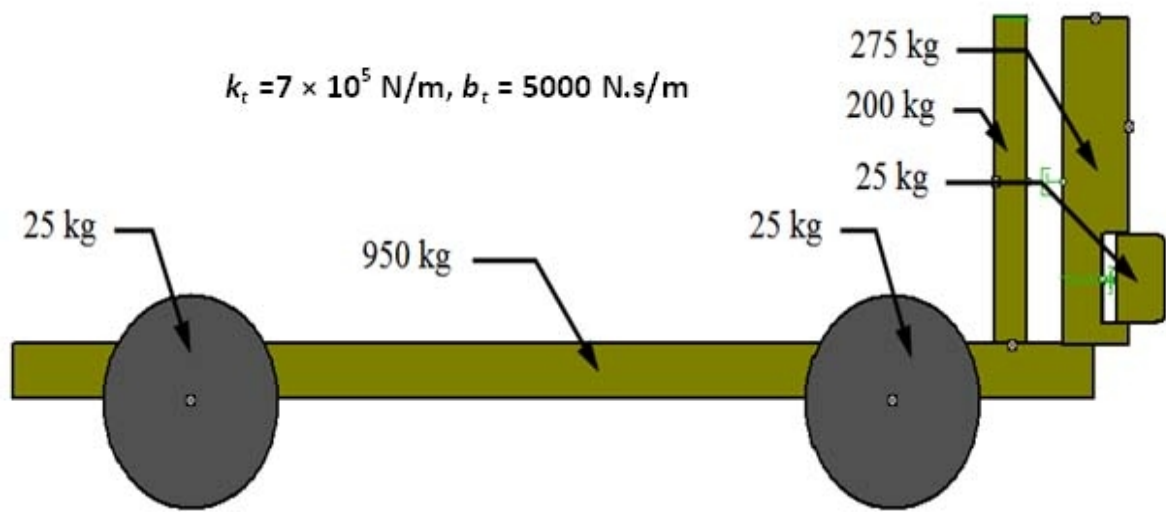


Figure 8.29: Model of moving deformable barrier with assumed masses

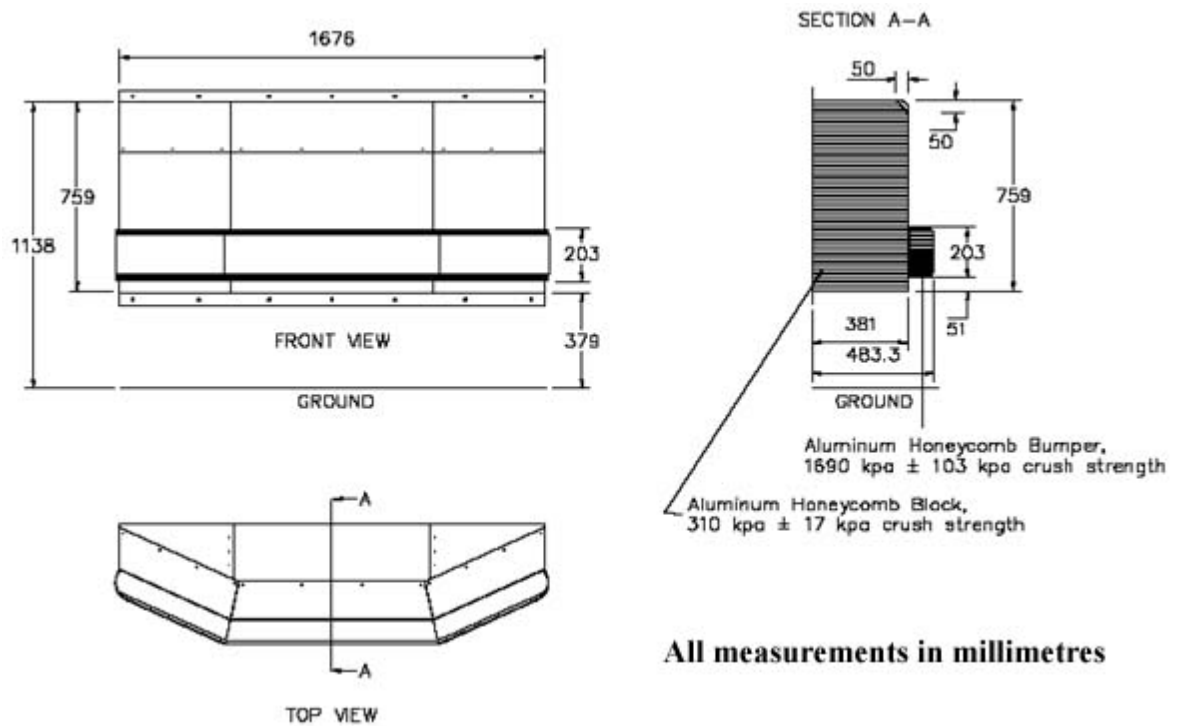


Figure 8.30: IHS deformable barrier element-version 4 (ESID, 1996)

8.4.3 Model of Driver in the Frontal Plane

Figure 8.31 shows the detailed human spine of the driver's model in the frontal plane. The model of driver for side impact simulations includes the head, cervical vertebra, thoracic vertebra, lumbar vertebra, and the upper and lower limbs.

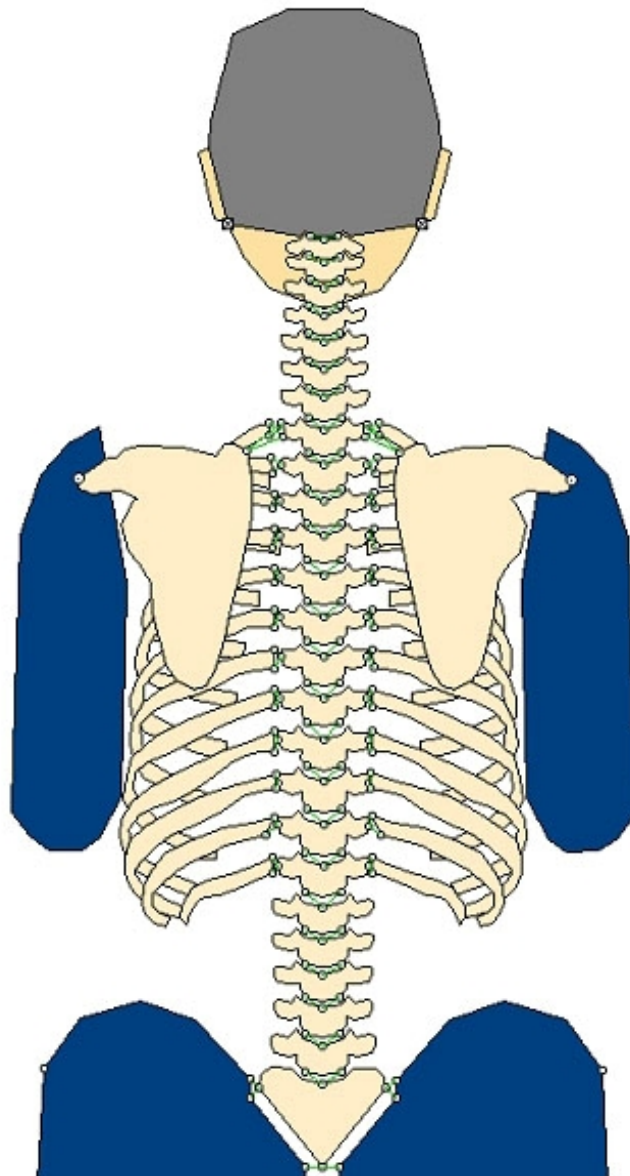


Figure 8.31: Modelling of the head and the whole spine in the frontal plane

Figures 8.32-33 show the detailed models for cervical and thoracic spine parts. The elements of the model are joined by articulated joints as an open kinematical chain. In addition spring-damper elements are added to get the appropriate stiffness and kinematics. The cervical part of the model consists of 7 cervical vertebrae, neck muscles, ligaments, intervertebral joints and discs. The model consists of 12 thoracic vertebrae, muscles connecting the ribs on each level with the rib on the other side of thorax and also with the upper and the lower rib, ligaments, intervertebral joints and discs. Shoulder blades in the thoracic model are connected to vertebrae with spring-damper elements.

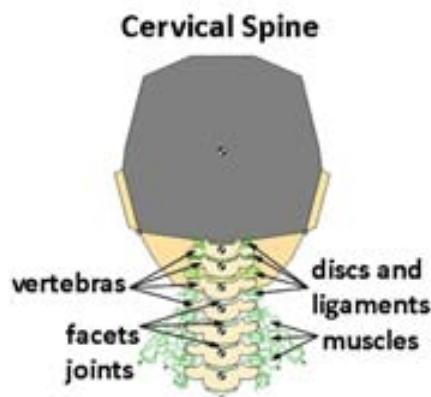


Figure 8.32: Modelling of head and cervical spine in the frontal plane

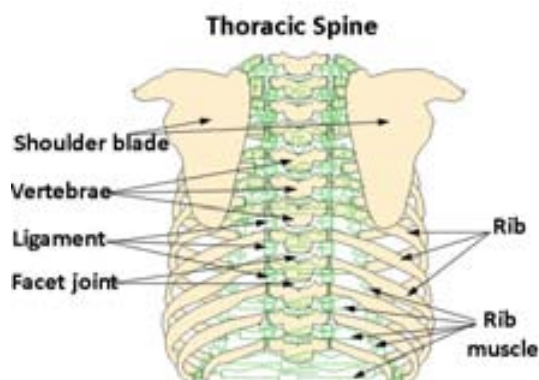


Figure 8.33: Modelling of the thoracic spine in the frontal plane

The lumbar part of the model consists of 5 lumbar vertebrae, back muscles, abdomen muscles, ligaments, intervertebral joints and discs as shown in **Figure 8.34**.

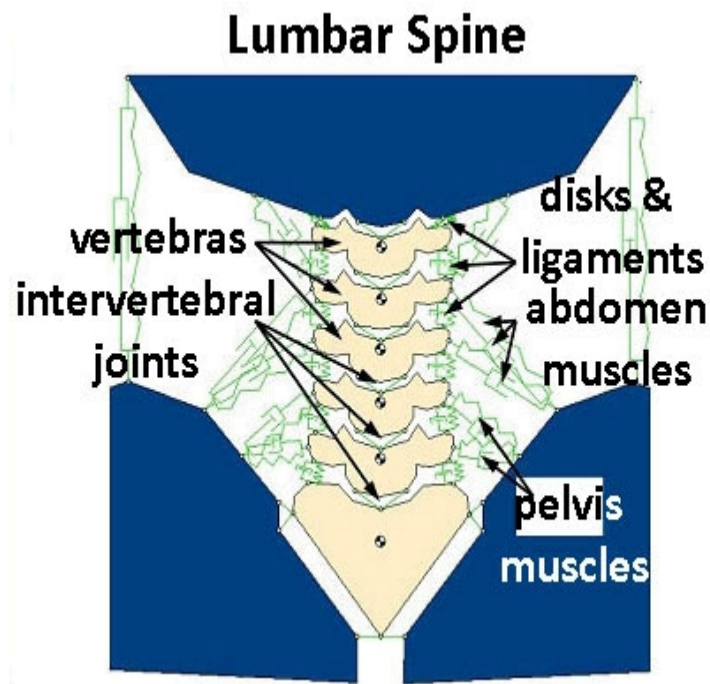


Figure 8.34: Modelling of the lumbar spine and sacrum in the frontal plane

The mass and moment of inertias (I_x) used for the main parts of driver model in the frontal plane are presented in **Tables 8.4** and **Table 8.12**. In addition the overall ribs mass: $(2 \times 6 \times 1 \text{ kg} + 2 \times 6 \times 1.5 \text{ kg})$ and shoulder plates mass $(2 \times 2.5 \text{ kg})$ match with upper body mass for a 50th percentile male (Schneider et al., 1983), and also with the sum of the chest and abdomen in previous model $(15 + 20 \text{ kg})$. The mechanical properties of the driver model in frontal plane are so similar to **Section 8.2.3**.

Table 8.12: Moments of inertia and mass of driver body parts in the frontal plane

Part of Driver Body	Mass [kg]	I_x [kg.m ²]
Head	5	0.025
Upper limb	4.5	0.031
Lower limb	12.5	0.046
Shoulder blade	2.5	0.007
T1 rib	1	2.35E-04
T2 rib	1	8.81E-04
T3 rib	1	0.001
T4 rib	1	0.002
T5 rib	1	0.002
T6 rib	1	0.002
T7 rib	1.5	0.003
T8 rib	1.5	0.003
T9 rib	1.5	0.003
T10 rib	1.5	0.002
T11 rib	1.5	0.002
T12 rib	1.5	7.41E-04

The driver is connected with the vehicle by spring-damper elements representing flexible connections between human body with the seat and seat belt (**Figure 8.35**). The stiffness coefficients for the upper and lower seatbelts are 4000 N/m and 5000 N/m respectively (Wismans et al., 1994). The head of driver can penetrate the window pane (indicated light blue on **Figure 8.36**) because the glass breaks first during a real collision, hence no interaction is defined between the two. The motion of the driver's body was analyzed in the lateral plane as shown in **Figure 8.35**.

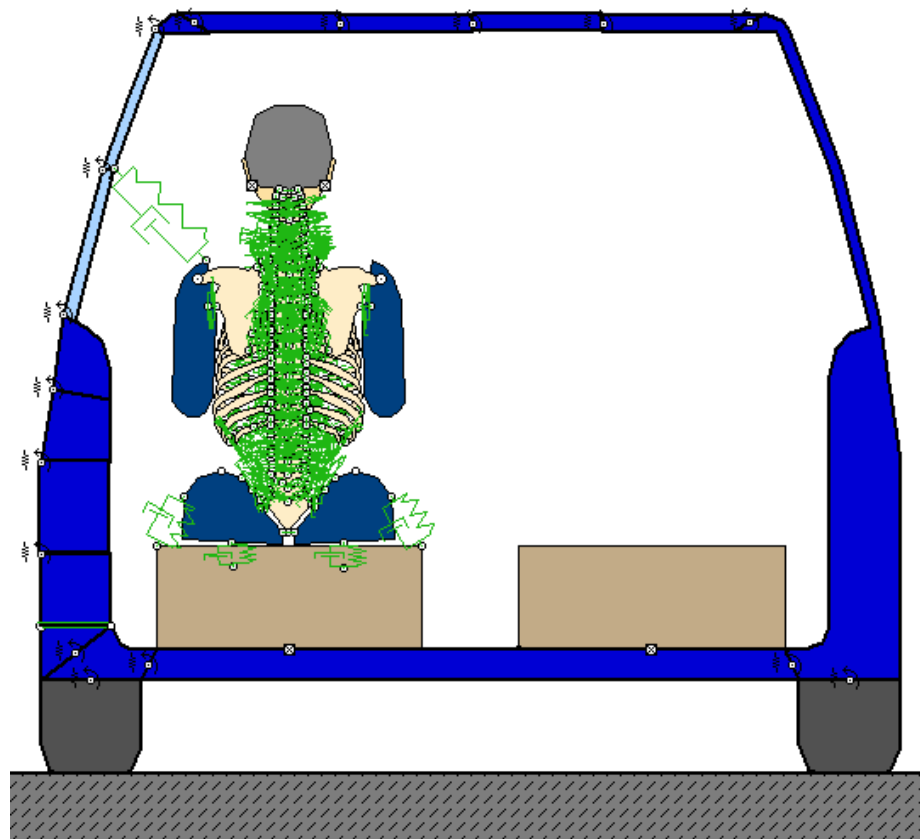


Figure 8.35: Positioning of the driver inside the car in the frontal plane

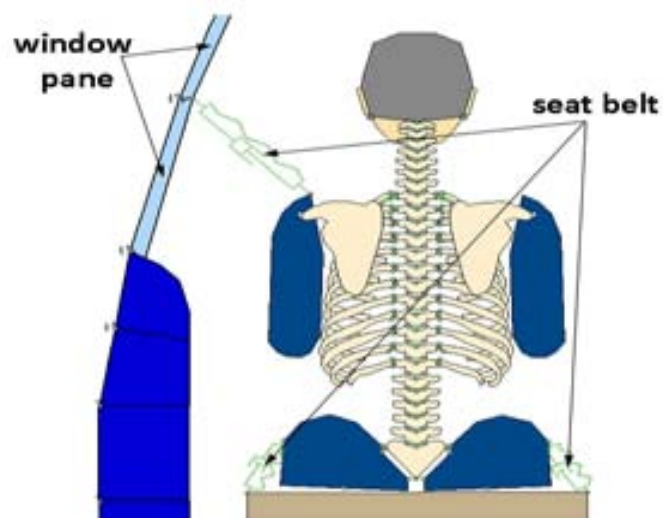


Figure 8.36: The connections between the driver and car for side impact

8.4.4 Side Impact Model Validation

The model has been verified on the basis of experimental tests performed at the Naval Biodynamics Laboratory (NBDL) as explained in **Section 8.2.4**. The same criteria for model quality assessment were used. The test conditions are summarized in **Table 8.13**.

Table 8.13: Test conditions of the side NBDL experiments

Parameter	Unit	Side
Reference		Ewing and Thomas, 1972
Subject		Volunteer
Total number of subjects		9
Total number of tests		9
Average mass	kg	76
Average height	m	1.77
Seat type		Rigid
Max sled pulse	g	7

In **Figure 8.37**, the overall response of the side impact is shown. During the first 200 ms the head remains stationary, without any significant rotation with respect to inertial space. Following this the head bends to the right, followed by a rotation around the Y-axis (twist).

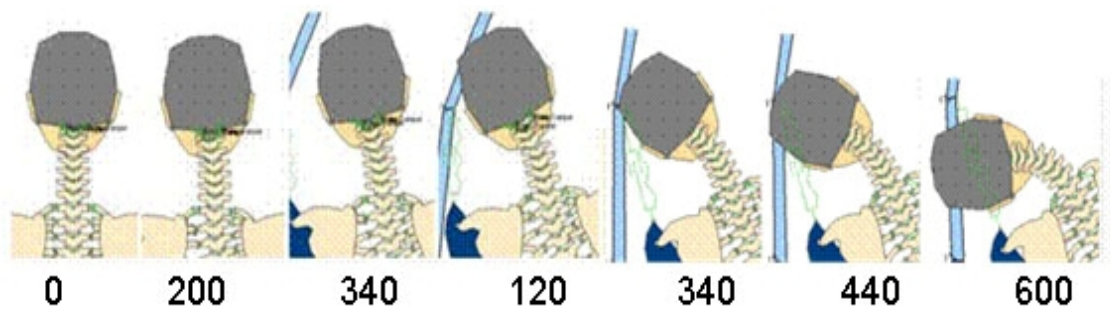


Figure 8.37: Simulations of human model for side impact at successive times

Figure 8.38 shows the head angle and the head CG displacements versus time. During the first 110 ms the kinematic responses are within the response corridor. After 110 ms, the head angle shows reasonable correlation with volunteer data, although the maximum head angle is about 20% larger than the experimentally reported head angle. The CG displacements of the model show a good correspondence with the response corridors.

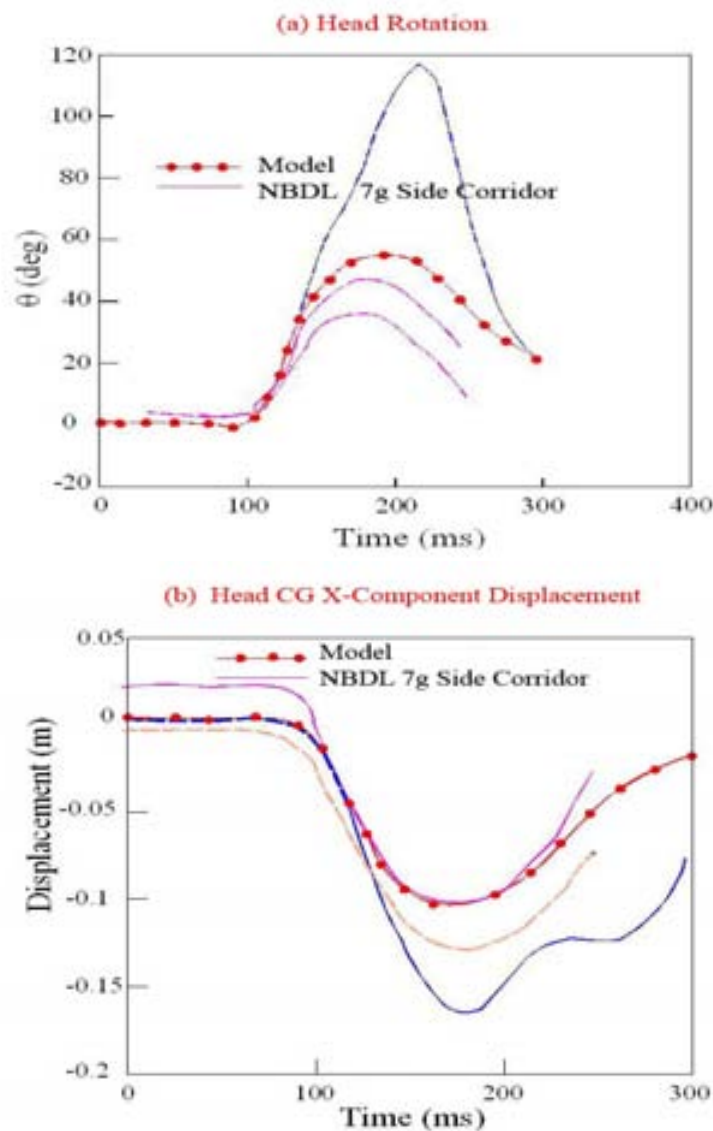


Figure 8.38: Simulated response to 7g side impact for model and NBDL

The verification has also been made according to the lab tests performed by the Insurance Institute for Highway Safety “Crashworthiness Evaluation Side Impact Crash Test Protocol” for side collision at 50 km/h Moving Deformable Barrier velocity. **Figure 8.39a** shows a comparison for the force applied through the door in the experiments and numerical simulations of the model. The car body deformation is quite important because energy transfer and dissipation has a great influence on the occupant’s body kinematics. As can be seen in the **Figure 8.39b** the bending mode of the door as observed in the simulation is similar to that reported in literature (IIHS, 2005). On the basis of the overall kinematics, i.e., acceleration responses, displacements and rotations, force responses as well as the deformation behavior, it is concluded that the model validation for the side impact is good.

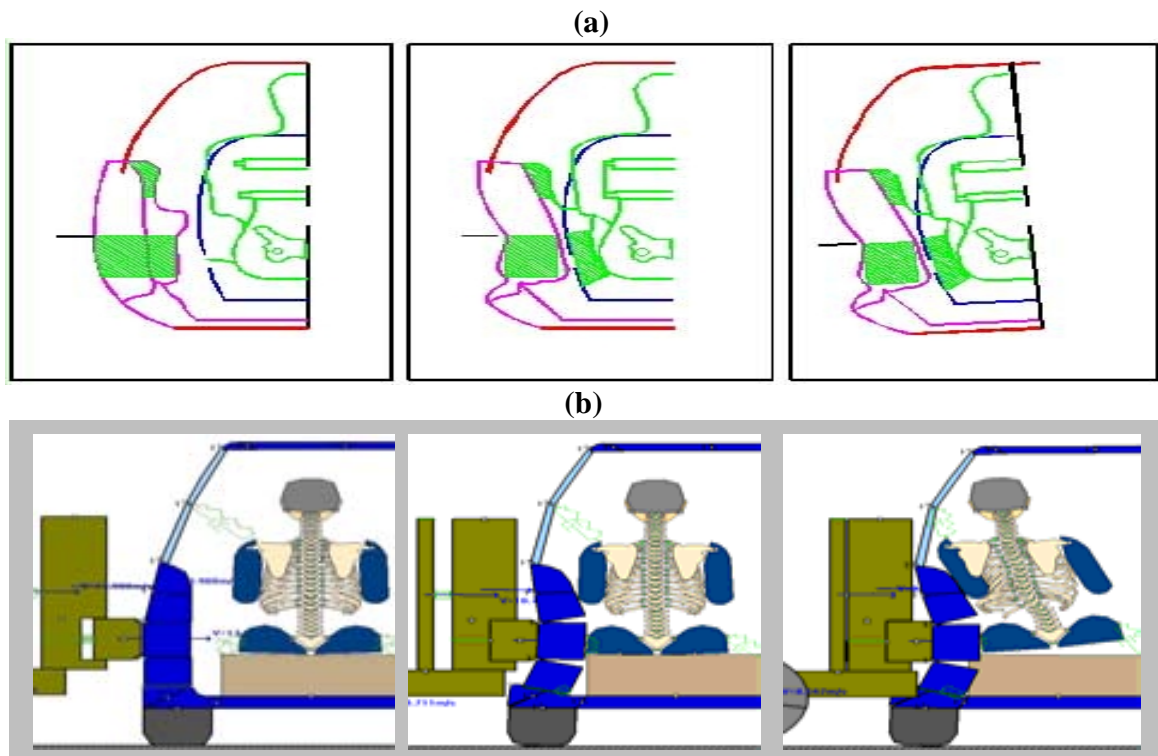


Figure 8.39: Comparison of force application through door: (a) literature example (EEVC, 2001; IIHS, 2005), (b) results of the model

8.5 SIMULATION OF SPINAL INJURY IN ROLLOVER

Trip-over accounts for over half of rollover initiations (Balavich, 2002). Tripped rollovers have been defined as when the lateral force acting on the wheels/tires has a sufficient magnitude and duration to create an overturning impulse that rotates the vehicle center of gravity past the tripping wheels (Ragan, 2000). Tripping mechanisms can be created with curbs, soil, road friction and the FMVSS 208 dolly. A number of rollover tests have been proposed in the literature (Viano and Parenteau, 2004; Chou et al., 2005). A dolly test as per SAE J2114 (Orlowski et al., 1985) has been used in the present study. The initial configuration of the rollover simulations is shown in **Figure 8.40**.

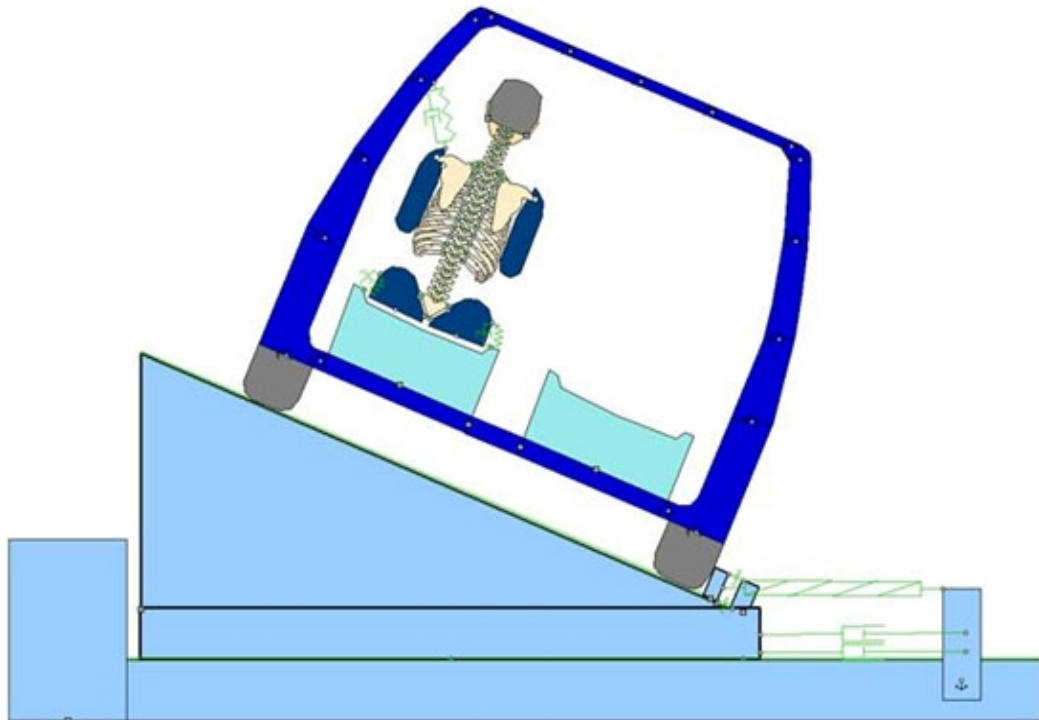


Figure 8.40: The initial configuration for simulation of a rollover of a vehicle

The Dolly Rollover test was first introduced by Mercedes-Benz in 1970 and incorporated into FMVSS 208 (Chou et al., 2005). It is also described in the Society of Automotive Engineers (SAE) Recommended Practice J2114 as a method of evaluating the performance of a vehicles' crashworthiness during rollover.

The Dolly Test consists of positioning a vehicle on a dolly fixture, which is inclined at 23° to the horizontal as shown in **Figure 8.41**. A curb of 102 mm holds the tire (and vehicle) in place. The fixture is towed at 48 km/h (30 mph) and stopped suddenly to generate the vehicle rollover. The number of rolls can vary from one to three or more under the same initial conditions depending on the vehicle tested. The main advantage of this test is its ability to generate a consistent initial rollover; especially for small vehicles with low center of gravity.

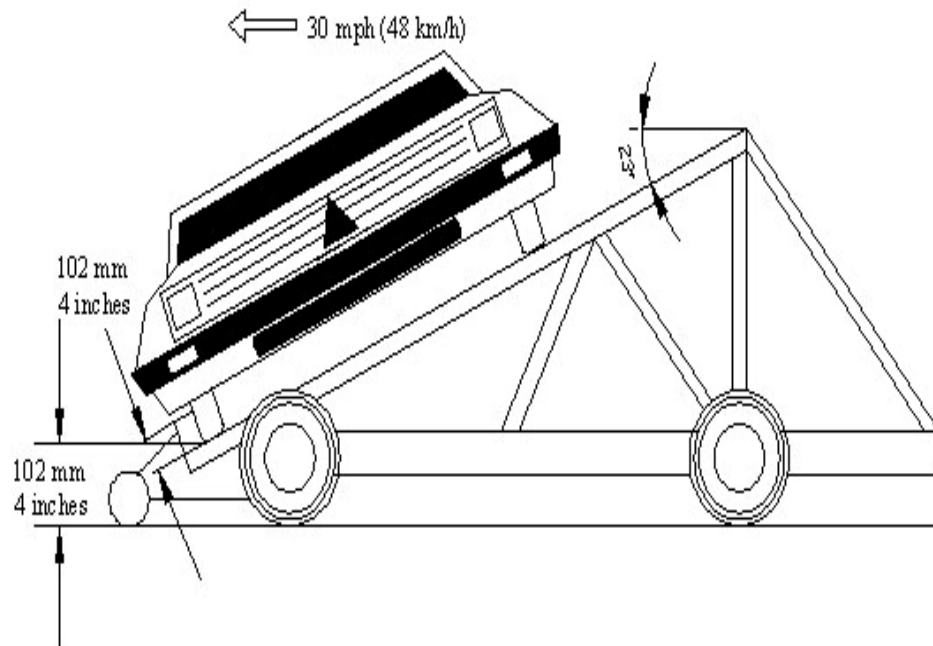


Figure 8.41: The dolly test setup (Chou et al., 2005)

The rollover simulations were modeled by creating: (a) a typical car model; (b) the dolly platform model; and (c) the dummy model in frontal plane. The vehicle and driver models have been described in **Section 8.4**. The model of the typical car used for rollover simulations is shown in **Figure 8.42**.

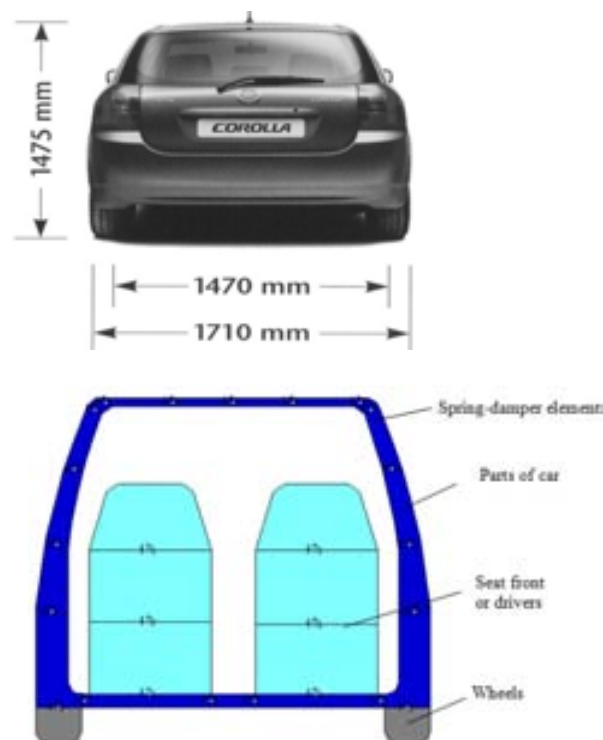


Figure 8.42: Car in rollover: geometry (Toyota), and model of car

The model takes into consideration car equipment having the main influence on the driver's body's behaviour during rollover. Initial simulation parameters (geometry, masses, moments of inertia, velocities, etc.) and accident configuration were based on the description in FMVSS 208. The vehicle is initially oriented at an angle of 23 degrees from the horizontal plane and resting against the flange as described above. In numerical simulations a change in the velocity during considered car collision is possible.

8.5.1 Model of Dolly

The design of the dolly is modeled as a system of rigid bodies as shown in **Figure 8.43**. The rollover standard stipulates placing the vehicle on a tilt table canted at 23 degrees with respect to the ground. The passenger side tires rest against the 4-inch high curb at the bottom of the table making the lowest point of the vehicle 9 inches from the ground. The vehicle is prescribed an initial velocity (48 km/h) along with the platform in the lateral direction with reference to the vehicle. The platform is then stopped in a short distance (< 3 feet) while maintaining a deceleration rate of at least 20g's for 40 ms. This is achieved by prescribing an acceleration field on the "platform alone" in the lateral direction opposite to its motion.

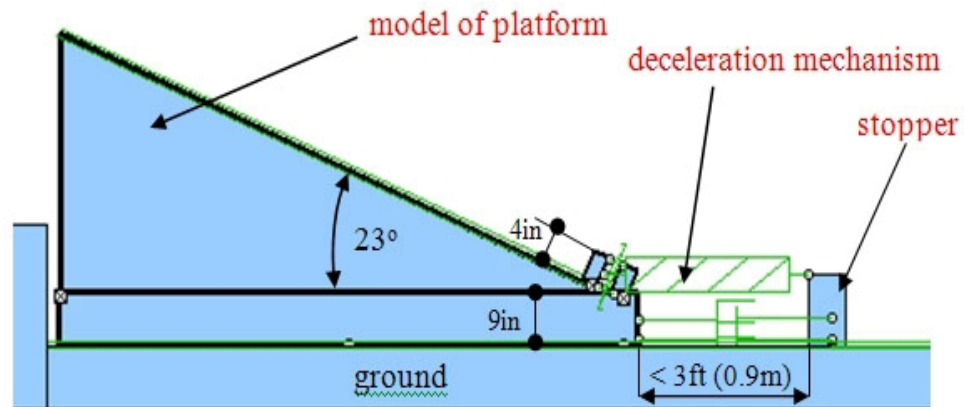


Figure 8.43: Model of platform used in the dolly system

In this study, the combined stopping system of the deceleration mechanism was simplified into a system of dampers ($b \cdot v^3 = 60 \text{ N} \cdot \text{s}^3/\text{m}'$). The ground is modeled as a plane in which all the parameters are in reference to the road. A friction coefficient 0.2 for the ground was used. These assumed parameters are presented in **Tables 8.14 and 8.15**.

Table 8.14: Parameters of model's platform

Parameters	Assumed properties
Deceleration pulse of dolly	20 G's for 40ms
Stopping mechanism	Hydraulic
"Curb" height	Currently 4"
Platform inclination	Currently 23 degree
Dolly height and tire pressures	Currently 9"
Platform orientation	0 degree in lateral direction

Table 8.15: Ground properties

Density	7,850 kg/m ³
Friction coefficient	0.2
Thickness	0.2 m

8.5.2 Rollover Model Validation

In order to validate the setup for rollover conditions, a 23° Dolly test has been simulated. The vehicle has been given a sideways velocity of 48 km/h. The vehicle trips from the dolly and rolls sideways. The test is as per SAE J2114 and the procedure is detailed in many surveys, Viano and Parenteau (2004) or Chou et al. (2005). **Figure 8.44** shows the vehicle rollover trajectory from the simulation was correlated to that from such a test (Viano and Parenteau, 2004). The comparison of the kinematics clearly shows that the model developed in WM predicts that the vehicle will roll over, turn completely and land again on its wheels.

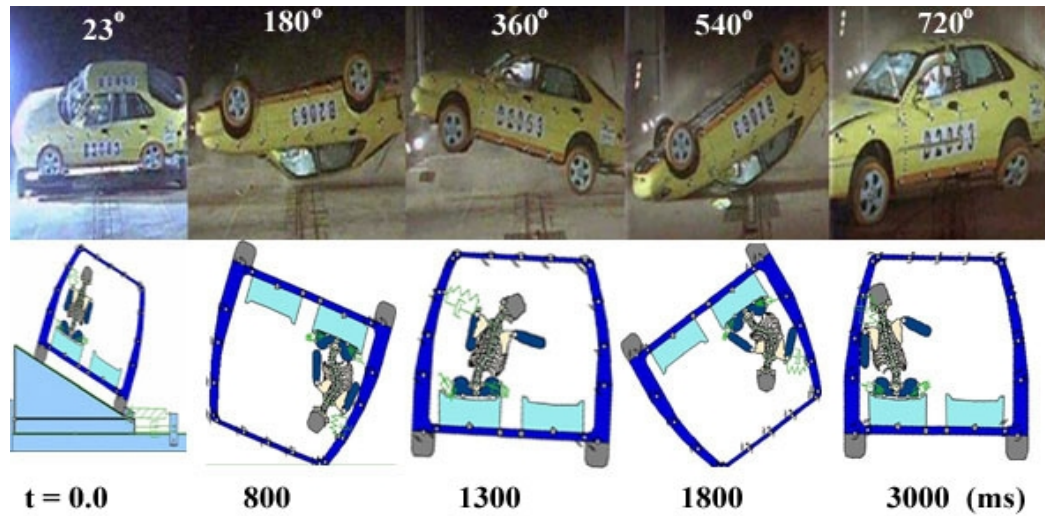


Figure 8.44: The vehicle kinematics during test of Viano and Parenteau, 2004 (upper) and simulation (lower) at successive times

The deceleration of the dolly is shown in **Figure 8.45** and compared with that obtained in the Dolly test (Chou et al., 2005). It can be clearly seen that the deceleration profile is very similar to the deceleration mechanisms generated by both cylinders in SAE J2114 tests.

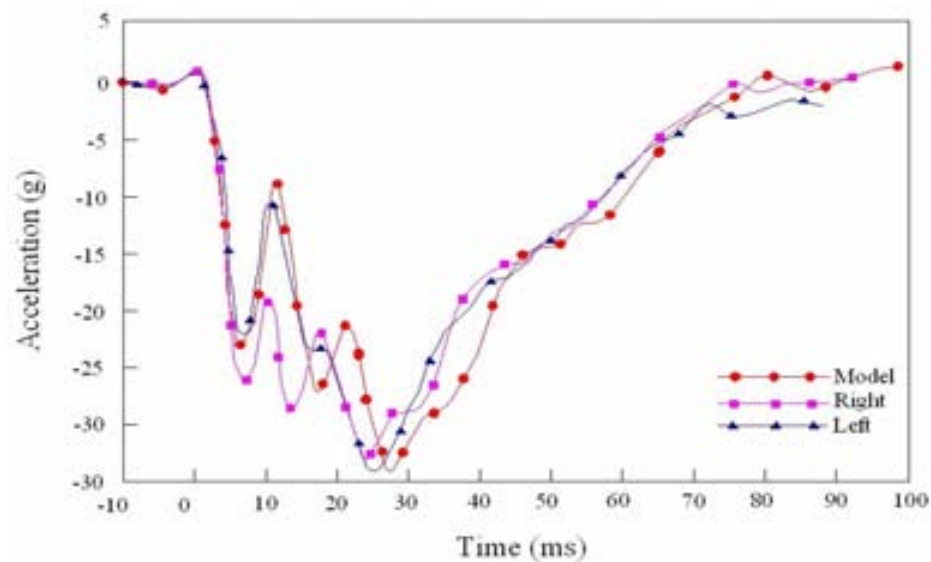


Figure 8.45: Decelerations generated for the model and tests in SAE J2114

Figure 8.46 compares the roll angle obtained from the WM simulation with that reported from tests (Gopal et al., 2004). The roll angle in the simulation is almost the same as that in the tests for the first 1.5 s. After that, even though it falls out of the experimental corridor, it is within the 25% band under which is considered to be good.

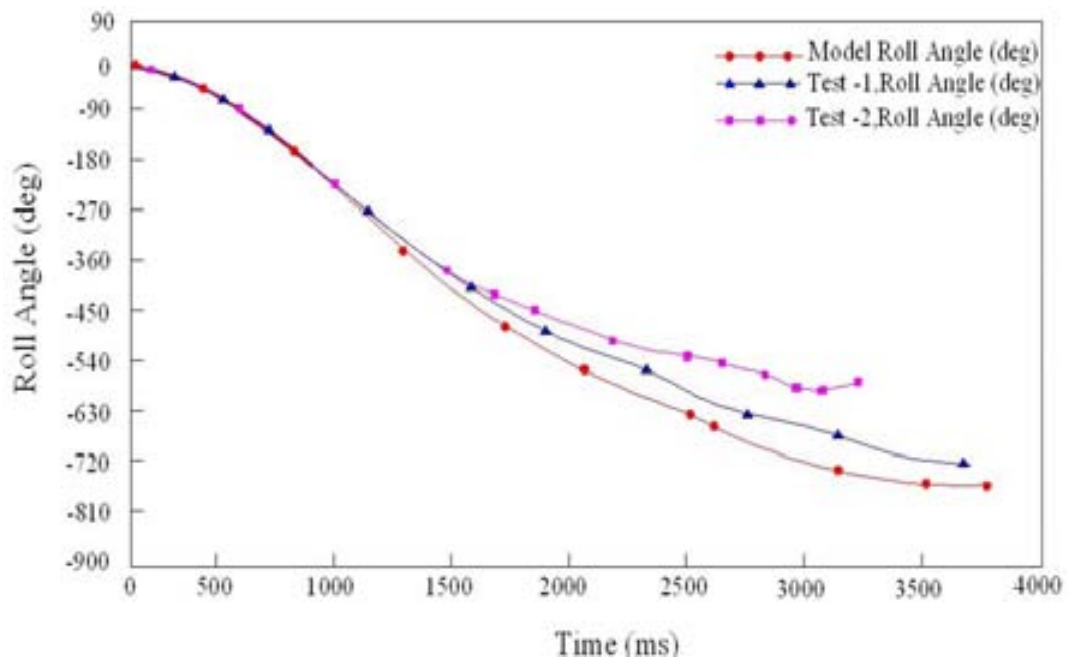


Figure 8.46: Roll angle of the SAE tests (Gopal et. al, 2004) and model simulation

The time–history of the vehicle’s CG height from the WM simulation is shown in **Figure 8.47**. Vehicle kinematics in rollover crashes along the longitudinal axis may be divided into three phases. The first phase includes contact between the car, platform and stopper. In the second phase the car turns during flight without ground contact. In the last phase the vehicle fall down on the ground and continues to move until it stopped. The vehicle’s CG height had two peak values. The first maximum value of the simulation appeared after the first impact with ground. The vehicle’s CG height decreased until it came to rest on its wheels.

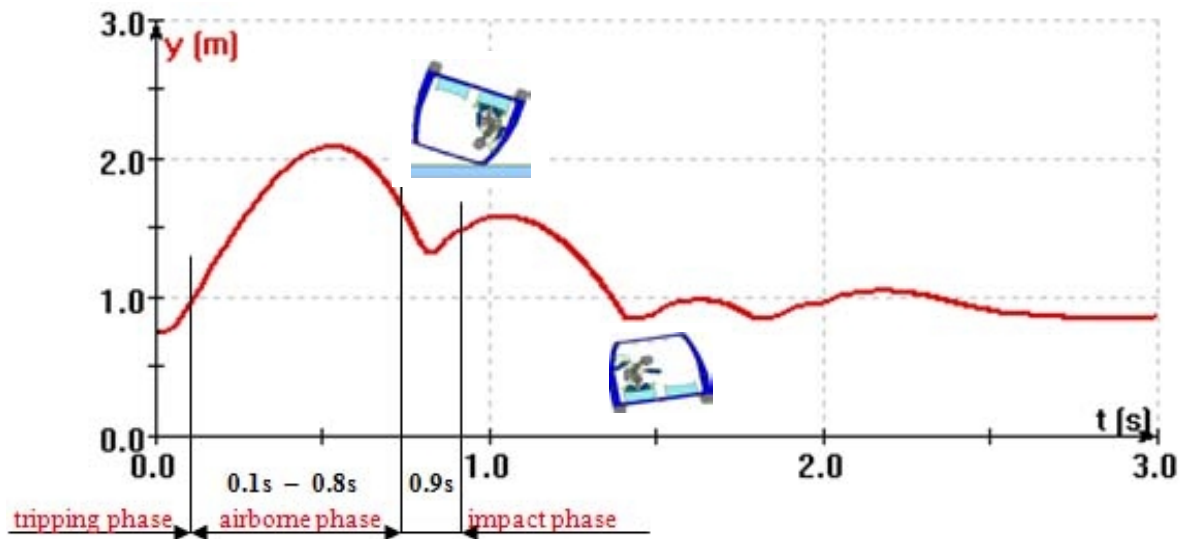


Figure 8.47: The vehicle CG height trajectory in the simulation

Figure 8.48 exhibits the vehicle roll-rate around the longitudinal axis over time from both the simulation and test (Parenteau et al., 2001).

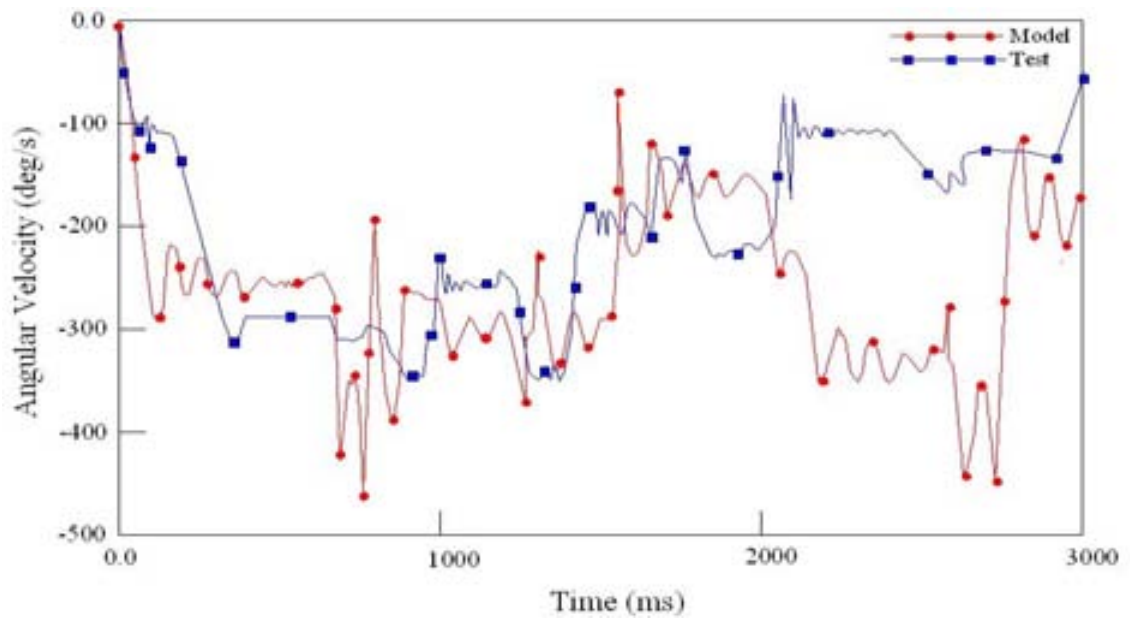


Figure 8.48: FMVSS 208 vehicle roll rate (deg/s) obtained from the laboratory tests (Parenteau et. al, 2001) and the model simulations

The correlation between the simulated vehicle roll angle and that from the experiment in **Figure 8.48** shows a good agreement of timing and peak values until 2.0 s. It is noted that after the first ground contact, there is an element of test-to-test variability that is somewhat challenging to capture in the model. Further in the time line this variability tends to increase. In addition, for the roll rate, data on only one test is available. It is thus not possible to establish a corridor for validation.

One of the most important driver injury parameters obtained from the simulation is the head acceleration. **Figure 8.49** compares the linear accelerations of the centre of gravity for the driver as obtained from the WM simulations and tests (Parenteau et al., 2001).

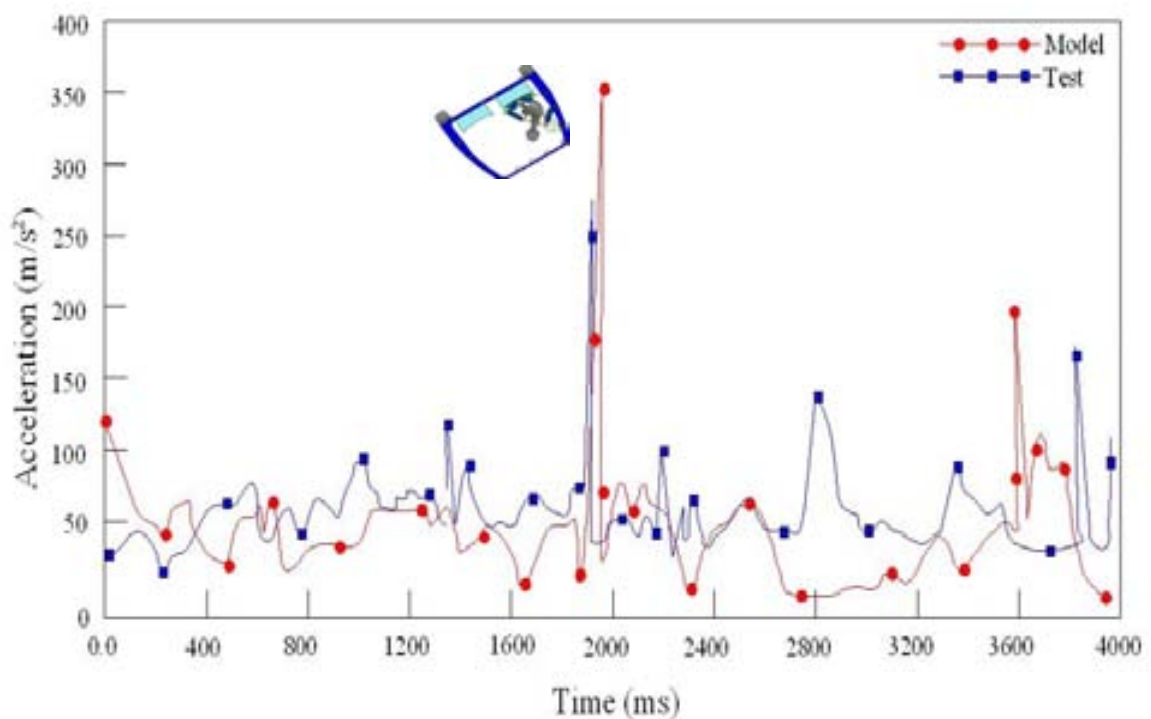


Figure 8.49: FMVSS 208 driver head acceleration obtained from laboratory tests (Parenteau et al., 2001) and the model simulations

The driver in the simulation experienced the maximum head acceleration during the second roof-ground contact. Though both the shoulder and lap belt hold the driver at the contact point, the driver's head hit the roof and reached about 35g linear acceleration. The head acceleration magnitude is also of the same order and is in the same range throughout the simulation period. There is no data available on the inter-vertebral forces from the tests. The validation is thus based on the head acceleration comparison.

It is clear that the the model simulations of rollover were capable of predicting the vehicle trajectory, the timing, the number of rolls and other relevant rollover parameters with reasonable accuracy. The differences between the simulation results and the laboratory tests may be due to the simplification of the suspension and type model. It is therefore concluded that the simulation matches well with the test, and the model can provide good simulation results which permitted the detailed analysis of the vehicle dynamics during rollover.

8.6 SIMULATION OF SPINAL INJURY IN COLLISION WITH CAMELS

The Camel–Vehicle Collision (CVC) problem has been increasing in Saudi Arabia and countermeasures are urgently needed to alleviate the heavy losses from such accidents. Every camel crash is unique. The speed at which the camel colliding the vehicle, and the size and design of the cars are important factors (Al-Shammari et al., 2010a). In this study, impacts of a typical passenger car have been simulated with a typical dromedary camel. The camel is taken to be impacted either from the side or from behind in the sagittal plane, as these were considered to be the most common orientations of crashes with camels as seen from field data in Saudi Arabia (Al-Amro et al., 1996; Al-Ghamdi and Al-Gadhi, 2004). The models of the vehicle and driver have been described in **Sections 8.2.2 and 8.2.3.**

8.6.1 The Anthropometry of the Dromedary Camel

Dromedary camels are one humped camels characterized by a long-curved neck, deep-narrow chest, and a single hump. Male dromedaries, in comparison to females, are about 10% heavier, weighing 600-800 kg, and are about 10 cm taller at shoulder height, measuring 1.8-2.0 m (Al-Habardi, 2000). The physical characteristics of camels vary widely according to their ages and types. However, the typical properties of a medium build camel which are usually involved in vehicle crashes of KSA are indicated in **Table 8.16** and **Figure 8.50**.

Table 8.16: Physical properties of a typical adult camel (Al-Habardi, 2000)

Property	Dimension (cm)
Ear's height	10
Width of eye	8
Distance from the front of the face to the gland	60
Length of neck	150
Distance between shoulder's joint and flank's joint	150
Length of tail	60
Distance from the tip of the hump to the ground	235
Distance from withers to the ground	205
Distance from withers to elbow pad	80
Distance from elbow pad to knee	60
Distance from knee to hoof	60
Distance from stifle pad to flank	80
Distance from stifle pad to hock	80
Distance from hock to hind hoof	60
Distance from one end of the hoof to the other	25
Distance of hoof joint to toenail	25

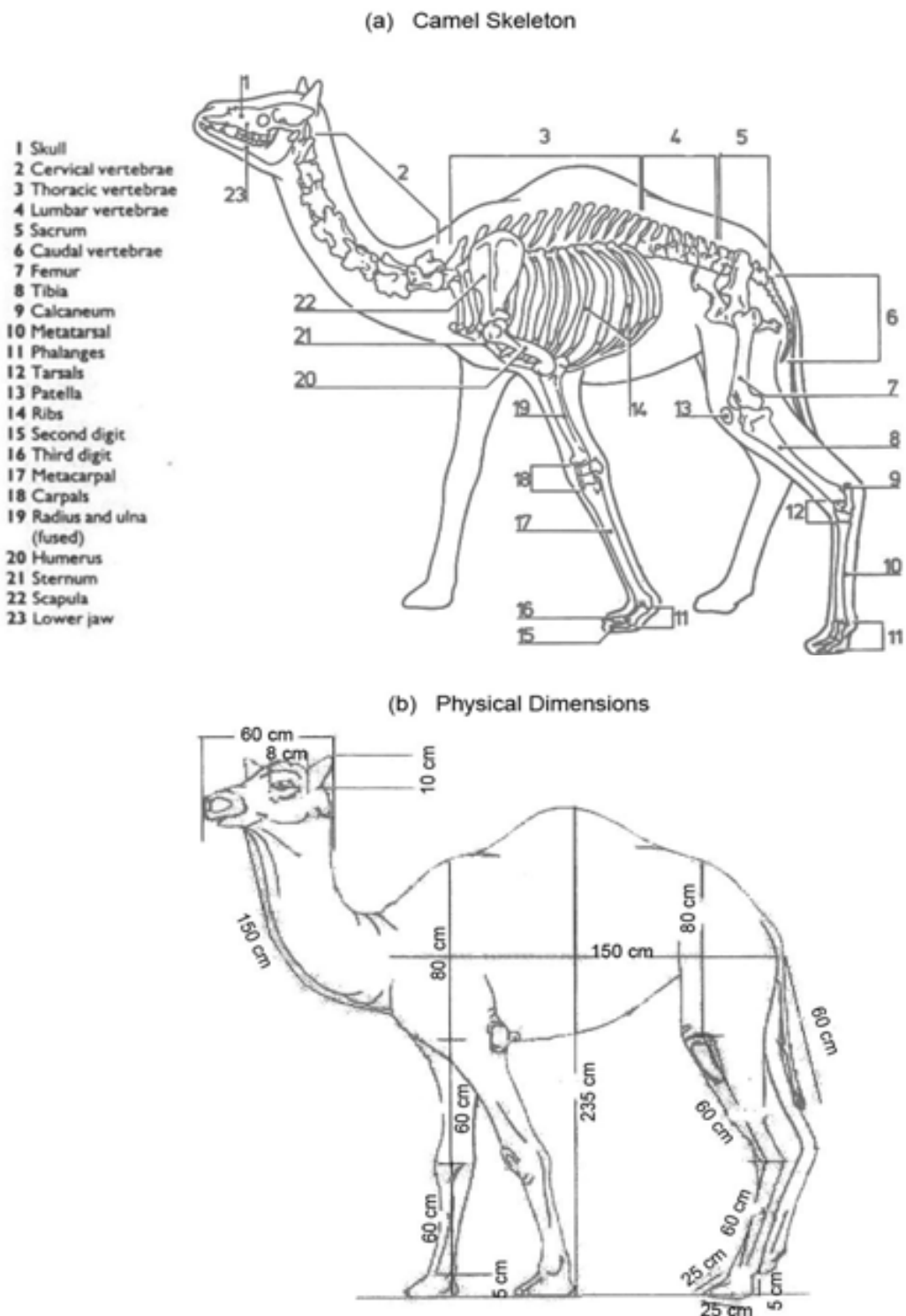


Figure 8.50: The typical characteristics of the camel's body (Al-Habardi, 2000)

8.6.2 Development of the Model of the Dromedary Camel

The camel's model has been made as per the anthropometric dimensions described above. The camel's body was divided into a head, neck, abdomen with single hump and the front and rear legs. These elements of the anatomical structure were joined by articulated joints as an open kinematic chain and additionally joined with spring-damper elements ($k_\phi = 5729 \text{ Nm/rad}$, $b_\phi = 57 \text{ Nms/rad}$) to capture the correct stiffness and kinematics. The movement of the camel models have been analysed into sagittal and frontal planes (**Figures 8.51-8.52**).

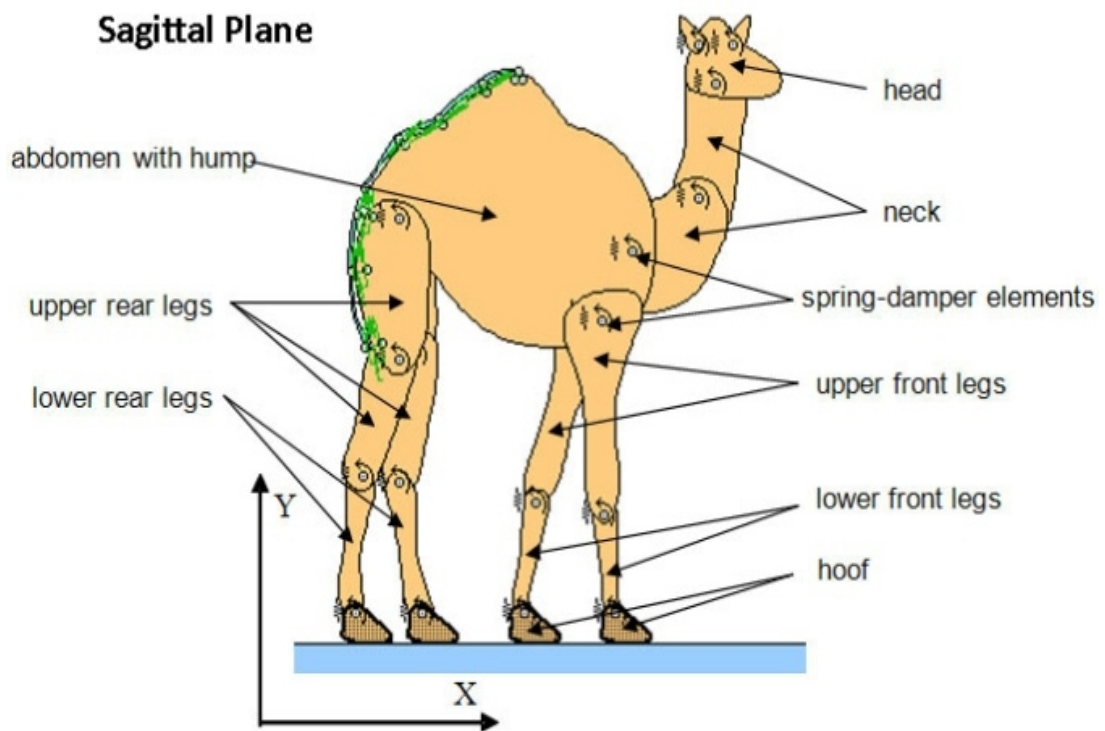


Figure 8.51: Coordinates of the camel models for the sagittal plane

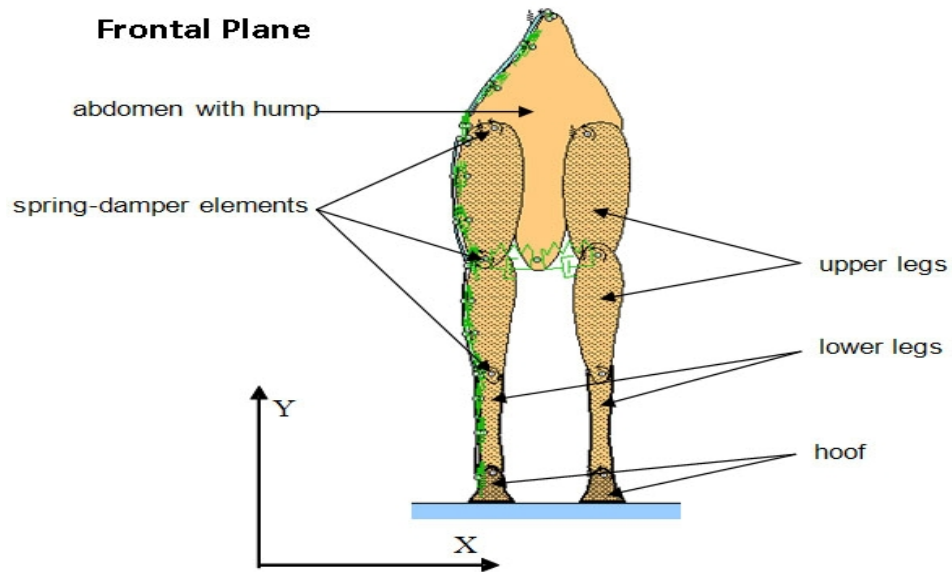


Figure 8.52: Coordinates of the camel models for the frontal plane

Table 8.17 presents the mass moment of inertia of the main parts in the camel models.

The typical mass of the camel was assumed to be 700 kg (Al-Habardi, 2000).

Table 8.17: Moments of inertia, and mass of parts of camel's body

Parts of Camel's Body	Mass (kg)	I_z [kg.m ²]
Sagittal Plane		
Head	20	0.3
Neck	35	1.1
Abdomen with hump	502	72.2
Upper front legs	12	0.8
Lower front legs	8	0.2
Upper rear leg	46.7	1.6
Lower rear leg	6	0.2
Hoof	1	0.26
Frontal Plane		
Abdomen with hump	502	49.9
Upper legs	58	1.8
Lower legs	14	0.2
Hoof	1	0.028

Camel collisions were simulated in the sagittal and frontal planes in the configurations shown in **Figures 8.53** and **8.54**.

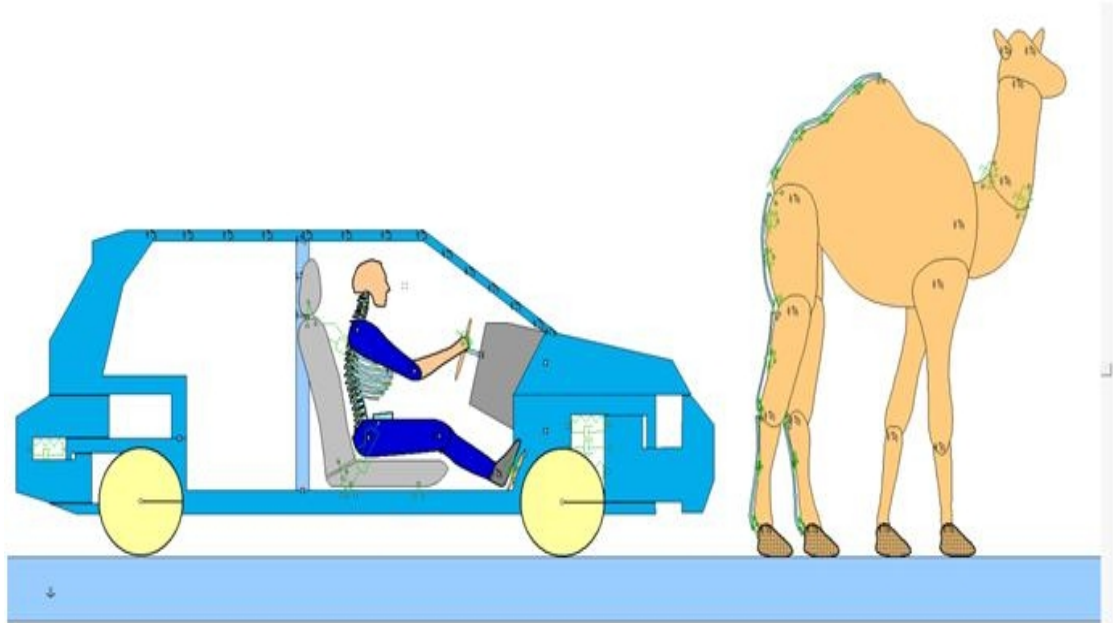


Figure 8.53: Model of camel collision in sagittal plane

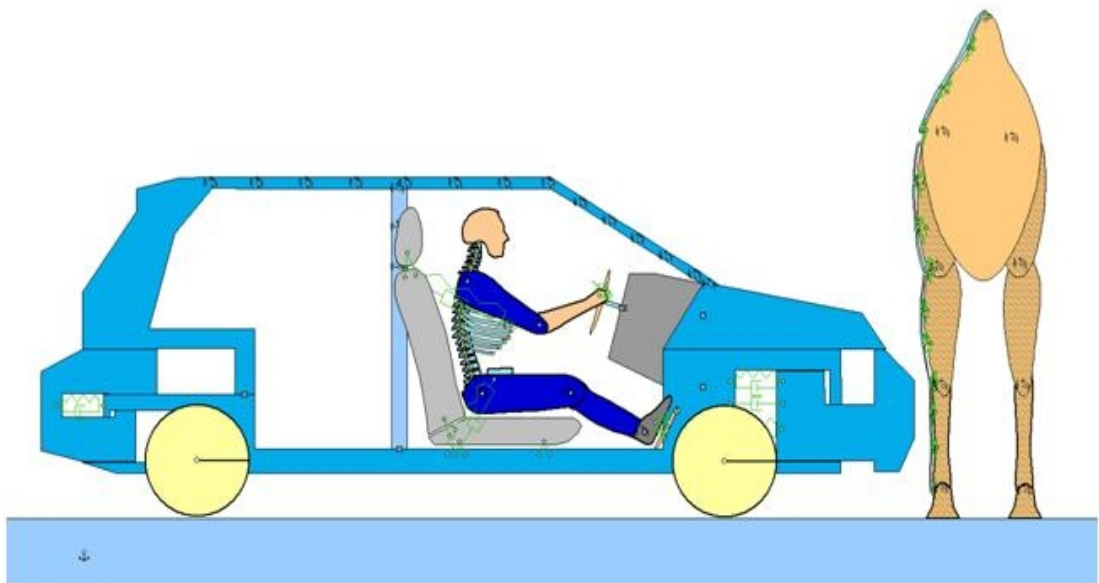


Figure 8.54: Model of camel collision in frontal plane

8.6.3 Camel Collision Model Validation

In order to validate the camel model and the simulation of camel impact, two typical cases of camel impacts were considered. Data for these cases was available from recorded crash data in this research and the crashes were simulated using the camel model developed.

8.6.3.1 Case I: Crash with the Camel in the Sagittal Plane

Crash Description: The vehicle in Case I, a 1997 Lumina, four door Sedan, was travelling eastbound at an estimated speed of 77 km/h on a rural two-lane road at night. The vehicle collided with a camel that appeared unexpectedly between the surrounding farms with a PDoF of zero degrees. The vehicle first struck the rear left leg of the camel and continued to move forward underneath since the bulk of the animal's mass and centre of gravity are higher than the bonnet height of the vehicle. This resulted in scooping up of the animal by the vehicle on to the bonnet. The animal slid across the bonnet contacted the windscreen area with its left side. The momentum of the camel pushed it through the windscreen, raising the front of the roof upwards, and came to rest in the front passenger compartment. The animal contacted the driver's upper body (head and torso) and pushed it onto the seat.

The direct impact between the animal and the driver's head and upper torso resulted in a subluxation at C4/C5, vertebral fracture of C3 cervical spine, and subarachnoid haemorrhage. The driver had other associated injuries, i.e., multiple lacerations to the chin, neck, scalp, limbs and right breast, and was in coma for two days. The hypothesized mechanism for cervical spine injuries is hyperextension and compression. The case description and contact sources of the injuries details are given in **Tables 8.18**, and **8.19**.

Table 8.18: Brief description of Case I

Sex	Male
Age (years)	28
Height (m)	1.75
Mass (kg)	80
Car speed (km/h)	77
Spinal injury	Fractures of C4/C5, C5
Physical Impairment	Intact

Table 8.19: Injuries of the driver in Case I

Injury	ISS Body Region	AIS	Source of Injury
Subluxation at C4/C5 Cervical spine	Cervical spine	650230.3	Camel/roof
Undisplaced fracture through C5	Cervical spine	650204.2	Camel/roof
Patterned abrasions around the neck	Cervical spine	310202.1	Camel/roof
Subarachnoid haemorrhage	Head	140684.3	Camel/roof
Scalp laceration vertex	Head	110600.1	Camel/roof
Abrasions with laceration to lower chin	Face	210600.1	Steering wheel
Abrasions over the forehead	Face	210202.1	A-pillar
Abrasion to right breast	Abdomen	410202.1	Steering wheel
Minor superficial abrasions to limbs	Extremities	710202.1	Dash board
ISS			11

Applying the law of the linear momentum to the camel crash yields:

$$V_2 = \frac{V_1 \times M_{car}}{M_{car} + M_{camel}} = \frac{77 \times 1499}{1499 + 786} \approx 51 \text{ km/h}$$

$$\therefore \Delta V = 51 - 77 \approx -26 \text{ km/h}$$

Where V_2 is the speed of car after impact in (km/h), V_1 is the speed before impact in (km/h), M_{car} is the mass of the car in kg, and M_{camel} is the mass of the camel in kg.

Figure 8.55 shows the points of impact in the crash. Points marked as ‘1’, ‘2’ and ‘3’ are the points where the camel first touches, where the legs come in contact with the car and where the camel back comes in contact on the car top. **Figure 8.56** shows the same locations as observed in the simulations. As can be seen, the simulation results of these points are very close to the landmarks seen on the vehicle. It can thus be seen that the developed model gives a good match with the crash in this case.

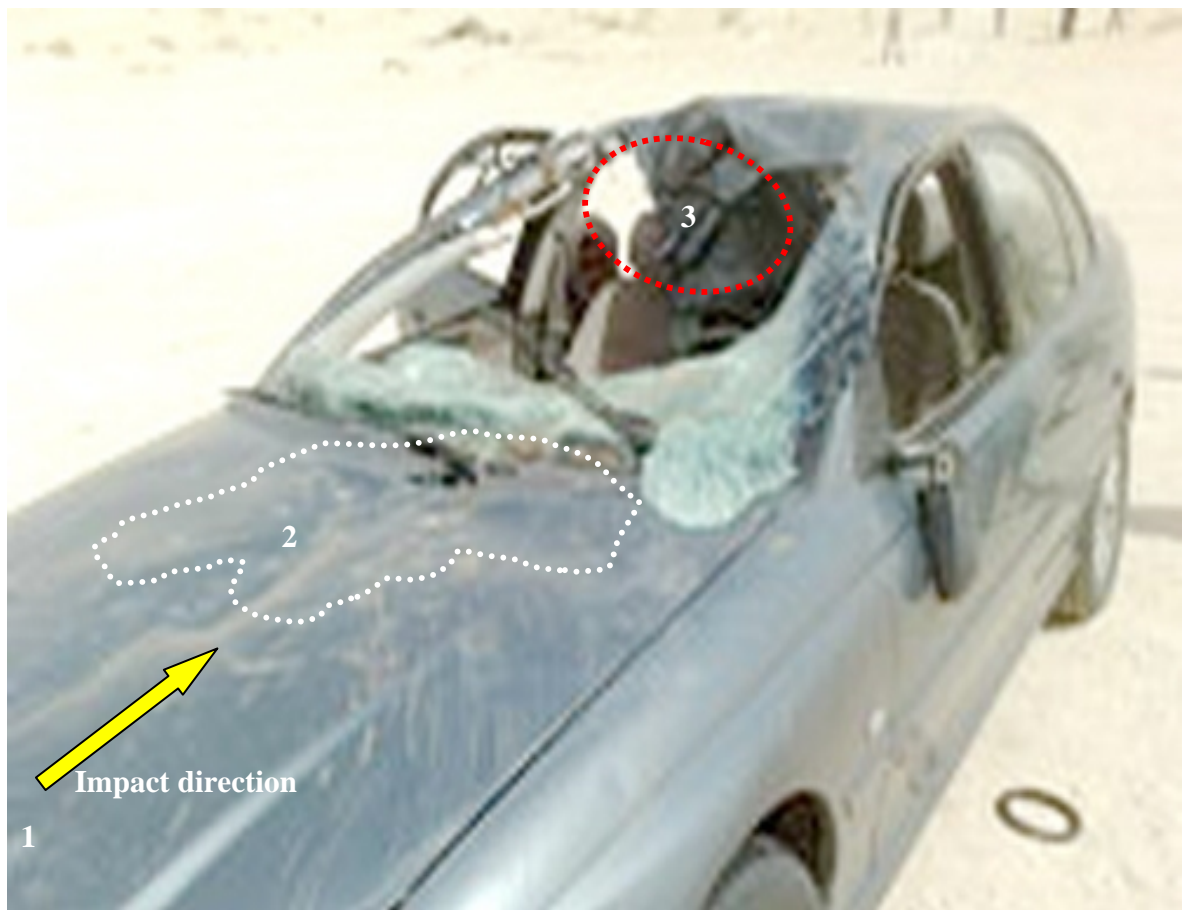
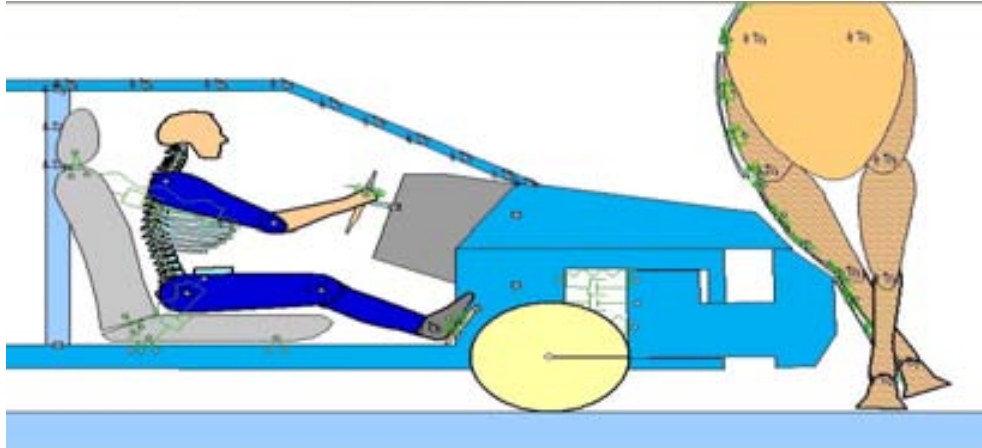
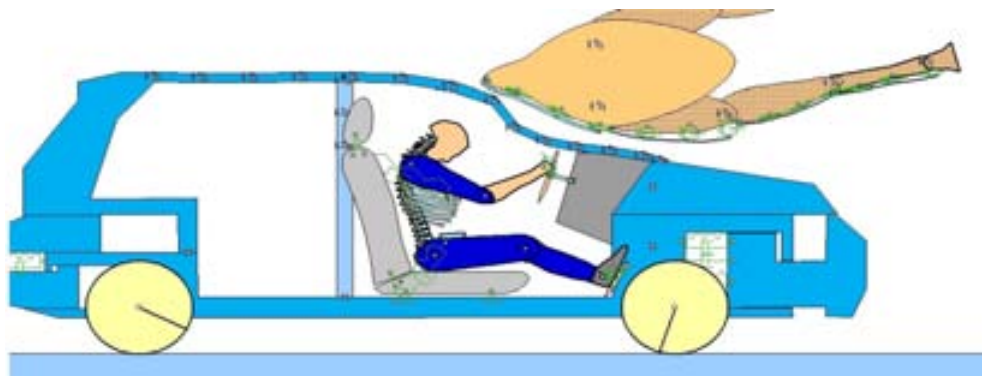


Figure 8.55: A picture of the damaged vehicle (having CDC: 12FLEW1) showing the major contact points on the vehicle

(a)



(b)



(c)



Figure 8.56: Snapshots from the simulation of the Case I crash showing the contact of the camel with the vehicle

8.6.3.2 Case II: Crash with the Camel in the Frontal Plane

Crash Description: On a weekend day, a driver and front seat passenger were travelling at approximately 110 km/h on an undivided highway, South of Riyadh. The 1990-Chevrolet, Caprice car in which they were travelling collided with a herd of camels that appeared suddenly on the road through the broken roadside fences.

The car struck the tall legs of the animal. The bulk mass of the animal and its centre of gravity are higher than the striking point on the vehicle. Therefore the vehicle is not arrested but continues in its forward motion underneath the animal. The animal's legs lose contact with the ground and are splayed on the bonnet as the animal's body is stationary because of inertia, making contact with the roof and the top of the windscreen. This contact collapses onto the passenger compartment on top of driver.

X-Ray and Computed Tomography (CT) Scans showed a burst fracture in C5, and fracture vertebral arch C5, along with sagittal fracture for C6-C7 resulting in complete quadriplegia. In addition to spinal injuries, the casualty sustained head, thoracic and facial injuries. The hypothesized mechanism of the spinal injury is axial compression with flexion. The case injury details are presented in **Tables 8.20** and **8.21**.

Table 8.20: Brief description of injuries in Case II

Sex	Male
Age (years)	23
Height (m)	1.68
Mass (kg)	76
Car speed (km/h)	110
Spinal injury	Fractures of C5, C6, C7
Physical Impairment	Complete quadriplegia

Table 8.21: Injuries of the driver in Case II

Injury	ISS Body Region	AIS	Source of Injury
Burst fracture of the 5 th cervical	Cervical spine	640263.5	Camel/roof
Sagittal fracture of the 6 th , 7 th vertebra	Cervical spine	650216.2	Camel/roof
Subdural oozing of blood	Head	140650.4	Camel/roof
Petechial haemorrhages	Head	140642.4	Camel/roof
Swelling of both temporal lobes	Head	140660.3	Camel/roof
Le fort fracture of maxilla	Face	250804.2	Camel/roof
Fractures of 2 nd , 3 rd and 5 th ribs	Thorax	450232.4	Steering wheel
Bilateral contusions to the lungs	Thorax	441410.4	Steering wheel
Large lacerations in the liver	Abdomen	541820.2	Steering wheel
Some lacerations to the spleen	Abdomen	544220.2	Steering wheel
Contusion into the root of the mesentery	Abdomen	542010.2	Steering wheel
Fracture of the left radius	Extremities	752800.2	Camel/roof
Fracture of the left ulna	Extremities	753200.2	Camel/roof
Fracture of the left tibia	Extremities	853404.2	Facia
Fracture of the left fibula	Extremities	851605.2	Facia
ISS			45

Applying the law of the linear momentum to the camel crash yields:

$$V_2 = \frac{V_1 \times M_{car}}{M_{car} + M_{camel}} = \frac{110 \times 1915}{1915 + 815} \approx 77 \text{ km/h}$$

$$\therefore \Delta V = 77 - 110 \approx -33 \text{ km/h}$$

Figure 8.57 shows the points of impact in the crash. Points marked as ‘1’, ‘2’ and ‘3’ are the points where the camel first touches, where the legs come in contact with the car and where the camel back comes to rest on the car top. **Figure 8.58** shows the same locations as observed in the simulations. As can be seen, the simulation results of these points are very close to the landmarks seen on the vehicle. It can thus be seen that the developed model gives a good match with the crash in this case.

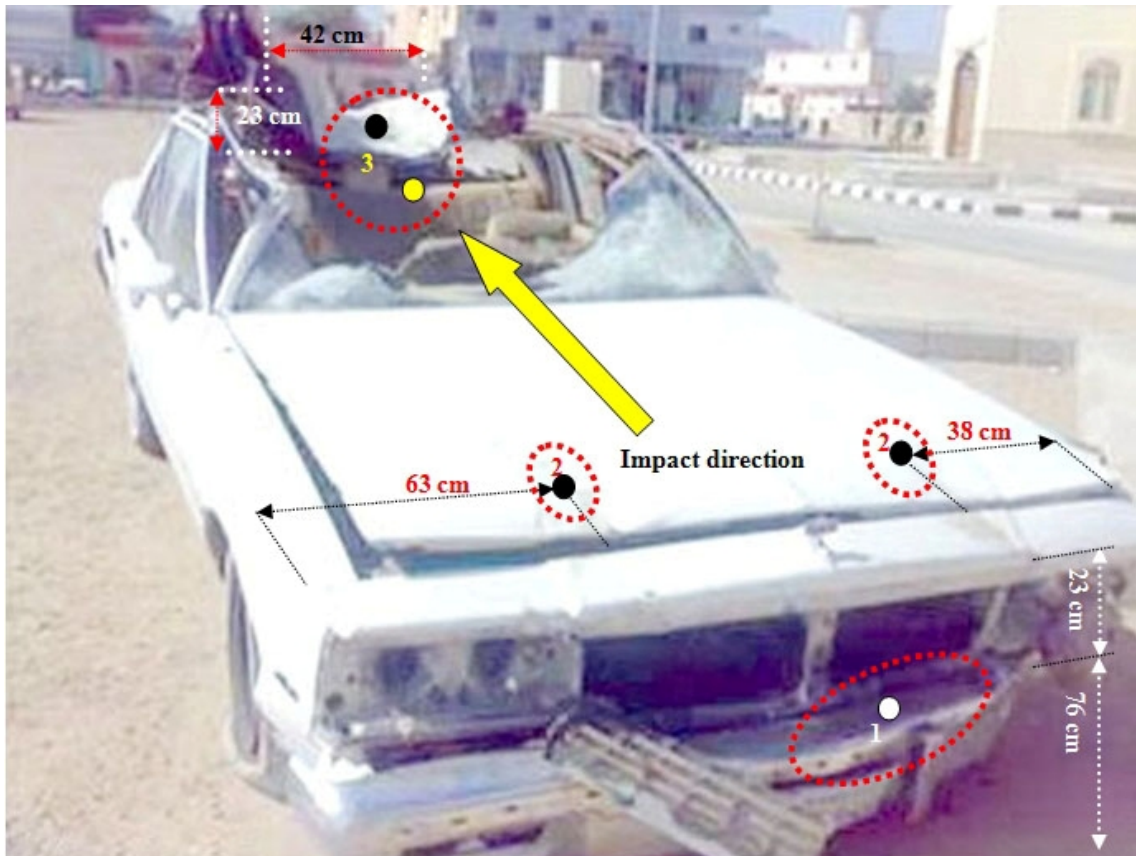


Figure 8.57: A picture of the damaged vehicle (having CDC: 12FLEW1) showing measurements: 1-position of first impact between the legs of animal and the vehicle, 2-second contact points due to sliding of the animal's legs over the bonnet of the vehicle, 3-third contact between the windscreen/roof and the back of the animal

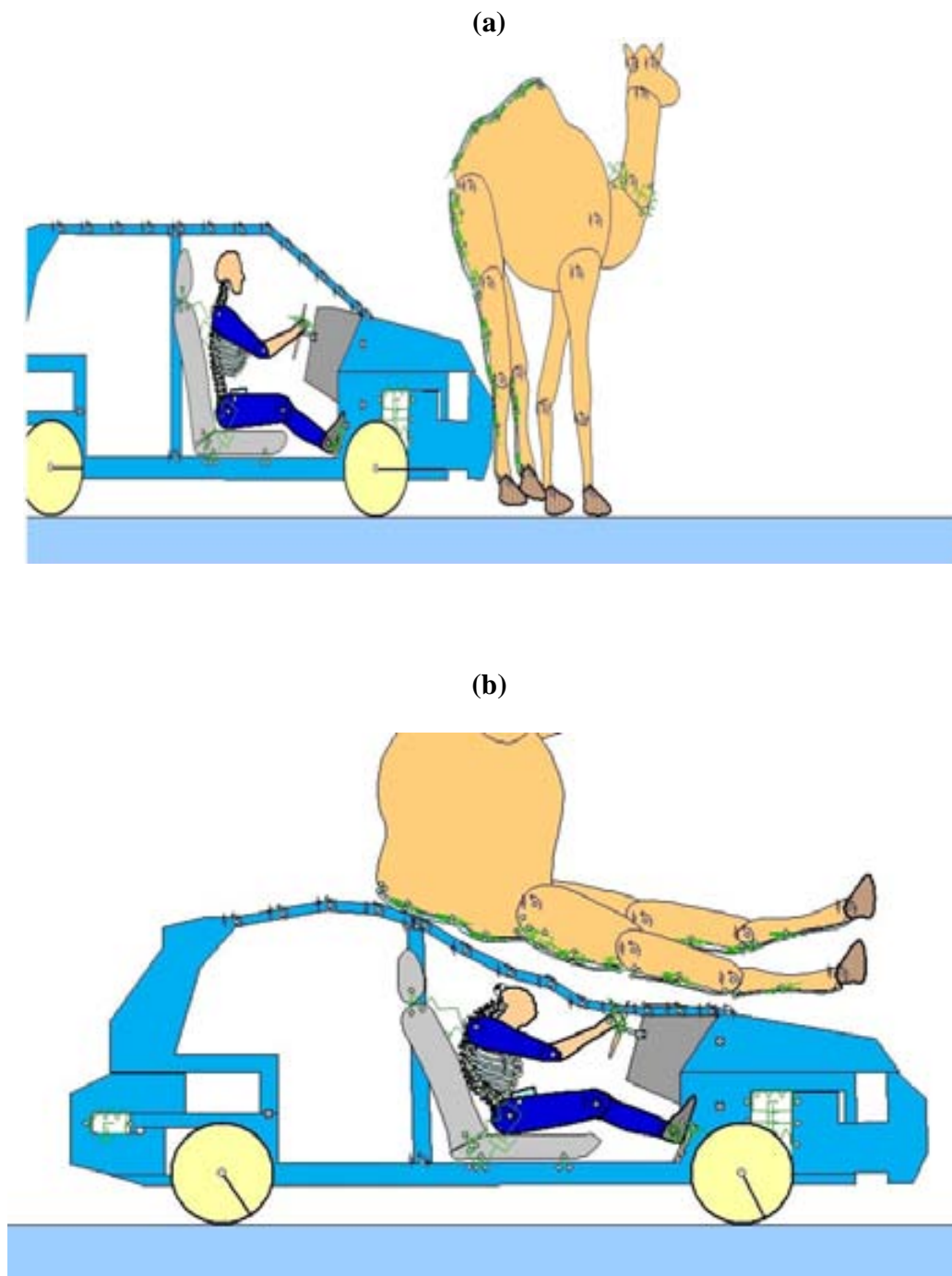


Figure 8.58: Snapshots from the simulation of the Case II crash showing the contact of the camel with the vehicle

From the analysis of these two camel crash cases, it can be seen that the simulation results of the present models are fairly close to the observations in the crash. It can thus be concluded that the camel model well predicts the camel kinematics and can be used for preliminary analysis of camel crashes.

8.7 DEVELOPMENT OF SPINAL INJURY OF PEDESTRIAN

Pedestrian simulations have been developed with a typical passenger car according to the Euro-NCAP pedestrian crash test (EEVC, 1994 and 1998). **Figure 8.59** shows the initial configuration in these simulations. The pedestrian model was created in the frontal plane in which the pedestrian to be impacted from the side as this is the most common orientation of pedestrian impact from field data (Yao et al., 2008; Sturges et al., 2002b; and Coley, 2004).

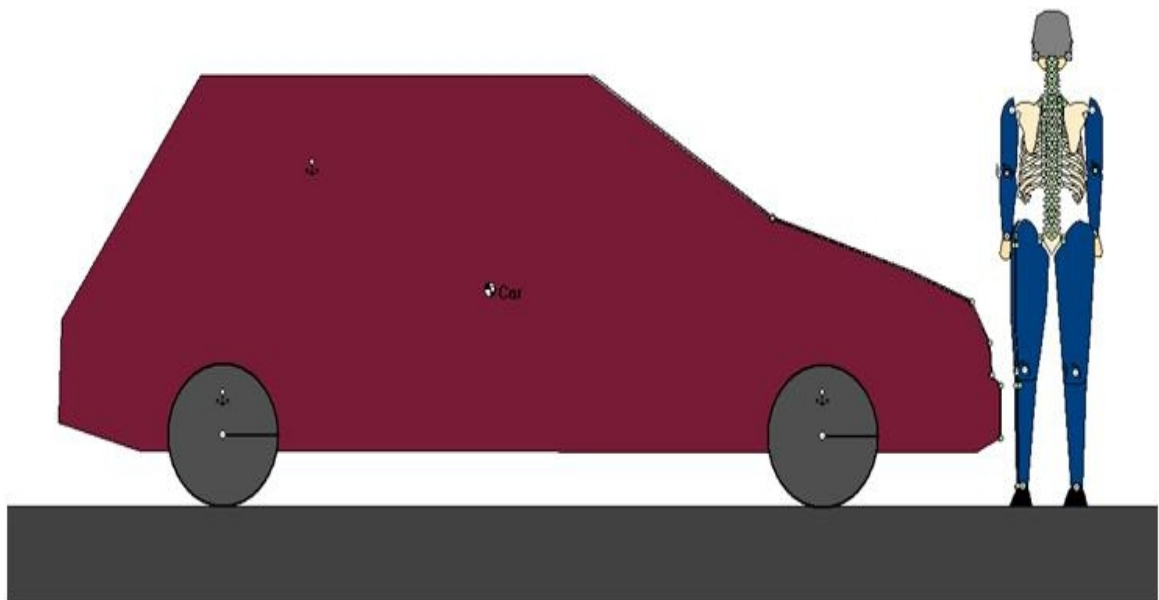


Figure 8.59: The initial configuration for the simulation of the pedestrian impact with a typical passenger car

8.7.1 Model of Passenger Car in the Pedestrian Impact Simulation

A typical passenger car has been developed for the pedestrian simulations as shown in **Figure 8.60**. The properties of the vehicle's model have been described in **Section 8.2.2** in more details. The mass of the vehicle was assumed to be 1200 kg.

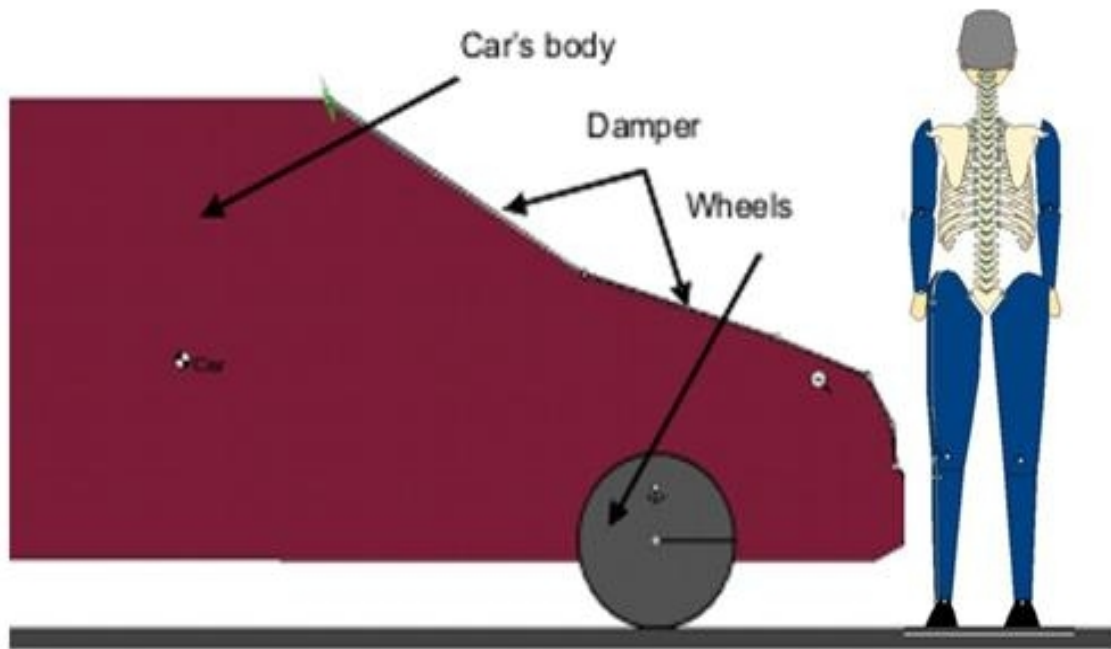


Figure 8.60: Model of passenger car

The vehicle was modeled from regular geometrical shapes representing rigid bodies (using software Working Model 2D) which were joined in appropriate ways to permit proper deformation as well as dissipation of energy at the moment of collision. The car was divided into three main parts, the body (consists of the main parts of the car), the wheels and the appropriate springs and dampers in the pedestrian contact area (Toyota, 2005).

8.7.2 Model of Pedestrian

The second part of the modelling process was focused on the formulation of pedestrian models, taking into the structure as well as the physiology of the cervical and lumbar spine. The model developed in the frontal plane is shown in **Figure 8.61**. The main anatomic parts involved in the model are the head, cervical, thorax and lumbar spine, upper and lower limbs connected with rotational joints and spring - damper elements as an open kinematics chain. The mechanical properties were according to the model described in **Section 8.4.3**.

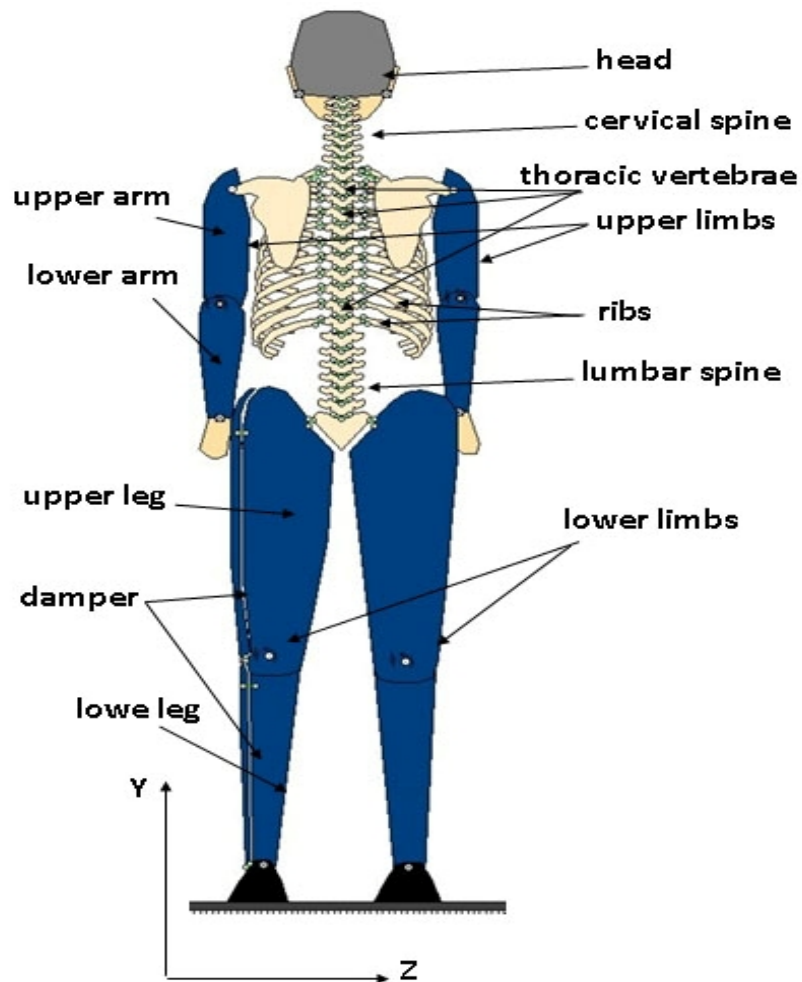


Figure 8.61: New model of pedestrian

Upper limbs are divided into upper arm and lower arm **Figure 8.62a**. Lower limbs are divided into upper leg and lower leg **Figure 8.62b**. Additionally an element-damper absorbing crash energy, simulating soft tissue is joined to the left leg (Silva and Ambrosio, 2004).

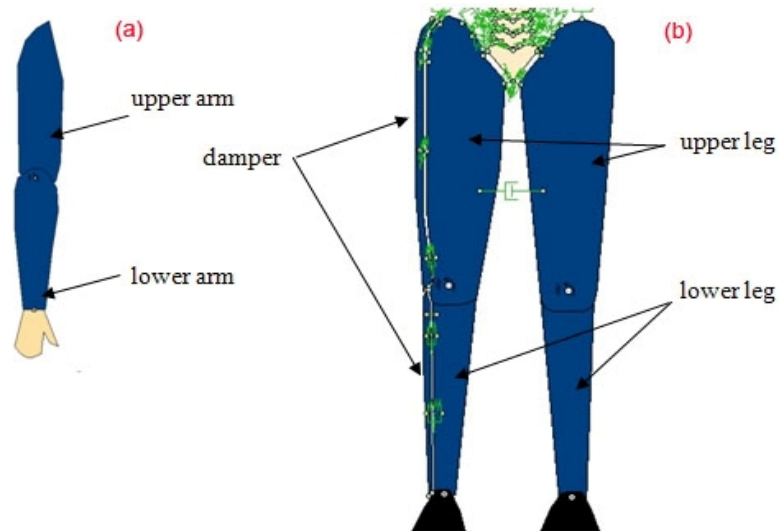


Figure 8.62: Model of limbs of pedestrian

The inertial parameters of the main parts of model of the pedestrian are presented in **Tables 8.4** and **8.22**. The movement of the model was analysed in the plane YZ of the coordinate system shown in **Figure 8.8**.

Table 8.22: Moments of inertia and mass of main parts of the pedestrian body

Parts of Driver Body	Demptster Coefficient (%)	Mass (kg)	I_x (kg.m ²)
Head	6.9	5	0.025
Upper limb	6.2	4.5	0.031
Lower limb	17.1	12.5	0.045

In order to verify the pedestrian model with previously undertaken cadaver experiments, computer simulations have been carried out with this model. The responses from the model, such as overall pedestrian behaviour, head resultant velocity and acceleration of the segments were validated though comparisons with cadaver test results from previous models.

8.7.3 Cadaver Tests

Ishikawa (2000) discusses a number of orientations that are possible in pedestrian crashes. Ishikawa et al. (1993) reported a set of ten cadaver tests conducted in the late 1980's and early 1990's at Hannover Medical University. The vehicle set-up consisted of the frontal parts of a medium sized production vehicle mounted on a test sled, enabling various frontal geometries to be attained, together with different stiffness values of the bumper (Figure 8.63).

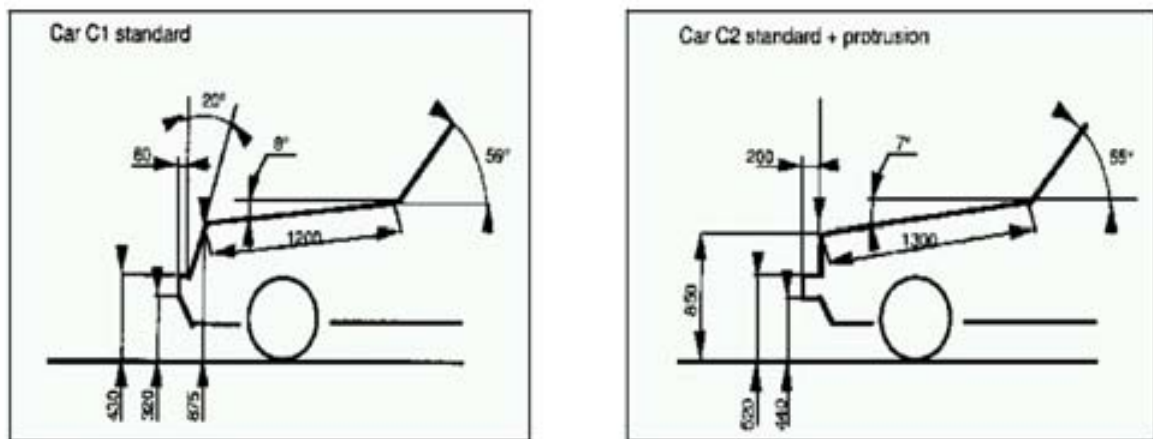


Figure 8.63: Vehicle frontal geometry used cadaver tests (Ishikawa et al., 1993)

The tests were conducted at four speeds, 25 km/h, 32 km/h, 39 km/h and 40 km/h, and one test from each of the speed groups was chosen for validation purposes.

During each of the tests, the cadaver kinematics was recorded with a high speed camera, which allowed the authors to recreate trajectory plots for the head, pelvis, knee and ankle. Also measured in each test was the resultant head velocity relative to the car. The latter of the published tests had the cadavers instrumented with four different accelerometers, to record data for acceleration of the head, chest, pelvis and impacted leg.

A test involving a 68-year-old male of height 1750 mm and weight 68 kg was simulated to achieve the validation. In test T9 the cadaver had its arm tied in front of the body to prevent its interaction in the impact sequence as shown in **Figure 8.64**.

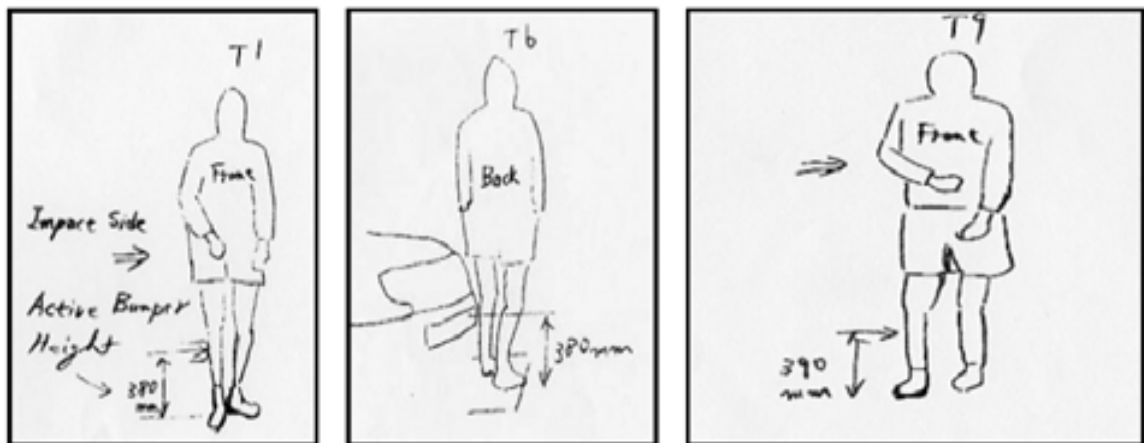


Figure 8.64: Sketches of pedestrian pre-impact positions (Ishikawa, 2000)

Test-T9 published by Ishikawa et al. (1993) was modeled using a simplified representation of the vehicle, with modelling for the bumper, bonnet top and windscreen. Stiffness values used in the simulations were taken directly from the publication. The frontal geometry of the impacting vehicle for this test set up was a 390 mm bumper height, a 720 mm leading edge height and a bumper lead of 200 mm. The test was conducted at 40 km/h.

8.7.4 Pedestrian Model Validation

The 40 km/h impact resulted in serious injury to the cadaver. The left leg had a fracture at the tibial lateral condyle, crush fracture at the head of fibula and total rupture of both collateral and crucial ligaments. The right leg sustained a crush fracture at the tibial medial condyle. There was also a fracture to the right side of the skull. The cadaver was orientated perpendicular to the vehicle, being struck on the right hand side.

Figure 8.65 illustrates the typical overall pedestrian kinematics obtained in the computer simulations for the test T9 and compares them with the responses of Linder's model created for a car's base line optimisation for injury prevention (Linder et al., 2004). Comparing the angle of the head relative to the upper body during impact sequence, it can be seen that the neck joints characteristics in the model seems to adequately predict the cadaver's head movement. However, the relative neck stiffness of a human, where muscle tone is active, should be investigated further for a reconstruction of real world car-pedestrian accidents.

The impacted elbow in both the cadaver tests and the model swings out and hits the bonnet, which may significantly affect the subsequent upper body motion and head impact with the bonnet or windscreen. This occurrence may be difficult to control and may decrease repeatability in experimental tests. In the cadaver test T9, the impacted hand of the cadaver specimen was tied across the front of the body, whereas in the simulations both arms were free. This difference caused a different swinging motion of the impacted arm and seemed to induce a different head impact with the bonnet or windscreen.

While 3D rotations have not been captured in these 2D simulations, the overall kinematics of T9 is similar in the cadaver test and computer simulations.

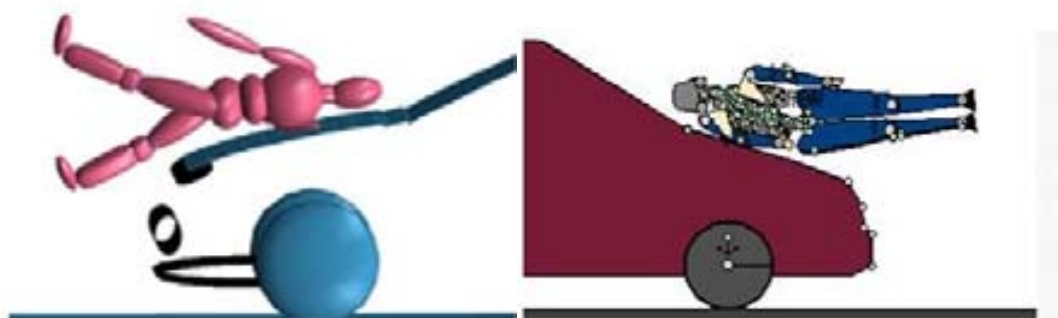
a) Linder's Model

b) Simulation Results

70 ms



110 ms



130 ms

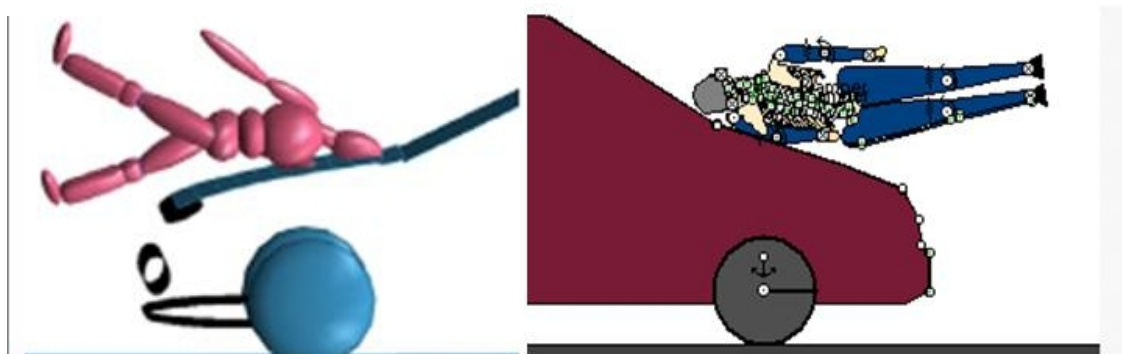


Figure 8.65: Pedestrian's kinematics at 40 km/h impact speed in the current 2D-Model and Linder's 3D-Model

The trajectories for head, pelvis, knee, and foot at a time step of 20 ms in the cadaver specimen tests are compared with that obtained from the computer simulations (**Figure 8.66**).

The trajectories of the head and pelvis appear to correlate reasonably to the cadaver results; however the impact location of the head falls short by approximately 20 cm. The foot joint appears to have the same trajectory again, but slightly offset, with the foot failing to rotate far enough under the vehicle front end, as seen and recorded from high speed film. It should be noted that previous attempts at modelling impacts at high speed have always struggled in correlating the lower extremity trajectory with the test (Ishikawa et al., 1993; Yoshida et al., 1998). However, Coley et al. (2001) with his detailed pedestrian models showed good correlations between human body trajectories and experiments. The trajectory of the knee shows a similar vertical movement initially, but then shows more of a rotating movement, whereas the cadaver knee closely followed the contours of the vehicle.

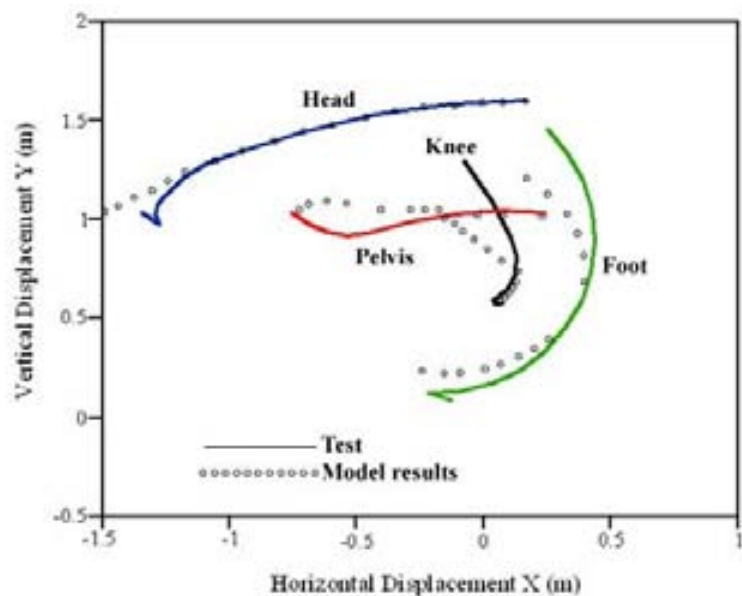


Figure 8.66: Trajectories of head, pelvis, knee and foot in the experiments (Ishikawa et al., 1993) and model simulations

Figure 8.67 compares the time histories for head resultant velocity (relative to the car body) obtained from the simulation with that obtained in the test. In none of the simulation intervals did the head attain the same peak resultant velocity at the same time as the cadaver test. However, overall the head velocity is generally correctly predicted by the pedestrian impact model. The point at which the head strike on the bonnet occurred showed that the head velocity was considerably greater than the initial impact velocity of the car, with deceleration levels being much higher in comparison with the cadaver test. It should be noted that the rising slope of the head resultant velocity appears to be quite similar in the test and corresponding simulation. The head velocity curve tends to peak too early due to the elbow interaction with the vehicle. The model showed a high peak head velocity which in turn led to a high deceleration and consequently would lead to greater injury risk.

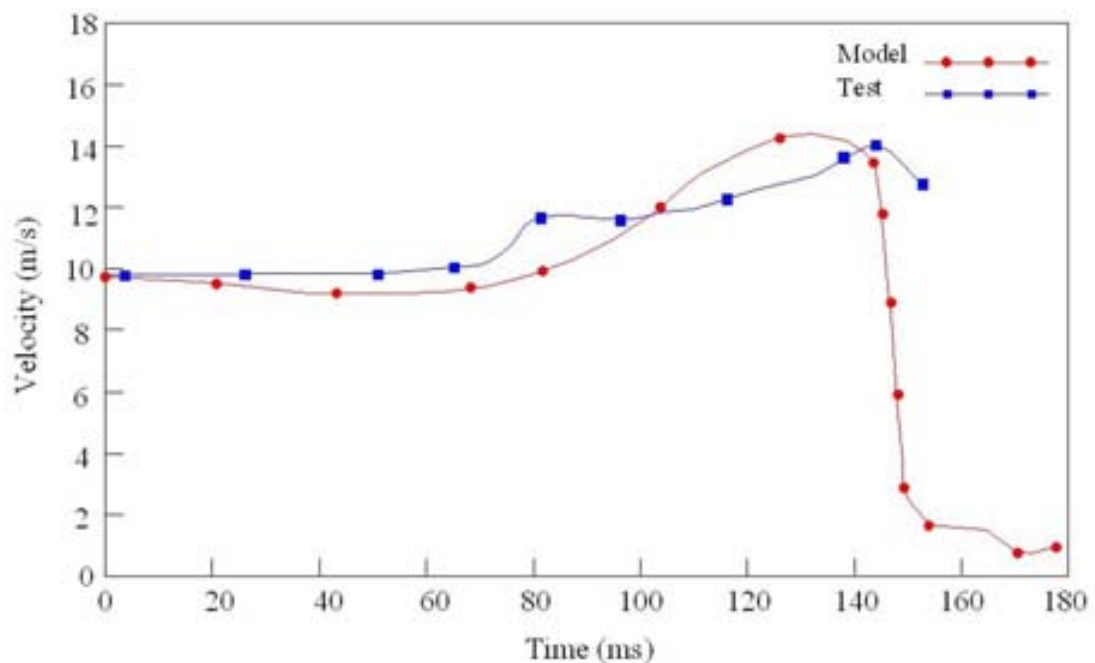


Figure 8.67: Comparison between the resultant head velocity relative to vehicle of the pedestrian in the experiments and computer simulations

In cadaver test T9, in addition to the measurements of displacement and velocity, the accelerometer output was recorded for the head resultant acceleration. Comparisons of the tests output with the test data, can be seen below in **Figure 8.68**. For the head impact, even with the most severe elbow strike on the bonnet, the timing of the peak head accelerations are substantially earlier than that which occurred in the cadaver test. This difference seems to be the result of the initial position of the impacted arm which was tied across the front of the body. The magnitude of the peak itself is probably of less importance as only a generic stiffness for the vehicle front end was given by Ishikawa et al. (1993) with no mention of the actual stiffness to use for the bonnet (2000 N/mm).

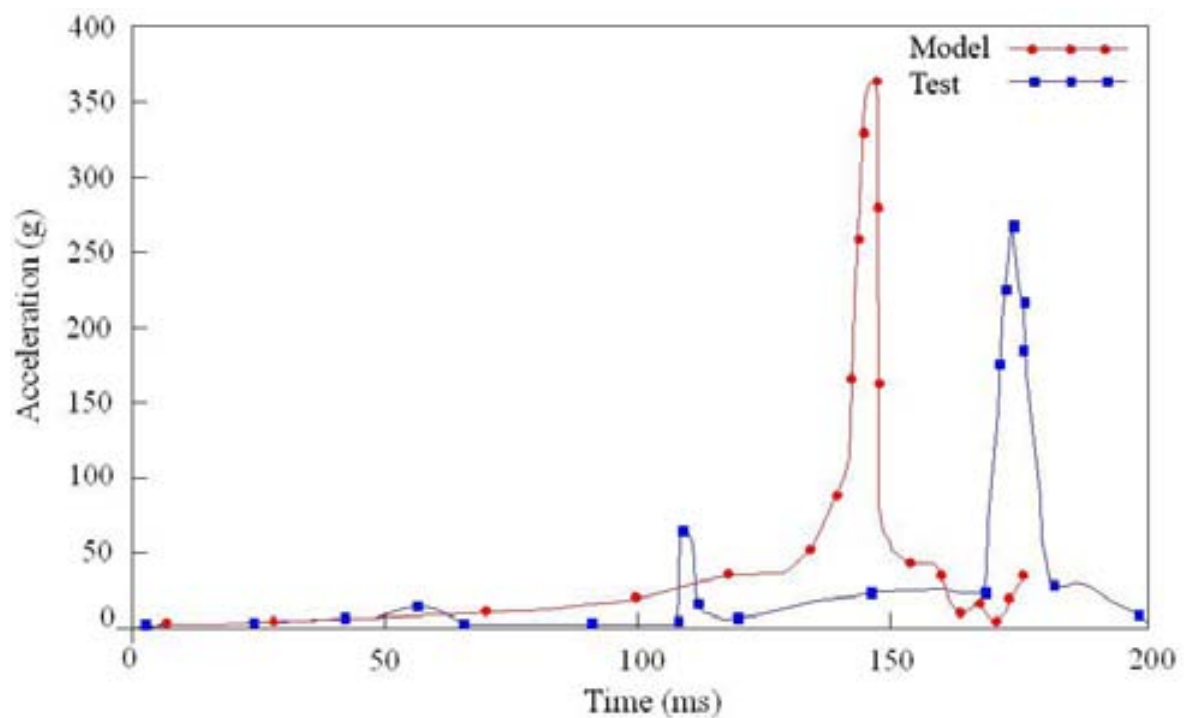


Figure 8.68: Comparison between the resultant head acceleration of the pedestrian in the experiments and computer simulations

Detailed work by Sturgess et al. (2002) has shown a linear relationship between injury and the stiffness of the impact object and also the effect of impact velocity. Tuning of the model based on bonnet stiffness could have been undertaken, however as described above, the resultant head velocity of the pedestrian never reached the peak seen in the testing. Use of the head impact velocity therefore proves a more useful measure under these circumstances.

It is known that the influence of the pedestrian arm can affect the impact characteristics especially the head strike to the vehicle, and in many cases both dummies and cadavers are set up in such a way as to prevent this (Suthurst and Hardy, 1985; Garrett, 1997).

Also one of the stipulations for these tests was that no severe facial injuries were sustained as the cadavers would be passed back to relatives for funerals. To ensure this the initial positions of the cadavers were set to be angled slightly away from the vehicle so that rotation occurs resulting in a strike to the rear of the head. In test T9 the cadaver had its arm tied in front of the body to prevent its interaction in the impact sequence. However, the outline kinematics at 50 ms intervals appeared to show that the arm still interacted with the vehicle albeit different to normal and caused a large elbow strike on the bonnet. The exact pre-impact set-up of these tests was not fully known, and was taken from sketch drawings provided in the Ishikawa et al publication to position and orientate that pedestrian body in **Figure 8.64**.

For these reasons, the model's initial position was optimised to give the closest match with the cadaver test data for the head impact velocity. To achieve the large elbow strike on the bonnet, the shoulder joint flexion and abduction values were altered between 5 and 10 degrees to cause this effect.

8.8 MAIS-ΔV ESTIMATED CURVES

In this section, an attempt was made to find the best relationship between the MAIS and ΔV for both restrained and un-restrained occupants based on data collected from real world accidents in Saudi Arabia (see **Section 4.1**). This is done by using square and cubic curve fitting as proportionality of severity of injury is known to be limited between square and cube of ΔV (Sturgess, 2002). The results are shown in **Figures 8.69-8.80**.

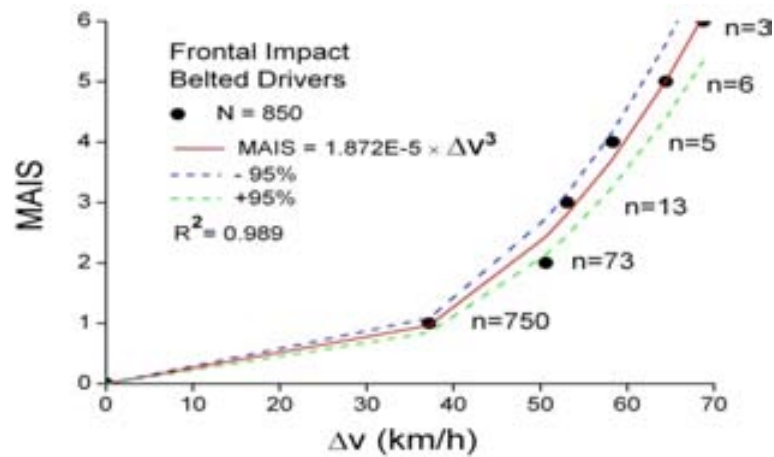


Figure 8.69: MAIS vs Delta-V for frontal impact, belted drivers, for spinal injuries

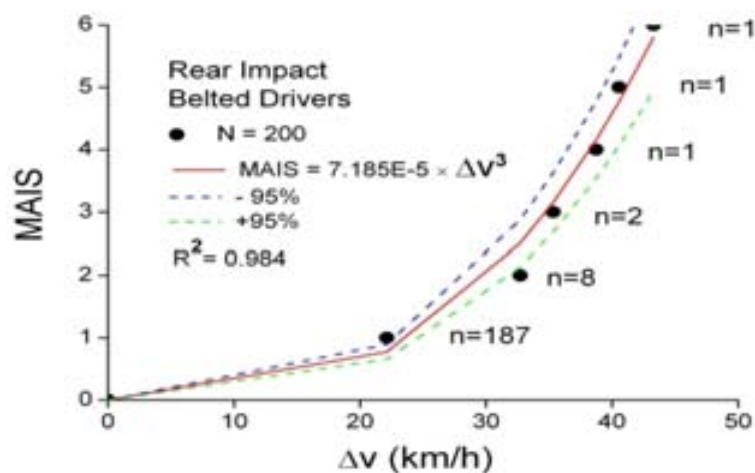


Figure 8.70: MAIS vs Delta-V for rear impact, belted drivers, for spinal injuries

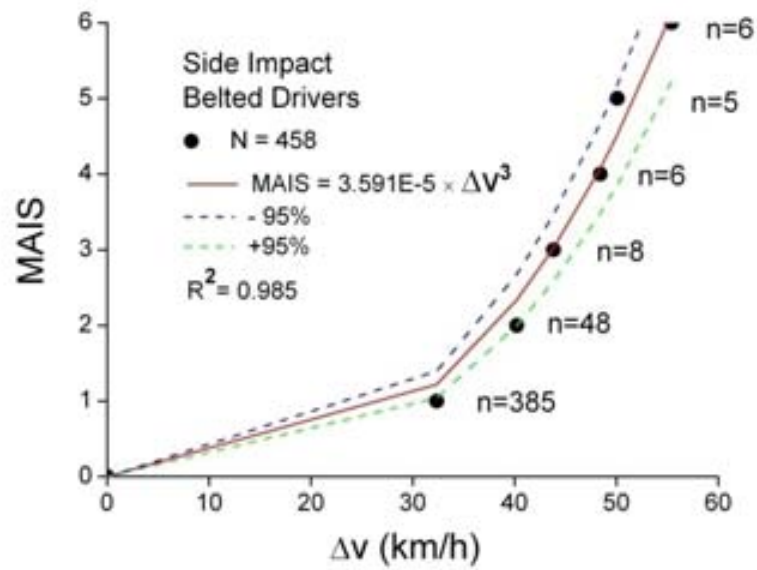


Figure 8.71: MAIS vs Delta-V for side, belted drivers, for spinal injuries

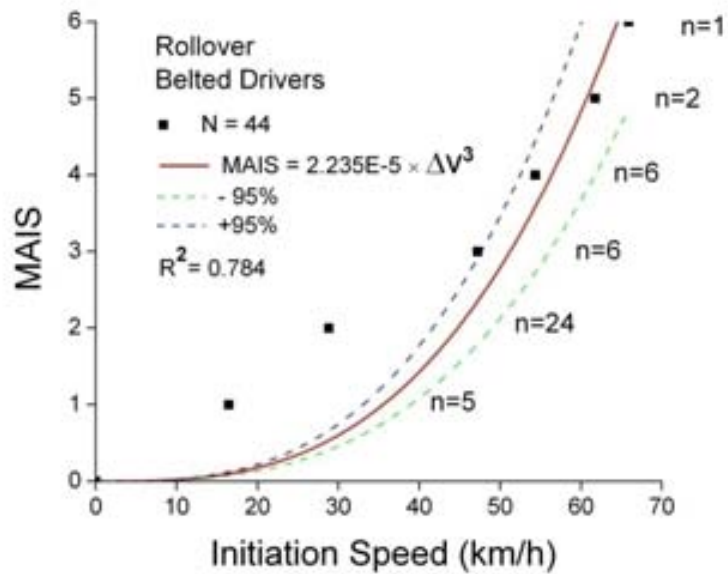


Figure 8.72: MAIS vs Delta-V for rollover, belted drivers, for spinal injuries

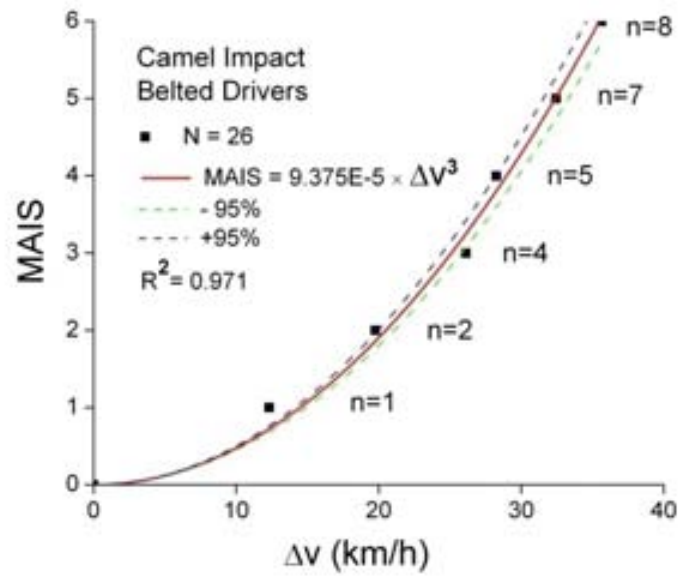


Figure 8.73: MAIS vs Delta-V for camel impact, belted drivers, for spinal injuries

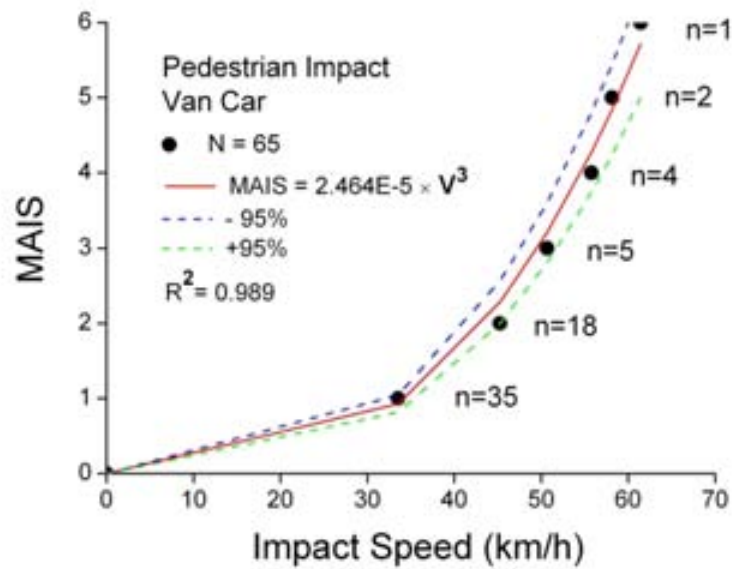


Figure 8.74: MAIS vs impact speed for pedestrians, van cars, for spinal injuries

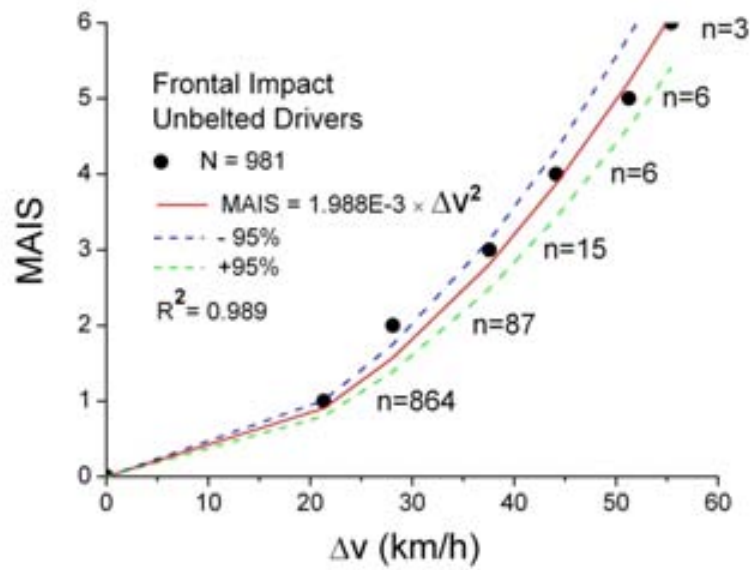


Figure 8.75: MAIS vs Delta-V for frontal impact, unbelted drivers, for spinal injuries

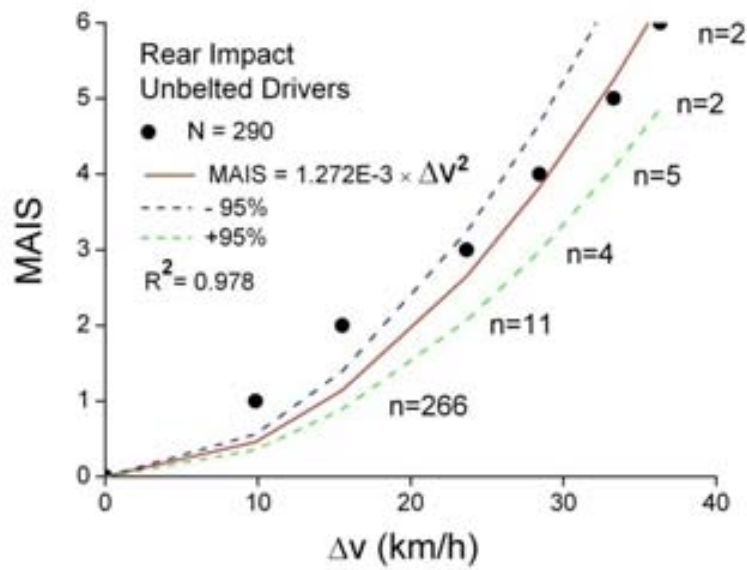


Figure 8.76: MAIS vs Delta-V for rear impact, unbelted drivers, for spinal injuries

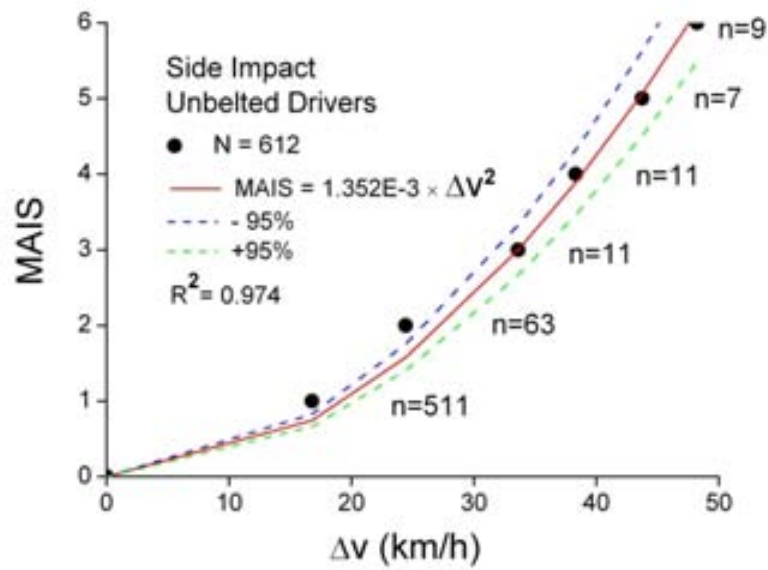


Figure 8.77: MAIS vs Delta-V for side impact, unbelted drivers, for spinal injuries

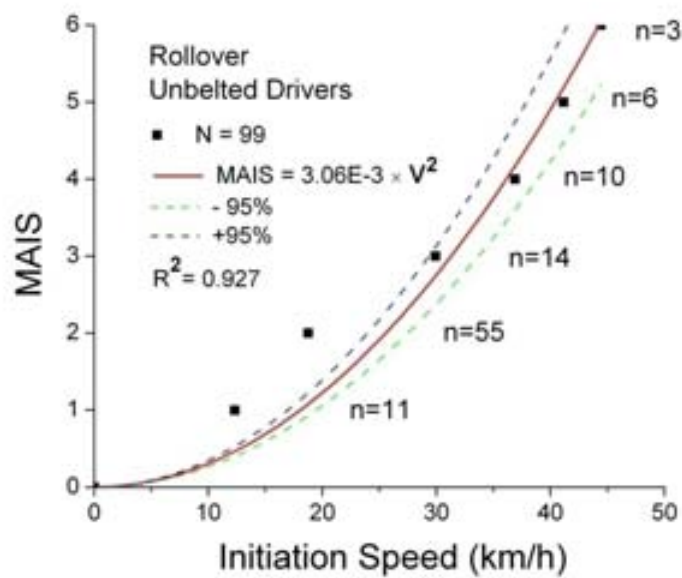


Figure 8.78: MAIS vs Delta-V for rollover, unbelted drivers, for spinal injuries

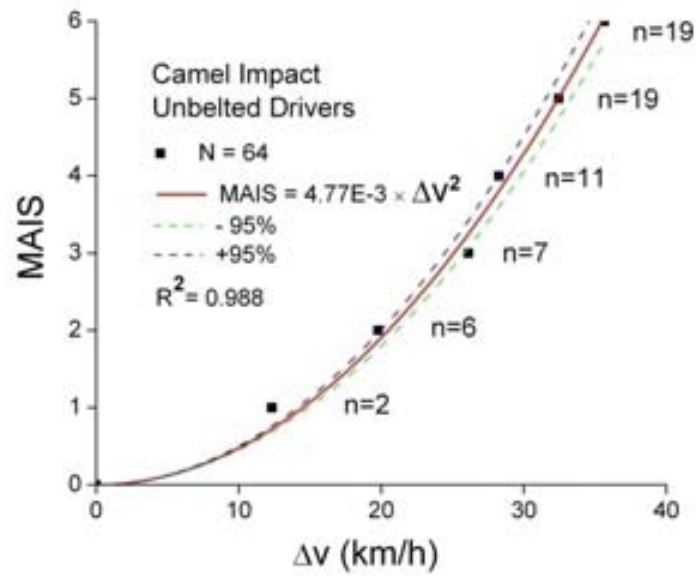


Figure 8.79: MAIS vs Delta-V for camel impact, unbelted drivers, for spinal injuries

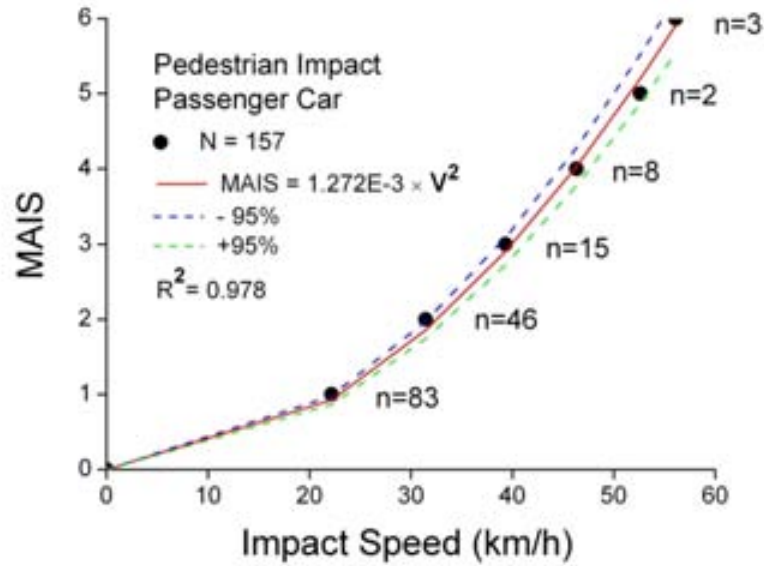


Figure 8.80: MAIS vs impact speed for pedestrians, passenger cars, for spinal injuries

From the relationships shown in **Figures 8.69-8.73**, it appears that ΔV^3 gives the best correlation for belted drivers, whereas for the unbelted drivers (**Figures 8.75-8.79**), the relationships were ΔV^2 . This simply quantifies what is generally observable, that unrestrained occupants suffer higher injury levels at lower ΔV than do restrained occupants, because they are subject to higher Peak Virtual Power (PVP) inputs for a given ΔV . The results of the present study confirm the same conclusion of previous studies by Sturgess (2001).

Also, for pedestrians, it can be seen that the correlation with V^3 is superior for the spinal injuries from van cars (**Figure 8.74**) whereas the correlation with the V^2 model is better for the spinal injuries from passenger cars (**Figure 8.80**). Sturgess et al. (2002) showed that the pedestrian is closely coupled to the vehicle during the injury phase of the contact, for serious and fatal injuries, and less closely coupled for the slight injuries. However, much more in-depth work would need to be done before this hypothesis could be considered proven.

As stated by Sturgess (2001), the high degree of correlation demonstrates that, by making very simple assumptions about idealized impact types, a simple theory can account for 85–90 per cent of the injuries obtained from vehicle collisions. The fact that all injuries require an expenditure of energy means that energy methods are independent of injury mechanisms; therefore, PVP is a good candidate for a universal injury criterion which can be correlated with real-world injury experiences. Furthermore, energy is the only physical quantity that remains unchanged at all scales, and so PVP can be applied at the micro, meso and macro scale.

The next step in this work is to calculate the ΔV which can be given by Eq. (8.1):

$$\Delta V = \vec{V}_{t2} + \vec{V}_{t1} \quad (8.1)$$

Where V_{t1} and V_{t2} are the vehicle velocities before and after the impact respectively.

Table 8.23 shows the estimated ΔV for each case in the simulations and the corresponding injury severity (MAIS) obtained from the previous figures.

Table 8.23: Delta-V measures for different impacts

Type of Impact	Speed (km/h)	ΔV (km/h)	MAIS
Front	27	18.09	1
	80	47.90	2
	120	65.18	5
	160	88.35	6
Rear	27	12.60	1
	80	38.70	4
	120	60.80	6
	160	76.70	6
Side	50	38.52	2
	80	45.54	3
	100	62.10	6
Rollover	48	-	3
Camel	27	25.11	2
	80	36.37	4
	120	55.83	6
Pedestrian	40	-	3

8.9 NECK INJURY CAUSATION ANALYSIS BY PVP

For the following neck injury evaluation, the PVPn (Neck) is based on the acceleration and velocity change of the neck (Sturgess et al., 2001). The PVPn at each intervertebra level can be defined as:

$$\text{PVPn} = F \cdot V + M \cdot \omega \quad (8.2)$$

Where F is the maxim force (N), V is the resultant linear velocity (m/s), M is the bending moment (Nm), and ω is the angular velocity (rad/s). Eq. (8.2) represents the power obtained in transitional and rotational motions at each intervertebral level.

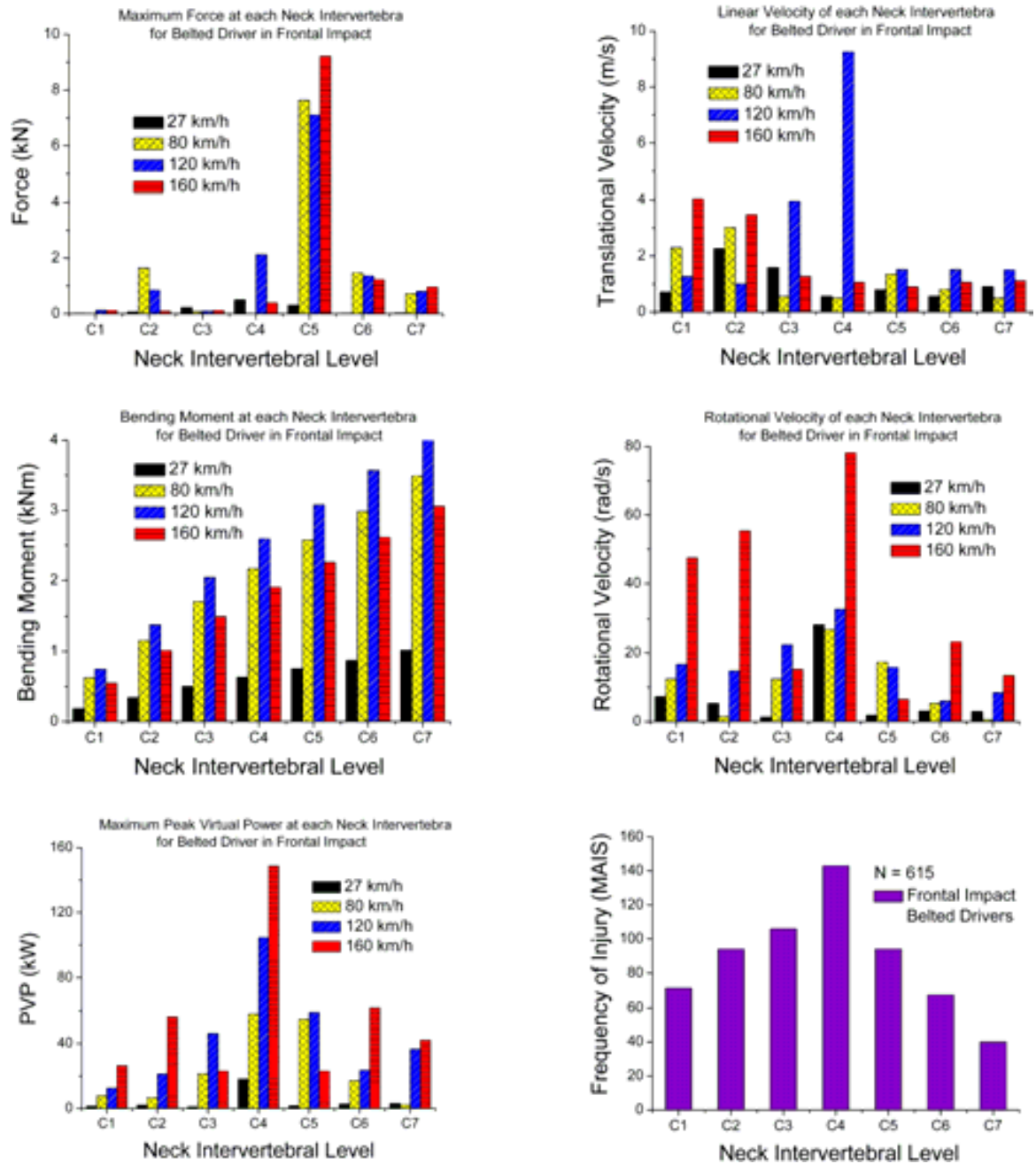


Figure 8.81: PVP for belted driver in frontal impacts

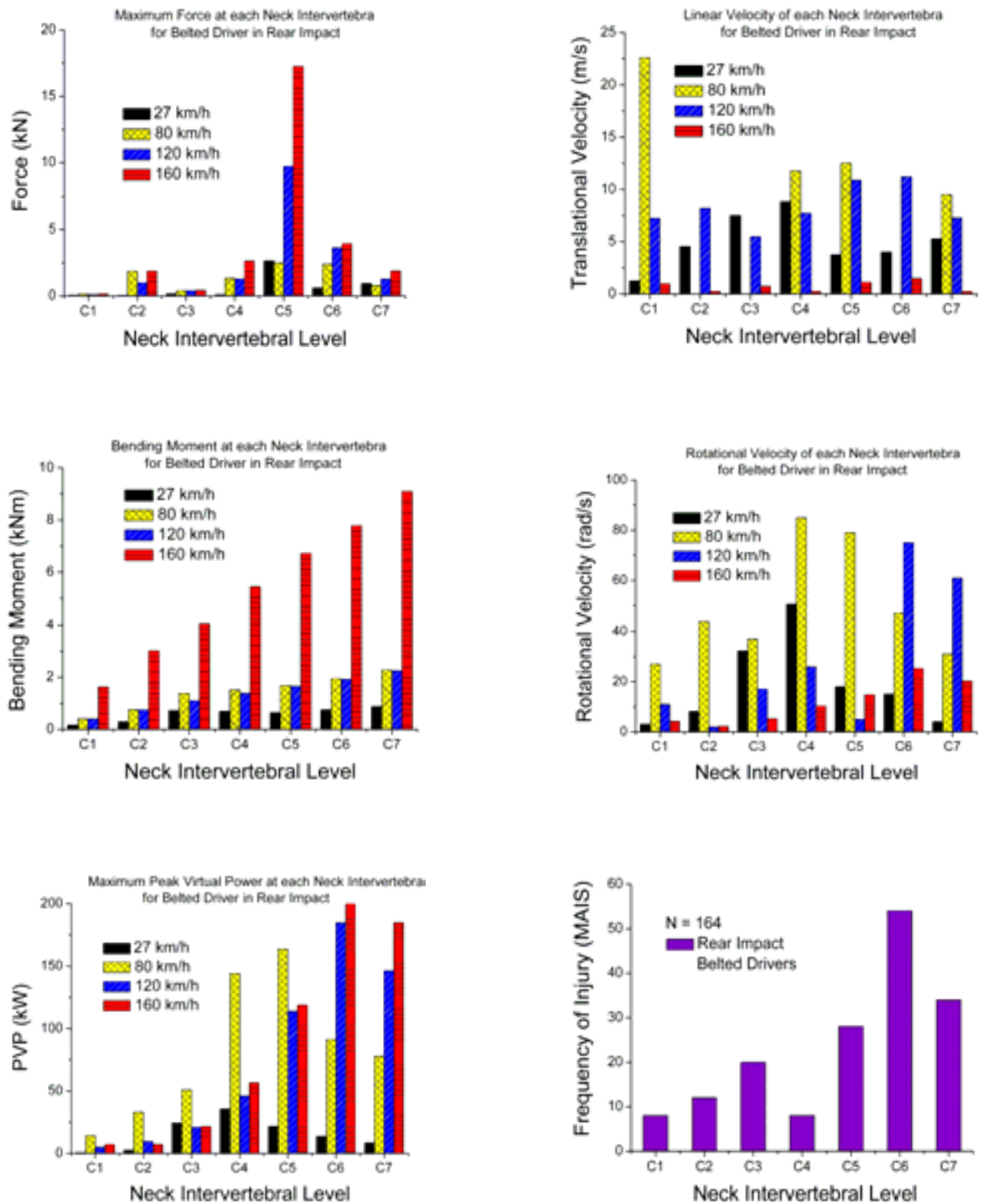


Figure 8.82: PVP for belted driver in rear impacts

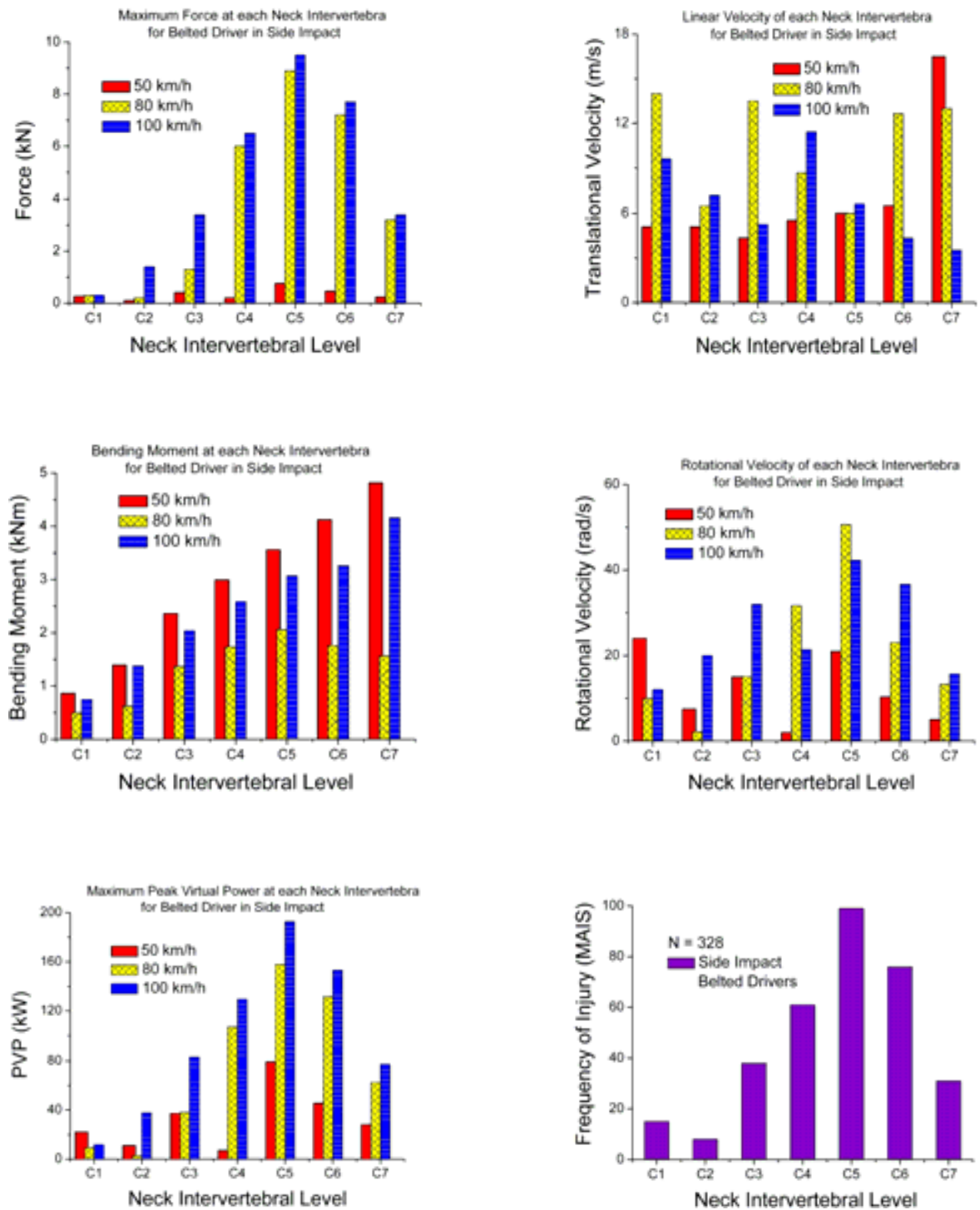


Figure 8.83: PVP for belted driver in side impacts

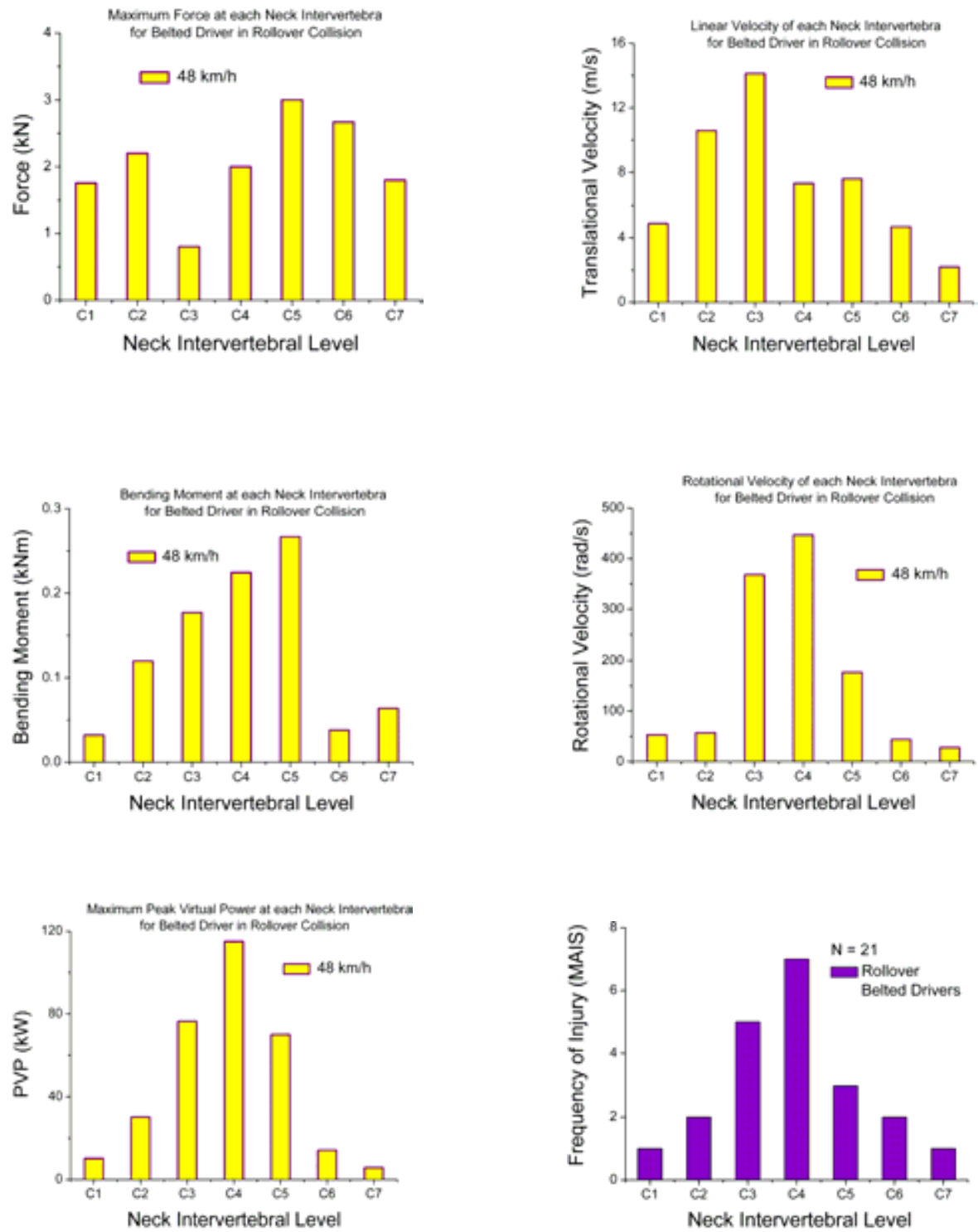


Figure 8.84: PVP for belted driver in rollover collisions

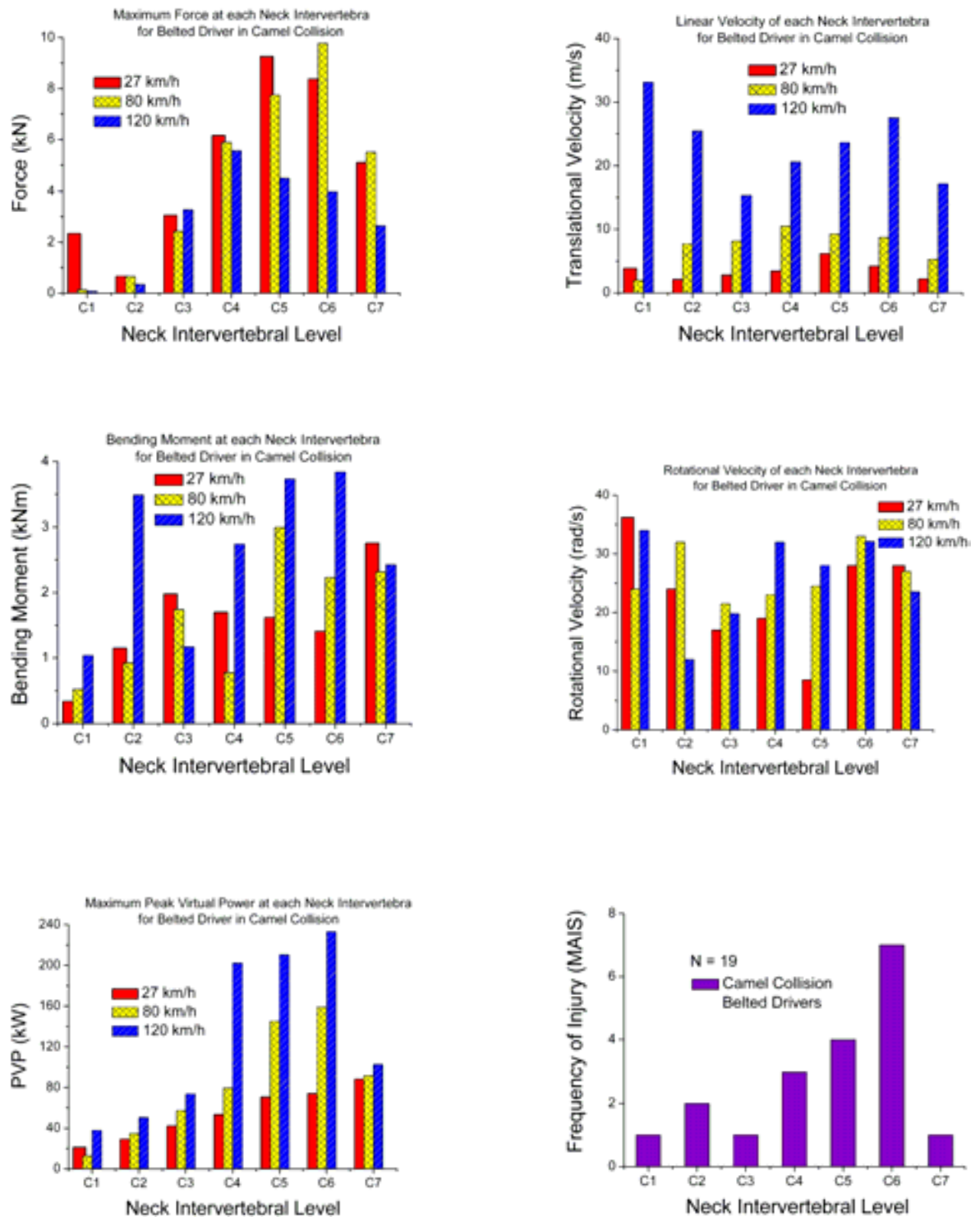


Figure 8.85: PVP for belted driver in camel collisions

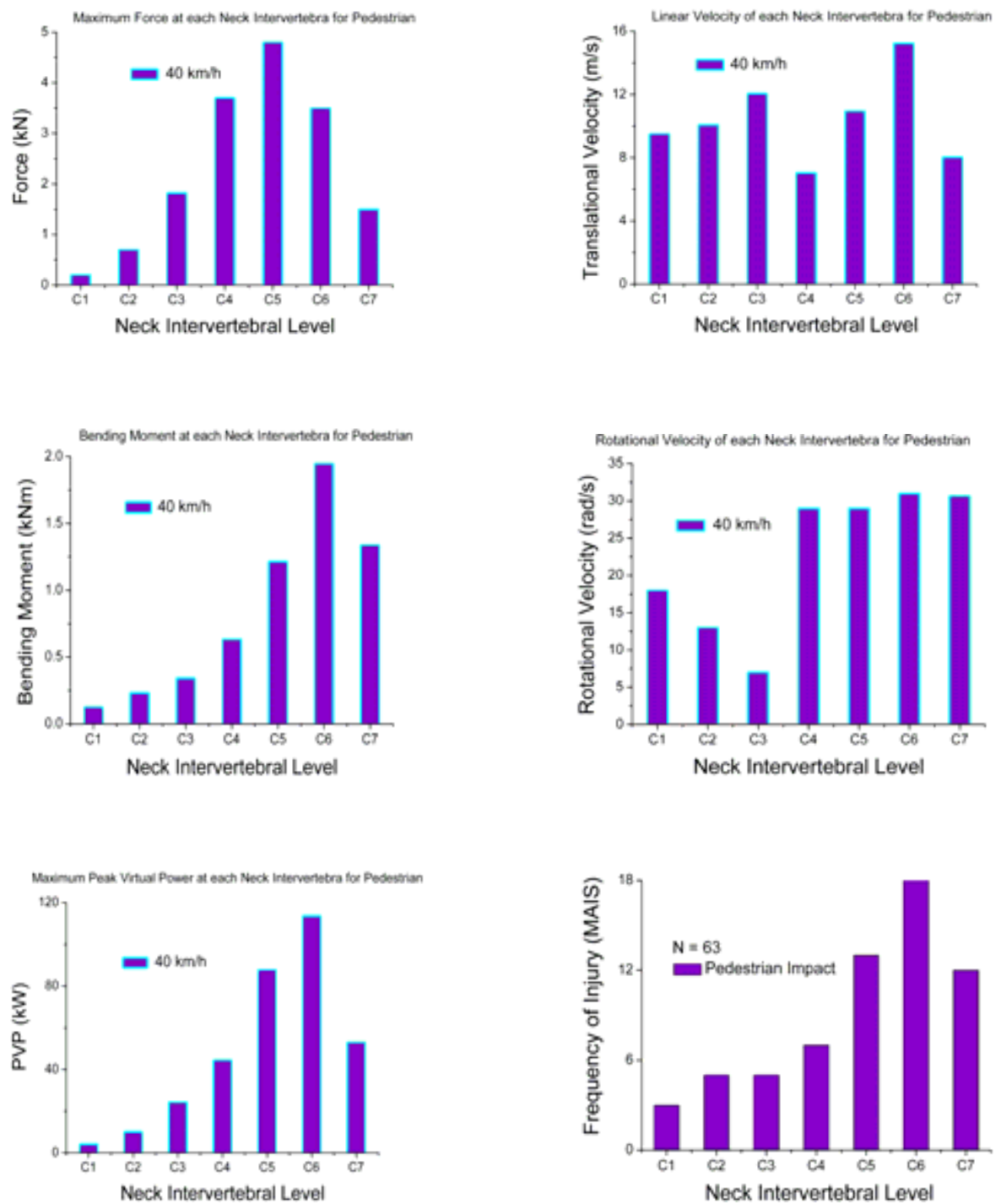


Figure 8.86: PVP for pedestrian impacts

Figures 8.81-86 show the peak virtual power calculations for different collisions using the typical passenger car model in this study. These results are represented for only the cervical spine, since that is the most important region considered in the whiplash injuries and neck injury criteria. In each figure, the first four figures show force, linear velocity, bending moment and angular velocity of each vertebra. The fifth graph shows the PVPn calculated. The last graph shows the incidence of neck injuries at each intervertebral level obtained from field survey of real world crashes in the same orientation.

A comparison of the last two graphs in each figure gives a quantitative comparison between the PVP and the injury likelihood. From the comparison it can be seen that whenever the PVPn is high, the neck injuries increase. The statistical analysis in **Table 8.24** shows that there is a high significant correlation ($P > 0.2$) between the PVP and the likelihood of spinal injury at a particular intervertebral level for the different impacts in the study.

Table 8.24: Statistical tests of PVP-Neck injury correlations (95% CL)

Impact Type	Person χ^2	d.f.	<i>P</i>
Front	35	30	0.243
Rear	35	30	0.266
Side	42	36	0.227
Rollover	28	20	0.260
Camel	26	18	0.310
Pedestrian	32	28	0.256

Figures 8.87 and 8.88 show the PVP and incidences of spinal injury for all the vertebra for two of the scenarios, frontal and rear impacts. In both the cases, it is observed that the cervical region is the most frequently injured region. It can also be seen that the distribution of the PVPn and that of the frequency of injury is similar. This further confirms the correlation between the PVP and the incidence of spinal injury.

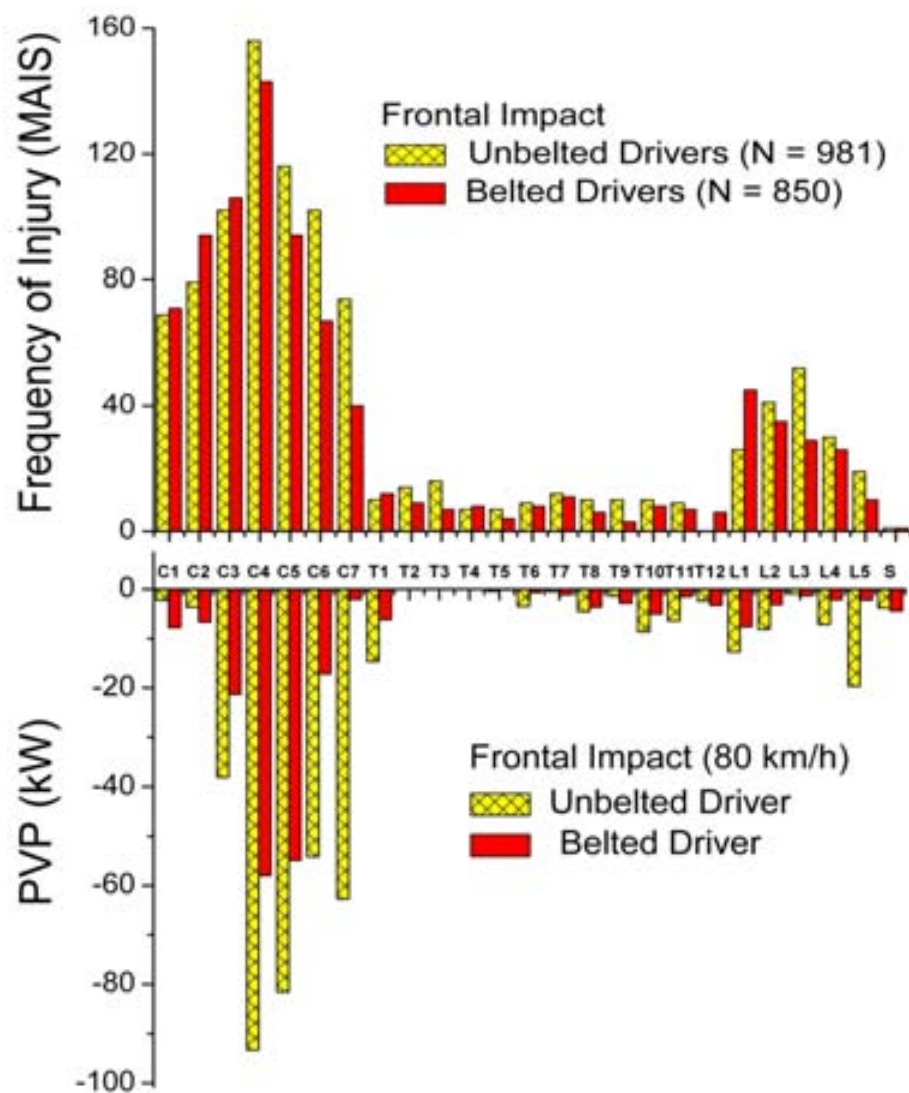


Figure 8.87: Distribution vertebral injuries of crash data vs PVP from simulations for belted and unbelted drives at 80 km/h frontal impact

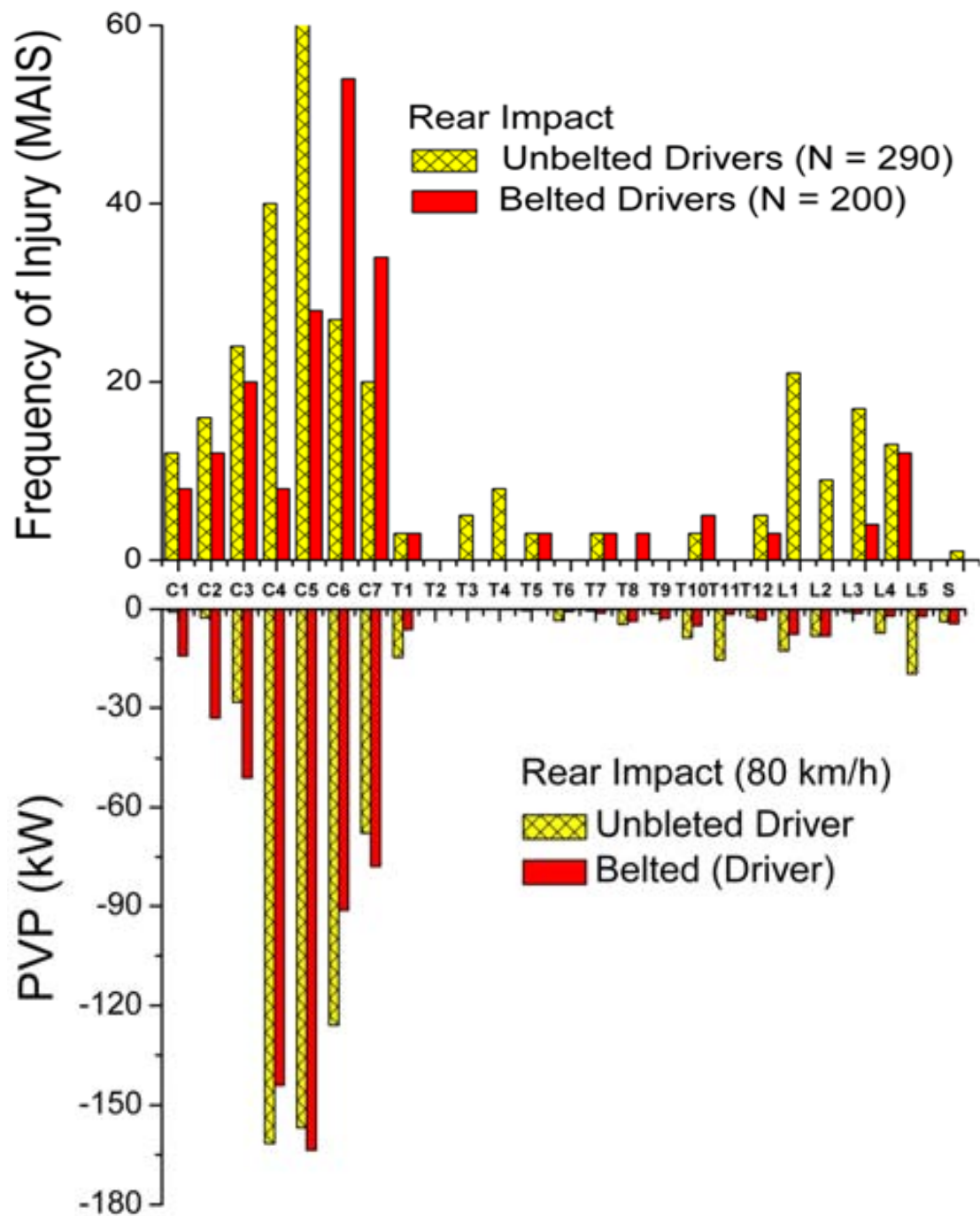


Figure 8.88: Distribution vertebral injuries in crash data vs PVP from simulations for belted and unbelted drives at 80 km/h rear impact

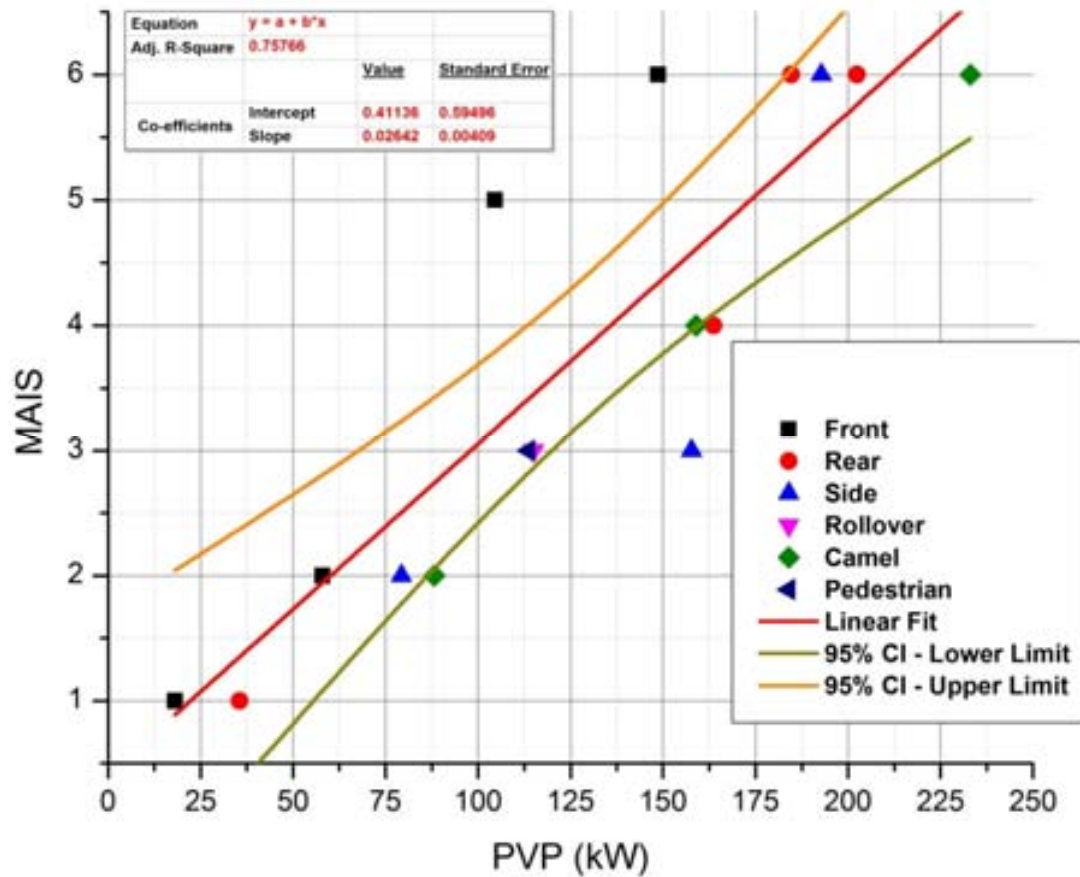


Figure 8.89: PVPn and MAIS based on the simulations

The previous results of the PVPn scores obtained by simulations using a typical passenger car model indicate the neck injury severity well. Besides, based on the “Master PVP Curve” where the MAIS is linearly proportional to PVP, (Sturgess, 2002a) the MAIS of the occupant can be depicted as shown in **Figure 8.89**. The MAIS results achieved from the “Master PVP Curve” indicates the neck injury severity well which shows the PVP is a good indicator of the occupant neck injury.

Also, the relationship between PVPn and N_{ij} was further investigated based on the simulations presented earlier using a typical passenger car model. To get the N_{ij} , forces and moments at the occipital condyle have been calculated according to Eq. (2.2) of **Section 2.2.2**. The critical values of $F_{YC} = 6160$ N and, $M_{ZC} = 310$ Nm (Lee et al., 2003) were used. The probability of neck injury in frontal and rear impacts was conducted based on the injury risk curves developed by Kleinberger et al. (1998). The results of N_{ij} are presented in **Table 8.25**.

Table 8.25: Neck Injury Criteria results for frontal and rear impact simulation

Simulation Case	F_Y (N)	M_{OCZ} (Nm)	N_{ij}	$p(AIS \geq 3)$ (%)
Front collision 28 km/h driver belted	600	164	0.626	7
Front collision 80 km/h driver belted	1800	853	3.04	94
Front collision 120 km/h driver belted	3600	1293	4.75	100
Front collision 160 km/h driver belted	5500	2032	7.44	100
Front collision 28 km/h driver unbelted	650	177	0.67	8
Front collision 80 km/h driver unbelted	1300	712	2.5	83
Front collision 120 km/h driver unbelted	2000	1276	4.44	100
Front collision 160 km/h driver unbelted	4500	2151	7.67	100
Rear collision 28 km/h driver belted	600	252	1.96	56
Rear collision 80 km/h driver belted	2500	762	6.04	100
Rear collision 120 km/h driver belted	9000	904	8.16	100
Rear collision 160 km/h driver belted	15500	1201	11.4	100
Rear collision 28 km/h driver unbelted	600	201	1.58	39
Rear collision 80 km/h driver unbelted	1900	557	4.43	100
Rear collision 120 km/h driver unbelted	4500	761	6.36	100
Rear collision 160 km/h driver unbelted	9800	809	7.6	100

Also, the results of the N_{ij} from the simulations of the frontal and rear impacts are presented graphically in **Figure 8.90**.

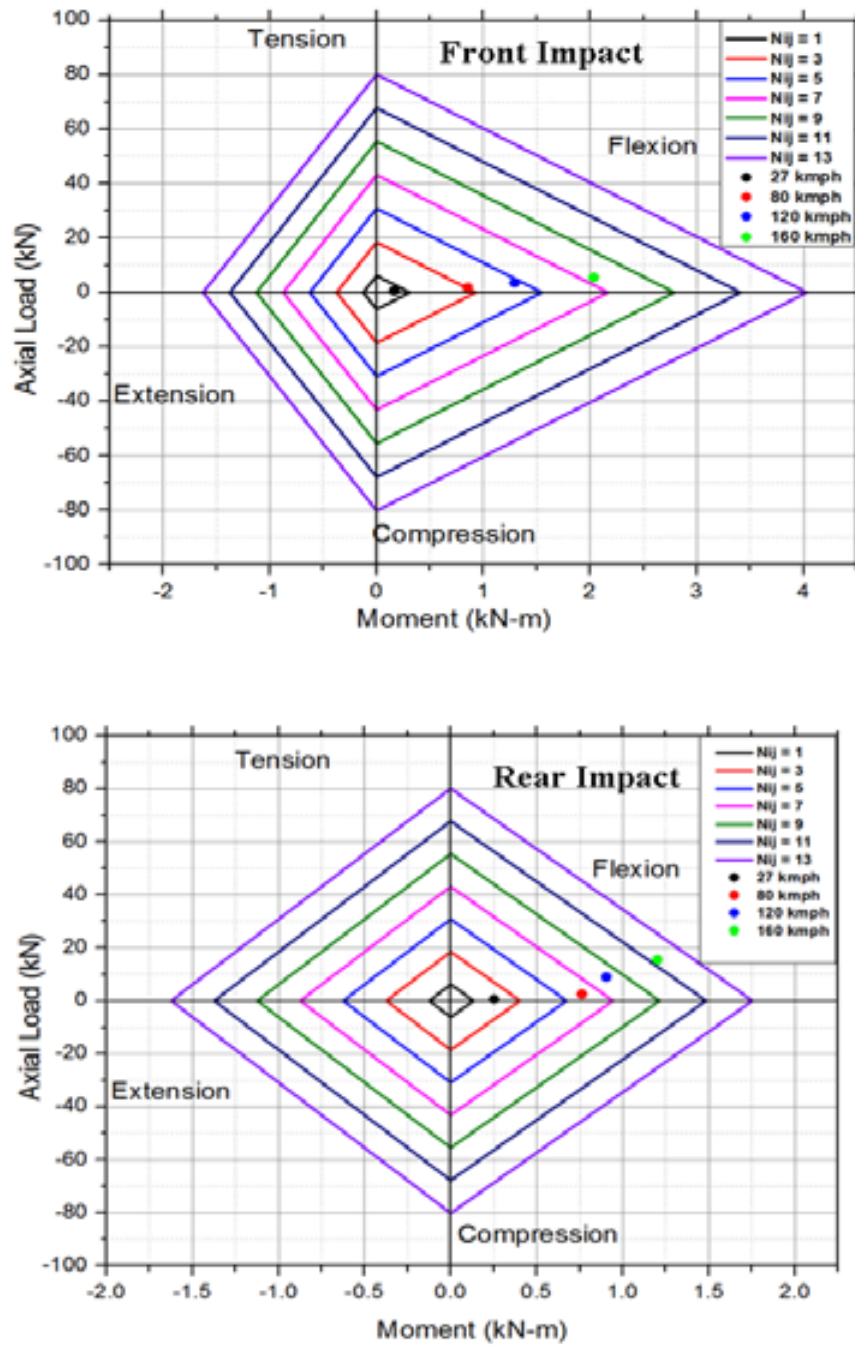


Figure 8.90: Graphical representation of N_{ij} for frontal and rear impacts

The correlation between N_{ij} and PVPn is shown in **Figure 8.91**. The results are very close for frontal impact. For rear impact, PVPn shows a significantly higher likelihood of neck injury at all car speeds more than N_{ij} and requires more research. However, N_{ij} cannot predict the distribution of injury along the spinal column, as is done with PVPn. This is considered to be a major advantage of using PVPn.

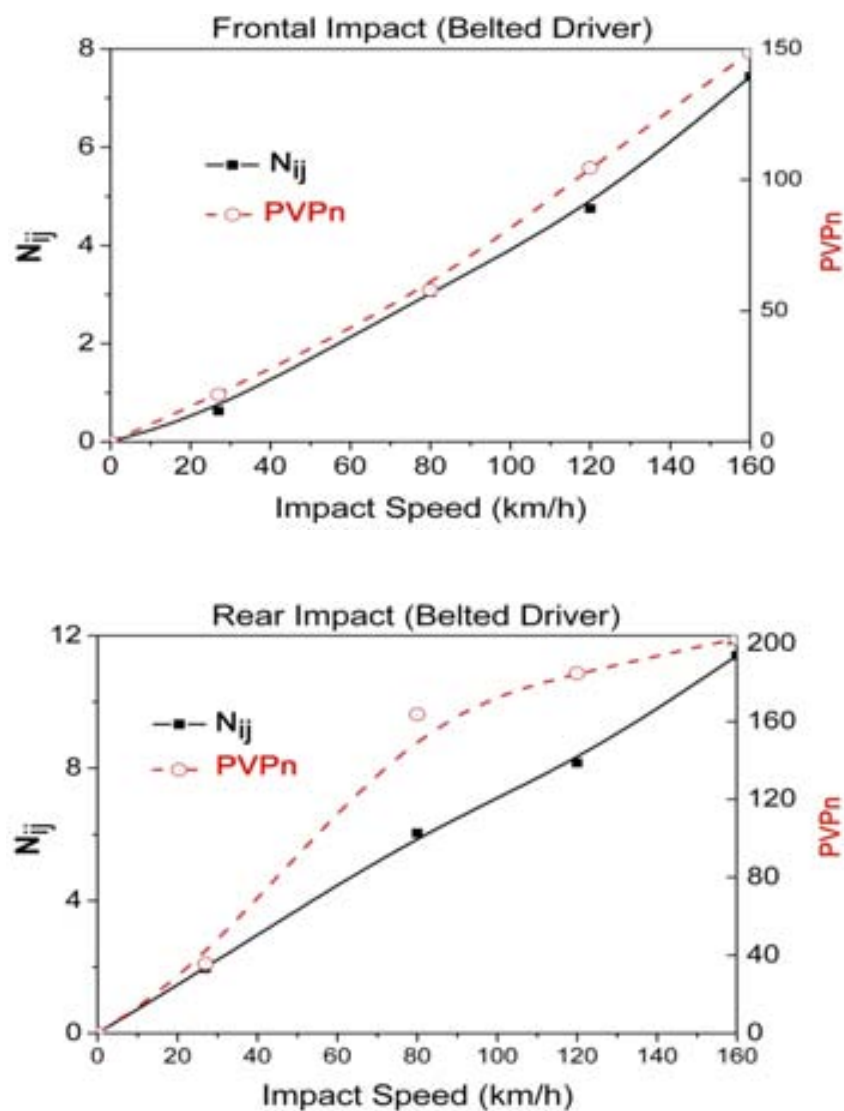


Figure 8.91: The Correlation between N_{ij} and PVPn for frontal and rear impacts

8.10 CONCLUSIONS

Spinal injury mechanism is especially connected with a head motion. Improvement of knowledge about correlation between crash dynamics, human body behaviour and internal cervical phenomena could contribute to the development of new protection systems. The best way to study the behaviour of the human body and internal interactions during car crashes is the mathematical modelling, with the use of latest numerical methods.

In this study, modelling research has been performed on the basis of principles from multibody dynamics, where rigid bodies are connected by articulated joints and spring-damper elements. The models were developed using professional Working Model 2D system, and were used to simulate head-on, rear collisions, side impact and rollover vehicle crashes as well as pedestrian and camel collisions. The following conclusions are reached:

- 1- The current set of simulations have been done using a typical car model. It will be worthwhile to do simulations as well as Full Scale Crash Tests with vehicles specific to the Saudi Arabian context. This will not only help conduct simulations, but would give a deeper insight into causation of neck injuries and will also give more insight into vehicle design issues and contribute to making vehicles in Saudi Arabia safer.
- 2- The kinematic analysis of driver motion reveals that the vertebral accelerations go as high as 75g during frontal impact.
- 3- The analysis demonstrates the efficacy of computer simulations in giving an insight into the injury likelihood of the individual vertebrae.
- 4- For the vehicle occupant, comparison of injury indices for belted and unbelted occupants indicates that the use of the seat belt is effective in reducing injury likelihood in most cases. The injury indices are also observed to increase with speed.

- 5- Pedestrians are seen to be relatively the safest in impacts with passenger cars. However, pedestrian impacts with trucks need additional investigations.
- 6- In camel impacts, it is observed that the most likely source of injury is likely to be the fall of the camel on top of the vehicle, thereby crushing the occupant. Laboratory experiments similar to Saab Moose Test should be conducted in future.
- 7- In an attempt to correlate injuries in these scenarios, it is observed that MAIS correlates best with ΔV^3 for belted drivers, whereas for the unbelted drivers, the relationships were ΔV^2 . This quantifies what is generally observable, that unrestrained occupants suffer higher injury levels at lower ΔV than do restrained occupants, because they are subject to higher PVP for a given ΔV .
- 8- The results show a very good quantitative correlation between the level of PVP and the injury levels in the clinical observations.
- 9- Also the results show a reasonable correlation between N_{ij} and PVP in the frontal impacts. However they diverge for rear impact. This requires more research. Moreover, N_{ij} cannot predict the distribution of injury along the spinal column, as is done with PVPn. This is considered to be a major advantage of using PVPn.
- 10- While the current N_{ij} is limited to only frontal impact, the new PVP measure provides a good prediction for neck injury in different types of impact.
- 11- The study provides evidence that the peak virtual power is a good indicator as to where the spinal injury is.

CHAPTER 9

OVERALL CONCLUSIONS AND FUTURE WORK

In spite of one of the most accident prone societies in the world, little research has been done in Saudi Arabia to identify the gravity of spinal injury related to road traffic accidents and to develop strategies to control them. Therefore, this study has been initiated to investigate the collision characteristics of spinal injuries as well as the simulation of occupant's kinematics during vehicle impacts and the likely mechanisms of spinal injuries.

As this thesis has explored a number of numerous aspects, the main findings and final recommendations for the future work are reviewed in the following sections.

9.1 OVERALL CONCLUSIONS

The fact that a very high percentage of road accidents cause spinal injury, creates an urge for the implementation of measures in order to decrease the number of car accidents in Saudi Arabia. Vehicle crashes-related spinal injuries are largely preventable and predictable. This study provides an attempt to identify most of these risk factors and presents some solutions. The work presents a methodology that has been proposed for collecting crash as well as injury data. While the data needs to be collected on a regular basis at the national level the study presents an insight into the epidemiology of the crashes as well as of spinal injuries.

The study highlighted the circumstances in which different parts of the spine are injured. The cervical spine was particularly prone to deceleration injury and over half of the spinal injuries were in the cervical region, and a significant number of these involved cord damage, and were life-threatening. It was found that seatbelt usage significantly reduced spinal injury severity outcome during the impact. This is expected as in an impact the seatbelt reduces head velocity at time of vehicle contact. This result indicates that a high proportion of spinal injuries in Saudi Arabia can be prevented if the seat belt usage increases.

It was also showed that the most common source of contact for AIS 2 spinal injuries was found to be vehicle interiors, while about a quarter are non-contact type injuries and about a quarter occurred through contact with exterior objects. The study also presents a correlation between likelihood of injury and direction of impact, crash severity (ΔV or ETS) and ejection. Even though, the data is currently not populated enough to understand these correlations completely, the study presents a methodology for data collection and correlation which needs to be implemented on a regular basis at the national level.

After studying the epidemiology of crashes and spinal injuries, a study was conducted at deriving an improved logistic regression model which would relate occupant, vehicle and impact characteristics to the probability of spinal injury based on real-world accidental data.

On the basis of the concept of deviance together with Wald statistic, the significant factors that contribute to the severity of spinal injury were found to be the level of spinal injury, restraint system, impact direction, and ETS. It is clear that these parameters will contribute to the severity of spinal injury from a biomechanical view point. Once this logistic model is strengthened by more data, it may serve as an initial prediction to establish the

severity of spinal injury sustained by occupants at road crash and a paramedic protocol as part of emergency response may be revised according to the developed model.

An analysis of the spinal cord injuries in Saudi Arabia revealed that cervical spine injuries were the most common spine injuries accounting for 38% with an incidence rate of 9.20 per 10^5 population. It was also found that the present average of incidence in Saudi Arabia (38 per million population) was the highest rate ever reported in 85% of the different countries in the world. And, the leading cause of SCI was identified as road traffic accidents, accounting for 63% of all causes. The situation is clearly alarming and warrants immediate attention.

In the current research crash reconstruction technique has been demonstrated as a tool to investigate crashes, to determine their probable cause, and to make recommendations to prevent crashes and/or mitigate the severity of the accidents and resulting injuries. An in-depth investigation for selected four cases of uncommon spinal injuries related to vehicle crashes was also done in the present study. In each of the cases the reconstruction was validated with the crash data available from site, and injuries were correlated with impact locations and injury mechanisms were studied in an attempt to see how these factors could be mitigated. The software reconstruction gave a good insight into the crash/injury mechanisms in the four cases.

A number of measures were identified on the basis of the reconstruction of the crashes. These included the need for installing appropriate traffic signals, modifications in vehicle design, the need of a dedicated emergency number, implementation of side airbags and curtains, roof-mounted side impact airbag in vehicles, ensuring proper seatbelt usage and many others which are detailed in the main body of the study.

Another important aspect studied was the dynamic mechanism of the injury. The behaviour of the human body and internal interactions during car crashes is best studied through mathematical modelling. Rigid body models were developed using Working Model 2D system, and were used to simulate head-on, rear collisions, side impact and rollover vehicle crashes as well as pedestrian and camel collisions and have been validated based on experimental data available in literature. The work has demonstrated how crashes can be simulated to estimate the injury parameters, and the likelihood of injuries on various parts of the body. In these simulations injury parameters like NIC and N_{ij} were computed to study the likelihood of neck injuries. These injury indices have been interpreted in terms of probability of injury to different parts of the body. Neck injuries have also been estimated based on the Peak Virtual Power in the vertebra during the impact as it is postulated that power may be a better estimate of neck injury than other measures.

For the vehicle occupant, it can be concluded that the use of the seat belt is effective in reducing spinal injury likelihood in most cases. Pedestrians are seen to be relatively the safest in impacts with cars. In camel impacts, it is observed that the most likely source of injury is likely to be the fall of the camel on top of the vehicle, thereby crushing the occupant or causing compressive injuries on the spinal column. In general simulations give a very good understanding of the kinematics of the crashes, and the likely mechanisms of injuries. This study has further demonstrated how these simulations can be used to evaluate the efficacy of different safety devices. It must be pointed out that most of vehicle design as well as design of safety devices today is done on the basis of similar computational simulation tools.

9.2 FUTURE WORK

As a conclusion of the foregoing study, the following is strongly recommended:

- i. Data on road accidents and spinal injuries should be collected regularly and in a systematic and scientific manner in the Kingdom of Saudi Arabia.
- ii. A national database for the same should be maintained centrally which can be queried by policy makers, government planners, industrial designers and others.
- iii. Computer simulations give a good insight into the dynamics of the crash and the injury. In order to understand crashes in Saudi Arabia it is proposed that reconstruction should be done regularly as a national activity.
- iv. Computer simulations should be done of the crashes using 3D models of the vehicles, as well as human dummies. These will help understand the injury mechanisms better as detailed Finite Element models would be able to better predict the outcome in the crash.
- v. Use of software like MadymoTM, and LSDynaTM for computer simulations is recommended for understanding crashes and also for optimizing the vehicle designs. Validated models of human dummies in these software would also be an added advantage.
- vi. Non availability of experimental data for using simulations and also for validation is a significant bottleneck in developing simulations. Appropriate testing facilities (full scale as well as Camel Crash Test) should be setup in Saudi Arabia for testing vehicles and their parts.

BIBLIOGRAPHY

1. AAAM (2005) *AIS 2005: The Injury Scale*, Eds. Gennarelli T and Wodzin E, Association of Advancement of Automotive Medicine.
2. AboAbat, A. M. (1999) *Spinal Cord Injury in Saudi Arabia: Characteristics, Bone Mineral Density, and Functional Electrical Stimulation for Upright Mobility*, PhD Thesis, University of Salford, UK.
3. ADA (2006) *The Economic Cost of Road Traffic Accidents in the Kingdom of Saudi Arabia*, The High Commission for the Development of Arriyadh (ADA), Research and Studies Dept., Final Report, Kingdom of Saudi Arabia, Riyadh, March 2006.
4. Agresti A. (2002) *Categorical Data Analysis* (2nd ed.), New York: Wiley.
5. Aits (2003) *Collision Suite, AiDamage3*, Ai Training Services Ltd (www.aitsuk.com), ISBN 5 702231 273076, Birdlip, Glos, UK, December 2003.
6. Al-Amro, S. A., Al-Hathloul, H. H., Al-Gadhi, S. A., Al-Ghamdi, A. S., Sharaf, E., and Al-Qahtani, K. N. (1996) *Study of the Influence of Stray Animals (Camels) on Traffic Safety in Saudi Arabia*, General Directorate of Research Grants Programs, King Abdulaziz City for Science and Technology (KACST), Final Report (Arabic), ART-14-72, Riyadh, Saudi Arabia.
7. Al-Ghamdi, A. S. (1998) *Injury Severity and Duration of Hospital Stay for Urban Road Accidents in Riyadh*, In: Transportation Research Record 1635, TRB, National Research Council, Washington, D.C, 125-132.
8. Al-Ghamdi, A. S. (2003) *Road Analysis of Traffic Accidents at Urban Intersections in Riyadh*, J. Accid Anal Prev, 35 (5): 717-724.
9. Al-Ghamdi, A. S. and Al-Gadhi, S. A. (2004) *Warning Signs as Countermeasures to Camel-Vehicle Collisions in Saudi Arabia*, J. Accid Anal Prev, 36 (5): 749-760.
10. Al-Habardi, A. M. (2000) *The Camels (Al-Eble)*, 1st ed., English, Translated by Murad, A. E., Ottawa, Canada, Al-Habardi Publishing, Al-Khobar, KSA.

11. Al-Shammari, N. K. (2008a) *Post Impact Care of Traumatic Spinal Injury From Road Crashes In Kingdom of Saudi Arabia*, Grant No. RCS-72-2007-DD-1, Prince Salman Center for Disability Research (PSCDR), Riyadh, Saudi Arabia, August 2008.
12. Al-Shammari, N. K.; Bendak, S., Al-Gadhi, S. (2010b) *In-Depth Analysis of Pedestrian Crashes in Riyadh*, J. Traffic Inj Prev, 10 (6): 552-559, 20 November 2010.
13. Al-Shammari, N. K.; Hassan, A. M.; Neal-Sturgess, C. E.; Al-Mejrad, A. S. (2010a) *Mechanism of Spinal Injuries Sustained by Drivers of Passenger Cars during Collisions with Camels*, In the Proceedings of the 6th World Congress on Biomechanics 2010, Singapore, 1-6 August 2010.
14. Al-Shammari, N. K.; Neal-Sturgess, C. E.; Hassan, A. M.; Al-Mejrad, A. S. (2008b) *Modeling Human Body Movement in Road Accidents and Consequences for the Cervical Spine*, In the Proceedings of the Saudi International Innovation Conference (SIIC-2008), 93-97, University of Leeds, Leeds, UK, Jun 9-10 2008.
15. Anderson, PA.; Henley, MB.; Rivara, FP.; and Maier, RV. (1991) *Flexion Distraction and Chance Injuries to the Thoracolumbar Spine*, J Orthop Trauma, 5: 153-160.
16. Anderson, PS., and Montesano, XP. (1988) *Morphology and Treatment of Occipital Condyle Fractures*, 13: 731-836, Spain.
17. ANSI (1996) *Manual on Classification of Motor Vehicle Traffic Accidents*, American National Standards Institute, Inc., D16.1, 6th ed, USA.
18. Asbridge, M., Poulin, C., Donato, A. (2005) *Motor Vehicle Collision Risk and Driving Under the Influence of Cannabis: Evidence from Adolescents in Atlantic Canada*, Accident Analysis and Prevention, 37 (6): 1025–1034.
19. ASIA (2002) *International Standards for Neurological Classification of SCI Revised*, <http://www.asia-spinalinjury.org/publications/store.php>
ASME, 124, No. 5, 504-511.
Available at <http://ntl.bts.gov/lib/17000/17800/17880/PB2001104885.pdf>,
20. Backaitis (ed) (1995) *Biomechanics of Impact Injuries and Human Tolerance of the Abdomen, Lumbar Spine, and Pelvis Complex*, Publication PT-47, SAE, Warrendale, PA.

21. Balavich, KM; Nayef, A. (2002) *Dummy Head Kinematics in Tripped Rollover Tests and a Test Method to Evaluate the Effect of Curtain Airbag Deployment*, SAE 2002-01-0690.
22. Bell, C. (1817) *Surgical Observations*, Middlesex Hosp J; 4:469-470.
23. Bendak, S. (2005) *Seat Belt Utilization in Saudi Arabia and its Impact on Road Accident Injuries*, J. Accid Anal Prev, 37: 367-371.
24. Bertholon, N.; Robin, S.; LeCoz, J.; Potier, P.; Lassau, J.; and Skalli, W. (2000) *Human Head and Cervical Spine Behavior During Low-Speed Rear-End Impacts: PMHS Sled Tests with a Rigid Seat*, In International IRCOBI Conference on the Biomechanics of Impacts, IRCOBI, 265-277.
25. Bostrom, O.; Svensson, M.; Aldman, B., Hansson, H.; Haland, Y.; Lovsund, P.; Seeman, T.; Suneson, A.; Saljo, A.; and Ortengren, T. (1996) *A New Neck Injury Criterion Candidate Based On Injury Findings In The Cervical Spinal Ganglia After Experimental Neck Extension Trauma*, Proc. IRCOBI Conf., 123-136
26. Camacho, D. L.; Nightingale, R. W.; Robinette, J. J.; Vanguri, S. K.; Coates, D. J.; and Myers, B. S. (1997) *Experimental Flexibility Measurements for the Development of a Computational Head-Neck Model Validated for Near-Vertex Head Impact*, Proceedings of the 41st Stapp Car Crash Conference, Society of Automotive Engineers, SAE Paper No. 973345, 473-486.
27. Campbell, B. J. (1966) *A Review of ACIR Findings*, In Proceedings of the Eighth Stapp Car Crash and Field Demonstration Conference.
28. Campbell-Kyureghyan N., Jorgensen M., Burr D., and Marras W. (2005) *The Prediction of Lumbar Spine Geometry: Method Development and Validation*, Clinical Biomechanics, 20: 455-464.
29. CDSI (1970-2010) *The Statistical Year Book, 1391-1430 AH (1970-2010 AD)*, Central Department of Statistics and Information, Ministry of Economy and Planning, Kingdom of Saudi Arabia, Riyadh.
30. Chance, GQ. (1948) *Note on A Type of Flexion Fracture of the Spine*, Br J Radiol, 21:452-453.

31. Chou, C.C.; McCoy, R.W.; and Le, J. (2005) *A Literature Review of Rollover Test Methodologies*, Int. J. Vehicle Safety, 1: 200-237.
32. Coley, G. (2004) *Modeling of Real-World Pedestrian Accidents*, PhD Dissertation, M0445281BU, University of Birmingham, Birmingham, UK, June 2004.
33. Conroy, C.; Hoyt, DB.; Eastman, AB.; Erwin, S.; Pacyna, S.; Holbrook, TL.; Vaughan, T.; Sise, M.; Kennedy, F.; Velky, T. (2006) *Rollover crashes: predicting serious injury based on occupant, vehicle, and crash characteristics*, Accid Anal Prev., 38(5):835-42, Sep 2006.
34. Cooper, R.; Cardan, C.; and Allen, R. (2001) *Computer Visualization of the Moving Human Lumbar Spine*, Computers in Biology and Medicine, 31, 451-469.
35. Cramer, D. (2003) *Advanced Quantitative Data Analysis* (Understanding Socialresearch), Open University Press; 1st ed., ISBN 978-0335200597, Berkshire, UK, July 2003.
36. Cuerden, R.W.; and Hassan, A.M. (1997) *Injury Patterns in Pedestrian Accidents and the Associated Methodology or Real World In-Depth Studies*, Pedestrian Safety, Automotive Environmental Impact and Safety, Proceedings Autotech '97 Conference, NEC, Birmingham, 4-6 November, IMechE Seminar Publication.
37. Cushman, LA.; Good, RG. ; States, JD. (1991) *Characteristics of Motor Vehicle Accidents Resulting in Spinal Cord Injury*, Accid Anal Prev., 23:557-560.
38. Dargay, J.; and Gately, D. (1999) *Transportation Research A* 33, 101.
39. Dauvilliers, F.; Bendjellal, F.; Weiss, M.; Lavaste, F.; and Tarriere, C. (1994) *Development of a Finite Element Model of the Neck*, Proceedings of the 38th Stapp Car Crash Conference, Society of Automotive Engineers, SAE Paper No. 942210, 77-91.
40. De Jager, M. K J. (1996) *Mathematical Head-Neck models for Acceleration Impacts*, PhD Thesis, Technical University of Eindhoven.
41. De Zee, M.; Hansen, L.; Andersen, T. B; Wong, C.; Rasmussen, J.; and Simonsen, E. B. (2003) *On the Development of a Detailed Rigid-Body Spine Model*, Proceedings of International Congress on Computational Bioengineering, Spain, pp 5.

42. Deng, Y. C.; and Goldsmith, W. (1987) *Response of a Human Head, Neck, Upper-Torso Replica to Dynamic Loading-II Analytical/Numerical Model*, Journal of Biomechanics, 20 (5): 471-486.
43. Denis, F (1983) *The Three Column Spine and its Significance in the Classification of Acute Thoracolumbar Spine Injuries*, Spine 8: 817-831.
44. Dietrich, M.; Kedzior, K.; and Zagrajek, T. (1991) *A Biomechanical Model Of The Human Spinal System*, Proceedings of the Institution of Mechanical Engineers, Part H: Journal of Engineering in Medicine, 205 (1): 19-26.
45. DSD (2006) *PC-Crash - A Simulation Program for Vehicle Accidents*, User's Manual, Version 7.0, English, Linz, Austria, October 2006.
46. EEVC (1994) *European Enhanced Vehicle-Safety Committee Working Group 10 Report - Proposals for Methods to Evaluate Pedestrian Protection for Passenger Cars*, European Experimental Vehicles Committee.
47. EEVC (1998) *European Enhanced Vehicle-Safety Committee Working Group 17 Report - Improved Test Methods to Evaluate Pedestrian Protection Afforded by Passenger Cars*, European Enhanced Vehicle-Safety Committee.
48. EEVC (2001) *European Enhanced Vehicle-Safety Committee Working Group 13 Report*, Head Contacts in Side Impact - An Accident Analysis, February 2001.
49. Esat, V.; and Acar, M. (2007) "A Multi-Body Model of the Whole Human Spine for Whiplash Investigations", Proceedings of 20th ESV - Enhanced Safety of Vehicles Conference (ESV 2007), DOT- HS 810 736, Paper No: 07-0437, Lyon, France, pp 7.
50. ESID (1996) *European Side Impact Directive 96/27/EC*, Plascore Deformable Barrier, available: http://www.plascore.eu/pdf/crash_layered.pdf, accessed 17 Sep 2008.
51. Ewing, C. L.; Thomas, D. J.; and Lustick, L. (1977) *Dynamic Response of the Human Head and Neck to +Gy Impact Acceleration*, In Proceedings of the 21st Stapp Car Crash Conference, Society of Automotive Engineers, 547-586.
52. Ewing, C. L.; and Thomas, D. J (1972) *Human Head and Neck Response to Impact Acceleration*, Monograph 21 USAARL 73-1, Naval Aerospace and Regional Medical Centre, Pensacola.

53. Feinberg, S. (1980) *The Analysis of Cross-Classified Categorical Data*, MIT Press, Cambridge, MA.
54. Gabler, HC.; Hampton, C.; and Roston, T. (2003) *Estimating Crash Severity: Can Event Data Recorders Replace Crash Reconstruction?*, Proceedings of the 18th International Conference on Enhanced Safety of Vehicles, May 19-22, pp 490.
55. Gardner-Morse, M. G.; and Stokes, I. A. F. (2004) *Structural behaviour of human lumbar spinal motion segments*, Journal of Biomechanics, 37: 205-212.
56. Garrett, M. (1997) *Head Impact Modelling using the MADYMO Simulations of Documented Pedestrian Accidents*, Proceedings of the 1997 Australian MADYMO Users Group Meeting, Melbourne.
57. GTZ (2005) *Saudi Arabian National Transportation Study*, Deutsche Gesellschaft fuer Technische Zusammenarbeit, SANTRAPLAN-3, Volume 1, Transport Sector Analysis, Part 2: Surface Transport – Roads, 68-90, *Ministry of Economy and Planning*, Final Report , Kingdom of Saudi Arabia, Riyadh, October 2005.
58. Haddon, W., Jr. (1968) *The Changing Approach to the Epidemiology, Prevention, and Amelioration of Trauma: The Transition to Approaches Etiologically Rather than Descriptively Based*, American Journal of Public Health, 58: 1431-1438.
59. Haddon, W., Jr. (1999) *The Changing Approach to the Epidemiology, Prevention, and Amelioration of Trauma: the transition to approaches etiologically rather than descriptively based*, Inj. Prev. 5 (3): 231-5.
60. Halidin, P. H.; Brolin, K.; Kleiven S.; Von Hoist, H.; Jakobsson, L.; and Palmertz, C. (2000) *Investigation of Conditions That Affect Neck Compression-Flexion Injuries Using Numerical Techniques*, Stapp Car Crash Journal, 44: 127-138.
61. Hassan, A. M.; and Mackay, M. (1996b), *Single Vehicle Accidents With Fixed Objects*, In Proceedings of the 2nd Malaysian Road Conference, Kuala Lumpur, Malaysia, 365-374.
62. Hassan, A. M., Mackay, M., Foret-Bruno, J. Y., Huere, J. F. and Langweider, K. (2001) *Influence of Intruder Resistance Glazing on Ejection and Entrapment*, Presented at the IRCOBI Conference, Isle of Man, October 2001.

63. Hassan, A. M.; Parkin, S.; and Mackay, G. (1996a) *Spinal Injuries: In Car Collisions, 40th Proceedings of the Association for the Advancement of Automotive Medicine*, Vancouver, Canada, October 9-11.
64. Hassan, A. M.; and Al-Shammari, N.K. (2009) *Investigation of Road Traffic Accident Disaster*, Internal Symposium on Disasters Management, Riyadh, KSA, Oct 3-6 2009.
65. Hassan, A.M.; Cuerden, R.W.; and Mackay, M. (1997) *Cervical Spine Injury Not Caused by Head Contact.*, Proceedings 41st Association for the Advancement of Automotive Medicine Conference, Orlando, Florida, 10-11 November 1997.
66. Heitplatz, F.; Sferco, R.; Fay, P.; Reim, J.; Kim, A.; and Prasad, P. (2003): *An Evaluation of Existing and Proposed Injury Criteria with Various Dummies to Determine their Ability to Predict the Levels of Soft Tissue Neck Injury Seen in Real World Accidents*, Proc. 18th ESV Conference.
67. Hooper, T.I.; DeBakey, S.F.; Bellis, K.S.; Kang, H.K.; Cowan, D.N.; Andrew, E.L.; and Gackstetter, G.D. (2006) *Understanding the Effect of Deployment on the Risk of Fatal Motor Vehicle Crashes: A Nested Case–Control Study of Fatalities in Gulf War Era Veterans, 199-1995*, Accident Analysis and Prevention, 38 (3): 518-525.
68. Hosmer, D. W; Lemeshow, S. (1989) *Applied Logistic Regression*. New York: Wiley.
69. Howland, W. J; Curry, J. L.; Buffington, C. B. (1965) *Fulcrum Fractures of the Lumbar Spine*. JAMA, 193: 240–241.
70. Huang, Y.; King, A.; and Cavanaugh, J. M. (1994) *FE Modeling of Gross Motion of Human Cadavers in Side Impact*, Proceedings of the 38th Stapp Car Crash Conference.
71. Huelke, D.F.; Ostrom, M.; Mackay, G.M.; and Morris, A.P. (1993) *Thoracic and Lumbar Spine Injuries and Lap-Shoulder Belt*; SAE International Congress and Exposition: Frontal impact protection: Seat Belts and Air Bags: 49-57.
72. IIHS (2005) *Crashworthiness Evaluation Side Impact Crash Test Protocol (version IV)*, Insurance Institute for Highway Safety (www.IIHS.org), August 2005.
73. IIHS (2008) *Frontal Offset Crashworthiness, Evaluation Offset Barrier Crash Test Protocol (version XIII)*, Insurance Institute for Highway Safety, May 2008.
74. IRF (2010) *The International Road Federation, World Road Statistics 2010*, Data 2002-2007, Geneva, Switzerland.

75. IRTAD (2009) *International Traffic Safety Data And Analysis Group*, Annual Report, OECD/ITF 2010, available: www.irtad.net, accessed 17 Oct 2010.
76. Ishaque, M. M.; Noland, R. B. (2006) *Making Roads Safe for Pedestrians or Keeping them out of the Way?* An historical perspective on pedestrian policies in Britain, *The Journal of Transport History*, 27(1): 115-137, March 2006.
77. Ishikawa, H.; Kajzer, J.; Schroeder, G. (1993) *Computer Simulation of Impact Response of the Human Body in Car-Pedestrian Accidents*, SAE Paper No.933129, 37th Stapp Car Crash Conference, November 1993.
78. Ishikawa, Y.; Shimada, Y.; Iwami, T.; Kamada, K.; Matsunaga, T.; Misawa, A.; Aizawa, T.; and Itot, E. (2005) *Model Simulation for Restoration of Trunk in Complete Paraplegia by Functional Electrical Simulation*, Proceedings of IFESS05 Conference, Montreal, Canada.
79. Jiang, C. (2008) *Head Injury Causation in Car Rollover Crashes*, PhD Dissertation, M0445281BU, University of Birmingham, Birmingham, UK, April 2008.
80. Jost, R.; and Nurick, G. N. (2001) *Finite Element Simulation of Biomechanical Response of the Human Body Subjected to Lateral Impact*, *International Journal of Crashworthiness*, 6 (1): 123-133.
81. Kaplan, F. S. (1995) *Prevention and Management of Osteoporosis*, *Clinical Symposia*, 47 (1), Ciba-Ceigy.
82. Kaushik, V.; Kelly, F.; Richards, SD.; Saeed, SR. (2002) *Isolated Unilateral Hypoglossal Nerve Palsy after Minor Head Trauma*, *Clin Neurol Neurosurg*, 105: 42–7.
83. Kleinberger, M.; Sun, E.; Eppinger, R. (1998) *Development of Improved Injury Criteria for the Assessment of Advanced Automotive Restraint Systems*, National Highway Traffic Safety Administration, September 1998.
84. Kleinberger, M. (1993) *Application of Finite Element Techniques to the Study of Cervical Spine Mechanics*, Proceedings of the 37th Stapp Car Crash Conference, San Antonio, TX, 261-272.

85. Klinich, K. D.; Saul, R. A.; Auguste, G.; Backaitis, S.; Kleinberger, M (1996): *NHTSA Child Injury Protection Team, Techniques for Developing Child Dummy Protection Reference Values*, NHTSA Docket No. 7414.
86. Lau, I. V.; and Viano, D. C. (1986) *The Viscous Criterion: Bases and Applications of an Injury Severity Index for Soft Tissues*, In 13th Stapp Car Crash Conference, Society of Automotive Engineers, Warrendale, Pennsylvania.
87. Lee, J.; Yoon, K.; Park, G. (2003) *A Study on Occupant Neck Injury in Rear End Collisions*, J Automobile Engineering, Vol. 217, Part D.
88. Lee, M.; Kelly, D. W.; and Steven, G. P. (1995) *A Model Of Spine, Ribcage And Pelvic Responses To A Specific Lumbar Manipulative Force In Relaxed Subjects*, Journal of Biomechanics, 28(11): 1403-1408.
89. Linder, A.; Clark, A.; Douglas, C.; Fildes, B.; Yang, J.; Sparke, L (2005) *Mathematical Modeling of Pedestrian Crashes: Review of Pedestrian Models and Parameter Study of the Influence of the Sedan Vehicle Contour*, Monash University, Accident Research Centre, Victoria, Australia.
90. Liu, Y. K (1986) *Finite Element Modeling of the Head and Spine*, Mechanical Engineering, 108(1): 60-64.
91. Lizee, E.; Robin, S.; Song, E.; Bertholon, N.; LeCoz, J. Y.; Besnault, B; and Lavaste, F. (1998) *Development of a 3D Finite Element Model of the Human Body*, Proceedings of the 38th Stapp Car Crash Conference, 115-138.
92. Mackay, M.; and Hassan, A. M. (2000) *Age and Gender Effects on Injury Outcome for Restrained Occupants in Frontal Crashes: A Comparison of UK and US data Bases*, In: *Proceedings of the Association for the Advancement of Automotive Medicine Conference*, Chicago, IL, USA, 2 - 4 October 2000, pp 75-91.
93. Mackay, G. M.; Galer, M. D.; Ashton, S. J. and Thomas, P. (1985) *The Methodology of In-Depth Studies of Car Crashes in Britain*, SAE Technical Paper Number 850556, Society of Automotive Engineers.
94. Magerl, F.; Aebi, M.; Gertzbein, SD.; Harms, J.; Nazarian, S. (1994) *A Comprehensive Classification of Thoracic and Lumbar Injuries*, Eur Spine J, 3:184-201.

95. Maquet, P. (1992) *Latrophysics to Biomechanics: From Borelli (1608-1679) to Pauwels (1885-1980)*, Bone Joint Surg Br, 74 (3): 335-339.
96. Margulies, S. S.; and Thibault, L. E. (1989) *An Analytical Model of Traumatic Diffuse Brain Injury*, J. Biomech. Engng, 111: 241–249.
97. McCann, H. R.; Al-Assar, F. S.; Fahleson, K.; Al-Ajmi, A.; Al-Omran, O. M. (1988) *Addressing the Camel-Vehicle Accident Problem in Saudi Arabia*, In: Proceedings of 3rd IRF Middle East Regional Meeting: Towards Better Road Performance, 2: 2.158-2.169, Ministry of Transport, Riyadh, Kingdom of Saudi Arabia, 13-18 Feb 1988.
98. McCullagh, P.; and Nelder, J. A. (1989) *Generalized Linear Models*, 2nd ed., London: Chapman and Hall.
99. McElhaney, J.H.; and Myers, B.S. (1993) *Biomechanical Aspects of Cervical Trauma Accidental Injury - Biomechanics and Prevention*: ISBN 0-387987881-X, ISBN 3-540-97881-X, Edited by Nahum and Melvin.
100. MCI (2008) *The Kingdom of Saudi Arabia: A Welfare State, Cultural Affairs Releases*, Ministry of Culture and Information, Kingdom of Saudi Arabia, Riyadh.
101. Menoret, P. (2005) *The Saudi Enigma: A History*, Zed Books, ISBN 1842776053.
102. Merrill, T.; Goldsmith, W.; and Deng, Y-C. (1984) *Three Dimensional Response of a Lumped Parameter Head - Neck Model Due to Impact and Impulsive Loading*, Journal of Biomechanics, 17 (2): 81-95.
103. Mofidi, A.; Tansey, C.; Mahapatra, SR.; Mirza, HA.; and Eisenstein, SM. (2007) *Cervical Spondylolysis, Radiologic Pointers of Stability and Acute Traumatic as Opposed to Chronic Spondylolysis*, J Spinal Disord Tech, 20:473-9.
104. MoH (1995-2010) *Health Statistical Year Book: Annual Mortality Report for Years 1416-1430H (1995-2010)*, Statistics Directorate, Ministry of Health, Kingdom of Saudi Arabia, Riyadh.
105. MoI (1970-2010) *Annual Statistics: The Publications of Road Accident Statistics for Years 1391-1430H (1970-2010)*, General Directorate of Traffic, Ministry of Interior, Kingdom of Saudi Arabia, Riyadh.
106. Momjian, S. (2003) *Occipital Condyle Fractures in Children*, Case Report and Review of the Literature, Pediatr Neurosurg, 38:265–70.

107. Moroney, S. P.; Schultz, A. B.; Miller, J. A. A.; and Andersson, G. B. J. (1988) *Load-Displacement Properties of Lower Cervical Spine Motion Segments*, Journal of Biomechanics, 21 (9): 769-779.
108. MoT (1970-2010) *Annual Statistical Book*, Reports for Years 1970–2010, Research and Studies Department, Ministry of Transport, Riyadh, Saudi Arabia.
109. MSC (2004) *MSC. Software Corporation*, User's Manual, Working Model Version 5.0TM, For Windows® 95/98/Me/2000/NT® 4.0 and later, WM2D*V5*Z*Z*Z*DC-TUTOR, <http://www.workingmodel.com>, Redwood City, CL, USA, May 2004.
110. Myers, B. S.; Winkelstein, B. A. (1995) *Epidemiology, Classification, Mechanism, and Tolerance of Human Cervical Spine Injuries*, Crit Rev Biomed Eng, 23 (5): 307-409.
111. Nafal, F.H.; Saeed, A.A.W.; Anokute, C.C. (1996) *Aetiological Factors Contributing to Road Traffic Accidents in Riyadh City, KSA*, Journal of Royal Society of Health, 116: 304–311.
112. Nahum, AM.; Melvin, JW. (2002) *Accidental Injury: Biomechanics and Prevention*, Springer Verlag, 2nd ed., ISBN 978-0387-98820-7, NY, USA.
113. NASS (1996) *National Automotive Sampling System, Pedestrian Crash Data Study*, Data Collection Coding and Editing Manual, U.S. Department of Transportation, National Highway Traffic Safety Administration, National Center for Statistics and Analysis, Washington, D.C. 20590.
114. NASS (2005) *National Automotive Sampling System (NASS)*, Crashworthiness Data System, Analytical User's Manual, 2005 File, National Highway Traffic Safety Administration, Department of Transportation.
115. NHTSA (2005) *Roof Crush Resistance*, National Highway Traffic Safety Administration, 49 CFR, Part 571, Docket No. NHTSA-2005-22143, RIN 2127-AG51.
116. Nicoll, EA. (1949) *Fractures of the Dorso-Lumbar Spine*, J Bone Joint Surg Br, 31:376–394.
117. Norton, R. (1992) *Design of Machinery*, McGraw-Hill.
118. Norusis, M. J. (2010) *SPSS 17.0 Guide to Data Analysis*, Upper Saddle River, NJ: Prentice-Hall, 28 Dec, 1st ed., ISBN 978-0321621436.

119. O'Connor P. (2002) *Injury to the Spinal Cord in Motor Vehicle Traffic Crashes*. *Accid Anal Prev.*, 34:477–485.
120. Oagana, A. (2010) *NHTSA and IIHS Crash Test Scores explained*, Available in <http://www.autoevolution.com/news/nhtsa-and-iihs-crash-test-scores-explained-4239.html>, accessed 27th August 2010.
121. Orlowski, K.; Bundorf, T.; Moffatt, E. (1985) *Rollover Crash Tests*. The Influence of Roof Strength on Injury Mechanics, SAE 851734, Society of Automotive Engineers, Warrendale, Pennsylvania.
122. Overaker, D. W.; Langrana, N. A.; and Cuitino, A. M. (1999) *A Nonlinear Micromechanical Model For Vertebral Trabecular Bone and Application in Whole Bone Finite Element Analysis*, American Society of Mechanical Engineers, Bioengineering Division (Publication) BED, Advances in Bioengineering, 42: 361-362.
123. Panjabi, M.; Wang, J.; Delson, N. (1999) *Neck Injury Criterion Based on Intervertebral Motions and its Evaluation using an Instrumented Neck Dummy*, Proc. IRCOBI Conf., pp 179-190.
124. Panjabi, M.; Dvorak, J.; Crisco, J.; Oda, T.; Hilibrand, A.; and Grob, D. (1998) *Simulation of Whiplash Trauma using Whole Cervical Spine Specimens*, *Spine*, 23 (1): 17-24.
125. Parenteau, C.; Gopal, M.; and Viano, DC. (2001) *Near and Far-Side Adult Front Passenger Kinematics in a Vehicle Rollover*, SAE 2001-01-0176, Society of Automotive Engineers, Warrendale, PA, USA.
126. Ragan, L. (2000) *Rollover Causal Analysis. SAE Passenger Car Rollover TOPTEC: Cause and Prevention*, Society of Automotive Engineers, Warrendale, Pennsylvania.
127. Reber, J. G; and Goldsmith, W. (1979) *Analysis of Large Head-Neck Motions*, *Journal of Biomechanics*, 12: 211-222.
128. Rivara, F.P.; Koepsell, T.D.; Grossman, D.C.; and Mock, C. (2000) *Effectiveness of Automatic Shoulder Belts Systems in Motor Vehicle Crashes*, *JAMA*, 283 (21): 2826-2828.

129. Roberson, R.E.; and Schwertassek, R. (1988) *Dynamics of Multibody Systems*, Springer-Verlag, ISBN 3-540-17447-8.
130. SAE (1984) *Collision Deformation Classification*, SAE Recommended Practice J-224BMAR84, Society of Automotive Engineers, Warrendale, PA, Mar 1984.
131. Sances, A., Jr.; Thomas, D. J.; Ewing, C. L.; Larson, S.J. (1986) *Mechanisms of Head and Spine Trauma*, Aloray Inc., NY, USA, ISBN 0-913690-11-2.
132. Schmitt, K. U.; Niederer, P.; Walz, F. (2004) *Trauma Biomechanics, Introduction to Accidental Injury*, Springer Science & Business Media, Inc., 1st ed., Germany, ISBN 3-540-22299-5.
133. Schneider, L.W.; Robbins, D.H.; Pflüg, M.A.; and Snyder R.G. (1983) *Development of Anthropometrically Based Design Specifications for an Advanced Adult Anthropomorphic Dummy Family*, Volume 1, DTNH22-80-C-07502, December 1983.
134. Shirazi-Adl, A.; and Parnianpour, M. (1996) *Stabilizing Role of Moments and Pelvic Rotation on the Human Spine in Compression*, Journal of Biomechanical Engineering, Transactions of the ASME, 118 (1): 26-31.
135. Shirazi-Adl, A.; and Parnianpour, M. (2000) *Load-Bearing and Stress Analysis of the Human Spine Under a Novel Wrapping Compression Loading*, Clinical Biomechanics, 15 (10): 718-725.
136. SIDA (2002) *Road Safety Analysis and Benchmarking*. In: Promemoria for an international Workshop. 21 May 2002. Swedish International Development Cooperation Agency, Stckholm.
137. Side, M. (1993) *Application of Finite Element Techniques to the Study of Cervical Spine Mechanics*, Proceedings of the 37th Stapp Car Crash Conference, San Antonio, TX, 261-272.
138. Silva M.P.; Ambrosio, J.A. (2004) *Human Motion Analysis Using Multibody Dynamics and Optimization Tool*, Technical report IDMEC/CPM - 2004/001, Lisbon.
139. Smith, J. A.; Siegel, J. H.; Siddiqi, S. Q. (2005) *Spine and Spinal Cord Injury in Motor Vehicle Crashes: A Function of Change in Velocity and Energy Dissipation on Impact with Respect to the Direction of Crash*, The Journal of Trauma, Injury Infection and Critical Care, 59 (1): 117-131.

140. SRCS (1970-2010) *Annual Report, The Publication Statistics for Years 1391-1430H*, Statistics Department, Saudi Red Crescent Society, Riyadh, Kingdom of Saudi Arabia.
141. Stemper, B. D. ; Yoganandan, N.; Pintar, F. A. (2004) *Validation of a Head-Neck Computer Model for Whiplash Simulation*, Med. Biol. Eng. Comput., 42: 333-338.
142. Sturgess, C.E.N. (2001) *A Continuum Damage Mechanics Theory of Impact Trauma*. Submitted to: Proc. IMechE, J. of Automobile Div.
143. Sturgess, C.E.N. (2002a) *Thermomechanical Theory of Impact Trauma*, Proc. IMechE, Part D: J. of Automobile Div., 216: 883-895.
144. Sturgess, C.E.N.; Coley, G.; and Oliveira, P De (2002b) *Pedestrian Injuries: Effects of Impact Speed and Contact Stiffness*, In Vehicle Safety 2002, IMechE London: MEP.
145. Suthurst, G.D; and Hardy, R.N. (1985) *Computer Simulations of a Range of Car-Pedestrian Collisions*, 10th International Technical Conference on Experimental Safety Vehicles, NHTSA, Oxford, July 1985.
146. Thunnissen, J.; Wismans, J.; Ewing, C. L.; and Thomas, D. J. (1995) *Human Volunteer Head-Neck Response in Frontal Flexion: A new Analysis*, In Proceedings of the 39th Stapp Car Crash Conference, Society of Automotive Engineers, SAE Paper No. 952721, 439-460.
147. Thurman, D.J.; Burnett, C.L.; Beaudoin, D.E.; Jeppson, L.; Snizek, J.E. (1995) *Risk Factors and Mechanism of Occurrence in Motorvehicle-Related Spinal Cord Injuries*: Utah, In: Proceedings of the 37th Annual Conference AAAM, San Antonio, Texas.
148. Toyota (2005) *Technical Specifications of Corolla model 2002*, Unpublished Report, Tech 2002-Toyt-28647-3, Motor Inspection Programme Meeting (124), Riyadh, Saudi Arabia, December 2005.
149. Valkonen, T., (1989) *The Calculation of the Values of Inequality Coefficients and Their Changes*. In: Fox, J. (ed.), Health Inequalities in European Countries, Gower Publishing Company, Aldershot, pp 161–162.
150. Van Der Horst, M. J. (2002) *Human Head Neck Response in Frontal, Side and Rear End Impact Loading - Modeling and Validation*, PhD Thesis, Technical University of Eindhoven.

151. Van Der Horst, M. J.; Thunnissen, J. G. M.; Happee, R.; Van Haaster, R. M. H. P.; and Wismans, J. S. H. M., (1997) *The Influence of Muscle Activity on the Head-Neck Response during Impact*, SAE Conference Proceedings, 315: 487-508.
152. Van Ee, C. A.; Nightingale, R. W.; Camacho, D. L. A.; Chancey, V. C.; Knaub, K. E.; Sun, E. A.; and Myers, B. A. (2000) *Tensile Properties of the Human Muscular and Ligamentous Cervical Spine*, Proceedings of 44th Stapp Car Crash Conference, Society of Automotive Engineers, 85-102.
153. Van Lopik, D.; and Acar, M. (2002) *The Development of a Multibody Head-Neck System for Impact Dynamics Using Visual Nastran 4D*, Proceedings of ESDA.
154. Viano, D.; Davidsson, J. (2001) *Neck Displacements of Volunteers, BioRID P3 and Hybrid III in Rear Impacts: Implications to Whiplash Assessment by a Neck Displacement Criterion (NDC)*, Proc. IIWPG/IRCOBI Symposium, Isle of Man.
155. Viano, DC.; Parenteau, CS. (2004) *Rollover Crash Sensing and Safety Overview*, SAE 2004-01-0342, Society of Automotive Engineers, Warrendale, PA, USA.
156. Wang, SL. (2001) *Motion Simulation with Working Model 2D and MSC.visualNastran 4D*, J. Comput. Inf. Sci. Eng., 1 (2): 193-196, June 2001.
157. WHO (2004) *Report on Road Traffic Injury Prevention*, World Health Organization World, ISBN 92 4 156260 9, Geneva, Switzerland.
158. WHO (2007) *International Statistical Classification of Diseases and Related Health Problems 10th Revision Version for 2007*, World Health Organization, available in <http://apps.who.int/classifications/apps/icd/icd10online/>, Retrieved February 2010.
159. WHO (2008) *The Global Burden of Disease the Global Burden of Disease, 2004 update*, World Health Organization, ISBN 97892 4 156371 0, Geneva, Switzerland.
160. Winkelstein, B. A.; and Myers, B. S. (2002) *Importance of Nonlinear and Multivariable Flexibility Coefficients in the Prediction of Human Cervical Spine Motion*, Journal of Biomechanical Engineering, Transactions of the ASME, 124 (5): 504-511.
161. Wismans, J.; Janssen, E.; Beusenbergh, M. (1994) *Injury Biomechanics - Course Notes*, Eindhoven University of Technology, Eindhoven.

162. Wismans, J.; Philippens, M.; Van Oorschot, E.; Kallieris, D; Mattern, R. (1987) *Comparison of Human Volunteer and Cadaver Head-Neck Response in Frontal Flexion*, In Proceedings of the 31st Stapp Car Crash Conference (P-202), pp 1-13, SAE Technical Paper #872194, Society of Automotive Engineers, Warrendale, PA.
163. Yang, K. H.; Zhu, F.; Luan, F.; Zhao, L.; and Begeman, P. C. (1998) *Development of a Finite Element Model of the Human Neck*, Proceedings of the 42nd Stapp Car Crash Conference, Society of Automotive Engineers, SAE Paper No. 983157, 195-205.
164. Yao, J.F; Yang, J.K; Otte, D. (2008) *Investigation of Head Injuries by Reconstructions of Real-World Vehicle-Versus-Adult-Pedestrian Accidents*, Safety Science, 46 (2008): 1103–1114.
165. Yochum, TR; Carton, JT; Barry, MS. (1995) *Cervical Spondylolysis: Three Levels of Simultaneous Involvement*. J Manipulative Physiol Ther, 18:411-5.
166. Yoganandan, N.; Haffner, M.; Maiman, D. J.; Nichols, H.; Pintar, F. A.; Jentzwn, J.; Weinshel, S; Larson, S. J.; Sances, A (1989) Jr: Epidemiology and Injury Biomechanics of Motor Vehicle Related Trauma to the Human Spine, Proceedings of the 33rd Stapp Car Crash Conference, SAE, Warrendale, PA, 223-242.
167. Yoganandan, N.; Kumaresan, S.; and Pintar, F. A. (2000) *Geometric and Mechanical Properties of Human Cervical Spine Ligaments*, Journal of Biomedical Engineering, 122 (6): 623-629.
168. Yoshida, S.; Matsuhashi, T.; and Matsuoka, Y. (1998) *Simulation of Car-Pedestrian Accident for Evaluating Car Structure*, Proc. 16th ESV Conf., 2344-2348.
169. Zander, T.; Rohlmann, A.; Klockner, C.; and Bergmann, G. (2002) *Effect of Bone Graft Characteristics on the Mechanical Behaviour of the Lumbar Spine*, Journal of Biomechanics, 35 (4): 491-497.
170. Zhang, Q. H.L; Tan, S. H.; and Teo, E. C (2008) *Finite Element Analysis of Head–Neck Kinematics Under Simulated Rear Impact at Different Accelerations*, Proc. IMechE, 222, Part H: J. Engineering in Medicine.

APPENDIX A

FIELDWORK OF REAL-WORLD ACCIDENTS STUDY

A.2 Field Study Forms (English)

Case					Veh		Occ		Form		Page		Position			
ACCIDENT DETAILS																
Total number of vehicles in accident					<input type="text"/>											
Date of accident					<input type="text"/> / <input type="text"/> / <input type="text"/>											
Time of accident					<input type="text"/> : <input type="text"/> : <input type="text"/> 24 hour clock											
Day of accident					<input type="text"/> Monday 1, Tuesday 2, etc											
Road classification					<input type="text"/> M, A, B, C (including unclassified)											
Speed limit					<input type="text"/> mph											
Region in which accident occurred					<input type="text"/>											
Maximum AIS in accident					<input type="text"/>											
Injury severity of accident					<input type="text"/> fatal 1, serious 2, slight 3, uninjured 4											
Account of accident																
Sketch of accident																

Case				Veh		Occ		Form		Page		Position			
------	--	--	--	-----	--	-----	--	------	--	------	--	----------	--	--	--

IMPACT DETAILS - EXTERIOR

Number of impacts	none 0, one 1, two 2, etc.
-------------------	----------------------------

Area of damage to this vehicle	front 1, offside 2, nearside 3, rear 4, roof 4, underside 5, multiple 7
--------------------------------	---

Rollover occurred		before impact 1, after impact 2, pure 3, in - between 4
	number of rolls (¼ rolls)	
	rest position	wheels 1, NS 2, OS 3, roof 4
	direction of roll rotation	to O/S 1, to N/S 2, rear over front 3, front over rear 4

Rollover CDC							
--------------	--	--	--	--	--	--	--

Under-ride occurred	
---------------------	--

Fire occurred		engine bay 1, passenger compartment 2, boot 4, sum for combinations
---------------	--	---

Water sub mersion		
-------------------	--	--

	N/S				O/S		
Length of vehicle (as found)			cm				cm

Distance wheel centres (as found)			cm					cm
-----------------------------------	--	--	----	--	--	--	--	----

Case					Veh	Occ	Form	Page	Position			
DAMAGE DETAILS - INTERIOR												
Windscreen	glass type		toughened 1, laminated 2									
	seal type		rubber seal 1, bonded 2									
	location (status)		in place 1, partial separation 2, ejection 3, missing 4									
	condition		broken & holed 1, broken, not holed 2, not broken 3									
	initial cause breakage		frame distortion 1, occupant 2, bonnet 3, external object 4,									
Front door	door attachment failure						hinge broken 1, latch broken 2					
							latch operated 4, (sum for multiples)					
	door status						opened out 1, unoperable 2, opened in 3,					
							restricted opening 4, torn off, removed 6					
	external object through door											
door bowed						out 1, in 2, both 3						
Rear door	door attachment failure						hinge broken 1, latch broken 2					
							latch operated 4, (sum for multiples)					
	door status						opened out 1, unoperable 2, opened in 3,					
							restricted opening 4, torn off, removed 6					
	external object through door											
door bowed						out 1, in 2, both 3						
Front row	relative intrusion						CHEST > pelvis 1, < pelvis 2, = pelvis 3					
	front door overrode sill											
	door beams	present										
		height					pelvis 1, abdomen 2, chest 3					
		damaged					beam 1, mounting plate 2, both 3					
		status					transmitted load to occupant 1					
						caused door to jam 2, both 3						
B pillar	relative intrusion						CHEST > pelvis 1, < pelvis 2, = pelvis 3					
	B pillar overrode sill											
Second row	relative intrusion						CHEST > pelvis 1, < pelvis 2, = pelvis 3					
	front door overrode sill											
	door beams	present										
		height					pelvis 1, abdomen 2, chest 3					
		damaged					beam 1, mounting plate 2, both 3					
		status					transmitted load to occupant 1					

Case					Veh	Occ	Form	Page	Position		
OCCUPANT DETAILS											
Seat row of occupant					first 1, second 2, etc.						
Seat position of occupant					offside 1, centre 2, nearside 3						
Occupant in child restraint					on lap 1, standing on seat 2, across seats 3, bearing another on lap 4						
Occupant not properly seated											
Occupant characteristics											
height					-		metres				
mass							kg				
age							years				
gender							male 1, female 2, pregnant female 3				
pregnancy							weeks				
pregnancy affected							Give details				
Hospitalisation											
status							outpatient 1, inpatient 2, dead on arrival 3, died in casualty 4				
duration of hospitalisation							nights				
time to die							days				
natural cause fatality											
Pre existing medical condition											
Severity for this occupant					fatal 1, serious 2, slight 3, uninjured 4						
Seat belt used					used 1, not used 2, not known if used 9						
Ejection											
ejection					known 1, suspected 2 (give details)						
type					full 1, partial 2 (give details)						
route					windscreen 1, side window 2, rear window 3, side door 4 hatch/estate door 5, sunroof 6						
Entrapment											
entrapment type					known 1, suspected 2, claimed 3 (give details)						
entrapment type					no doors openable by occupant* 1, body part trapped 2 occupant unable to release belt *4, multiple causes (sum codes)						
* due to vehicle damage, not occupant injury or presence of external objects.											

A.3 Field Study Forms (Arabic)

دراسة السجلات العمود الفقري الناجمة عن حوادث المرور بالململكة العربية السعودية - دراسة ميدانية على مدينة الرياض

[illegible]

ملخص الحادث

أسماء عدد الملاحظات المشتركة مع الحادث					
أسماء عدد الملاحظات المشتركة مع الحادث					
أسماء عدد الملاحظات المشتركة مع الحادث					
أسماء عدد الملاحظات					
أسماء عدد الملاحظات					
وصاية الحادث حسب تصنيف المرور					جسيم 1، عطر 2، طفيف 3، تلفيات 4
تاريخ الحادث			/	/	يوم / شهر / سنة
يوم الأسبوع					السيات 1، الأحد 2، الاثنين 3، الثلاثاء 4، الأربعاء 5، الخميس 6، الجمعة 7
وقت البلاغ عن الحادث					نظام 24 ساعة
مواقع الحادث					داخل المدينة 1، خارجي المدينة 2
التج حسب تقسيمات مدينة الرياض					شمال ش، جنوب ج، شرق ق، غرب غ
قراءة الكاميرات	N				شمال
	E				شرق
مطابق رقم الحادث					داخل حدود الطريق 1، خارج حدود الطريق 2
السرعة المحددة بالموقع					كم / س
تصنيف المرور					الناصرة 1، الشرق 2، الشمال 3، الغرب 4
رقم الحادث المروري					

رسم التقرير		رقم الحادث		رقم الحادث	
الشاهد الأول		رقم الحادث		رقم الحادث	
الشاهد الثاني		رقم الحادث		رقم الحادث	

[illegible]

ملخص الحادث

تم برسم كروكي لواقع الحادث مع تحديد الأبعاد والتفاصيل حسب المعاينة

رقم التوجه	المؤدىل	نوع المركبة	تسلسل المركبات
			1
			2
			3
			4
			5
			6
			7
			8
			9
			10

دراسة اصابات العمود الفقري الناجمة عن حوادث المرور بالململكة العربية السعودية - دراسة ميدانية على مدينة الرياض

البلد سنة شهر يوم طرف الحادث البركة الحالة

تفاصيل الحادث

حالة اليوم	معايير الموقع	الطريق الأول
1 صحو (بدون رياح قوية)	1 جزيرة وسطية	1 طريق سريع
2 مطر (بدون رياح قوية)	2 عند مدخل أو نهاية مخرج	2 طريق خدمة
3 صحو (مع رياح قوية)	3 على شبكة طرق سريعة	3 طريق رئيسي
4 مطر (مع رياح قوية)	4 طريق مستقيم	4 طريق فرعي
5 حباب	5 طريق منحني	5 غير محدد
6 غائم	6 دوار	عدد اسم الطريق :
7 غبار	7 تقاطع سكة حديد	
8 أخرى	8 تقاطع	يوم التفتيش بالتقاطير
9 غير معروف	9 مرتفع أو منحدر	1 رجل مرور
	10 غير معروف	2 اشارة ضوئية
		3 لوحة مرور
		4 اشارة ضوئية
		5 لا يوجد تحكيم

حالة الطريق	يوم التفتيش	الطريق الثاني
1 جاف	1 دوار	1 طريق سريع
2 زلق	2 شارع باتجاه واحد (احادي)	2 طريق خدمة
3 تلج	3 طريق مفرد (بدون جزيرة وسطية) - النجاش	3 طريق رئيسي
4 رطب	4 طريق مزدوج - مسارين في كل اتجاه	4 طريق فرعي
5 مغمور بالمياه (> 3)	5 طريق مزدوج - 3 مسارات أو أكثر في كل اتجاه	5 غير محدد
	6 طريق زراعي	عدد اسم الطريق :
	7 غير معروف	

دراسة اصابات العمود الفقري الناجمة عن حوادث المرور بالململكة العربية السعودية - دراسة ميدانية على مدينة الرياض

المرحلة 01 من 02 صفحة 03 عدد ملاحظات 04 طرف الحادث 05 البرقبة 06 الملاحظة

تفاصيل الحادث

تفاصيل الحادث	أنشطة المشاة	الاشارة
1 أكثر من 20 م عن التقاطع	0 لا يوجد نظام للمشاة	الترفع منضاه
2 دوار كبير	1 علامات عبور للمشاة في الشارع	1 يوجد أعمدة أنارة < 7
3 دوار صغير	2 علامات عبور لطلاب المدارس	2 يوجد أعمدة أنارة > 7
4 حرف تي (T)	3 علامات عبور تنظيم برجل مرور	3 لا يوجد أنارة
5 حرف واي (Y)	4 اشارة صوتية مزودة بأنظمة المشاة الذكية	4 نوع الاشارة غير معروف
6 مدخل او مخرج طريق سريع	5 ممر مشاة مزود بوسيلة تحكم آلي	الترفع منظم
7 الملاء اكثر من ثلاثة شوارع	6 جسر للمشاة	5 يوجد أعمدة أنارة < 7
8 تقاطع طرق مزدوج	7 نفق للمشاة	6 يوجد أعمدة أنارة > 7
9 بوابة خاصة		7 لا يوجد أنارة
10 غير معروف		8 الاضاءة متعطله
		9 نوع الاشارة غير معروف

العوامل على الطريق	ظروف المواقع
0 لا يوجد	0 لا يوجد
1 سقوط حولة من مركبة	1 الاشارة الصوتية خارج الخدمة
2 وجود جسم آخر على الطريق	2 الاشارة الصوتية معطلة جزئيا
3 وجود حادث سابق	3 التوسعات المرورية نالقة
4 وجود حيوان على الطريق	4 يوجد أعمال صيانة
5 عدم وجود سباح للطريق	5 سطح الطريق معطوب

دراسة اصابات العمود الفقري الناجمة عن حوادث المرور بالملكة العربية السعودية - دراسة ميدانية على مدينة الرياض

المرحلة 01 02 03 04 05 06 07 08 09 10 11 12 13 14 15 16 17 18 19 20 21 22 23 24 25 26 27 28

تفاصيل الحادث

يوم الحادث	1	2	3	4	5	6	7	8	9	10	11
تصادم مع مركبة أخرى متحركة											
الطريق											
دعس مشاة											
صدم دراجة هوائية											
صدم دراجة نارية											
صدم جسم ثابت											
تصادم مع حافلة أو شاحنة											
تصادم مع حيوان											
احتراق مركبة											
سقوط من جسر											
سقوط من منحدر											

تلفيات عامة	0	1	2	3	4	5	6	7	8	9	10	11	12	13	14	15	16	17	18	19	20	21	22	23	24	25	26	27	28
لا يوجد																													
شاحنة أو سيارة بحجم > 40																													
شاحنة أو سيارة بحجم < 40																													
رحيل																													
دوار																													
إشارة ضوئية																													
لوحات مرورية																													
أشجار																													
حوادث مرورية																													
حوادث مرورية																													
جدار أو سور																													
جسر																													
عمود إنارة																													
منطقة انتظار للسيارات																													
قناة مائية																													
مساح معدن حول الطريق																													
حوادث سابقة																													
أعمال صيانة بالطريق																													
مركبة متوقفة (إضاءة الرؤية)																													
مركبة متوقفة (غير واضحة)																													
جزيرة وسطية																													
حواجز تقاطع																													
لوحات أسماء الشوارع																													
لوحات إعلانية																													
خزان مياه																													
غرفة كهرباء																													
كثبان هوائية																													
بنية الطريق (غير محددة)																													
جسم ثابت آخر غير معروف																													

موقع الحادث بالمدينة للطريق	1	2
داخلي حدود الطريق		
خارج حدود الطريق		

موقع الحادث بالمدينة للطريق	0	1	2	3	4	5	6	7	8
لم يخرج عن مساره									
خرجت باتجاه اليمين									
خرجت باتجاه اليمين ثم عادت									
خرجت لالتقاء باتجاه تقاطع									
خرجت باتجاه المسار									
خرجت باتجاه المسار ثم عادت									
خرجت جهة المسار على الجزيرة									
خرجت جهة المسار على الجزيرة الوسطية ثم عادت إلى حالتها الأولى									
خرجت جهة المسار وغابت الجزيرة الوسطية إلى الاتجاه الآخر									

الوقت: دقيقة ساعة يوم شهر سنة

معلومات عامة

اسم المنتج										
نوع المادة										
رقم الملف										
اللون										
رقم الوحدة										
الموديل										

نوع المركبة	نوع التصادم
1 مركبة صغيرة صالون (مثل كامري ، كرميدا...) وغيرها	1 تصادم أمامي
2 جيب (مثل لاندكروزر ، بنترول ، سوزوكي...) وغيرها	2 تصادم جانبي
3 مركبة صغيرة ، صندوق الأمتعة باب خلفي مثل مازدا بوكس.	3 تصادم خلفي
4 مركبة ذات سقف متحرك (مثل بي إم دبليو 330 سي أي	4 احتكاك جانبي
5 وانيت (مثل داتسون ، هيلكس...)	5 زوازي
6 فان / حافلة صغيرة (أكثر من مرتين مثل سيارات التوالت)	6 متعدد
7 مركبة توصيل طلمات (عمارة واحدة مع حوض مصندوق)	
8 سيارات سائق التلقد منخفض والقوة اقل من مثل بورش ..	
9 مركبة أجرة (ليموزين)	

هل غلقت المركبة بشاحنة ؟	
--------------------------	--

1. اعمد

المتنوع		
مطابقة الشركة	1	
مقصورة الركاب	2	
حزان الأمعة (شبكة العنكبوت)	3	
أكثر من مكان	4	

هل قام رجال الدفاع المدني بأعماله؟

[illegible]

<p>وهم صبي الترييل . والمساكن . والداعيات الناجمة عن هذا المثل</p>	

APPENDIX B

NATIONWIDE SURVEY

OF

SCI

B.1 Main Questionnaire Survey of Study (Part I) - Demographic Background

I. Personal Information:

Name: _____ Hospital No.: _____
Address: _____ Telephone No.: _____
Nationality: Saudi _____ Non Saudi _____
If non-Saudi, specify: _____
Age : _____ years Sex: Male _____ Female _____

Education Level:

- | | |
|-----------------------|---------------------------|
| 1. Illiterate _____ | 4. Secondary _____ |
| 2. Primary _____ | 5. University _____ |
| 3. Intermediate _____ | 6. Higher education _____ |

Marital Status:

- | | |
|------------------|-------------------|
| 1. Married _____ | 3. Divorced _____ |
| 2. Single _____ | 4. Others _____ |

Occupation:

- | | |
|-------------------------|-----------------------------------|
| 1. Student _____ | 4. Self-Employed _____ |
| 2. Private Sector _____ | 5. Unemployed _____ |
| 3. Govt Employee _____ | Military _____ Non-military _____ |

Time, Day and Date of Injury _____

Date of Admission _____ Date of discharge: _____

Length of hospital stay _____ Referred from: _____

II. Cause of Injury

- | | |
|----------------------|------------------|
| 1. R.T.A _____ | 4. Gunshot _____ |
| 2. Industrial _____ | 5. Others _____ |
| 3. Domicillary _____ | |

If due to R.T.A., specify whether:

- A- 1. Pedestrian _____ 3. Passenger _____
 2. Driver _____ 4. Others _____
- B- 1. Seat belt: _____ Fastened _____ Unfastened
- C- 1. Head on collision _____ 3. Roll over _____
 2. Collision with camel _____ 4. Others _____

If due to industrial trauma, specify whether:

- | | |
|-----------------------|--------------------------|
| 1. Fall _____ | 3. Others, specify _____ |
| 2. Heavy object _____ | |

If due to Domiciliary trauma, specify whether:

- | | |
|-----------------------|--------------------------|
| 1. Fall _____ | 3. Others, specify _____ |
| 2. Heavy Object _____ | |

III. Acute Management

First Aid at site: Yes _____ No _____

If yes, specify whether:

- | | |
|--------------------------------|------------------|
| 1. Trained medical staff _____ | 3. Police _____ |
| 2. Passerby _____ | 4. Unknown _____ |

Mode of Transport to Hospital

1. Ambulance _____ 2. Normal Transport _____ 3. Aircraft _____

First Aid for Transport Time after Trauma

<1 hr _____ 1-4 hr _____ 4-6 hr _____ more than 6hr _____

Time from injury 1st ER services

1-2 hr _____ 2-4 hr _____ 4-6 hr _____ more than 6 hr _____

Time from injury 1st ER to SCI center (where casualty is operated first or treated conservatively)

0-6hr _____ 6-12hr _____ 12-24hr _____ >24hr _____ specify _____

Time from injury to SCI center

0-6hr _____ 6-12hr _____ 12-24hr _____ >24hr _____ specify _____

Position at scene: Supine _____ Side _____

Position during transfer Supine _____ Side _____

Immobilization

1. Neck _____ 2. Back _____

Respiratory Support:

1. Blind nasotracheal intubation _____ 2. Oxygen mask _____

3. Manual in line traction _____ 4. Oral intubation _____

Haemodynamic Management

1. Intravenous replacement _____ 3. Atropine _____

2. Bagonists _____ 4. Swan Ganz catheterization _____

Time from injury to start Methyl Prednisolone (MP) Bolus

0-2hr _____ 2-4hr _____ 4-6hr _____ 6-8hr _____ >8hr _____

Time from MP to SCI center

0-4hr _____ 4-8hr _____ 8-12hr _____ 12-24hr _____ >24hr _____

Time from injury to start traction

0-6hr _____ 6-12 hr _____ 12-24 hr _____ \geq 24hr _____

Time from injury to start 1st surgery

0-6 hr _____ 6-12 hr _____ 12-24 hr _____ \geq 24hr _____

B.2 Main Questionnaire Survey of Study (Part II) – Social Effects / Life Satisfaction in SCI

Age: _____ Sex: M ☐ F ☐

Average Family Income / Month:

< 3000 ☐ <5000 ☐ <7000 ☐ 7000> ☐

Number of Siblings:

1-3 ☐ 3-5 ☐ 5-8 ☐ 8 and above ☐

Education

None ☐ School ☐ Undergraduate ☐ Graduate ☐
Postgraduate ☐

Years since obtained a driving license:

1-3 yrs ☐ 3-5 yrs ☐ 5-8 yrs ☐ 8 and above ☐

Residence

Rural ☐ City ☐

If city, duration of stay

1-3 yrs ☐ 3-5 yrs ☐ 5-8 yrs ☐ 8 and above ☐

Cause of trauma:

Accident ☐ Fall ☐ Violence ☐
Sport related ☐ Other ☐

Who is the care provider for you?

None ☐ Servant / Maid ☐ Brother ☐
Father ☐ Wife ☐ Sister ☐ Other ☐

Is the residence modified?

Yes ☐ No ☐

Questions to care provider:

Limitations in physical activity:

Yes ☐ No ☐
Manageable ☐
Severe ☐

Limitations in social activity:

Yes ☐ No ☐
Manageable ☐
Severe ☐

Health Problems;

Yes ☐ No ☐

Emotional Problems:

Yes ☐ No ☐

General Mental Health:

No change ☐
Small change ☐
Severe change ☐

Limitations in usual role activity:

No ☐
Little ☐
Manageable ☐
Severe ☐





B.3 Summary Results of Poisson Model

Descriptive Statistics			alpha			p-value	Annual % change
			Model Coefficient	95% Confidence Interval			
Variable Name	Mean	Std. Deviation		Lower	Upper		
asrF35to44	2963.40	423.860	-0.057	-0.061	-0.053	0.000	-5.508
asrF45to54	2450.60	662.553	-0.074	-0.078	-0.070	0.000	-7.133
asrF55to64	3443.10	349.814	-0.025	-0.029	-0.021	0.000	-2.476
asrF65plus	3036.20	642.034	-0.019	-0.023	-0.015	0.000	-1.877
CIRtransport	2221.80	95.638	-0.022	-0.027	-0.018	0.000	-2.187
CIRfall	969.30	112.366	-0.018	-0.025	-0.011	0.000	-1.763
CIRother	332.70	63.607	0.035	0.023	0.047	0.000	3.589
CIRcomtetra	284.80	37.944	-0.046	-0.059	-0.033	0.000	-4.511
CIRintetra	589.50	186.200	-0.101	-0.111	-0.092	0.000	-9.650
CIRcompara	601.80	68.847	-0.047	-0.056	-0.039	0.000	-4.630
CIRinpara	1303.60	314.868	0.044	0.038	0.050	0.000	4.501
TransM0to14	796.60	194.317	0.035	0.027	0.042	0.000	3.532
TransM15to24	2.50	.527	-0.007	-0.144	0.129	0.916	-0.735
TransM25to34	165.40	41.661	-0.026	-0.043	-0.009	0.003	-2.541
TransM35to44	2802.30	276.252	-0.040	299.000	-0.036	0.000	-3.913
TransM45to54	613.60	155.467	-0.082	-0.090	-0.073	0.000	-7.835
TransM55to64	273.00	118.078	0.094	0.081	0.108	0.000	9.877
TransM65plus	6735.50	490.147	-0.013	-0.015	-0.010	0.000	-1.279
FallM0to14	2527.60	517.854	0.015	0.011	0.020	0.000	1.547
FallM15to24	727.30	318.798	0.091	0.082	0.099	0.000	9.494
FallM25to34	3922.20	756.092	-0.074	-0.078	-0.071	0.000	-7.175
FallM35to44	1381.20	353.027	-0.097	-0.103	-0.091	0.000	-9.221
FallM45to54	41960.00	12929.398	0.051	0.050	0.052	0.000	5.210
FallM55to64	4573.70	1419.983	-0.121	-0.124	-0.118	0.000	-11.387
FallM65plus	2700.60	482.031	-0.081	-0.085	-0.077	0.000	-7.783
OtherM0to14	336.40	122.531	-0.082	-0.094	-0.070	0.000	-7.906
OtherM15to24	4145.60	1253.735	-0.006	-0.010	-0.003	0.000	-0.641
OtherM25to34	4382.60	1462.285	-0.002	-0.005	0.001	0.188	-0.219
OtherM35to44	768.90	252.891	0.033	0.025	0.041	0.000	3.372
OtherM45to54	1681.30	795.631	-0.044	-0.050	-0.039	0.000	-4.334
OtherM55to64	4807.40	2619.494	-0.012	-0.015	-0.009	0.000	-1.185
OtherM65plus	2620.00	1071.689	-0.005	-0.009	-0.001	0.018	-0.509

Descriptive Statistics			alpha			p-value	Annual % change
			Model Coefficient	95% Confidence Interval			
Variable Name	Mean	Std. Deviation		Lower	Upper		
TransF0to14	273.80	60.578	-0.048	-0.061	-0.035	0.000	-4.700
TransF15to24	6860.00	2732.602	-0.123	-0.126	-0.120	0.000	-11.583
TransF25to34	83.70	33.744	-0.100	-0.123	-0.076	0.000	-9.476
TransF35to44	693.10	175.720	0.032	0.023	0.040	0.000	3.203
TransF45to54	1.00	.000	-0.024	-0.240	0.191	0.825	-2.406
TransF55to64	87.30	62.329	0.145	0.120	0.169	0.000	15.564
TransF65plus	1289.40	178.936	-0.048	-0.054	-0.042	0.000	-4.646
FallF0to14	416.20	122.304	-0.108	-0.118	-0.097	0.000	-10.201
FallF15to24	197.70	49.815	0.013	-0.002	0.028	0.097	1.313
FallF25to34	1112.80	162.288	-0.053	-0.060	-0.047	0.000	-5.170
FallF35to44	488.90	146.329	-0.102	-0.112	-0.092	0.000	-9.701
FallF45to54	148.60	30.420	-0.037	-0.055	-0.020	0.000	-3.656
FallF55to64	744.90	274.341	-0.109	-0.117	-0.101	0.000	-10.339
FallF65plus	557.70	162.964	-0.077	-0.086	-0.068	0.000	-7.397
OtherF0to14	204.40	116.152	-0.029	-0.044	-0.014	0.000	-2.833
OtherF15to24	1031.80	182.257	-0.017	-0.024	-0.010	0.000	-1.683
OtherF25to34	1457.60	246.639	-0.054	-0.060	-0.049	0.000	-5.288
OtherF35to44	324.80	237.543	-0.112	-0.124	-0.100	0.000	-10.606
OtherF45to54	627.00	109.122	-0.030	-0.039	-0.022	0.000	-2.972
OtherF55to64	1310.70	389.619	0.008	0.002	0.014	0.008	0.811
OtherF65plus	851.80	238.703	0.039	0.032	0.047	0.000	4.010
ComtetraTrans	244.20	39.883	-0.054	-0.068	-0.040	0.000	-5.283
ComtetraFall	13.80	4.158	-0.008	-0.066	0.050	0.796	-0.763
ComtetraOther	26.80	6.125	0.007	-0.035	0.049	0.746	0.693
IncomtetraTrans	474.10	197.788	-0.135	-0.145	-0.125	0.000	-12.619
IncomtetraFall	21.00	3.197	-0.048	-0.095	-0.001	0.046	-4.690
IncomtetraOther	94.60	23.486	0.049	0.026	0.071	0.000	4.989
ComparaTrans	504.90	67.831	-0.053	-0.063	-0.043	0.000	-5.154
ComparaFall	42.00	4.784	-0.049	-0.083	-0.016	0.004	-4.828
ComparaOther	54.70	10.100	0.004	-0.025	0.033	0.780	0.417
IncomparaTrans	998.70	280.719	0.055	0.048	0.062	0.000	5.616
IncomparaFall	148.50	14.924	-0.025	-0.043	-0.007	0.006	-2.449
IncomparaOther	156.40	38.437	0.043	0.026	0.061	0.000	4.439

APPENDIX C

CLINICAL SYMPTOMS OF SOFT TISSUE NECK INJURY

 1-2
 3-10
 11-13
 14

Name Sticker

Phone: Work.....Home.....

Gender

Hobby (24 – 26)

Time Of Accident
.....
41 – 44

1. Approximate speed of vehicle in km/h:

Self	<input type="checkbox"/>	<input type="checkbox"/>	<input type="checkbox"/>	45 - 47
Other	<input type="checkbox"/>	<input type="checkbox"/>	<input type="checkbox"/>	48 - 50

2. Make & Model of Vehicles:

Self	<input type="checkbox"/>	<input type="checkbox"/>	<input type="checkbox"/>	51 - 52
Other	<input type="checkbox"/>	<input type="checkbox"/>	<input type="checkbox"/>	53 - 54

3. Momentum	Low/High	(=1/2)	<input type="checkbox"/>	55
-------------	----------	--------	--------------------------	----

4. 1. Driver 2. Passenger **Front** 3. Passenger **Rear Rt**

4. Passenger **Rear Lt** 5. Passenger **Rear Middle**

<input type="checkbox"/>	56
--------------------------	----

5. Head rest – Yes / No	<input type="checkbox"/>	57
-------------------------	--------------------------	----

6. Height of Head rest: (Please use the diagrams to answer the following question)

Adequate (diag.1)

Not adequate (diag. 1)	<input type="checkbox"/>	58
------------------------	--------------------------	----

7. At the time of the accident your were

Wearing a SASH / LAP belt (1)

Wearing a LAP belt (2)

Not wearing a seat belt (3)	<input type="checkbox"/>	59
----------------------------------	--------------------------	----

8. Type of collision: Rear End (1)\

Head on (2)

Side (3)

Pile up (4)

Frontal (5)

Others (6)

☐ ☐

60 – 65

Specify:

.....

9. Were you aware of the impending accident?

Yes / No

☐

66

10. Were you unconscious after the accident?

Yes / No

☐

67

11. If yes for how long? Mins

☐ ☐

68 – 69

11. Within 24 hrs after the accident did you experience any of the following?

Nausea yes / no	<input type="checkbox"/>	70
Head ache yes / no	<input type="checkbox"/>	71
Blured vision yes / no	<input type="checkbox"/>	72
Double vision yes / no	<input type="checkbox"/>	73
Black spots in the visual field		
Yes / no	<input type="checkbox"/>	74
Difficulty in focusing your eyes		
Yes / no	<input type="checkbox"/>	75
Pain behind the eyes		
Yes / no	<input type="checkbox"/>	76
Dizziness yes/no	<input type="checkbox"/>	77

Specify:

.....

.....

.....

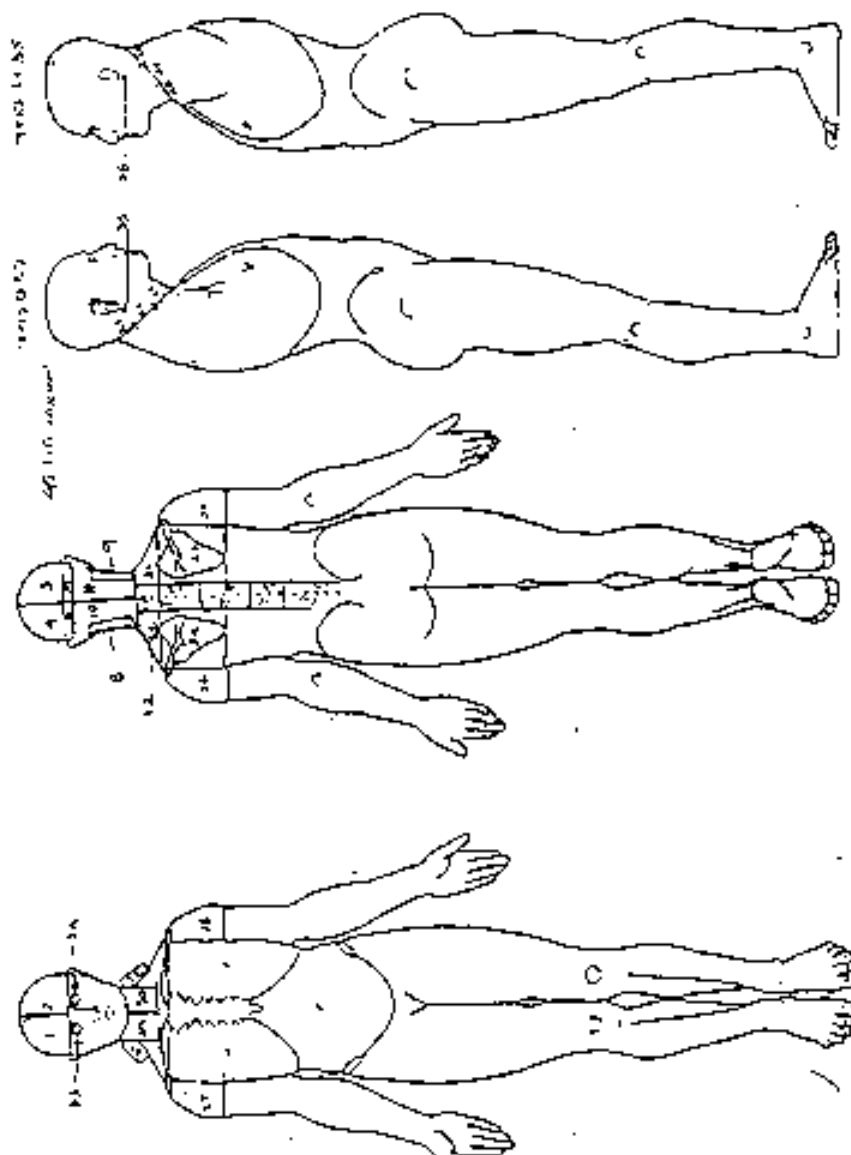
.....

.....

.....

Yes =1, No=2 Yes (Right) =3, Yes (Left)=4

12. Please use the body diagram (**Chart 1**) to show pain or pins and needles sensation or numbness that you noticed within 24 hours after the accident.



1-2

3-10

13. Please use the following expressions to describe the pain that you experienced (chart 1) and how severe it was at that time. (Please read explanation of 0-100 pain scale from the chart).

- 1- Dull ache

2- Deep ache

3- Sharp pain
- 4- Throbbing pain

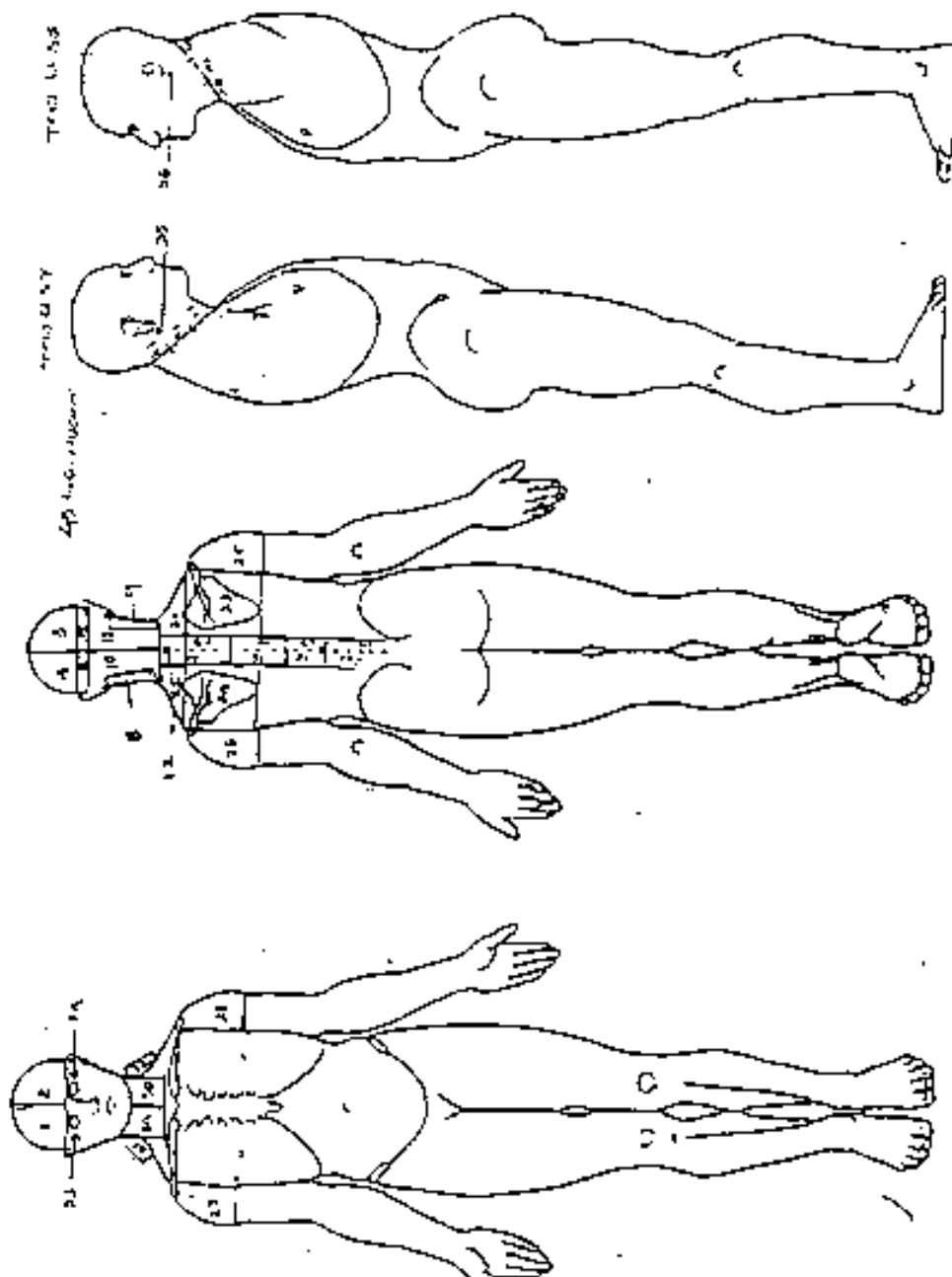
5- Stabbing pain

6- Tooth ache
- 7- Burning pain

8- Stretching pain

Area	Description of Pain		Intensity	
<div><div></div><div></div></div>	11-12	<div><div></div>13</div>	<div><div></div><div></div><div></div></div>	14-16
<div><div></div><div></div></div>	17-18	<div><div></div>19</div>	<div><div></div><div></div><div></div></div>	20-22
<div><div></div><div></div></div>	23-24	<div><div></div>25</div>	<div><div></div><div></div><div></div></div>	26-28
<div><div></div><div></div></div>	29-30	<div><div></div>31</div>	<div><div></div><div></div><div></div></div>	32-34
<div><div></div><div></div></div>	35-36	<div><div></div>37</div>	<div><div></div><div></div><div></div></div>	38-40
<div><div></div><div></div></div>	41-42	<div><div></div>43</div>	<div><div></div><div></div><div></div></div>	44-46
<div><div></div><div></div></div>	47-48	<div><div></div>49</div>	<div><div></div><div></div><div></div></div>	50-52
<div><div></div><div></div></div>	53-54	<div><div></div>55</div>	<div><div></div><div></div><div></div></div>	56-58
<div><div></div><div></div></div>	59-60	<div><div></div>61</div>	<div><div></div><div></div><div></div></div>	62-64
<div><div></div><div></div></div>	65-66	<div><div></div>67</div>	<div><div></div><div></div><div></div></div>	68-70
<div><div></div><div></div></div>	71-72	<div><div></div>73</div>	<div><div></div><div></div><div></div></div>	74-76
<div><div></div><div></div></div>	77-78	<div><div></div>79</div>	<div><div></div><div></div><div></div></div>	80-82

14. Current Symptoms: Please use the body diagram (**Chart 2**) to show either pain or pins and needles sensation or numbness that you might have at present.



1-2

3-10

15. Please use the following expressions to describe the pain experienced by you (Chart 2) and how severe it is (Please read the explanation of 0-100 pain scale from the chart).

- | | | |
|-------------------|--------------------|---------------|
| 1- Dull ache | 2- Deep ache | 3- Sharp pain |
| 4- Throbbing pain | 5- Stabbing pain | 6- Tooth ache |
| 7- Burning pain | 8- Stretching pain | |

Area		Description of Pain		Intensity	
<input type="text"/> <input type="text"/>	11-12	<input type="text"/> 13		<input type="text"/> <input type="text"/> <input type="text"/>	14-16
<input type="text"/> <input type="text"/>	17-18	<input type="text"/> 19		<input type="text"/> <input type="text"/> <input type="text"/>	20-22
<input type="text"/> <input type="text"/>	23-24	<input type="text"/> 25		<input type="text"/> <input type="text"/> <input type="text"/>	26-28
<input type="text"/> <input type="text"/>	29-30	<input type="text"/> 31		<input type="text"/> <input type="text"/> <input type="text"/>	32-34
<input type="text"/> <input type="text"/>	35-36	<input type="text"/> 37		<input type="text"/> <input type="text"/> <input type="text"/>	38-40
<input type="text"/> <input type="text"/>	41-42	<input type="text"/> 43		<input type="text"/> <input type="text"/> <input type="text"/>	44-46
<input type="text"/> <input type="text"/>	47-48	<input type="text"/> 49		<input type="text"/> <input type="text"/> <input type="text"/>	50-52
<input type="text"/> <input type="text"/>	53-54	<input type="text"/> 55		<input type="text"/> <input type="text"/> <input type="text"/>	56-58
<input type="text"/> <input type="text"/>	59-60	<input type="text"/> 61		<input type="text"/> <input type="text"/> <input type="text"/>	62-64
<input type="text"/> <input type="text"/>	65-66	<input type="text"/> 67		<input type="text"/> <input type="text"/> <input type="text"/>	68-70
<input type="text"/> <input type="text"/>	71-72	<input type="text"/> 73		<input type="text"/> <input type="text"/> <input type="text"/>	74-76
<input type="text"/> <input type="text"/>	77-78	<input type="text"/> 79		<input type="text"/> <input type="text"/> <input type="text"/>	80-82

1-2

3-10

16. Please indicate how often you have been noticing the pain and pins and needles sensation that you have show in the body diagram 2?

1. All the time
2. Most of the time
3. Now and then
4. After moving the part
5. Occasionally
6. All the time made worse by movement
7. Bending the head forward for a long time (15 minute +)

Area of Pain	Frequency	Area of P&N	Frequency
<input type="text"/> <input type="text"/> 11-12	<input type="text"/> 13	<input type="text"/> <input type="text"/> <input type="text"/> 14-15	<input type="text"/> 16
<input type="text"/> <input type="text"/> 17-18	<input type="text"/> 19	<input type="text"/> <input type="text"/> <input type="text"/> 20-21	<input type="text"/> 22
<input type="text"/> <input type="text"/> 23-24	<input type="text"/> 25	<input type="text"/> <input type="text"/> <input type="text"/> 26-27	<input type="text"/> 28
<input type="text"/> <input type="text"/> 29-30	<input type="text"/> 31	<input type="text"/> <input type="text"/> <input type="text"/> 32-33	<input type="text"/> 34
<input type="text"/> <input type="text"/> 35-36	<input type="text"/> 37	<input type="text"/> <input type="text"/> <input type="text"/> 38-39	<input type="text"/> 40
<input type="text"/> <input type="text"/> 41-42	<input type="text"/> 43	<input type="text"/> <input type="text"/> <input type="text"/> 44-45	<input type="text"/> 46
<input type="text"/> <input type="text"/> 47-48	<input type="text"/> 49	<input type="text"/> <input type="text"/> <input type="text"/> 50-51	<input type="text"/> 52
<input type="text"/> <input type="text"/> 53-54	<input type="text"/> 55	<input type="text"/> <input type="text"/> <input type="text"/> 56-57	<input type="text"/> 58
<input type="text"/> <input type="text"/> 59-60	<input type="text"/> 61	<input type="text"/> <input type="text"/> <input type="text"/> 62-63	<input type="text"/> 64
<input type="text"/> <input type="text"/> 65-66	<input type="text"/> 67	<input type="text"/> <input type="text"/> <input type="text"/> 68-69	<input type="text"/> 70
<input type="text"/> <input type="text"/> 71-72	<input type="text"/> 73	<input type="text"/> <input type="text"/> <input type="text"/> 74-75	<input type="text"/> 76
<input type="text"/> <input type="text"/> 77-78	<input type="text"/> 79	<input type="text"/> <input type="text"/> <input type="text"/> 80-81	<input type="text"/> 82

Others specify:

.....
.....
.....

☐☐ 1-2

☐☐☐☐☐☐☐☐ 3-10

17. Area you suffering from any of the following:

Nausea Yes / No ☐ 11

Blured vision Yes / No ☐ 12

Double vision Yes / No ☐ 13

Black spots in the visual field Yes / No ☐ 14

Difficulty in focusing your eyes Yes / No ☐ 15

Dizziness Yes / No ☐ 16

Loss of balance Yes / No ☐ 17

Ringing in the ear Yes / No ☐ 18

Pain behind the eyes Yes / No ☐ 19

Specify:

.....
.....
.....
.....

Yes =1, No=2 Yes (Right) =3, Yes (Left)=4